UNIVERSITY OF THE
WITWATERSRAND,
JOHANNESBURG

REGULATION OF PXDN IN EYE DEVELOPMENT AND PXDN GENE VARIANT SCREENING WITHIN A SOUTH AFRICAN COHORT OF PATIENTS PRESENTING WITH ANTERIOR SEGMENT DYSGENESIS

By

TEBOGO RECTOR MARUTHA

Thesis

Submitted in fulfilment of the requirements for the degree

Doctor of Philosophy

in

Molecular and Cell Biology

in the Faculty of Science, University of the Witwatersrand, Johannesburg, South Africa

Supervisor: Prof D. Mavri-Damelin

Co-supervisor: Dr N. Carstens

December 2022

Declaration

I, **Tebogo Rector Marutha** (**1111612**), am a student registered for the degree of Doctor of Philosophy in the academic year 2022.

I hereby declare the following:

- I am aware that plagiarism (the use of someone else's work without their permission and/or without acknowledging the original source) is wrong.
- I confirm that the research proposal submitted for assessment for the above degree is my own unaided work except where explicitly indicated otherwise and acknowledged.
- I have followed the required conventions in referencing the thoughts and ideas of others.
- I understand that the University of the Witwatersrand may take disciplinary action against me if there is a belief that this is not my own unaided work or that I have failed to acknowledge the source of the ideas or words in my writing.

Signature_____T.R Marutha_____ 07th day of December 2022_ YEAR

I would like to dedicate this work to my loving parents and family for all the support they have given me.

Abstract

Peroxidasin (PXDN) is an extracellular matrix-associated haem-peroxidase predominantly expressed in the vasculature and eye. PXDN crosslinks collagen IV through sulfilimine bond formation in the basement membrane. Aberrant PXDN expression is associated with fibrosis, heart failure and cancer, and various pathologies of the eye, where PXDN likely provides structural support via basement membrane synthesis in the cornea and lens during eye development, as well as protect the lens, trabecular meshwork and cornea against oxidative damage. Furthermore, *PXDN* pathogenic variants have been associated with anterior segment dysgenesis (ASD), congenital cataracts and corneal opacity. To further understand the role of *PXDN* in the eye, first we aimed to identify *PXDN* as a novel target of key transcriptional regulators of eye development, namely PAX6, FOXC1 and PITX2, and second, to screen a cohort of South African patients with ASD to look for pathogenic variants in *PXDN* and other ASD genes. Protein expression of PAX6, FOXC1, PITX2 and PXDN, in response to Fibroblast Growth Factor-2 (FGF-2) were quantified by western blotting and localisation visualised using immunofluorescence confocal microscopy. Chromatin immunoprecipitation-PCR and luciferase assays were employed to detect transcription factor-*PXDN* promoter interactions. Expression data established that PXDN, PAX6, FOXC1 and PITX2 were induced by FGF2 at varying time points. Putative binding sites for all three transcription factors were identified in the *PXDN* promoter and ChIP-PCR confirmed that PAX6, FOXC1 and PITX2 interact with various regions of the promoter. Luciferase reporter assays are currently underway. Next Generation Sequencing of genomic DNA from South African patients exhibiting ASD disorders. identified disease causing variants in *PAX6* and *GJA8*. Variants of uncertain significance were identified in *PXDN*, *BCOR*, *EPHA2* and *LTBP2* genes and are being investigated further. In conclusion, we identified PXDN as a novel target of PAX6, FOXC1 and PITX2 that further supports for the integral role of PXDN in eye development.

Research output

Original Publication: Marutha, T.R., Williams, S., Novellie, M., Dillon, B., Carstens, N., and Mavri-Damelin, D., 2022. Exome sequencing in South African patients presenting with Anterior segment dysgenesis. Submitted manuscript to Ophthalmic Genetics Journal, **ISSN:** 1744-5094.

Conferences:

Marutha, T.R., Williams, S., Novellie, M., Dillon, B., Carstens, N., and Mavri-Damelin, D., 2018. Regulation of PXDN in eye development and *PXDN* gene variant screening within a South African cohort of patients presenting with anterior segment dysgenesis. Life sciences imaging facility research day, University of the Witwatersrand, Johannesburg, Oral presentation.

Marutha, T.R., Williams, S., Novellie, M., Dillon, B., Carstens, N., and Mavri-Damelin, D., 2019. Regulation of PXDN in eye development and *PXDN* gene variant screening within a South African cohort of patients presenting with anterior segment dysgenesis. University of the Witwatersrand 10th Cross-Faculty postgraduate symposium, Johannesburg, Poster presentation.

Marutha, T.R., Williams, S., Novellie, M., Dillon, B., Carstens, N., and Mavri-Damelin, D., 2020. Regulation of PXDN in eye development and *PXDN* gene variant screening within a South African cohort of patients presenting with anterior segment dysgenesis. University of the Witwatersrand 11th Cross-Faculty postgraduate symposium, Johannesburg, Grad-flash presentation.

Marutha, T.R., Williams, S., Novellie, M., Dillon, B., Carstens, N., and Mavri-Damelin, D., 2022. Regulation of PXDN in eye development and *PXDN* gene variant screening within a South African cohort of patients presenting with anterior segment dysgenesis. South African Society of Biochemistry and Molecular Biology (SASBMB), Virtual event, Poster presentation.

Marutha, T.R., Williams, S., Novellie, M., Dillon, B., Carstens, N., and Mavri-Damelin, D., 2023. Regulation of PXDN in eye development and *PXDN* gene variant screening within a South African cohort of patients presenting with anterior segment dysgenesis. 14th International Congress of Human Genetics (ICHG2023), Poster presentation.

Acknowledgements

This project has been one of the most challenging journeys in my quest for scientific knowledge and as such I would like to thank the following individuals as well as organisations for their contribution towards the success of this study.

I would like to thank my supervisor, Prof Demetra Mavri-Damelin, first for designing the project and setting it in motion by granting me the opportunity to join her research lab. Secondly for her support, encouragement and guidance which enabled me to achieve more than I thought possible in the years spent in the Functional Genetics Research Laboratory. It was indeed a blessing to have been under her guidance for the duration of this research project.

I would also like to thank my co-supervisor Dr Nadia Carstens, for collaborating with us on this project which enabled me to learn even more techniques and acquire more skills. Thank you for the support with analysis of the NGS data, exposure to various bioinformatics tools and the co-supervision.

I am grateful to the funding bodies that supported me, and this work, financially, through the provision of bursaries and awards. This work was funded by scholarship from the National Research Foundation. I would also like to thank the National Health Laboratory services for technical assistance with Next generation sequencing and the University of the Witwatersrand. I would like to thank the participants as well as their families for their participation in this study. Dr Susan Williams, Dr Michael Novellie, Dr Bronwyn Dillon and Mrs Prescilla January for recruitment of patients, diagnosis, as well as sample collection.

To my colleagues in the Functional Genetics Research Laboratory whom have become very close and precious friends, Kayleen Jegels, Thokozile Makhanya, Lebogang Moshupya, Jemma Falkov, Eunice Niyobuntu and Ntakadzeni Nemuvumoni thank you for all the memories, support, encouragement advice and most importantly the laughs in both rainy and sunny days.

I would like to thank Dr. Clement Penny and Dr. Aurelie Deroubaix for so much assistance with the Carl Zeiss LSM 780 confocal microscope at the Life Sciences Imaging Facility at the University of the Witwatersrand Medical School. Dr Angela Botes for access to the Qsonica probe sonicator, Daniesha Govender and Bronwyn Mol for access to HEK293 cell line, finally Dr Kerry Hanmer and Dr Boitumelo Sitole for optimisation of some section of the methods.

To my parents, Headman Marutha and Agnes Marutha thank you for all your unwavering support throughout my academic journey and life in general. Each of you in your own unique ways have imparted wisdom to me that has strengthened me through difficult times of this journey.

And over and above I thank the all-mighty God for everything he has made possible.

Table of contents

List of figures

List of tables

List of abbreviations

A	Adenine
ACMG	American college of medical genetics and genomics
ARS	Axenfeld-Rieger syndrome
ASD	Anterior Segment Dysgenesis
ASD	Anteror segment dysgenesis
BAM	Binary annotation map
BCOR	BCL6 corepressor
BM	Basement Membrane
Br^-	Bromine
C	Cytosine
CADD	Combined annotation-dependent depletion
ChIP	Chromatin immunoprecipitation
ChIP	Chromatin Immunoprecipitation
Cl^-	Chlorine
COL4A	Collagen IV
COPD	Chronic Obstructive Pulmonary Disease
Cx50	Connexin50
DANN	Deleterious annotation of Genetic Variants using Neural Network
DAP	4',6-Diamidino-2-Phenylindole
DMEM	Dulbecco's Modified Eagle's Medium

DUOX	Dual Oxidase
ECL1	Extracellular loop one
ECL2	Extracellular loop two
ECM	Extracellular Matrix
EMT	Epithelial-Mesenchymal Transition
EPHA2	Ephrin receptor tyrosine kinase A2
EPO	Eosinophil Peroxidase
ExAC	Exome Aggregation Consortium
FATHMM	Functional Analysis through Hidden Markov Models
FBN1	Fibrillin
FBS	Foetal Bovine Serum
FOXC1	Forkhead box c1
G	Guanine
GBM	Glomerular Basement Membrane
GJA8	Gap junction alpha 8
gnomAD	Genome aggregation database
H_2O_2	Hydrogen Peroxide
HO-1	Heme Oxygenase 1
HOBr	Hypobromous Acid
HOCI	Hypochlorus Acid
HOSCN	Hypothiocyanous Acid
IGV	Integrative genomics viewer

IOP	Intraocular pressure
IOP	Intra-Ocular Pressure
IR	Ischemia Reperfusion
LPO	Lactoperoxidase
LTBP2	Latent Transforming Growth Factor Beta Binding Protein 2
MAC	Microphthalmia, Anophthalmia and Coloboma
MAF	Minor allele frequency
Met	Methionine
MG50	Melanoma Associated Gene 50
MPO	Myeloperoxidase
NaCl	Sodium Chloride
NADPH	Nicotinamide Adenine Dinucleotide Phosphate
NC1	Non-Collagenous Domain 1
NCBI	National Center for Biotechnology Information
NGS	Next generation sequencing
NGS	Next Generation Sequencing
NOX	NADPH Oxidase
NRF2	Nuclear factor-erythroid factor 2-related factor 2
NT	N-terminal domain
O_2	Oxygen
$O2^-$	Superoxide
OCFD	Oculofaciocardiodental

PAX6	Paired Box 6
PCG	Primary Congenital Glaucoma
PH	Pulmonary Hyperfusion
PITX2	Paired-like homeodomain transcription factor 2
Polyphen2	Polymorphism Phenotyping v2
PRG2	P53-Responsive Gene 2 Protein
PST	Proline serine threonine
PUFD	PCGF Ub-like fold discriminator domain
PXDN	Peroxidasin
PXDNL	Peroxidasin Like
ROS	Reactive Oxygen Species
SNAI1	Snail Family Transcriptional Repressor 1
SCN^-	Thiocyanate
SDS	Sodium Dodecyl Sulfate
SIFT	Sorting intolerant from tolerant
SNP	Single Nucleotide Polymorphism
SNV	Single nucleotide variation
T	Thymine
TGF-β1	Transforming Growth Factor Beta 1
TM1	Transmembrane one
TM2	Transmembrane two
TPO	Thyroid Peroxidase

URE	Uncorrected Refractive Errors
VCF	Variant caller file type
VPO1	Vascular Peroxidasin 1
VUS	Variant of uncertain significance
vWF	Von Willebrand Factor
WES	Whole exome sequencing

CHAPTER 1: Introduction

1.1 Peroxidasin overview of structure and functions

Peroxidasin (PXDN) was first isolated from *Drosophila*, as being secreted by mesoderm derived haemocytes (Nelson et al., 1994). Since then, the human gene has been identified to encode for a secreted enzyme that contains both a peroxidase catalytic domain and multiple motifs found in extracellular matrix (ECM) proteins (Nelson et al., 1994; Péterfi and Geiszt, 2014). In humans, PXDN is predominantly expressed in the cardiovascular system by cardiomyocytes (Zhang et al., 2012) and it is also expressed in the developing eye, more specifically in the layers of lens and corneal epithelium (Khan et al., 2011). Some suggested general functions of PXDN include innate immune defence (Li et al., 2012), catalysis of oxidative reactions using hydrogen peroxide (H_2O_2) (Ma et al., 2013), and in the biogenesis of basement membrane in cells and tissues (Bhave et al., 2012). PXDN belongs to the haem containing cyclooxygenase peroxidase family that consists of: thyroid peroxidase (TPO), lactoperoxidase (LPO), eosinophil peroxidase (EPO) and myeloperoxidase (MPO) (Davies et al., 2008; Soudi et al., 2012; Lázár et al., 2015). In addition, a peroxidasin like protein (PXDNL) has also been identified, which was found to have a high level of sequence similarity to PXDN but lacks peroxidase activity (**Figure 1.1**); to date it has only been found to be expressed in humans (Peterfi et al., 2014).

The *PXDN* gene is located at chromosome 2 (2p25.3) and consists of 23 exons that encode a 1479 amino acid protein. *PXDN* has also been referred to in the literature as *MG50* (melanoma-associated gene 50) (Weiler et al., 1994; Mitchell et al., 2002), *PRG2* (p53-responsive gene 2 protein) (Horikoshi et al., 1999) and *VPO1* (vascular peroxidase 1) (Cheng et al., 2008). Besides containing a peroxidase domain, which is highly homologous to other animal peroxidases (**Figure 1.1**), PXDN also contains domains with characteristics of proteins of the ECM, these include: Ig-like C2 domains, which have been found to have various biological functions with the most common function being pattern recognition and cell adhesion (Von Castelmur et al., 2008); von Willebrand Factor domain (vWF), which aids in oligomerisation of proteins as well as regulation of bone morphogenetic binding (Sadler, 2009) and leucine-rich repeats which have been found in numerous proteins, which seem to be involved in protein to protein interactions including ECM assembly, RNA

processing, cell adhesion, platelet aggregation, neural development and signal transduction (Bella et al., 2008) (**Figure 1.1**). These motifs often function in interactions between proteins although the exact role of each domain in PXDN remains largely un-investigated (Péterfi and Geiszt, 2014). In a study by Ero-Tolliver etal., (2015) it was found that the catalytic and Ig domains were required for successful sulfilimine bond formation between collagen IV molecules. The leucine-rich repeats domain was also found to be required for efficient binding of laminin in basement membrane (BM) (Sevcnikar et al., 2020).

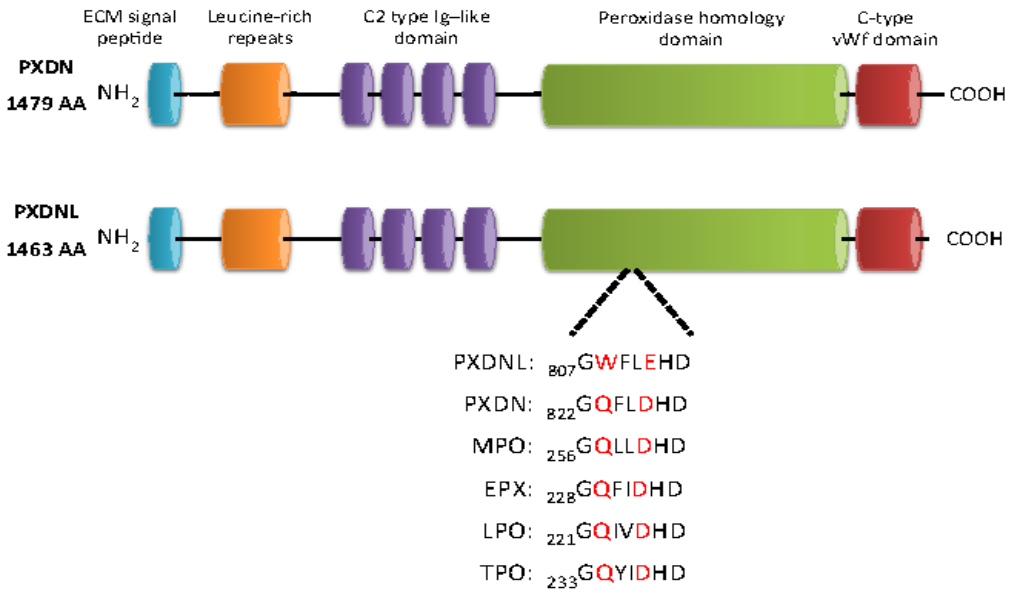

Figure 1.1: Comparison of PXDN and PXDNL structure. The structure of both PXDN and PXDNL show similar domains (vWF C type, Leucine rich repeats, Peroxidase, Ig like and N terminal secretory signal) and share homology with other haem peroxidases within the peroxidase domain (Modified from Péterfi and Geiszt, 2014).

Among the haem containing cyclooxygenase family of peroxidases, PXDN has a larger molecular size of approximately 165 Kilodalton (kDa) and shares greatest 86% similarity with MPO (Cheng et al., 2008). Despite the additional domains of PXDN, the amino acid residues that form the core of PXDN within the peroxidase

domain are highly conserved, which suggest that the PXDN haem catalytic site functions in a similar manner (Cheng et al., 2011).

1.2 Functions of other haem peroxidase-cyclooxygenases

Peroxidase cyclooxygenases is a family of haem containing peroxidases with a central structure of coordinated haem iron which is used as a redox cofactor and H_2O_2 as the electron acceptor in the catalysis of various oxidative reactions (Zámocký et al., 2015). Peroxidase-cyclooxygenases can also use haem to catalyse electron oxidation of other molecules such as proteins, anions, cations as well as tyrosine (Zámocký et al., 2015). PXDN has been found to likely be the ancestral member of the haem containing peroxidase family conserved to the basal phylum Cnidaria (**Figure 1.2**), which reflects its function in the critical aspect of tissue formation in animals and BM assembly (Soudi et al., 2012).

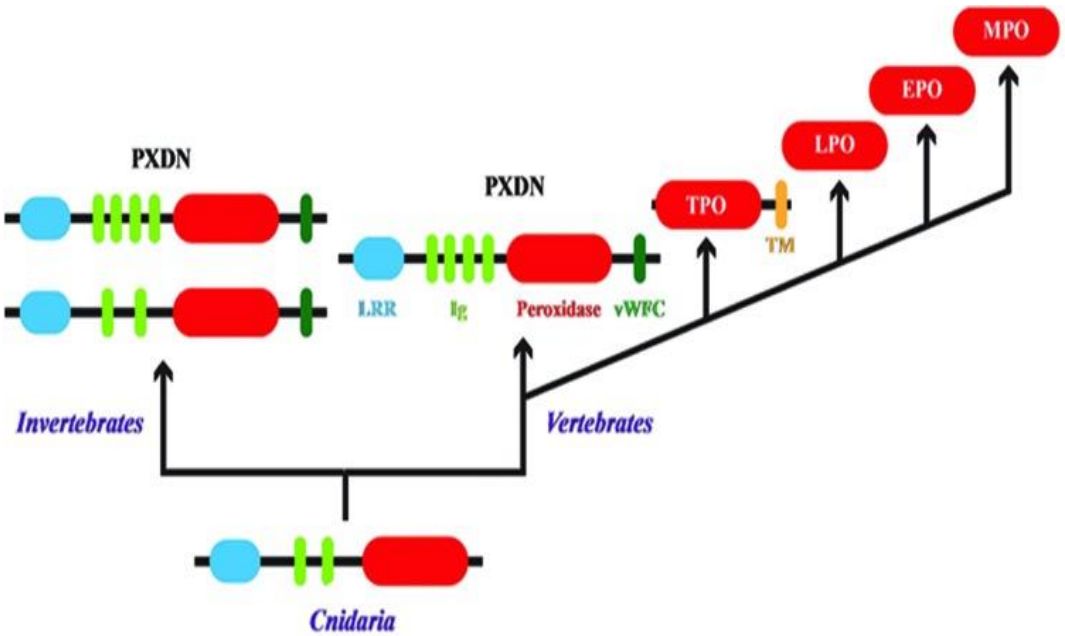

Figure 1.2: A diagrammatic representation of the evolution of PXDN originally in Cnidaria then to invertebrates to vertebrates through a series of gene duplication, loss of non-catalytic domain and loss of TM domain to give rise to EPO, MPO and LPO (Ero-Tolliver et al., 2015).

Through gene duplication, loss of the non-catalytic domains and merging with transmembrane domain, PXDN was observed to have likely given rise to TPO in early Chordates with thyroid hormone signalling which may be associated with endothermy (Little and Seebacher, 2014; Ero-Tolliver et al., 2015). After the loss of the transmembrane domain in TPO, coupled with successive gene duplication, this may have likely given rise to LPO, which is primarily expressed by the glandular epithelium; MPO, which appears in vertebrates for the development of neutrophils and EPO, which appears in eosinophils (Zámocký et al., 2008). The human genome location of TPO and PXDN on chromosome 2 adjacent to one another, and MPO, LPO and EPO forming a cluster on chromosome 17, reflects the evolutionary ontogeny of animal haem peroxidases (Ero-Tolliver et al., 2015).

Much of the activity of this family of enzymes is used in antimicrobial defense. The antimicrobial toolbox of neutrophils comprises MPO as one of its key components, which enables neutrophils in both adaptive and innate immunity to serves as effector cells (Nauseef and Borregaard, 2014). MPO which is expressed by activated neutrophils, is released at sites of tissue injury to phagolysosomes containing engulfed pathogens. This is achieved by infiltrating inflammatory cells to provide defence against invading pathogenic microbes via assembly of nicotinamide adenine dinucleotide phosphate (NADPH) oxidases (NOX) membrane which produces superoxide that dismutase H_2O_2 to provide a substrate for production of hypochlorous acid (HOCl). MPO may also be secreted extracellularly in the normal degranulation process, packaged within neutrophil extracellular traps, or released after neutrophil cell death (Van der Veen et al., 2009; Davies, 2011). Lower concentrations of MPO are also secreted by macrophages and monocytes which are required for host defense (McMillen et al., 2005).

LPO is released from mucosal glands and found in secretions like saliva, milk or tears where it exhibits antimicrobial activity due to the ability to catalyse oxidative reactions with H_2O_2 as a substrate and a halide ion such as SCN^- in the above-mentioned tissues (Kussendrager and Hooijdonk, 2000; Köksal et al., 2016).

EPO is also part of the antimicrobial arsenal, which is secreted by eosinophils tasked to destroy viral and bacterial infections as well as parasitic-worms or helminths. Granules containing EPO are secreted towards the target rather than phagocytise their target pathogens since parasites are bigger in size and this is a primary function unique to EPO (Furtmüller et al., 2006; Davies et al., 2008).

TPO is expressed in the thyroid gland and aids with the synthesis of thyroid hormone via initiation of the biosynthetic pathway for thyroxine, which involves the detection of low concentrations in millimolar range and leading to iodide oxidation to modify thyroglobulin (Taurog et al., 1996; Ruf and Carayon, 2006; Le et al., 2015). More recently this class of peroxidases have been discovered to also regulate the development of the ECM (DeNichilo et al., 2015), initiation of angiogenesis (Panagopoulos et al., 2015) and are therefore involved in tissue regeneration (Péterfi and Geiszt, 2014; DeNichilo et al., 2015). The addition of PXDN to this family has helped to clarify the role of peroxidases in this context.

1.3 Peroxidasin Expression

1.3.1 PXDN in the cardiovascular system

PXDN was originally found to be highly expressed in the vasculature, including cardiomyocytes, and due to this distribution, the protein was termed VPO1 (Cheng et al., 2008; Zhang et al., 2012; Ma et al., 2013). Cardiovascular cells express PXDN and secrete the protein into the blood stream (Cheng et al., 2011). The normal physiological functions of PXDN circulating in plasma are largely unknown. In general, oxidative reactions involve catalysis of H_2O_2 as a substrate to produce HOCl, with the dissociation of H_2O_2 which generates water (Battistuzzi et al., 2010). PXDN contains essential features that are not found in MPO and might aid in its ability to confine to exact vascular sites where it performs biological functions such as ECM modification (Cheng et al., 2011). Whether animal peroxidases assist in cross linking of dityrosine molecules during the development of the ECM in the vascular tissue is largely unknown, while the data presented by Cheng et al., (2011) make evident the capability of PXDN to promote such modifications, which was

further confirmed by Bathish et al., (2020) who showed that PXDN mediates bromination of tyrosine residues in ECM. Dityrosine cross links result when tyrosine molecules are oxidised therefore producing tyrosine radicals which when joined together form dityrosine (Cheng et al., 2011).

1.3.2 PXDN in the eye

PXDN is believed to contribute in providing support of the lens and cornea framework during their construction in the early stages of eye development (Khan et al., 2011; Choi et al., 2015). *In-situ* hybridisation found that PXDN is expressed in the eye forming region and in particular the lens of *Xenopus tropicalis* (Tindall et al., 2005). In mice, expression was observed in the lens and retina and during development of eye of the mouse, PXDN expression was detected from embryonic age (E11.5) onwards which is equivalent to 33 days in human embryology, and furthermore PXDN knock-out animals showed absence of collagen IV crosslinking (Homma et al., 2009; Lázár et al., 2015). As such, PXDN is understood to be essential for normal growth of eye structures such as the lens epithelium and cornea via collagen IV crosslinking, which promotes consolidation of ocular BM (Yan et al., 2014).

Evidence for a role of PXDN in human eye development has been found in pathology context with various genetic variants in *PXDN* being direct cause of various disorders affecting eye development; currently there are only three papers (Khan et al., 2011; Choi et al., 2015; Michel et al., 2016). Aberrant PXDN expression causes loss of structural integrity of the lens capsule and lens molecules such as g-crystallin seem to be extruded into the anterior and posterior chamber of the eye (Yan et al., 2014). These results presented by Yan et al. (2014) confirmed that indeed PXDN plays a pivotal role in consolidation of the BM and that PXDN is required for normal BM integrity along with adhesion of cells during embryonic eye development in higher organisms. Studies that have investigated *PXDN* gene mutations in association with ocular phenotypes in humans are discussed further in **section 1.6.5**.

1.4 Physiological Functions of Peroxidasin

1.4.1 Extracellular Matrix Formation in Basement Membrane

The extracellular matrix (ECM) is a non- cellular, organised network of proteins that provides a structural framework for cells. This framework provides for both chemical and mechanical signals between cells. Surface cell receptors such as integrins detect these signals and relay them intracellularly (Hynes, 2009). This relationship between the ECM and cells enables the ECM to modify behaviour of cells and for cells to modify their surrounding ECM (Hynes, 2009; Bonnans et al., 2014). Biological processes such as tissue development, response to injury and maintenance are critically dependent on the interaction of cells with the ECM (Rosario and DeSimone, 2010; Clause and Baker, 2013). ECM composition varies in specific tissues and the composition changes during and after development and upon tissue injury (Frantz et al., 2010; Rosario and DeSimone, 2010).

The ECM is divided into two subtypes namely, basement membrane (BM) and interstitial matrix (Frantz et al., 2010; Bonnans et al., 2014). The BM and interstitial matrix form separate but adjacent structures *in vivo* (Laurila and Leivo, 1993). The structural support and protection against compression is provided by the interstitial matrix, which surrounds mesenchymal cells (Yurchenco, 2011). The BM is a specialised sheet- like network arrangement of the ECM (Koshnoodi et al., 2008) and it underlies cells of the muscle, epithelial and endothelial tissues, and separates them from underlying stroma (**Figure 1.3**) (Yurchenco, 2011). The proliferation, differentiation, migration and polarity of primary cells in almost all tissues is regulated by the BM (Yurchenco, 2011). Consequently, the BM is essential for the maintenance and development of tissues and plays a critical role in normal physiology and pathogenesis of disease.

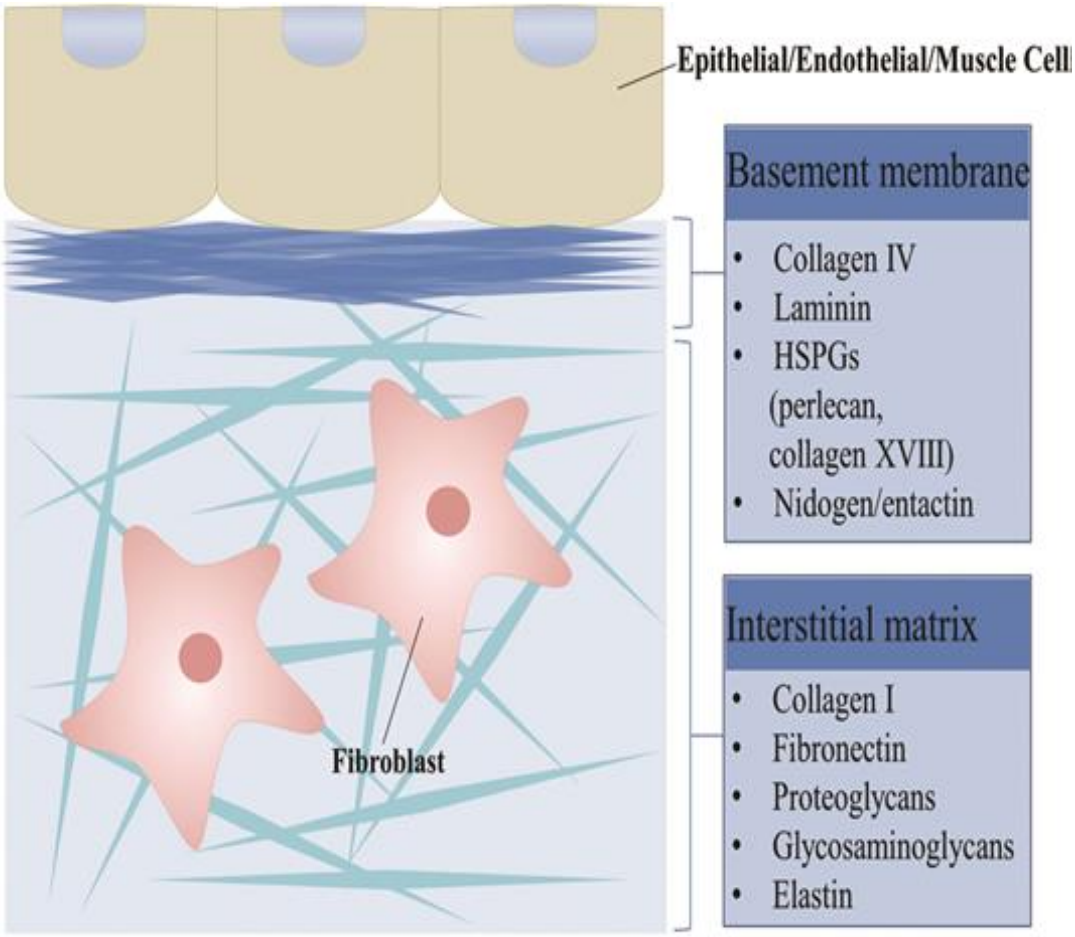

Figure 1.3: **Two subtypes of ECM. The diagram depicts two main types of ECM.** The BM underlies cells of various tissues and comprises collagen IV, nidogen, laminin, collagen XVIII and perlecan. The interstitial matrix which consists of elastin, proteoglycans, collagen I and glycosaminoglycans, surrounds cells (Colon et al., 2017).

The core BM proteins are collagen IV, laminins, proteoglycans, and nidogens (Yurchenco, 2011). Recently, PXDN has been found to be responsible for consolidating collagen IV (Bhave et al., 2012). Specifically, PXDN generates hypohalous acids to cross- link collagen IV protomers (**Figure 1.4**) (Cheng et al., 2011; Ma et al., 2013), which are key to BM formation and maintaining the integrity of tissues during formation and development (Bhave et al., 2012; Péterfi and Geiszt, 2014; Ero-Tolliver et al., 2015). The mechanism of how PXDN cross-links collagen IV promoters is discussed in detail in the section below.

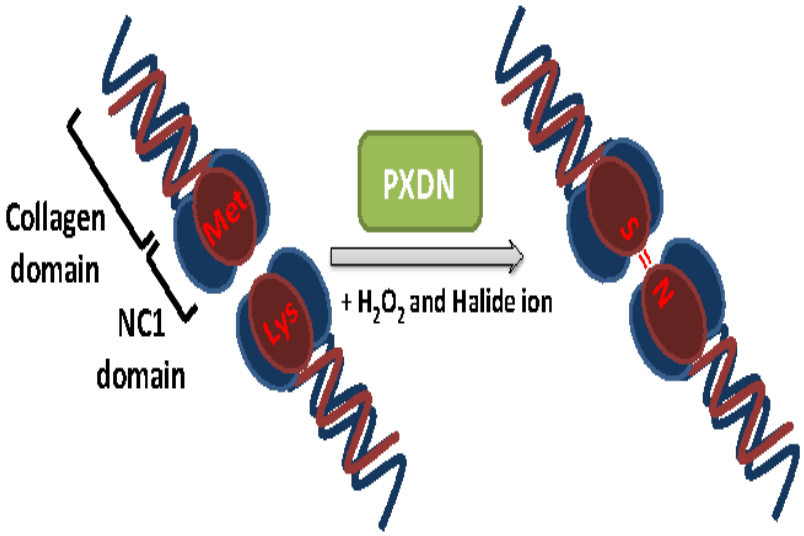

Figure 1.4: Crosslinking of collagen IV is mediated by PXDN which utilises H_2O_2 and a halide ion to produce a sulfilimine (S = N) bond (Modified from Péterfi and Geiszt, 2014).

1.4.2 Collagen IV and Reaction Mechanism of PXDN

The most predominant proteins in animals making up approximately 30% of total protein are collagens. Collagens are mainly characterised by the presence of a triple helical structure, a collagenous domain, and an amino acid repeat structure in which glycine residues occur every third residue (Shoulders and Raines, 2009; Ricard-Blum, 2011). Collagen IV is the predominant collagen found in BM and is comprised of six alpha chains that form heterotrimeric triple helical molecules. There are three distinct domains on each alpha chain, namely a C- terminal non- collagenous domain (NC1), a triple helical collagenous domain and an N- terminal 7S domain (Söder and Pöschl, 2004). Collagen IV also contains protomers, which exist in mammals only [α1α1α2 (α112), α3α4α5 (α345) and α5α5α6 (α556)], which further assemble into three major networks (α112:α112, α112:α556, α345:α345) (Borza et al., 2001). In nearly all mammalian tissues the α112 network is the most predominant (Koshnoodi et al., 2008; Yurchenco, 2011). Conversely, the α345 and α1256 networks have restricted tissue localization, for example, the α345 network is restricted to the glomerular BM (GBM) of kidney, the lens epithelial BM, cochlear BM, and in small quantities in lung alveolar and testicular BM (Gunwar et al., 1991; Kahsai et al., 1997; Kalluri et al., 1998, Abrahamson et al., 2009; Saito et al., 2011).

In order to form the BM, the collagen protomers self- oligomerise to form three sheet- like networks (Koshnoodi et al., 2008). Oligomerisation enables the networks to assemble and these are further stabilised by sulfilimine chemical bonds (S = N). To date, the sulfilimine bond is considered to be exclusive to collagen IV molecules in living organisms (Vanacore et al., 2009). Methionine at position 93 (Met93) and hydroxylysine at position 211 (Hyl211) are joined covalently and stabilise the edges of adjacent NC1 in the protomers of collagen IV (Risteli et al., 1980; Bhave et al., 2012; Ronsein et al., 2014; Anazco et al., 2016). The formation of these crosslinks in collagen IV has recently been assigned to PXDN (Bhave et al., 2012).

PXDN catalyses the crosslinking of collagen IV using hypohalous acids. Firstly, hypohalous acids (hypoiodous acid (HOI), hypobromous acid (HOBr), hypochlorous acid (HOCl), and hypothiocyanous acid (HOSCN)) are produced by haem peroxidases in the presence of H_2O_2, in this case PXDN, via oxidation of halide ions such as bromide (Br^-), thiocyanate (SCN^-) and chloride (Cl^-) (**Figure 1.5**) (Ronsein et al., 2007; Bhave et al., 2012; Colon et al., 2017). The halide from the hypochlorous acid is donated to the sulfur atom from methionine producing a halosulfonium cation that in turn links with the lysine amino group of the subsequent collagen IV (; Vanacore et al., 2009; Bhave et al., 2012; Ronsein et al., 2014). The source of extracellular H_2O_2 is currently unknown, but NOX, which are membrane proteins have been suggested to be the source of H_2O_2 in bronchial epithelial cells (Geiszt et al., 2003). NOX consist of NOX (1 to 5) and dual oxidase (DUOX) 1 to 2: NOX1, NOX2, NOX3 and NOX5 have the ability to reduce extracellular oxygen (O_2) to superoxide (O_2^-) and NOX4, DUOX1 and DUOX2 to hydrogen peroxide, while oxidizing NADPH intracellularly (Lamberth and Neish, 2014). Superoxide, spontaneously or via superoxide dismutase, forms the hydrogen peroxide required for the reaction (Fukai and Ushio-Fukai, 2011). The role of PXDN in collagen IV and BM consolidation is still undergoing investigation with a recent study by Sirokmány et al. (2018), finding that PXDN catalysed collagen IV synthesis may be independent of H_2O_2 generated by the NOX/DUOX system. This was done by testing crosslinks of collagen IV in mouse models deficient of the NOX/DUOX isoforms, and the results were in support of the view that other ECM proteins might act as the source of H_2O_2 (Sirokmány et al., 2018). Lévigne et al. (2016) also showed that mice

with wounds and deficient in NOX4 healed significantly slower as compared to mice with wounds and active NOX4, this was thought to be because of insufficient dityrosine cross-links in the ECM (Lévigne et al., 2016).

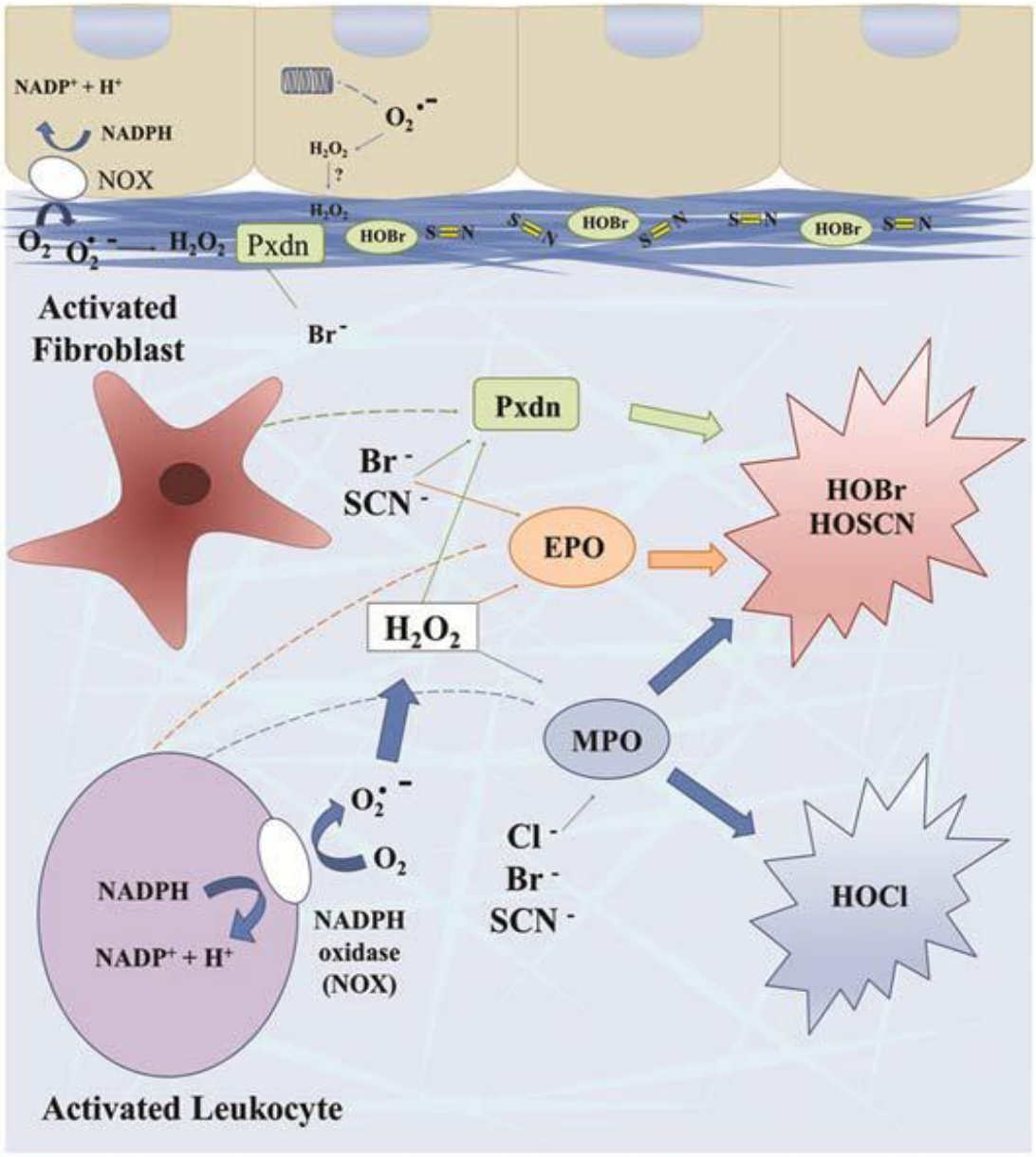

Figure 1.5: PXDN catalysis of HOBr to produce sulfilimine (S=N) cross- links in collagen IV. PXDN is secreted into the ECM by activated fibroblasts, while activated infiltrating leukocytes release MPO and EPO. The NADPH oxidases generate superoxide ($O_2^{\cdot -}$), which dismutates into H_2O_2, and along with Br^- and Cl^- halides or SCN- anions, lead to the generation of hypohalous acids by PXDN during sulfilimine bond formation in the BM (Colon et al., 2017).

1.4.3 Role in Host Immune Defence

Phagocytes such as the neutrophils which have the ability to move from blood into various organs, provide the key mechanism for upkeep of a sterile environment in tissues by employing both oxidative and non-oxidative mechanisms to kill invading microbial agents (Rada and Leto, 2008). The primary mechanism usually involves the NADPH oxidase system by using NOX2 (Rada and Leto, 2008). For example, MPO, by combining H_2O_2 and Cl^-, synthesises HOCl; this reaction was previously thought to be exclusive to MPO and EPO but is now also attributed to PXDN (Klebanoff et al., 2005; Li et al., 2012). LPO, MPO and EPO also predominantly mediate host defence functions but are restricted to specific cell types, for instance in the body fluids saliva and breast milk this is performed by LPO and in phagocytic cells this is carried out by MPO and EPO (Klebanoff et al., 2005). MPO is usually retained inside phagocytes, and PXDN is secreted into plasma by vascular endothelial cells (Cheng et al., 2011), where it is understood to demonstrate a role in host defence (Li et al., 2012). It was initially thought that since PXDN lacks a methionine (Met) at position 981 (corresponding to position Met409 in MPO), it was thought to render the catalysis of HOCl by PXDN impossible, since PXDN has glutamine (Gln981) at that position (Li et al., 2012). The methionine at position 409 is a distinctive feature of MPO that has been suggested to be a main factor of its unique capability to produce HOCl (Klebanoff et al., 2005). However, Li et al. (2012), showed that PXDN like MPO, can synthesise HOCl and further hypothesised that PXDN may be localised at infected and injured tissues. HOCl is a very potent microbicidal agent that can kill microorganisms, for example, the incubation of *Escherichia coli* (*E. coli*) bacteria with PXDN supplemented with H_2O_2 and Cl^- halide completely killed the *E. coli* via HOCl synthesis (Cheng et al., 2011; Li et al., 2012). As such, the findings by Li et al. (2012) propose that methionine at position 409 of MPO is not compulsory but its presence can augment the synthesis of HOCl by peroxidases.

1.5 Peroxidasin in Pathophysiological conditions

PXDN with its various functions has been implicated in various diseases, most notably those affecting the cardiovascular system (Cheng et al., 2008; Zhang et al., 2012; Ma et al., 2013), cancer (Desmond et al., 2007; Tauber et al., 2010; Liu et al., 2010; Jayachandran et al., 2016; Sitole and Mavri-Damelin, 2018), fibrosis (Peterfi et al 2009), and the eye (Khan et al., 2011, Choi et al., 2015; Micheal et al., 2016).

1.5.1 Cardiovascular Disorders

Oxidative stress refers to an imbalance between free radicals and antioxidants resulting from oxidation within cells, tissues or organs and is caused by increased reactive oxygen species (ROS) (Lu et al., 2011). This can cause pathophysiological conditions such as atherosclerosis (Lu et al., 2011), heart failure and heart attack (Strobel et al., 2011). PXDN expression may be altered under conditions of oxidative stress and may therefore have a role to play in these conditions (Ma et al., 2013). The HOCl derived from reactions catalysed by PXDN has been implicated in injury of the cardiovascular system since it is a stronger oxidant than to H_2O_2 and O_2^- (Goud et al., 2008). HOCl has been found to induce direct oxidative damage to lipids, deoxyribonucleic acid (DNA) and proteins (Kang and Neidigh, 2008) which can lead to apoptosis. Oxidation of lipids by HOCl has been suggested as a possible cause of atherosclerosis, since it produces chlorinated products which may form plaques (Ford, 2010; Yang et al., 2013). PXDN generated HOCl has been found to also activate apoptosis in cardiac and endothelial cells (Bai et al., 2011). Bai et al. (2011) hypothesised that the activation of apoptosis in endothelial cells might be induced by oxidised low-density lipoproteins (ox-LDL), which is the key constituent of serum lipids and is a critical risk factor for atherosclerosis and endothelial dysfunction (Kita et al., 2001). Ox-LDL further upregulates the expression of NADPH oxidase, which results in elevated ROS, PXDN and HOCl, thereby forming a positive loop between PXDN (which forms HOCl) and NADPH oxidase (to form ROS). HOCl production was inhibited when PXDN was silenced. This loop is thought to activate the p38 MAPK/caspace-3-dependent signaling pathway, which in turn induces ox-LDL endothelial cell apoptosis (Bai et al., 2011).

Other studies using rat model/tissue also provided evidence showing that PXDN mediates oxidative stress causing oxidative injury (Shi et al., 2011; Zhang et al., 2012; Li et al., 2012). In a rat model of myocardial ischemia reperfusion (IR) injury, it was found that PXDN expression was up regulated and was accompanied by oxidative injury. When NOX activity was inhibited, PXDN expression was suppressed thereby attenuating the IR injury. Shi et al. (2011) found that arterial tissue of spontaneously hypertensive rats had elevated PXDN, which was accompanied by vascular remodelling. In a case-control study by Zhuan et al. (2017) patients diagnosed with chronic obstructive pulmonary disease (COPD) combined with Pulmonary hypertension (PH) had significantly high levels of plasma PXDN, NADPH oxidase, ROS activity and NF-κB as compared to the controls, thus suggesting that PXDN and the NADPH oxidase/ROS/NF-κB pathway may be actively involved in the pathogenesis of COPD combined with PH via the resulting oxidative stress (Zhuan et al., 2017).

1.5.2 Cancer

PXDN displays irregular expression patterns in different cancers affecting different tissues such as melanoma, colon, breast, ovarian cancers along with metastatic gliomas as well as renal carcinoma, (Mitchell, 2000; Desmond et al., 2007; Tauber et al., 2010; Liu et al., 2010; Jayachandran et al., 2016; Sitole and Mavri-Damelin, 2018; Paumann-Page et al., 2021;). The precise function of PXDN in cancer remains unclear but has been associated with changes to cell attachment, migration and invasion of cancer cells. Two studies characterised PXDN as being involved in melanoma development (Paumann-Page et al., 2021), but one did not study the normal physiological function of PXDN (Mitchel et al., 2000). In another study by Tauber et al. (2010), gene expression profiling technique was employed with an aim to pinpoint a group of genes associated with haem oxygenase 1 (HO-1) in 14 different types of cancer. PXDN was found to be a key player in adhesion of neoplastic cells, which are dependent on HO-1, and PXDN silencing stopped the increase in adhesion in response to HO-1 in various cell lines, whilst cells deficient of HO-1 and reduced PXDN expression did not affect cell adhesion.

Madden et al. (2004) previously showed a 17-fold increase in PXDN expression in glioma endothelial cells as compared to non-neoplastic endothelial brain cells. Subsequently, PXDN was found to be selectively upregulated in a set of endothelial marker genes in the microvasculature of metastatic brain tumours glioblastoma and pilocytic astrocytomas, while it was absent or detected at low quantity in the controls (non-neoplastic temporal lobe) specimens (Liu et al., 2010). PXDN protein was localised in microvascular endothelial cells, which was also reported by Castronovo et al. (2006) when it was found that PXDN localised in vascular structures in kidney cancer, thus it was hypothesised that PXDN may be playing a role in tumour angiogenesis in various cancers. One other major feature of cancer is the ability of cells to undergo epithelial-to-mesenchymal transition (EMT), a process that enables cancer cells to typically acquire invasive ability (Kalluri and Weinberg, 2009). As a result of EMT, immobile cells of the epithelial phenotype attain a mesenchymal phenotype as well as the capability to invade and migrate during tumour metastasis and developmental morphogenesis (Nieto, 2013; Lamouille et al., 2014). Jayachandran et al. (2016) investigated genes that regulate cellular invasion with the aim of inhibiting their effect in melanoma invasion. In mesenchymal like melanoma cells PXDN was found to be upregulated and silencing of PXDN reduced melanoma invasion *in vitro*. As to how PXDN exerts its effect in the development of cancer is not known and the studies discussed above shows that the role of PXDN may differ per cancer type. Studies in our laboratory have found that Snai1 which is a key player in EMT modification regulates PXDN in cervical carcinoma cell lines (Sitole and Mavri-Damelin, 2018).

1.5.3 Kidney Disorders

Almost every organ can undergo fibrosis and it is predominantly observed in diseases affecting the liver, heart, kidney and lung tissues (Wynn, 2007). It has been observed that PXDN is also expressed in dermal fibroblasts (Peterfi et al., 2009). Elevated expression of PXDN was found in myofibroblasts that were undergoing differentiation induced by TFG-β1. The fibrillar like structure forming the ECM was formed by PXDN secreted from myofibroblasts (Peterfi et al., 2009). In a normal healthy kidney PXDN was undetectable, while in a mouse model with kidney

fibrosis PXDN expression was found to be elevated and the expression paralleled fibrotic kidney remodelling (Peterfi et al., 2009).

Goodpasture (GP) is an autoimmune disease which affect the kidneys when circulating autoantibodies bind to regions within the NC1 of collagen IV which is required for BM synthesis under normal physiological functions (Pedchenko et al., 2010). The formation of sulfilimine bonds which crosslinks collagen IV molecules in glomerular basement membrane (GBM) confers protection against GP given that the binding of circulating autoantibodies to NC1 domain of collagen IV prevents normal formation of GBM (Pedchenko et al., 2010). A study by McCall et al., 2018 showed that approximately 46% of patients diagnosed with GP disease show reduced HOBr syntheses due to autoantibodies against PXDN. Alteration of collagen IV crosslinking has been proposed as key pathogenic mechanism for GP via anti-PXDN autoantibodies, and this was based on in vitro data that showed autoantibodies had the ability to inhibit HOBr syntheses (McCall et al., 2018). The resulting reduced crosslinking of collagen IV in GBM is vital for the pathogenesis of GP disease (McCall et al., 2018). PXDN has also been discovered to be a novel target of autoantibodies for Lupus nephritis (Manral et al., 2019).

1.5.4 Eye Disorders

Various mutations in *PXDN* have been found to be present in patients diagnosed with developmental eye disorders, specifically anterior segment dysgenesis (ASD), lending support to the significance of PXDN in eye development (Khan et al., 2011; Choi et al., 2015). Whilst the precise functions of PXDN in the eye are as yet unknown, PXDN is understood to be involved in supporting the cornea as well as lens framework during development of the eye as well as acting as an antioxidant enzyme to protect various eye structures from oxidative damage (Khan et al., 2011; Yan et al., 2014; Choi et al., 2015). The protein seems to be involved in number of pathways, yet the exact route through which it exerts its function is not well understood especially with regards to development of the eye. Support from an animal model showed that a mutant *KTA048* mouse model Yan et al. (2014), displayed similar phenotypes observed in individuals harbouring mutations in PXDN. The mutant mouse model was induced via N-ethyl-N-nitrosourea of which

upon sequencing revealed a recessive mutation (c.T3816A) causing a premature stop codon in the peroxidase domain, which resulted in development of ASD as well as microphthalmia (Yan et al., 2014). No precise mechanisms are known currently as to how mutations discovered in *PXDN* cause ASD disorders, which include glaucoma, abnormal lens and cornea development. Few possible mechanisms have been suggested: (1) the lack of PXDN protein in the cornea as well as in the epithelial layers of the lens causes accumulation of ROS that generally oxidise lipids also proteins, producing aggregates that are insoluble leading to cataractogenesis and corneal clouding and (2) the accumulation of ROS in the aqueous humour can affect the differentiation also development of the structures found in the anterior segment which is involved in the development of glaucoma (Izzotti et al., 2006, Khan et al., 2011). For instance, aqueous humour of glaucoma patients contains elevated enzymes induced by oxidative stress and reduced antioxidants which promotes oxidative stress (Ferreira et al., 2004) and the trabecular meshwork is very sensitive to damage by oxidation (Khan et al., 2011). The specific mutations detected in PXDN are discussed in **section 1.6.5** that follows along with other genes that may interact with PXDN to bring about various ocular phenotypes.

The primary focus of this study is to understand the regulation of PXDN in eye development. Formation of the human eye is discussed in detail in the sections that follow to create a link between successful eye development and PXDN requirement.

1.6 Anatomy of the human eye

1.6.1 The anterior segment of the eye

The human eye is a unique and complex part of the human body which is broadly divided into two segments (**Figure 1.6**) namely the anterior and posterior segments (Addo et al., 2016). The anterior chamber and posterior chamber are filled with aqueous humour which provides nutrients to tissues in the anterior segment of the eye. The anterior segment of the eye comprises of trabecular meshwork, cornea, lens, iris, ciliary body and Schlemm's canal while the retina and optic nerve form the posterior segment of the eye (Ito and Walter, 2014). In order for the eye to form a

clear image, different structures within the eye contribute to the process. The cornea as a curved membrane which encompasses the front section of the eye allows light to pass through which leads to the light rays bending and focusing as they pass through the iris on the way to the lens. The dilator muscles and pupillary sphincter generate a synchronised action that helps the pupil to constrict and dilate in order to regulate the amount of incoming light. The lens with the aid of ciliary muscles focuses the light which will travel through the vitreous humour then straight to the retina (Kaplan, 2007).

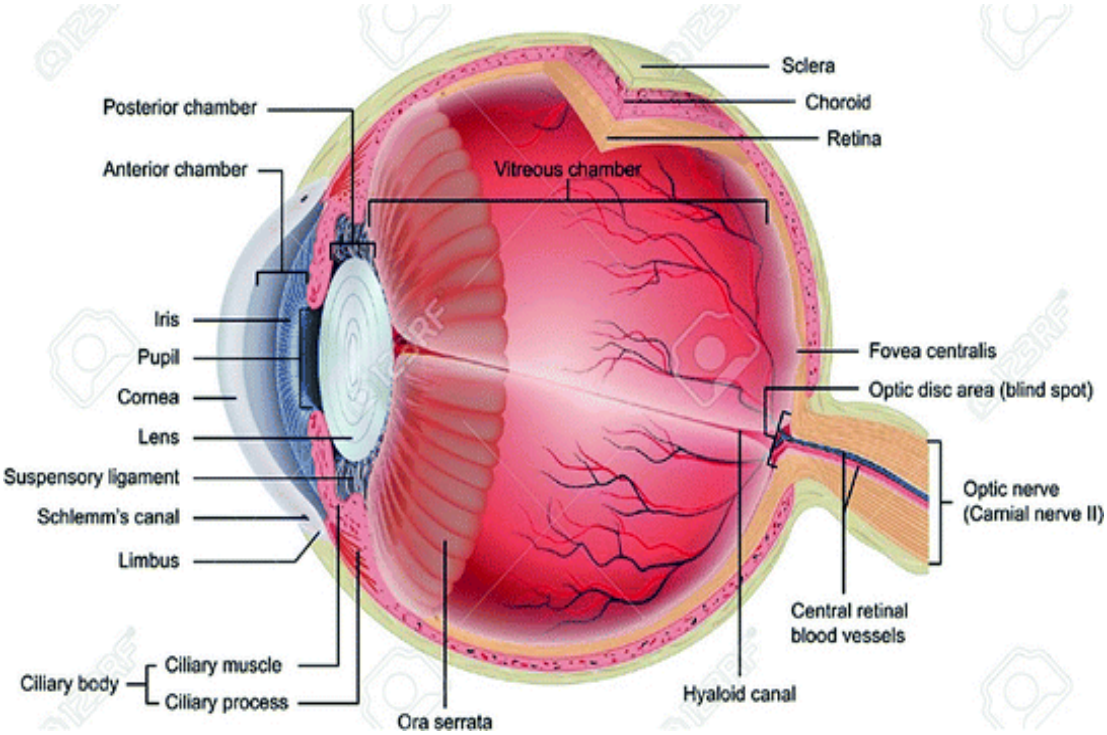

Figure 1.6: Anatomical structure of a fully developed human eye. In this study only the disorders affecting the anterior segment structures such as iris, cornea, lens, ciliary body and Schlemm's canal were discussed (Addo et al., 2016).

In humans, the eye starts developing within 21 days of gestation through a highly organised process, which is tightly regulated by various transcription factors and multiple cell signalling pathways which can lead to development of various eye disorders if perturbed (Dash et al., 2016; Budak et al., 2018).

1.6.2 Anterior segment morphogenesis

Starting from the sixth week of human development, morphogenesis of various eye structures is initiated, such as the embryonic optic cup (bi-layered) from neuroectoderm of the forebrain and the lens vesicle is invaginated thus separating from the ectoderm (Cvekl and Tamm, 2004; Sowden, 2007). **Figure 1.7a** show a rudimentary diagram of the eye which is surrounded by progenitor cells (mesenchyme) most of which originate from the neural crest migrating anteriorly (Sowden, 2007). Tissue differentiation and morphogenesis driven by the progenitor cells along with those from the surface ectoderm and optic cup peripheral region will give rise to the cornea, iris and drainage structures of the irido-cornea (Cvekl and Tamm, 2004). The normal development of the anterior segment of the eye is dependent on the correct differentiation and specification of the progenitor cells (mesenchymal) in early embryogenesis (Gage et al., 2005). **Figure 1.7b** shows that the cornea is formed first from the primitive endothelium, then the trabecular meshwork which is situated posterior to the surface ectoderm (Sowden, 2007).

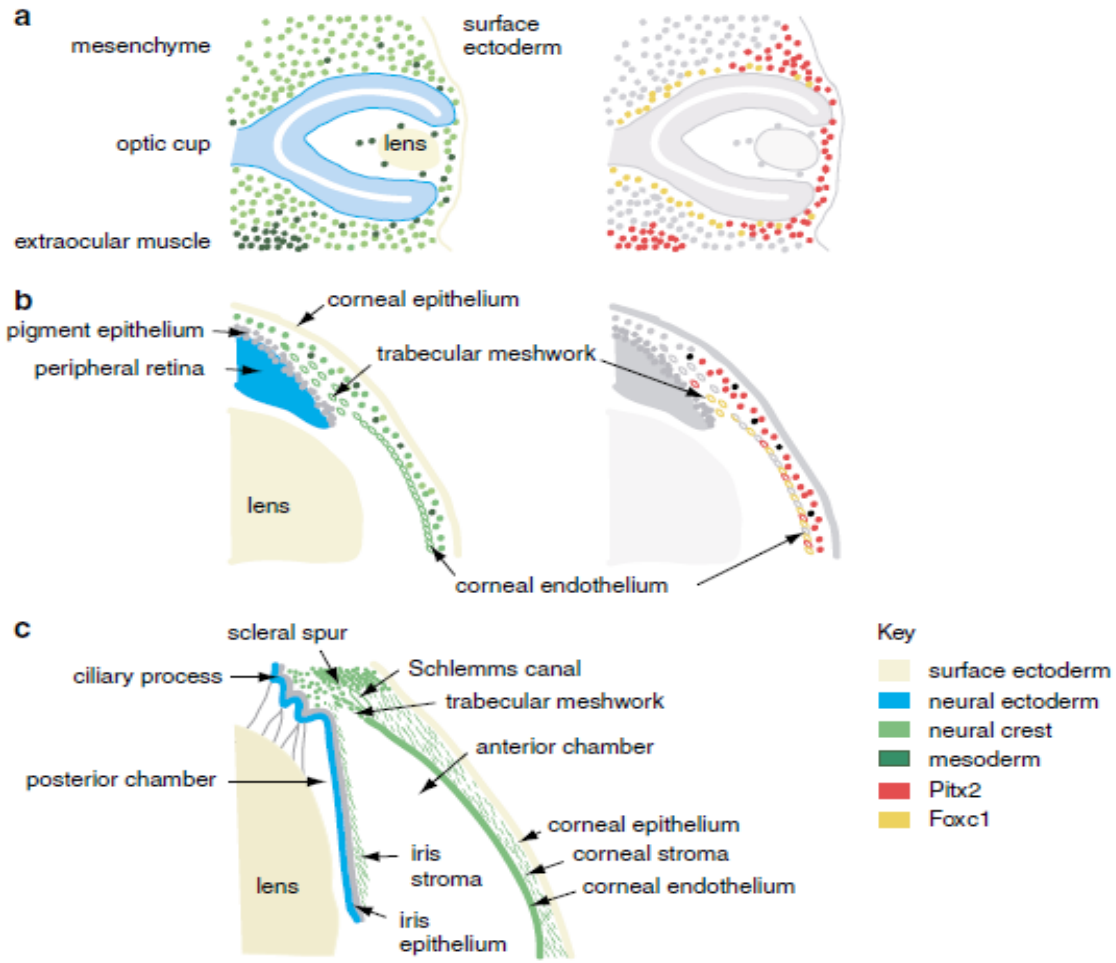

Figure 1.7.: **Anterior segment development of the human (foetal) eye.** (a) 5th week of embryogenesis, the optic cup stage (b) 5th month of development, formation of the anterior chamber (c) fully developed anterior segment showing all structures including the iris, lens, cornea. Key colours indicate two important genes expressed during anterior segment development and origin of cells that form the anterior segment tissues (Sowden, 2007).

Collagen, which is usually in a lamellar arrangement, is synthesised when the corneal (epithelium and endothelium) cells form corneal stroma (Beebe and Coats, 2000). In the 5th month of gestation, the cornea, iris and the anterior chamber will be well developed. Further development, as well as maturation of the tissues, involves more differentiation where the sclera spur separates the iris root and ciliary body from the trabecular meshwork (Gage et al., 2005; Sowden, 2007). The trabecular meshwork will be situated anterior to the iris root as well as visible to the aqueous humour as shown in **Figure 1.7c** (Sowden, 2007).

1.6.2.1 Optic cup morphogenesis

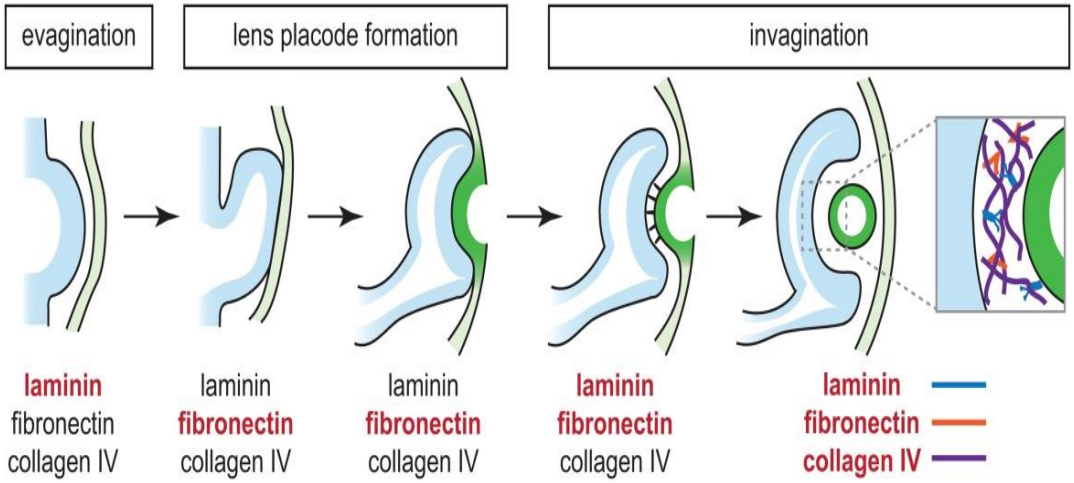

Figure 1.8: Morphogenesis of the optic cup and involvement of the ECM proteins through the stages of evagination, lens placode formation and invagination. The ECM components collagen IV (purple), fibronectin (orange) and laminin (blue) when labelled in red colour it means the component is required for that specific stage and when in grey colour it is not required for that specific stage of eye development (Kwan, 2014).

Optic cup formation initiates establishment of the basic structures of the eye which are derived from various origins of embryonic nature such as mesenchyme, surface ectoderm and neuroectoderm (Graw, 2003). Optic vesicle evagination from either side of the brain neuroepithelium signals the commencement of optic cup development with formation of single eye fields in the anterior neural plate median region (**Figure 1.8**). Adjacent to the surface ectoderm, the single eye field will then move laterally, separate and form the optic vesicle (Yang, 2004). The optic cup is generated by this out-pocketing of tissue which undergoes a series of cell and tissue rearrangements which further leads to formation of retinal pigmented epithelium, neural retina and lens (Chow and Lang, 2001; Fuhrmann, 2010). The ECM components collagen IV, laminin and fibronectin are present from evagination, lens placode formation and invagination stages of eye development with laminin and fibronectin required in the first early stages and all three required for the last stages including collagen IV (**Figure 1.8**) (Kwan, 2014).

1.6.2.2 Lens morphogenesis

At day 33 of gestation post optic cup formation, formation of the lens placode will be the next step during human eye development (Graw, 2003). A region of contact with the overlying ectoderm is established with the developing optic vesicle following evagination, lens placode development will begin. The ECM is found in abundance in the region between lens placode and prospective retina separating the tissues (Kwan, 2014). The lens will be formed by the mesenchymal cells as they also differentiate to form melanocytes and fibroblasts of the iris stroma (Gage et al., 2005). The iris epithelium is formed when cells within the two layers of peripheral optic cup spread inwardly after proliferation amid the iris stroma as well as the lens (Beebe and Coats, 2000). The lens placode composed of lens progenitor cells will invaginate to form the lens cup which will close up and form the lens vesicle by separating from the surface ectoderm. The lens vesicle and surface ectoderm will be connected by a temporary link from a lens stalk which will be retracted later on with the surface ectoderm giving rise to epithelium (**Figure 1.7b**) that will form the cornea at later stage (Graw, 2003; Snowden, 2007).

A spherical shape with an empty cavity is representative of a lens vesicle, with the cuboidal lens epithelium formed from the anterior cells while elongation of the posterior epithelial cells via filling of the lumen will give rise to primary lens fibre cells which will in turn form embryonic nucleus (Graw, 2010). This process is initiated at the 44^{th} day of human eye development, with much of the lens formation driven by the posterior epithelial cells in the first two months of lens formation. The secondary lens fibre cells are formed from the actively dividing anterior progenitor cells through migration from the central to the equatorial region, proliferation and differentiation which will be displaced inwards flanked by embryonic nucleus and the capsule (Cvekl and Ashery-Padan 2014). As humans continue to grow, the epithelial cells (anterior) mitotically continue to divide to form secondary lens fibre cells and only stop when they are displaced into the inner layer since by then they will be mature and start losing their differentiation ability as well as their organelles (Graw, 2010). Lens fibres at the periphery are therefore newly formed young cells,

as the lens fibres are successively displaced to the inner cortex (Cvekl and Ashery-Padan 2014).

1.6.2.3 Cornea morphogenesis

The epithelium (anterior and posterior) forms the components of the cornea along with the corneal stroma in between them. The optic vesicle along with lens vesicle induce the formation of the cornea via the continued proliferation of the surface ectoderm to form the corneal epithelium even after the lens vesicle has completely separated from the surface ectoderm. The corneal stroma formation results from production of glycosaminoglycans and collagen fibres by corneal epithelium in the basal lamina (Graw, 2010).

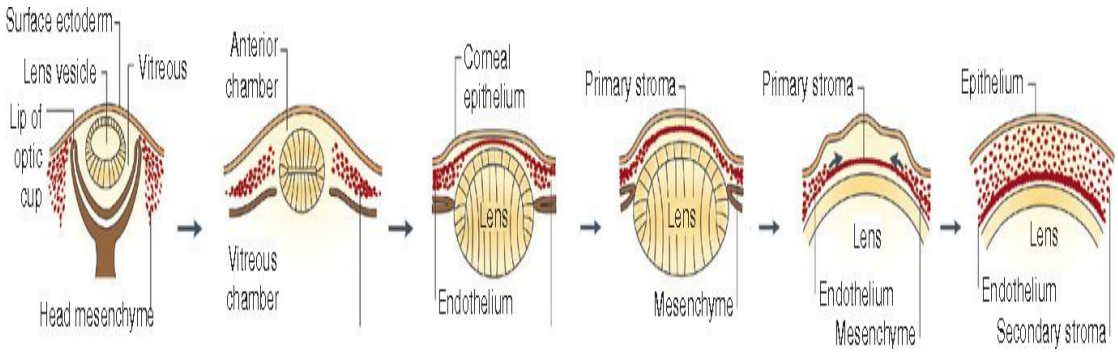

Figure 1.9: Diagram illustration of development of the cornea during embryogenesis (Graw, 2010).

The space between the lens vesicle and surface ectoderm will be filled by mesenchymal cells of the neural crest origin in three waves (**Figure 1.9**) (Graw, 2010). The first wave gives rise to corneal endothelium, while the second wave of cells condense and contribute to various corneal structures and the third wave form keratocytes in the stroma via migration between epithelium and endothelium (Cvekl and Tamm 2004). The secondary corneal stroma is formed from the organisation of type 1 collagen and proteoglycans (synthesised by keratocytes) as lamellae while the basal membrane derives the formation of Descemet's membrane (Cvekl and Tamm 2004).

1.6.2.4 Iris and Ciliary body morphogenesis

The neuroectoderm which comprises of two layers, the outer pigmented and inner non pigmented epitheliums is formed when the optical cup distal tips proliferate and extend in parallel to the formation of the lens as well as the cornea which leads to formation of iris and ciliary body (Graw, 2010). Anterior to the iris is the iris stroma and the iris muscles, while the posterior layer has the iris pigmented epithelium (**Figure 1.7c**) and the base of the iris is attached to the ciliary body in addition to irido-corneal angle (Davis-Silberman and Ashery-Padan 2008).

The formation of the iris results from derivation of two embryonic origins: Periocular mesenchyme which forms iris stroma and neuroectoderm which forms iris sphincter, dilator muscles as well as the iris pigmented epithelium. Pupillary membrane is formed when the aforementioned second wave of mesenchymal cells condensed, while the two distal tips of the optic cup extend to reach the pupillary membrane fusing to give rise to the iris (Davis-Silberman and Ashery-Padan 2008; Graw 2010).

Myofibrils, which result from differentiating iris pigmented epithelium, form the iris sphincter and dilator muscles; these regulate (in an antagonist manner) the constriction and dilation of the pupil in response to light (Graw, 2003). The iris stroma is composed of melanocytes as well as fibroblast derived from periocular mesenchymal cells. When migrating to the anterior section of the lens while in peripheral part of the pupillary membrane these cells secrete collagen fibrils in ECM which aids in formation of the anterior stroma of the iris. Different melanin quantity in the iris stroma results in various colours of the iris in different individuals (Davis-Silberman and Ashery-Padan 2008).

The proximal non pigmented layers result in the formation of ciliary body when the distal tips of the optic cup neuroectoderm form the iris. The ciliary body muscles are formed from proliferating periocular mesenchyme myofilament, while the stroma of the ciliary body is formed when the periocular mesenchyme condenses at the anterior section of the ciliary body (Graw, 2003). The pupil develops from the degeneration of the pupillary membrane when gestation reaches the 8^{th} month, while the ciliary

body, iris stroma and dilator muscle continue to develop even after birth since they would have been immature after birth (Davis-Silberman and Ashery-Padan 2008).

1.6.2.5 Anterior chamber morphogenesis

During the 3rd month of gestation between the iris epithelium and corneal endothelium a presumptive anterior chamber can be observed (Graw, 2010). Within the anterior chamber the mesenchyme forms the trabecular meshwork while the venous canaliculi form the Schlemm's canal from the small plexus (Sampaolesi et al., 2009). The ciliary body muscle continues to develop even after 7 months of gestation which enables the extension of Schlemm's canal in the direction of the anterior chamber while the anterior chamber angle continues to recede as well as widen in a triangular shape. The anterior chamber continues to further deepen as well as surpasses the spur even after birth and the anterior chamber angle also continues to develop to maturity a year after birth (Sampaolesi et al., 2009).

1.6.3 Regulatory networks involved in the anterior segment of the eye.

The regulatory programmes that control eye development are complex and involves a myriad of both transcriptional and post transcriptional events (Dash et al., 2016; Budak et al., 2018). Master control genes of eye development refers to the genes that drive eye development at the early stages, and most of which code for transcription factors and signalling molecules (Graw, 2010). Transcription factors such as Sry-box 2 (SOX2), sine oculis homeobox homolog 3 (SIX3), retina and anterior neural fold homeobox (RAX), sonic hedgehog (SHH) and Paired box 6 protein (PAX6) are at the top of the hierarchy of master control genes for eye development since they are responsible for the formation of the optic vesicle through patterning and splitting of the single eye field (Graw, 2003). PAX6, Paired-like homeodomain 2 (PITX2) and Forkhead box C1 (FOXC1) are among the key role players in the development of the anterior segment by directing the proper differentiation of ocular mesenchyme (Baulmann et al., 2002; Graw, 2003).

PAX6 like many other transcription factors induces embryonic differentiation along major body axes in response to the concentration gradient of other regulatory

proteins or transcription factors, which bind to DNA sequences of other genes and regulate their expression (Friedman, 1998). PAX6 belongs to the *PAX* multigene family of transcription factors that aid in the regulation of embryonic differentiation (Friedman, 1998). PAX6 is termed a master control gene since mutations in the highly conserved transcription factor interrupts development of the eye in both insects and mammals (Hill et al., 1991; Quiring et al., 1994). The study of the transcription factor PAX6 has improved the understanding of how ocular tissues develop and mis-expression of PAX6 induces ectopic eyes (Zuber et al., 2003; Kenyon et al., 2003; Kozmik, 2005). In vertebrates, this factor is essential for normal development of several organs including the brain, pancreas and the eye (Kenyon et al., 2003). PAX6 as a transcription factor, leads the cascade of eye development pathways and it initiates development of the eye in almost any tissue in which it is ectopically expressed (Ashery-Padan and Gruss, 2001). Lens differentiation and proliferation is dependent on PAX6 expression, while aberrant expression causes disruption of lens formation (Yan et al., 2014). *PAX6* is expressed from the early stages of eye development, on the surface of neuroectoderms, and then expressed in the differentiating cells in the retina, lens, ciliary body and cornea throughout development (Nishina et al., 1999; Chanas et al., 2009). Expression of *PAX6* is very precise within the different tissues, therefore normal eye development requires the correct dosage of PAX6. Reduced expression of *PAX6*, due to mutations, results in clinical phenotypes such as small eye in mice and rats (Kroeber et al., 2010), whereas in humans it induces Aniridia (Yokoi et al., 2016; Lim et al., 2017). Overexpression in mice was found to also cause severe eye phenotypes (Schedl et al., 1996; Chanas et al., 2009). The functional studies conducted on PAX6 and the observed expression pattern which is conserved have implicated this protein in various pathways essential for normal eye development (Ashery-Padan and Gruss, 2001).

The transcription factor SIX3 has been found to be a regulator of PAX6 in the development of the lens (Liu et al., 2006). SIX3 is present during early eye development in the optic stalk, in the presumptive retina and in the lens vesicle and later also in the lens (Oliver et al., 1995). In SIX3 mutant embryos it was found that *PAX6* was downregulated while SOX2 was absent (Liu et al., 2006). PAX6 was

found to be interacting with *SOX2* gene promoter therefore initiating expression of the SOX2 protein (Liu et al., 2006; Lengler et al., 2005), while SIX3 was found to not interact with the *SOX2* gene promoter (Lengler et al., 2005). Meis homeobox 1 (MEIS1) and homeobox 2 (MEIS2) were found to bind upstream of the *PAX6* gene promoter and induce expression in vertebrate lens ectoderm (Zhang et al., 2002). Both MEIS1 and MEIS2 are expressed throughout development in a similar manner like PAX6, but their expression occurs independently of PAX6. In the lens of mice, it was found that MEIS2 overexpression caused increased expression of PAX6 (Zhang et al., 2002).

PITX (Paired-like homeodomain), *MAF* (bZIP transcription factor) and *FOX* (Forkhead box) transcription factor genes act downstream of the master control genes such as *PAX6* in specific regions of the anterior segment of the eye such as the cornea, lens and iris (Graw, 2003). A wide variety of genes are regulated by the FOX class of transcription factors, with FOXC1 and FOXE3 being the most critical transcription factors required for development of the anterior segment of the eye (Graw, 2010).

FOXC1 is composed of a Forkhead domain which enables DNA-binding and has 110 amino acid protein which is highly conserved. The transcription factor has a single exon that codes for 553 amino acid protein and is located on the short arm of chromosome 6 band 25 (6p25). In both various ocular and non-ocular structures FOXC1 protein has been observed to be expressed (Erickson, 2001; Mathew et al., 2002; Walter, 2003; Seo and Kume, 2006). The periocular mesenchyme cells express FOXC1 protein which enables the cells to give rise to anterior segment structures such as trabecular meshwork, iris and cornea (Wang et al., 2001; Sowden, 2007).

PITX2 encodes a 33 kDa protein which comprises of homeodomain with 60 amino acids at the N terminus as well as a 14 amino acid C terminal domain which enables protein to protein interaction (Amendt et al., 2000). The involvement of PITX2 protein in regulation of cellular differentiation in optic nerves, heart, nerves, pituitary, midbrain neurons and anterior segment of the eye indicates the various

roles the protein plays during development (Gage et al., 1999; Martin et al., 2004; Houssaye et al., 2006).

Figure 1.7 shows that during development of anterior segment of the eye both FOXC1 and PITX2 are highly expressed (Sowden, 2007), which is also the case in animal models such as the mouse; in mouse eye development *PITX2* mRNA is expressed in the mesenchyme that surrounds the optic eminence as early as E8.5 in preparation for the formation of the lens vesicle and optic cup (Mucchielli et al., 1997). At the stage of E11.5 after both the optic cup and lens vesicle have developed, the migrating periocular mesenchyme highly expresses PITX2 (Gage and Camper, 1997; Hjalt et al., 2000). Corneal endothelium and trabecular meshwork which are mesenchymal derivatives retains the expression of PITX2 and by E18.5 PITX2 becomes restricted to the angle (Kidson et al., 1999). Like PITX2, FOXC1 expression in mouse eye development is similar in that it is initiated in the periocular mesenchyme by E11.5 which is prior to the commencement of mesenchymal cell migration (Hjalt et al., 2000; Wang et al., 2017). FOXC1 continues to be expressed in the hyaloid plexus at E12.5, conjunctiva and trabecular meshwork which persist until parturition and potentially thereafter and also in the precorneal mesenchyme (Hjalt et al., 2000; Sowden, 2007).

A study by Berry et al., 2006 showed that PITX2 and FOXC1 are co-expressed during eye development in discreet cell types and that they share a subnuclear compartment as well as interact with each other physically. The data further showed that both FOXC1 and PITX2 are crucial for the proper development as well as function of the anterior segment of the eye as they form a higher order transcription factor complex (Berry et al., 2006). Signals which are essential for proper migration and condensation into endothelia such as those of trabecular meshwork as well as cornea may be initiated by FOXC1 and PITX2 (Berry et al., 2006). Both transcription factors are likely to be the ones to initiate elaboration of the anterior chamber angle along with other mechanical messages during migration transduced by the ECM and cytoskeleton (Berry et al., 2006).

The interaction between the genes that regulate the development of the anterior segment of the eye is not fully understood especially PAX6, FOXC1, PITX2 interaction with PXDN. Even though specific functions of PXDN are yet unknown in eye development, it is understood that PXDN is involved in supporting the cornea as well as lens by syntheses of BM which provides a structural framework and acting as an antioxidant enzyme to protect various eye structures from oxidative damage (Khan et al., 2011; Yan et al., 2014; Choi et al., 2015). Mutations in the genes that facilitate the development of the anterior segment of the eye results in poor development of the structures such as iris, cornea, lens, trabecular meshwork etc which leads to impaired vision. Eye development disorders resulting from mutations and/or aberrant expression of the genes discussed above (FOXC1, PITX2, PAX6 and PXDN, with relevance to the current study) are discussed in detail in below.

1.6.4 Anterior segment dysgenesis

Anterior segment dysgenesis (ASD) defines a collection of various congenital eye disorders that affect structures within the anterior segment of the eye such as the cornea, iris, trabecular meshwork, and ciliary body (Sowden, 2007; Reis and Semina, 2011). ASD is comprised of disorders such as Peter's anomaly, Axenfeld-Rieger Syndrome (ARS), Sclerocornea and microphthalmia, while ARS, Peter's anomaly and sclerocornea can lead to cataract formation, corneal opacity and glaucoma (Reis and Semina, 2011).

ASD congenital disorders are usually accompanied by a 50% increased predisposition to glaucoma (Alward, 2000; Sowden, 2007; Ito and Walter, 2014). The congenital disorders typically involve modifications to adhesions between the lens and cornea or cornea and iris, corneal opacity, iris hypoplasia and posterior embryotoxon, these can present themselves separately or in combination (Reis and Semina; 2011). The most common disorders associated with ASD are (1) ARS which is usually noted by a combination of adhesion of the cornea, iris hypoplasia and polycoria (more than one pupillary opening in the iris), (2) Peter's anomaly which denotes the trio of malformations in the layers of the cornea, corneal opacity and adhesion of the cornea. (3) Sclerocornea is characterised by the anterior extension of scleral tissue to replace the peripheral cornea (Ito and Walter, 2014).

1.6.4.1 Axenfeld Rieger syndrome

ARS was first described by Axenfield in 1920 in patients presenting with iris strands adhesion, iris atrophy, pseudopolycoria and further described a sequence of mesodermal dysgenesis of the cornea and iris (Stahl, 2014). The syndrome at times it is accompanied by systemic complications such as facial bone defects, dental abnormalities, pituitary and umbilical abnormalities (Idrees et al., 2006). ARS has varying severity can be from delicate findings (which can be detected using gonioscopy) to a more severe malformation (Stahl, 2014).

1.6.4.2 Peters anomaly and Peters-plus syndrome

Peters' anomaly is a developmental abnormality in the anterior section of the eye. In 1906, Peters described the syndrome as it was characterised by cornea-iris adhesion, corneal leukoma and shallow anterior chamber (Harissi-Dagher and Colby, 2008). The severity of the disorder can vary from mild opacification of the cornea to severe glaucoma, cataract and microphthalmia (Stahl, 2014). Peters-plus syndrome results when abnormality of the system such as developmental delay and skeletal changes also occur (Yang and Lambert, 2001). The two modes of inheritance (autosomal recessive and dominant) have been reported for peters anomaly, which involves mutations in *PAX6*, *FOXC1*, *PITX2* and *CYP1B1* genes (Doward *et al.* 1999; Nishimura *et al.* 2001; Vincent *et al.* 2001).

1.6.4.3 Aniridia

Aniridia (lack of iris), is a rare autosomal dominant disease which is described by varying eye abnormalities such as corneal opacity, lens dislocation, ciliary body hypoplasia, and iris hypoplasia (Lee et al., 2008). The following can also lead to impaired or complete loss of vision, foveal hypoplasia, cataract, glaucoma early onset, retinal detachment and aniridia-associated keratopathy. Systemic abnormalities do not usually present with aniridia but deletions in genes such as FOXC1 and PAX6 enables the presentation of systemic anomalies in aniridia patients (Ito et al., 2009).

1.6.4.4 Sclerocornea

Sclerocornea is a congenital anomaly that is characterised by noninflammatory, nonprogressive asymmetric scleralisation of the cornea (Kenyon, 1975). In Sclerocornea the scleral tissue is extended anteriorly which in turn replaces the peripheral cornea leading to the vessels of both the conjunctiva and episclera crossing the cornea, this disorder may associate with cataracts and coloboma (Harissi-Dagher and Colby, 2008).

1.6.4.5 Primary congenital glaucoma

Primary congenital glaucoma (PCG) is part of infantile glaucoma which can lead to eye defects and can be associated with ARS (Sarfarazi et al., 2003, Micheal et al., 2016). At the age of 6 months about 60% of the patients presenting with such disorders can be diagnosed and 80% within the first year. PCG accounts for approximately 0.04% of blindness and can cause permanent visual impairment (Gould and John, 2002). Across various populations the incidence rate of PCG varies such that in western population it affects 1 in 10000, 1 in 3300 in Indians, 1 in 2500 in Saudi Arabians and 1 in 1250 Slovakian gypsies (Bejjani et al., 1998; Plásilová et al., 1999; Tanwar et al., 2009).

Elevated intraocular pressure (IOP), coupled with optic nerve damage and elevated corneal diameter are the characteristics of PCG (Tanwar et al., 2009; Kim et al., 2011). Some of the clinical features of PCG include descemet membrane opacification coupled with rupture, buphthalmos, edema of the cornea, anterior sclera thinning, iris atrophy, and deep anterior chamber (Sarfarazi et al., 2003; Micheal et al., 2016). Some of the less common features include photophobia, epiphora, and blepharospasm. GLC3A, GLC3B, GLC3C at 2p21, 1p36.2-1p36.1, and 14q24.3 respectively have been associated with PCG pathogenesis. CYP1B1 along with LTBP2 are the only target genes that have be located thus far, while CYP1B1 gene was found to be frequently mutated, in about 20% to 100% cases of PCG from Saudi Arabia, Slovakian gypsies and Japan (Kim et al., 2011; Plásilová et al., 1999; Tanwar et al., 2009; Bejjani et al., 1998).

1.6.4.6 Microphthalmia

Microphthalmia, anophthalmia and coloboma disorders, usually referred to as MAC, present as a syndrome rather than separate malformations (FitzPatrick and Van Heyningen, 2005; Ragge et al., 2007). The disruption of normal formation of anterior segment and congenital cataracts may be seen in patients with microphthalmia, this will lead to opacification of the cornea, abnormal irides and small abnormal lenses (Verma and FitzPatrick, 2012). A study of congenital eye disease at a teaching hospital in Sagamu, Nigeria, found that corneal opacities is the fourth most common congenital eye disorder causing blindness in 5.7% of infants with congenital eye diseases (Bodunde and Ajibode, 2006).

Microphthalmia (small eyes) refers to an eye with reduced volume and may be associated with Anophthalmia (complete absence of the eye) and Coloboma (a defect in the iris of the eye) (Skalicky et al., 2013). MAC contributes an important percentage of congenital ocular disorders worldwide (Hornby et al., 2000). The presence of any of the three disorders always increases the risk of development of cataracts and glaucoma if left untreated. The aetiology of the spectrum of eye disease is yet to be fully understood. The evidence gathered from experimental and clinical investigations suggests a heterogenous genetic basis which also includes a disruption (Local) in development of the eye (Verma and Fitzpatrick, 2007; Bardakjian and Schneider, 2011). There are various factors involved in the early stages of eye development such as transcription factors, complex signalling molecules, and structural proteins, adhesion factors, cell cycle regulators which are downstream targets (Yun et al., 2009; Fuhrmann, 2010; Eiraku et al., 2011). The regulation of eye development pathways interacts in a specific manner which may be time and tissue specific. This may help explain the overlap of the underlying genetic heterogeneity of the disorders with the clinical phenotypes (Bardakjian and Schneider, 2011).

1.6.5 The genetics of anterior segment dysgenesis

Mutations in genes that initiate and regulate the complex pathways involved in eye development can cause a spectrum of disorders such as ASD which can present with MAC. Mutations in genes such as *PXDN*, *PAX6*, *SOX2*, *ALDH1A3*, *STRA6*, *OTX2*, *RAX*, *BMP4*, *VSX2*, *GDF6*, *VAX1*, *SMOC1* and *SIX6* to name a few have been found in patients presenting with ASD and MAC disorders (Schneider et al., 2009; Khan et al., 2011; Slavotinek et al., 2011; Aldahmesh et al., 2013; Yan et al., 2014; Choi et al., 2015). Genes such as *FOXE3*, *PITX3*, *PAX6*, *B3GALTL*, *COL4A1* and *SH3PXD2B* have been screened for mutations and deletions in patients with ASD, and there is substantial heterogeneity in both MAC and ASD disorders which causes overlap thus (**Figure 1.10**) leading to no clear-cut molecular diagnosis (Semina et al., 2001; Mao et al., 2012; Alzuhairy et al., 2013; Prokudin et al., 2013).

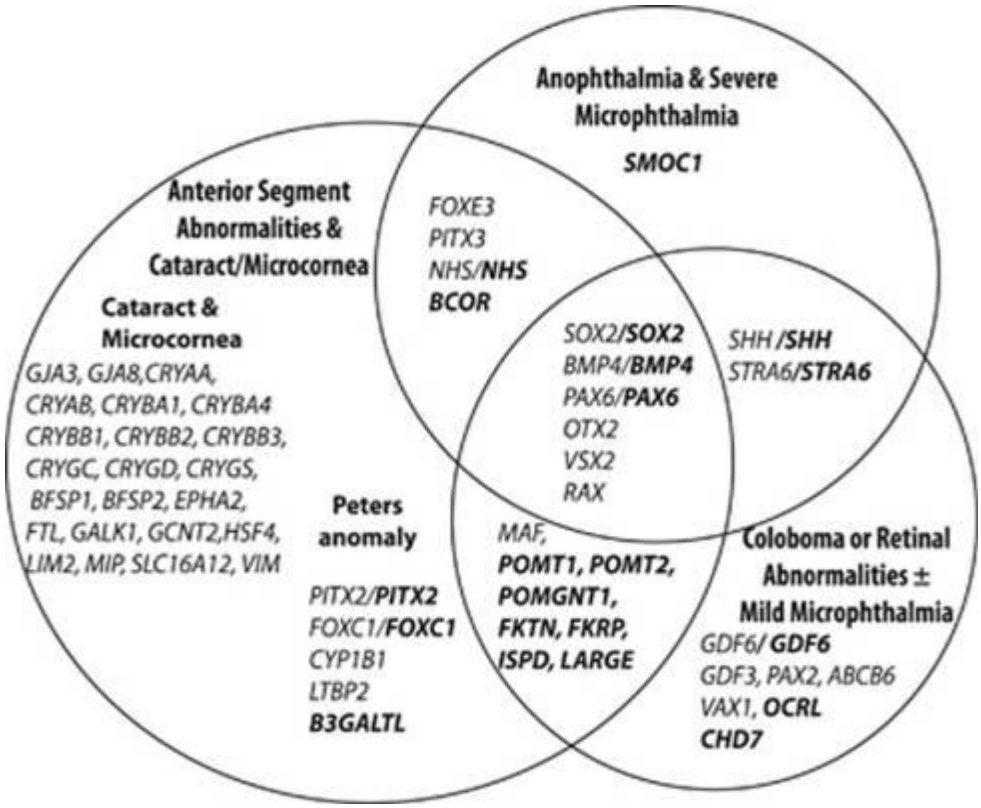

Figure 1.10: Genes that overlap in clinical features of congenital eye disorders due to genetic heterogeneity. Most common congenital eye disorders are shown along with the genes that can cause them. Eye disorders that manifest without abnormality of the system are represented by genes in normal font. The bolded genes are mostly found in eye disorders with syndromic features (Choi et al., 2015).

Whilst there are many unidentified genes that are involved in the development of congenital eye disorders, **Figure 1.11** shows some of the genes known to be active at different stages of eye development (Sinn and Wittbrodt, 2013) and the chromosomal location along with the function of the corresponding proteins is listed in **Table 1.1**. It is imperative to recognise ASD because it is commonly linked with cataracts and influences congenital glaucoma development in 50% of diagnosed patients as well as an increase in ocular pressure (Reis and Semina; 2011; Choi et al., 2015).

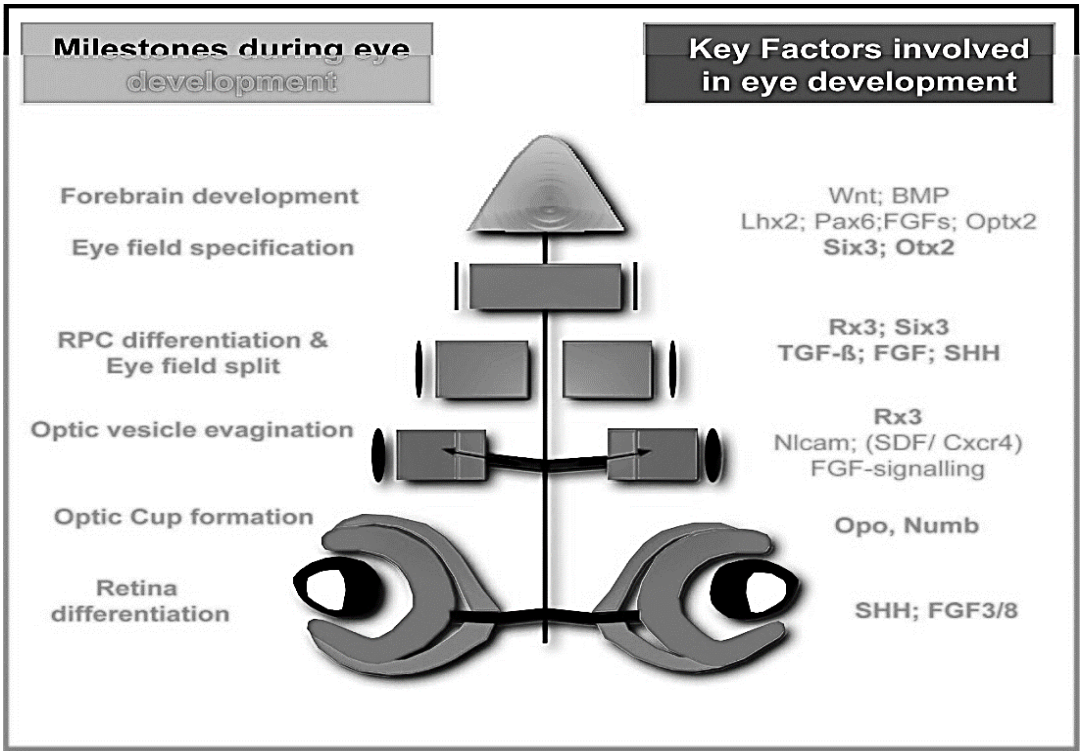

Figure 1.11: Various genes activated at different stages in the development of the eye in vertebrates. Various key transcription factors such as PAX6, SIX3, OTX2, WNT as well as LHX2 are required for normal eye development starting from the forebrain development and eye field specification stages in the presence FGF. Expression of FGF as well as TGF-β leads to upregulation of SHH, SIX3 and RX3 which drive eye field split with RX3 further expressed for optic vesicle evagination. NUMB and OPO which regulated cell differentiation are expressed to enable optic cup formation, with FGF 3 and 8 expression enabling SHH to initiate retina differentiation. (Sinn and Wittbrodt, 2013).

Investigations have been carried out with regards to some of the above-mentioned genes in cohorts of various ethnic groups. Several other genes other than *PXDN* were also investigated in other cohorts for their association with ocular congenital disorders (**Table 1.2**). Mutations in genes such as *PNPT1, COL4A1, OTX2, GDF6, RARB,* and *STRA6* were detected in 32 patients diagnosed with microphthalmia and other defects of the eye (Slavotinek et al., 2015). A Pakistani family of seven and an Indian family were screened for mutations via sequencing, and three mutations (novel) were detected in the gene *ALDH1A3* [c.964G>A (p.V322M), c.1310_1311delAT (p.Tyr437Trpfs*44)] as well as c.289A>G (p.Ile97Val) missense mutation in *FOXE3*. Families harbouring these mutations were presenting with microphthalmia (Ullah et al., 2016). In a study by (Prokudin et al., 2014) five causal variants in *PAX6, CRYGC, CYP1B1,* and *GJA8* were identified from 11 Indian families (unrelated) with Peter's anomaly, cataract, coloboma and microphthalmia.

Recently, mutations in PXDN have been associated with ASD. In a study by Khan et al. (2011), it was found that two Pakistan families (consanguineous) and one Cambodian family (consanguineous) harboured homozygous mutations in *PXDN* gene (Khan et al., 2011). The two Pakistani families presented with congenital cataract and corneal opacity which was mild and moderate, while the Cambodian family presented with severe corneal opacification and congenital glaucoma. An exon 17 missense mutation c.2638C>T (p.Arg880Cys) was detected in *PXDN* via direct sequencing. Having scored 0.98 with PolyPhen the mutation was likely to be deleterious and the amino acid change was within the conserved peroxidase domain, which could affect both protein structure and enzymatic ability of the domain (Khan et al., 2011). Another variant in exon 10 of *PXDN* c.1021C>T (p.Arg341X) was found to likely cause protein truncation, which can also be deleterious. These mutations were only observed in the affected patients and absent in the controls.

Additional mutations in *PXDN* have since been identified: a paternally inherited 23-base-pair deletion causing a frameshift and premature protein truncation c.2375_2397del23 predicting p.(Leu792Hisfs*67) was observed in two siblings presenting with microphthalmia, developmental delays, ASD, hypotonia and Sclerocornea from a Caucasian family with no history of consanguinity (Choi et al.,

2015). Data from another 20 patients was investigated for any *PXDN* gene mutations and two were identified in one patient (male) presenting with ASD, microphthalmia and cataracts: the mutations were a c.1192delT, frameshift mutation which is inherited maternally p.(Tyr398Thrfs*40) and a c.947 A4C (p.Gln316Pro) a missense mutation considered to be deleterious and paternally inherited.

Table 1.1: Candidate genes selected for sequencing in the current study. Aberrant expression of the proteins below has been associated with various specific and a spectrum of congenital ocular disorders.

Protein	Gene	Omim #	Inheritance	Location	Function	Reference(s) Protein function
Aldehyde Dehydrogenase 1 family member 3	*ALDH1A3*	600463	Autosomal Recessive	15q26.3	Required for the biosynthesis of normal levels of retinoic acid in the embryonic ocular and nasal regions; retinoic acid is required for normal embryonic development of the eye and the nasal region.	Duester, 2009
Beta-1,3-glucosyltransferase	*B3GALTL*	610308	Autosomal Recessive	13q12.3	Regulates glycosylation in cells.	Lesnik Oberstein et al., 2006
BCL6 corepressor	*BCOR*	300485	X-linked Dominant	Xp11.4	It is involved in formation of organs and tissues including the eyes.	Ng et al., 2004
Beaded Filament Structural Protein 1	*BFSP1*	603307	Autosomal Recessive/ Dominant	20p12.1	Functions as a component of the beaded filament which is a cytoskeletal structure found in lens fiber cells.	Alizadeh et al., 2003 Wang et al., 2013
Beaded Filament Structural Protein 2	*BFSP2*	603212	Autosomal Dominant	3q22.1	Function as part of the fiber cell-beaded filament.	

Protein	Gene	Omim #	Inheritance	Location	Function	Reference(s) Protein function
Crystallin Alpha B	*CRYAB*	123590	Autosomal Recessive/ Dominant	11q23.1	Involved in lens development and aids in prevention against protein aggregation under a wide range of stress conditions.	Graw, 2009
Crystallin Beta A1	*CRYBA1*	123610	Autosomal Dominant	17q11.2	Crystallins are key dominant components in the structure of the lens in eyes of vertebrate.	Graw, 2009
Crystallin Beta A4	*CRYBA4*	123631	-	22q12.1		
Crystallin Beta B1	*CRYBB1*	600929	Autosomal Recessive/ Dominant	22q12.1	The lens refractive index and transparency are maintained by these proteins. These crystallins are made and then retained throughout life, making them extremely stable proteins because lens central fiber cells lose their nuclei during development.	Graw, 2009
Crystallin Beta B2	*CRYBB2*	123620	Autosomal Dominant	22q11.23		
Crystallin Beta B3	*CRYBB3*	123630	Autosomal Recessive/ Dominant	22q11.23		Graw, 2009
Crystallin Gamma C	*CRYGC*	123680	Autosomal Dominant	2q33.3		
Crystallin Gamma D	*CRYGD*	123690	Autosomal Dominant	2q33.3		
Crystallin Gamma S	*CRYGS*	123730	Autosomal Dominant	3q27.3		

Protein	Gene	Omim #	Inheritance	Location	Function	Reference(s) Protein function
Cytochrome P450 Family 1 Subfamily B Member 1	*CYP1B1*	601771	Autosomal Recessive	2p22.2	The enzyme also metabolizes a signalling molecule involved in eye development.	Vasiliou and Gonzalez et al., 2009
EPH receptor A2	*EPHA2*	176946	Autosomal Dominant	1p36.13	Controls the development, shape and maintenance of lens fibre cells.	Cheng et al., 2022
Fukutin Related Protein	*FKRP*	606596	Autosomal Recessive	19q13.32	Necessary for posttranslational modification of dystroglycan.	Chan et al., 2010
Fukitin	*FKTN*	607440	Autosomal Recessive	9q31.2	Protein is thought to be a glycosyltransferase and could play a role in brain development.	Haro et al., 2018
Forkhead Box C1	*FOXC1*	601090	Autosomal Dominant	6p25.3	Involved in embryonic and ocular development regulation.	Berry et al., 2008 Lehmann et al., 2003
Ferritin Light Chain	*FTL*	134790	Autosomal Dominant	19q.13.33	Plays a role in delivery of iron to cells.	Girelli et al., 1995
Galactokinase 1	*GALK1*	604313	Autosomal Recessive	17q25.1	Metabolises galactose sugar.	Rubio-Gozalbo et al., 2021
Growth Differentiation Factor 6	*GDF6*	601147	Autosomal Dominant	8q22.1	Plays a key role in regulating apoptosis during retinal development.	Asai-Coakwell et al., 2007

Protein	Gene	Omim #	Inheritance	Location	Function	Reference(s) Protein function
Gap Junction Protein Alpha 3	*GJA3*	121015	Autosomal Dominant	13q12.11	Regulates lens-fibre junctions	Gerido and White, 2004
Gap Junction Protein Alpha 8	*GJA8*	600897	Autosomal Dominant	1q21.2	Necessary for lens growth and maturation of lens fiber cells.	Ceroni et al., 2019
Heat Shock Transcription Factor 4	*HSF4*	602438	Autosomal Dominant	16q22.1	Involved in the negative regulation of DNA binding activity	Shiels and Hejtmancik, 2015
Lens Intrinsic Membrane Protein 2	*LIM2*	154045	Autosomal Recessive	19q13.41	Play an important role in both lens development and cataractogenesis.	Arneson and Louis, 1998
Latent Transforming Growth Factor Beta Binding Protein 2	*LTBP2*	602091	Autosomal Recessive	14q24.3	Play an integral structural role in elastic-fiber architectural organization and/or assembly.	Shi et al., 2021
Transcription Factor Maf	*MAF*	177075	Autosomal Dominant	16q23.2	Acts as a transcriptional activator or repressor. Involved in embryonic lens fiber cell development.	Reza and Yasuda, 2004
Major Intrinsic Protein of Lens Fiber	*MIP*	154050	Autosomal Dominant	12q13.3	Responsible for regulating the osmolarity of the lens.	Long et al., 2018
Nance-Horan Syndrome	*NHS*	300457	X-linked Dominant	Xp22.2	Involved in the regulation eye, tooth, brain and craniofacial development.	Burdon et al., 2003

Protein	Gene	Omim #	Inheritance	Location	Function	Reference(s) Protein function
Orthodenticle Homeobox 2	*OTX2*	600037	Autosomal Dominant	14q22.3	Transcription factor and plays a role in brain, craniofacial, sensory organ development.	Beby and Lamonerie, 2013
Paired box 6	*PAX6*	607108	Autosomal Dominant	11p13	Key in the development of neural tissues, particularly the eye.	Nishina et al., 1999
Paired Like Homeodomain 2	*PITX2*	601542	Autosomal Dominant	4q25	Controls cell proliferation in a tissue-specific manner and is involved in morphogenesis.	Markintantova et al., 2008
Paired Like Homeodomain 3	*PITX3*	602669	Autosomal Recessive/ Dominant	10q24.32	Involved in lens formation during eye development.	Wu et al., 2019
Peroxidasin	*PXDN*	605158	Autosomal Recessive	2p25.3	Involved in extracellular matrix formation	Nelson et al., 1994 Bhave et al., 2012
Retinoic Acid Receptor Beta	*RARB*	180220	Autosomal Recessive/ Dominant	3p24.2	Mediates cellular signalling in embryonic morphogenesis.	Busby and Burris, 2012
Retina and Anterior Neural Fold Homeobox	*RAX*	601881	Autosomal Recessive	18q21.32	Is required for retinal cell fate determination.	Furukawa et al., 1997

Protein	Gene	Omim #	Inheritance	Location	Function	Reference(s) Protein function
Sonic Hedgehog	*SHH*	600725	Autosomal Dominant	7q36.3	Crucial in the development of all animals.	Cavodeassi et al., 2019
Solute Carrier Family 16 Member 12	*SLC16A12*	611910	Autosomal Dominant	10q23.31	Functions in monocarboxylic acid transport.	Halestrap and Meredith, 2003
Secreted Modular Calcium-Binding 1	*SMOC1*	608488	Autosomal Recessive	14q24.2	Essential roles in eye and limb development.	Okada et al., 2011
Sex Determining Region Y-Box 2	*SOX2*	184429	Autosomal Dominant	3q26.33	Regulation of embryonic development.	Taranova et al., 2006
Stimulated By Retinoic Acid 6	*STRA6*	610745	Autosomal Recessive	15q24.1	acts as a receptor for retinol/binding protein.	Casey et al., 2011
Vimentin	*VIM*	193060	Autosomal Dominant	10p13	Responsible for maintaining cell shape.	Battaglia et al., 2018
Visual System Homeobox 2	*VSX2*	142993	-	14q24.3	Plays a significant role in the specification and morphogenesis of the sensory retina.	Zou and Levine, 2012

With the aid of next generation sequencing (NGS), screening of deleterious mutations associated with human disease has taken an important leap and the technique has been effective when employed in the detection of causal mutations (**Table 1.2**) in patients diagnosed with congenital ocular disorders (Gupta et al., 2017).

Table 1.2: Studies that employed NGS in the interrogation of various genes in patients diagnosed with congenital ocular diseases (Gupta et al., 2017).

Type of ocular phenotypes	**Study cohort origin**	**Case type examined**	**Genes harbouring causal variants**	**References**
Micropthalmia and Anophthalmia	Hispanic	25 trios, two duos and five single probands	*GDF6, STRA6 COL4A1, OTX2, RARB, FBLN1, PNPT1* and *GCNT2,*	Slavotinek et al., 2015
	Indian and Pakistani	Familial	*FOXE3, ALDH1A3* and *VSX2*	Ullah et al., 2016
ASD and Micropthalmia	Caucasian	Familial Sporadic	*PXDN*	Choi et al., 2015
MAC, Peters anomaly and Cataract	-	Familial	*PAX6, ABCB6, GJA8, CRYGC, CYP1B1,* and *GDF3*	Prokudin et al., 2014
PCG	Pakistani	Familial	*LTBP2* and *PXDN*	Micheal et al., 2016

Currently there are no research studies conducted for the association of *PXDN* gene variants in Africans. There are currently a few studies which have investigated PXDN gene mutations in association with congenital eye disorders. **Table 1.3** shows currently known mutations, but none of the examined cohorts is comprised of Africans.

Table 1.3: Studies conducted in various population and *PXDN* mutations detected in patients with congenital eye disorders.

Type of ocular phenotypes	Study cohort origin	Case type examined	Variant	References
congenital cataract, corneal opacity, and developmental glaucoma	Pakistani Cambodian	Familial	exon 17 missense mutation c.2638C>T (p.Arg880Cys) exon 10 c.1021C>T (p.Arg341X) exon 17 c.2568delC (p.Cys857Alafs*5)	Khan et al., 2011
developmental ocular disorder and primary glaucoma	Pakistani	Familial	(c.3496G>A;p.G1166R)	Micheal et al., 2016
micropthalmia and anterior segment dysgenesis	Caucasian	Familial Sporadic	c.1021C>T predicting p.(Arg341*); c.2375_2397del23 predicting p.(Leu792Hisfs*67); c.1192delT, predicting p.(Tyr398Thrfs*40) and c.947 A4C, predicting p.(Gln316Pro)	Choi et al., 2015

1.6.6 Eye disorders in South Africa

In South Africa there is limited epidemiological data regarding the burden of eye diseases, since data is hardly collected or reported on the burden of eye diseases. The most common challenge faced by advancement of genetics in South Africa is genetic diversity which is exhibited by the populace comprising of both local and immigrant. Although even within these groups severe admixture exists, this has contributed to the varying population frequencies of genetic variants adding to the difficulty in genetic diagnosis of most congenital eye disorders (Roberts et al., 2016). Glaucoma, cataract, corneal scarring and refractive errors were found to be major causes of blindness as well as impaired vision in South Africa (Butcher and Ijsselmuiden, 1988; Verwey and Mahomed, 2020). Less than a handful of studies have been conducted in a South African cohort with regards to the genetic aspect of eye disease such as Macular corneal dystrophy (MCD), Familial congenital cataract, nystagmus and coloboma (Carstens et al., 2016; Goolam et al., 2018).

A study by Carstens et al., (2016) investigated the genetic cause of type 1 MCD (a corneal stromal dystrophy which leads to progressive vision loss) in a consanguineous South African family. The gene carbohydrate sulfotransferase (*CHST6*) encodes an enzyme that catalyses the synthesis of keratan sulfate in the cornea. Aberrant synthesis of the enzyme causes abnormal organisation of fibril in the cornea. A novel mutation (p.E71Q) in the gene carbohydrate sulfotransferase (*CHST6*) was identified as the causal mutation in the family. A *PAX6* p.R208W mutation (NM_000280.3: c.622G>A) was identified in a total of 27 admixed South African family members diagnosed with nystagmus, coloboma as well as familial congenital cataracts and co-segregation of the variant with the clinical phenotypes was observed in all 27 family members (Goolam et al., 2018).

In summary the current study seeks to determine whether genetic mutations exist in South African patients diagnosed with ASD and whether transcription factors PAX6, FOXC1 and PITX2 regulates the transcription of PXDN.

1.7 Aims and Objectives

i. Determine whether the master regulators of eye development PAX6, FOXC1 and PITX2 are involved in regulating *PXDN* gene expression.

- To use western blotting and immunofluorescence confocal microscopy to quantify and observe protein localisation of PAX6, FOXC1, PITX2 and PXDN within cells upon treatment.

- To employ chromatin immunoprecipitation (ChIP) and PCR to determine PAX6, FOXC1 and PITX2 interaction with *PXDN* gene promoter.

- To employ the Luciferase reporter, assay to assess the ability of PAX6, FOXC1 and PITX2 to express reporter gene expression from the *PXDN* promoter.

ii. Determine whether genetic variants exist in *PXDN* gene within a cohort of South African patients presenting with congenital ocular diseases.

- To select a panel of 50 candidate genes associated with the development of congenital eye disorders.

- To use Next Generation Sequencing based method to perform mutation screening in the genes of interest in a cohort of South African patients with congenital eye disorders.

- To use the American college of medical genetics and genomics (ACMG) guidelines for variant filtering to identify putative disease-causing mutations.

CHAPTER 2: Regulation of *PXDN* by PAX6, FOXC1 and PITX2

2.1 Introduction

2.1.1 PXDN in eye development

PXDN belongs to the haem containing cyclooxygenase peroxidase family and in humans, PXDN is predominantly expressed in the cardiovascular system by cardiomyocytes (Zhang et al., 2012) and in the developing eye, more specifically in the layers of lens and corneal epithelium (Khan et al., 2011). In mouse animal models, the developing eye expresses PXDN from embryonic age (E11.5) onwards, which is equivalent to 33 days in human embryology, and when PXDN is knocked out, the outcome is absence of collagen IV crosslinking (Lázár et al., 2015). As such, PXDN is understood to be essential for normal development of eye structures such as the lens epithelium and cornea via collagen IV crosslinking, which promotes consolidation of ocular BM (Yan et al., 2014). Aberrant PXDN expression causes loss of structural integrity of the lens capsule and lens molecules such as γ-crystallin, which as a result seem to be extruded into the anterior and posterior chamber of the eye (Yan et al., 2014). Various mutations in *PXDN* have been found to be present in patients diagnosed with developmental eye disorders, specifically ASD, lending support to the significance of PXDN in eye development (Khan et al., 2011; Choi et al., 2015). PXDN displays expression in a variety of tissues, indicating that transcription is likely regulated in a tissue specific manner. To date, there is no information about the regulators of PXDN in the context of eye development.

2.1.2 PAX6, FOXC1 and PITX2 in development and maintenance of the eye

The three transcription factors of interest are key players in the development as well as maintenance of the anterior segment structures of the eye with PAX6 expressed in the very early stages of eye development to drive the organisation of the anterior segment (Takamiya et al., 2020), while FOXC1 and PITX2 act downstream of the master control gene *PAX6* (Graw, 2003). PITX2 and FOXC1 are co-expressed during eye development in discreet cell types and they share a subnuclear compartment as well as interact with each other physically; as such they are crucial for the proper development as well as functioning of the anterior segment of the eye as they form a higher order transcription factor complex (Berry et al., 2006).

During the optic cup formation stage of eye development FOXC1 and PITX2 expression is elevated showing their requirements for the process (Sowden, 2007). ECM proteins such as laminin, fibronectin, and collagen IV are also crucial for a successful optical cup formation (Kwan, 2014). Collagen IV requirement means that PXDN expression will be elevated since crosslinking of collagen IV is required in the formation of BM which is essential for normal development of the eye with the process exclusive to PXDN (Bhave et al., 2012; Lee et al., 2020). The continuous expression of PAX6 throughout eye development stages in both anterior and posterior segments as well as post-development is indicative that *PXDN* could be a target of PAX6, just as FOXC1 and PITX2 are known PAX6 targets (Wang et al., 2017). FOXC1 as well as PITX2 do not regulate collagen IV crosslinking or BM synthesis, but the absence of PAX6 during lens formation results in ECM proteins being significantly diminished between the optic vesicle and ectoderm via the reduction of transcripts encoding components of the ECM (Huang et al., 2011).

Once the eye is fully developed, proteins such as FOXC1, PAX6 and PXDN continue to be expressed, with FOXC1 required for cell viability as well as resistance to oxidative stress (Berry et al., 2006), while PXDN is thought to protect eye structures against oxidative stress damage (Khan et al., 2011). In a study by Shukla and Mishra, (2018), it was shown that levels of hydrogen peroxide in corneal cell lines affect expression levels and localisation of PAX6. This work was conducted using human embryonic kidney cells (HEK293) as a model cell line due to its embryonic nature, which enables elevated expression of proteins required for normal development, and has been shown to endogenously express PXDN (Hanmer and Mavri-Damelin, 2018). HEK293 cells are also considered a healthy cell line that also have high transfectability, which is advantageous for luciferase reporter assay, as used in our study to investigate gene regulation (Wurm et al., 2004). In murine cells, it has been shown that FOXC1 is expressed in developing kidney cells and it is required for kidney organogenesis (Kume et al., 2000), while no studies have been conducted to date that examined expression levels of PAX6 as well as PITX2 in kidney cells, we used data obtained from protein atlas database, which has expression profiles of proteins in various commonly used cell lines and showed that both proteins are endogenously expressed (www.proteinatlas.org).

The interaction between the genes that regulate the development of the anterior segment of the eye is not fully understood, especially PAX6, FOXC1, PITX2 interaction with *PXDN*, which brings about the primary aim of the current study, which is to interrogate whether there is any interaction of PAX6, FOXC1 as well as PITX2 with *PXDN*.

2.2 Methodology

2.2.1 Reagents

General reagents were purchased from Sigma Aldrich (St Louis, Missouri, USA) unless stated otherwise. The recipes of buffers and solutions used in the experiments explained below are listed in **Appendix C**. Antibodies used in this study are listed in **Table 2.1** below and were purchased from Santa Cruz® Biotechnology Inc and Sigma-Aldrich (indicated by SC- code and HPA- code, respectively). The application of the methods explained in this chapter were adopted and/or modified from the studies which investigated the interaction of NRF2 with *PXDN* (Hanmer and Mavri-Damelin, 2018) and SNAi1 with *PXDN*, from our laboratory (Sitole and Mavri-Damelin, 2018).

Table 2.1: **Antibodies used in immunochemistry techniques in the current study.**

Antibodies		**Immunoassay Techniques**
Primary	**Secondary**	
PXDN (SC-293408) Mouse monoclonal IgG2b κ	m-IgGκ BP-FITC (SC-516140)	Immunofluorescence Confocal Microscopy
PAX6 (SC-32766) Mouse monoclonal IgG_1 λ	m-IgGλ BP-CFL (SC-516192)	
FOXC1 (HPA040670) Rabbit polyclonal	Anti-Rabbit-FITC (SC-2012)	
PITX2 (HPA050074) Rabbit polyclonal	Anti-Rabbit-FITC (SC-2012)	
PXDN (HPA012375) Rabbit polyclonal	Anti-Rabbit IgG-HRP (SC-2004)	Western Blot Chromatin Immunoprecipitation Assay (Primary Antibody only)
PAX6 (SC-32766)	m-IgGλ IgG-HRP (SC-516132)	
FOXC1 (HPA040670)	Anti-Rabbit IgG-HRP (SC-2004)	
PITX2 (HPA050074)	Anti-Rabbit IgG-HRP (SC-2004)	
B-Actin (D6A8/#8457) Rabbit monoclonal	Anti-Rabbit IgG-HRP (#7074)	

2.2.2 Cell culture

HEK293 were cultured in 10 ml of Dulbecco's Modified Eagle's Medium (DMEM)/Hams with Glutamax-F12 (Gibco), containing 10% (v/v) fetal bovine serum (FBS) (Gibco) and 1% (v/v) Pen-Strep (5000 units/mL penicillin and 5000 µg/mL streptomycin) (Gibco) in a 100 mm cell culture dish (NEST®). The cells were maintained in a humidified incubator with 5% carbon dioxide (CO_2) at 37 °C.

HEK293 cells were monitored every 24 hours with medium change when they reached a confluency of about 70% to 80%. Cells were then sub-cultured by first discarding the old medium followed by rinsing with 1X phosphate buffered saline (PBS) (Gibco). The cells were detached by adding 500 µl of 1X PBS and 500 µl of 1X Trypsin-ethylenediaminetetraacetic acid (EDTA) (Gibco) followed by incubation of the cells at 37 °C for 3 minutes. Trypsin-EDTA was then deactivated by adding 1 ml of fresh DMEM to the resuspended cells, then cell clumps were broken via multiple pipetting in the plate with 300 µl of the resuspended cell mixture aspirated and the remaining volume of cells discarded. The aspirated 300 µl was pipetted into a clean plate, 9.7 ml of fresh DMEM added, then placed into the incubator for maintenance. For experiments that required specific cellular densities, a cell count was conducted. With the aid of a haemocytometer, 10 µl of 0.2% (w/v) trypan blue was mixed with 10 µl of resuspended cells for counting and further calculation of the volume required to seed cells for a specific density. Once the HEK293 cells were seeded, the culture plate was incubated at 37°C for 24 hours prior to performing any treatments/experiments unless stated otherwise. DMEM supplemented with 10% FBS was replaced with serum free medium (SFM) to starve the cells prior to treatment with FGF-2. HEK293 cells represented a healthy model cell line previously shown to endogenously express PXDN protein (Hanmer and Mavri-Damelin, 2018), as well as the transcription factors of interest (Kume et al., 2000; www.proteinatlas.org).

Fibroblast growth factor 2 (FGF-2) which is a potent mitogen (Ornitz and Itoh, 2015) was used for treatment of cells with an attempt to determine as to whether expression levels of our target proteins can be elevated. As shown in **section 1.6.5** by **Figure 1.11**, FGF pathway activation drives expression of transcription factors

required for normal development as well as maintenance of the eye and further induces cellular proliferation (Sinn and Wittbrodt, 2013). FGF2 has also been shown to be required for normal proliferation as well as differentiation of corneal epithelial cells during eye development (Zhang et al., 2015) and Iris-Lens regeneration (Hayashi et al., 2004) which require transcription factors PAX6 (Yan et al., 2014; Nishina et al., 1999; Chanas et al., 2009), FOXC1 (Wang et al., 2001; Sowden, 2007) and PITX2 (Gage and Camper, 1997; Hjalt et al., 2000; Sowden, 2007) for normal development of these structures. In a study by Tassi et al., (2001), a final concentration of 2ng/ml of recombinant FGF-2 was used to treat fibroblast cells with the addition of heparan sulphate to help prevent FGF-2 degradation and increase proliferation. In the current study we used the same concentration of 2 ng/ml of FGF-2 without addition of heparan sulphate which was also shown to have transient effects lasting for 24 hours in the absence of heparan sulphate (Tassi et al., 2001). The FGF-2 solution was applied to cells with the exact volume depending on the size of the culture flask.

2.2.3 Immunofluorescence confocal microscopy

To observe the localisation of proteins (PXDN, FOXC1, PAX6 and PITX2) in cells upon treatment with FGF-2, confocal immunofluorescence (IF) microscopy technique was utilised. IF microscopy employs the use of target specific primary antibodies as well as fluorescent tagged secondary antibodies to visualise localisation and endogenous expression of specific target proteins (Shakes et al., 2012). Glass coverslips were used for seeding of cells in 6 well plates (120 000 cells/well) with the cells incubated for 24 hours to allow them to attach on to the coverslips. DMEM supplemented with 10% FBS was replaced with SFM to starve the cells prior to treatment with FGF-2, as described in the previous (section 2.2.2). Once the treatment period/incubation was complete, cells were washed for 5 minutes with ice cold 1X PBS then fixed on to the coverslips by adding 3% (v/v) formaldehyde in 1X PBS at room temperature for approximately 15 minutes while agitating on a shaker and finally three 5-minute washes were performed in cold 1X PBS. In order to allow antibodies to permeate membrane of the cells, Triton X-100 0.25% (v/v) in 1X PBS was added to the cells at room temperature for 1 hour with

gentle agitation on a shaker and washed three times for 5 minutes with 1X PBS. To reduce non-specificity of antibodies, the coverslips were blocked with Bovine Serum Albumin (BSA) 0.5% (w/v) at room temperature for 30 minutes followed by a single wash of 5 minutes in 1X PBS. A primary antibody listed in **Table 2.1** (1:200) targeting each of the proteins of interest was diluted in 0.25% (BSA) in 1X PBS, added into each corresponding well then incubated at 4 °C overnight with gentle agitation on a shaker. Three 5 minutes washes using 0.5% (w/v) BSA in 1X PBS were performed prior to addition of secondary antibody corresponding to each primary antibody (**Table 2.1**) was diluted in 0.5% (w/v) BSA in 1X PBS then added to each corresponding well then incubated for 2 hours on a shaker at room temperature in the dark. In order to avoid photobleaching of the secondary antibody, all steps after the 2 hours incubation period were performed in the dark. Cells were washed three times for 5 minutes with 1X PBS followed by nuclei staining with 0.1 µg/ml 4',6-diamidino-2-phenylindole (DAPI) for 5 minutes at room temperature with gentle agitation on a shaker. Finally, four 5-minute washes were performed in 1X PBS with the coverslips attached onto the slides using Fluoromount aqueous mounting medium then placed in the dark for 2 hours to allow the Fluoromount to dry. Cells were visualised with the aid of Carl Zeiss LSM 780 confocal microscope using the Zen software (2010), with FITC tagged secondary antibody having excitation of 494 nm and emission of 525 nm, while CFL tagged secondary antibody had excitation of 650 nm and emission of 670 nm.

2.2.4 Protein quantification and Western blot

The quantification of protein expression was achieved by culturing of cells as described in **section 2.2.2** and employing the western blot technique. Western blot was used to identify proteins using molecular weight and protein type via gel electrophoresis (Mahmood and Yang, 2012). The proteins on the electrophoresed gel were transferred to a nitrocellulose membrane which was followed by incubation with specific antibody for target protein (**Table 2.1**). The unbound antibodies were washed off. The thickness of the band was directly proportional to the concentration of the target protein (Mahmood and Yang, 2012).

2.2.4.1 Cell lysate preparation

HEK293 cells were cultured in 10 cm dishes and treated with 2 ng/ml of FGF-2 for 12, 24 and 48 hours, while a 0-hour untreated control served as a negative control. The treatment time points were analysed for differences in contrast to the 0-hour untreated control. The serum medium control which had no FGF-2 but only DMEM supplemented with 10% FBS was used to assess the effect of FGF-2 in contrast with FBS serum in expressing proteins of interest. Once incubation period of cells with FGF-2 was complete, culture medium was discarded with cold 1X PBS used to wash the cells twice. Cells were scraped from the surface of the plate collected into 1 ml of 1X PBS in a 1.5 ml microcentrifuge tube which was centrifuged at 11 000 rpm for 10 minutes at 4 °C to pellet the cells. The pelleted cells were re-suspended in 1X radioimmunoprecipitation assay (RIPA) buffer supplemented with 10 μM Leupeptin as well as 1 mM phenylmethanesulfonylfluoride fluoride (PMSF) protease inhibitors for lysis after discarding the supernatant. Lysis was achieved by vortexing the samples for 1 minute to rupture the cells, then placed on an orbital shaker for 60 minutes with vibration every 5 minutes at 90° angle in a 4 °C walking fridge. To separate proteins from cellular debris, lysates were centrifuged at 12 500 rpm for 5 minutes at 4 °C. Total protein, which was in the supernatant, was aliquoted into autoclaved PCR tubes with one used for quantification and the rest stored at -70 °C for future use.

2.2.4.2 Protein estimation using the Bramhall assay

The normal Bradford assay technique could not be employed due to the high levels of SDS from the 1X RIPA buffer, which was used to lyse the cells, as it interferes with one of the ingredients of Bradford reagent, coomassie blue (Bradford, 1976). Therefore; quantification of total protein from cell lysate resulting from 1X RIPA buffer was achieved with the aid of a modified version of the Bradford assay (Bramhall *et al*., 1969). A container was filled with enough dH_2O to fully soak Whatman™ filter paper (Grade 1) for 20 minutes on a shaker. Then the filter paper was further incubated in ethanol 95% (v/v), 100% (v/v) and acetone 100% (v/v) for 5 minutes in each solution in the order presented here. The filter paper was then placed in a safety cabinet to air dry followed by set up of standard curve using a

stock solution of 1 mg/ml BSA. Different volumes of 1 mg/ml BSA (1 µl, 3 µl, 6 µl, 12 µl, 16 µl and 20 µl) were pipetted across the filter paper separately as well as 2 µl from the cell lysate with unknown protein concentration to create a standard curve for protein estimation in cell samples. The filter paper was then air dried in a safety cabinet and to fix as well as to precipitate the proteins on the filter paper, 7.5% (v/v) trichloroacetic acid (TCA) was used to soak the filter paper for 45 minutes with gentle shaking (Link and LaBaer, 2011). The TCA and 1X RIPA buffer in the samples on the filter paper were removed by briefly rinsing the filter paper with coomassie blue dye. To stain the proteins, the filter paper was then soaked in fresh coomassie blue dye for 60 minutes on a shaker followed by removal of the filter paper from coomassie blue dye into a container filled with a destain solution to remove the dye on sections without proteins on the filter paper. The destain step was carried out for 60 minutes on a shaker followed by air-drying of the paper and each protein sample as well as the standard sample area cut-out. Bradford tubes were filled with 5 ml of elution buffer with the cut-out samples individually placed into each tube followed by overnight incubation in the dark. All eluted samples were pipetted into a 96-well plate by adding 160 µl of each sample per well. The Multiskan GO microplate reader (ThermoFisher Scientific) was used to measure the absorbance at 595 nm and readings used to subsequently plot a standard curve of protein concentration against absorbance using Microsoft Office Excel 2016, with unknown protein concentrations calculated using the equation generated from the standard curve.

2.2.4.3 SDS-PAGE

The dual vertical electrophoresis and electroblotting system Mini-PROTEAN® Tetra Cell and Mini Trans-Blot® Module (Bio-Rad, #1658035) was used to perform reducing SDS-PAGE. To identify PAX6, FOXC1, ACTB and PITX2, total protein of 30 µg for PAX6, FOXC1 as well as ACTB and 40 µg for PITX2 was electrophoresed on either a 10% or 12% separating gel with 5% stacking gel while PXDN was detected in total protein of 150 µg electrophoresed on 8% separating gel with 5% stacking gel. Extracted protein lysate was mixed with a 4X protein loading buffer in a 3:1 ratio with the mixture placed in boiling water for 5 to 7

minutes to induce protein denaturation. The SDS-PAGE gel and running buffer were placed in the tank and the boiled samples were briefly vortexed then centrifuged prior to loading into the gel. The gel was electrophoresed at a constant voltage of 180V until the dye front had just run-off of the gel into the buffer for PXDN since it was a big protein. The colour pre-stained protein standard ladder (New England Biolabs # P7712) was used to measure sizes of proteins of interest prior to transfer of proteins from gels to nitrocellulose membranes.

2.2.4.4 Electrophoretic Transfer and Antibody Probing

Upon completion of electrophoresis, the SDS-PAGE gel was removed from the tank and placed in a container with transfer buffer. Using the protein ladder markers, the sizes that flanked target proteins of interest were excised then placed into transfer buffer. The remaining gel pieces which were not of interest were placed in a beaker containing coomassie blue dye (protein staining) for 60 minutes followed by replacement of the coomassie blue with a destain solution overnight to assess the quality of the electrophoresis. The gel sizes of interest were placed on to a nitrocellulose membrane of similar size then sandwiched between fibre pad and filter paper finally placed into the transfer tank filled with ice cold transfer buffer. The electrophoretic transfer was carried out at a constant current of 300 mA for 2 hours (PAX6, FOXC1, PITX2 and β-ACTIN) and 3 hours (PXDN) at 4 °C and upon completion the SDS-PAGE gels were placed into a beaker with coomassie blue dye for 60 minutes then destained overnight to assess the quality of the transfer. 1X Tris buffered saline with Tween-20 (TBS/T) was used to rinse the nitrocellulose membranes prior to blocking the membranes in blocking buffer for 60 minutes at room temperature with gentle shaking. The nitrocellulose membranes were then individually washed five times for 5 minutes in 1X TBS/T on a shaker at 180 rpm. Once the washes were completed, the membranes were placed into primary antibody solutions which were prepared either in 5% (w/v) BSA or fat-free powder milk diluted in 1X TBS/T then incubated at 4 °C overnight with gentle agitation. Then the nitrocellulose membranes were washed four times for 5 minutes in cold 1X TBST prior to them being incubated with a corresponding horse radish peroxidase-conjugated secondary antibody (HRP) diluted in 5% (w/v) fat-free milk

in 1X TBS/T for 1 h at RT in the dark, with gentle agitation. Nitrocellulose membranes were washed another four times with cold 1X TBS/T and taken to a dark room for visualisation. All the antibodies used in the current study were purchased from Sigma-Aldrich and Santa Cruz biotechnology, as indicated in **Table 2.1**.

2.2.4.5 Protein Visualisation and Quantification

Chemiluminescence substrates (WesternBright^{TM} Advansta) A and B were mixed into a microcentrifuge tube wrapped in foil in a 1:1 ratio, according to manufacturers' instructions, then added onto each nitrocellulose membrane for about 2 minutes to allow the signal to develop between the HRP and chemiluminescent reagents. The excess substrate was poured off on to a piece of paper towel with the membranes then covered in a plastic wrap. X-ray films were used to detect bands by exposing them to the nitrocellulose membranes then developing using the following solutions in the same order: placing the exposed X-ray film into a developer solution, rinsed in water, placed into a fixer solution, one final rinse in water then allowed to air dry. The x-ray film for each protein after performing biological triplicates (n=3) were scanned and saved as TIF images of which were uploaded onto Image Studio Lite Software (version 5.2.5) to capture signal values used to quantify intensity of the developed bands via densitometric calculations.

2.2.5 Chromatin immunoprecipitation assay

2.2.5.1 Analysis of the *PXDN* promoter region and ChIP-PCR primer design

The interaction of PAX6, FOXC1 and PITX2 with the *PXDN* gene promoter was determined by employing the technique of chromatin immunoprecipitation (ChIP) followed by PCR. ChIP is a technique that is used to determine whether a given protein binds to or is localized to a specific DNA sequence in vivo (Gavrilov et al., 2009). A bioinformatics analysis of *PXDN* gene promoter was conducted using JASPAR software (Mathelier et al., 2016) and CONTRAV3 (Kreft et al., 2017). The *PXDN* promoter sequence of 5000 base pairs (bp) from the translation start site (TSS) was uploaded to both JASPAR and CONTRAV3 to scan for any putative

binding sites for PAX6, FOXC1 and PITX2. Using default settings on both databases, putative binding sites with sequences on either the sense or antisense strand were generated for all three transcription factors of interest (**Table 2.2**) and polymerase chain reaction (PCR) primers flanking each potential binding site were designed.

Table 2.2: Putative binding sites of PAX6, FOXC1 and PITX2 in the *PXDN* gene promoter covering 5000 bp upstream of the translation start site (+1).

Transcription Factor (TF)	Predicted binding site (Sequence)	Position From TSS (bp)	Database
PAX6	ATGTAGAGCGTGAA	-1802/-1788	JASPAR
	AACTGGAGTGTGAA	-2277/-2263	
	AACTGGAGTGTGAA	-2396/-2382	
FOXC1	AATGTAAACTG	-2782/2771-	JASPAR
	AGTGTAAACTG	-2211/2200-	
	TGTGTGAATAG	-1654/-1643	
	TGTGTGAATAG	-1537/-1526	
	TCATTTTCCCA	-677/-666	
	ATAATTTCCTA	-506/-495	
PITX2	GGATCA	-432/-426	JASPAR
	TCTAATCTGA	-3269/-3279	CONTRAV3

The designed primers amplified regions covering the putative binding sites and another set was designed to serve as a negative control containing no putative binding site. In addition, known target genes of PAX6, FOXC1, and PITX2 were selected from the literature to use as known targets of the transcription factors to server as positive controls. **Table 2.3** shows ChIP-PCR primers for transcription factor PITX2, PAX6, FOXC1 target: *PXDN* and known targets Inhibin Subunit Beta A (*INHBA*), Wnt Family Member 5A (*WNT5A*) and Heat Shock Protein Family A (*HSPA6*), respectively. The ChIP-PCR primers were designed with the aid of National centre for biotechnology information (NCBI) primer blast online bioinformatics tool (Ye et al., 2012). The putative binding sites listed in **Table 2.2** as well as few flanking nucleotides were individually loaded onto primer blast to generated region specific primers to amplify each putative binding sites and these primers are listed in **Table 2.3** below.

We identified six putative FOXC1 binding sites $PXDN^{FOXC1}$ (A-F), three sites for PAX6 $PXDN^{PAX6}$ (A-C), only two sites for PITX2 $PXDN^{PITX2}$ (A-B) and the negative control primers amplifying a region with no known putative binding sites on *PXDN* gene promoter $PXDN^{Negative}$. PCR primers that flank the multiple cloning site of the pGL4.10 vector were designed as described above with the aid of Primer Blast and were used to amplify successfully ligated putative binding sites in preparation for luciferase assay.

Table 2.3: ChIP-PCR primers for target and control genes for each putative binding site on *PXDN* promoter region.

Primer	Forward (5'-3')	Reverse (5'-3')	Annealing Temperature (°C)	Amplicon Size
PXDN$^{\text{Foxc1 A}}$	ATGGCATCTGCATCTGGACC	AAAGATTCCAGTGGGTCCGC	50	540 bp
PXDN$^{\text{Foxc1 B}}$	TGGGACCCAAACTCAACCAC	CTCACAGTCCAGAAGCCGTT	60	547 bp
PXDN$^{\text{Foxc1 C}}$	GCACCGGTGGAATGTGTAGA	GCAGACATCTCTCCTGCAA	50	334 bp
PXDN$^{\text{Foxc1 D}}$	TGGACCCACTTCTGTGTGTG	CCGGATTCCATTTCTCCTGC	50	111 bp
PXDN$^{\text{Foxc1 E}}$	TCTGAATCTGGCACCGTCACCCTG	AAAGCCCCTCATTCCTTTTGAGGA	55	476 bp
PXDN$^{\text{Foxc1 F}}$	CAGACTCCCTTGCTGTGCGCTTTG	AGCTGTGCACATGCGCGAGGCT	58	471 bp
PXDN$^{\text{Pax6 A}}$	TGGGACCCAAACTCAACCAC	CATCCCAACCTCTCACTCAAG	50	339 bp
PXDN$^{\text{Pax6 B}}$	ACTGGACCCACTTGAGTGTA	CTCACAGTCCAGAAGCCGTT	50	180 bp
PXDN$^{\text{Pax6 C}}$	GCACCGGTGGAATGTGTAGA	CCGGATTCCATTTCTCCTGC	50	464 bp
PXDN$^{\text{PITX2 A}}$	ATGGCATCTGCATCTGGACC	AAAGATTCCAGTGGGTCCGC	50	540 bp
PXDN$^{\text{PITX2 B}}$	CAGACTCCCTTGCTGTGCGCTTTG	AGCTGTGCACATGCGCGAGGCT	58	471 bp
PXDN$^{\text{Negative}}$	GAAGACGGTGGGAACCAGG	GCCCCTTCTCTCCACAAACA	50	139 bp
HSPA6$^{\text{Foxc1+}}$	GTAGGGTGAGTGCCCCTCTT	GGGAAAATAGCAGTGCAGGA	50	196 bp
HSPA6$^{\text{Foxc1-}}$	CCCAAAGGCTTTCAGAAGCAGA	CATTGTAAGTCTCAATCCTCTCCTC	50	189 bp
WNT5A$^{\text{Pax6+}}$	GACACAATTTGGGGCTGACT	ACAGACACACACCCCAACAC	50	145 bp
WNT5A$^{\text{Pax6-}}$	AGCCAGCACAAGGAGGAATC	TACGGCCCACCCATTCATTC	50	308 bp
INHBA$^{\text{Pitx2+}}$	GGCTTATGTGTGGGAAAGAA	ACCAGTGCATTCATAGACAG	50	265 bp
INHBA$^{\text{Pitx2-}}$	TGTTTGCTCTAGGAGAAAGGC	CAATGTTCCTCTTGGGCAACC	50	301 bp
pGL4.10	CTAGCAAAATAGGCTGTCCC	TTCATGGCTTTGTGCAGCT	60	243 bp

2.2.5.2 Phenol-Chloroform gDNA extraction and optimisation of primers

The DNA used for primer optimisation was extracted using Phenol Chloroform method (Green and Sambrook, 2017). HEK293 cells were cultured in 10 cm dishes with the medium aspirated then cells washed three times with 10 ml of ice cold 1X PBS followed by scraping of the cells into 1 ml of 1X PBS. The scrapped cells were collected into a microcentrifuge tube and centrifuged for 5 minutes at 4 °C at 5000 rpm. The 1X PBS was removed with the pellet resuspended in 50 µl of cold 1X PBS and 450 µl of lysis buffer which was supplemented with 1 µl RNase A (ThermoFisher Scientific) from stock concentration of 20 µg/ml followed by 60 minutes incubation at 37 °C. Protein digestion and removal was achieved by addition 2.37 µl of Proteinase K (ThermoFisher Scientific) from stock concentration of 21.2 mg/ml incubated for 2 hours at 50 °C followed by gentle agitation of the sample every 20 minutes. Phenol (Buffered), Chloroform and 2-Propanol were mixed at a ratio of 25:24:1 respectively, with phenol (half the total volume of the lysate) added to the sample and briefly vortexed. This was subsequently followed by addition of chloroform:2-propanol (24:1) to make up the remaining half of the total volume of the total lysate. The mixture was briefly vortexed and centrifuged for 25 minutes at 13 000 rpm at room temperature. The supernatant (upper aqueous phase) was transferred into a new microcentrifuge tube and Phenol:Chloroform:2-propanol in equal volume of the supernatant was added to the upper aqueous phase then vortexed briefly finally centrifuged at room temperature for 25 minutes at 13 000 rpm. The new upper aqueous phase was transferred into a new microcentrifuge tube and an equal amount of Chloroform:2-Propanol without Phenol was added then centrifuged for 25 minutes at 13 000 rpm at 4 °C with this step repeated once in a new microcentrifuge tube. The final aqueous phase was transferred into a new microcentrifuge tube with 3M sodium acetate ($1/10^{th}$) and 100% ethanol (v/v) (2 volumes) added to the tube followed by overnight incubation at -20 °C. The sample was then centrifuged at 13 000 rpm at 4 °C to collect the DNA, then the pellet was washed three times for 5 minutes with 70% ethanol (v/v) at 13 000 rpm. The excess DNA was discarded with the DNA pellet air dried then resuspended 50 µl of 10 mM Tris-HCl buffer pH 7.8 and finally quantified with NanoDrop one spectrophotometer (ThermoFisher Scientific) then

stored at -20 °C. The DNA was then diluted into a working concentration for use in optimisation of the PCR primers listed in Table 2.3 in order to obtain optimum annealing temperature for each primer set.

2.2.5.3 ChIP protocol

ChIP was performed on HEK293 cells which were cultured in 10 cm dishes until the confluency reached 70% with the DMEM medium aspirated and fresh serum free DMEM added to the plates overnight to starve the cells. Using data from confocal microscopy and western blot analysis, a single time point which showed elevated expression levels of each protein, or clear nuclear localisation, was selected. The cells were treated with 2 ng/ml of FGF-2 for the selected time points. Once treatment was complete, serum free medium was aspirated and fresh DMEM with 10% FBS (v/v) as well as 1% (v/v) formaldehyde were added to each plate to cross link protein-DNA interaction for 10 minutes with gentle agitation at room temperature. This was followed by addition of 125 mM glycine to the plates for 5 minutes to quench the proteins which were now crosslinked to DNA. The mixture of DMEM, formaldehyde and glycine solution was discarded from the plates with the cells washed for 5 minutes three times with 1X PBS. The cells were scrapped in 1 ml cold 1X PBS into 1.5 ml microcentrifuge tube then centrifuged for 5 minutes at 4 °C and 5 000 rpm to collect cell pellet. Each cell pellet was resuspended in 300 µl of 1X RIPA lyses buffer supplemented with 1.25 µl of 0.1M PMSF as well as 0.5 µl of 10 mM Leupeptin protease inhibitors then vortexed to lyse the cells. The samples were sonicated using Qsonica (Q125) probe sonicator at 60% amplitude with 15 seconds on and 30 seconds off with cooling on ice for a total of 25 minutes per sample. Samples were then centrifuged at 10 000 rpm for 10 minutes at 4 °C to collect cellular debris and the supernatant transferred into a new microcentrifuge tube. To ensure that fragmented DNA was within the 1000 bp range, 5 µl of the sonicated DNA was loaded then resolved on 1.5% (w/v) agarose gel at 100 V for 45 minutes. 50 µl of the sonicated DNA was set aside to use as input control DNA after extraction. ChIP dilution buffer (900 µl) supplemented with 10 mM Leupeptin and 0.1M PMSF was added to 100 µl of sonication lysate in a 1:10 dilution for each protein of interest and a no antibody control tube. In each tube, 5 µl of antibody

specific to each protein of interest was added to the corresponding tube except in the no antibody control tube. The tubes were placed on a rotator for 4 hours in a 4 °C Walk-In fridge, which was followed by addition of 20 µl protein A/G beads (sc-2003) to each tube then returned to the rotator for overnight incubation at 4 °C. The following washes were performed in a walk-In fridge at 4 °C on a rotator. The tubes were centrifuged at 5 000 rpm for 1 minute with the supernatant discarded and the protein A/G beads (bound to Antibody-protein-DNA) resuspended in 1 ml of ChIP wash buffer. The beads were washed three times at 20 rpm for 1 minute followed by 1 minute centrifugation to remove the ChIP wash buffer. The above step was repeated once with 1 ml of ChIP final wash buffer with the sample then kept on ice after discarding the wash buffer. In each tube, 120 µl of ChIP elution buffer (pre-warmed) was added then incubated at 65 °C in a water bath for 1 hour with the tubes briefly vortexed/flicked every 15 minutes to reverse the protein-DNA crosslinks. The tubes were then centrifuged for 1 minute at 5 000 rpm with the supernatant transferred into a new microcentrifuge tube for purification with the aid of GeneJET PCR Purification Kit/Zymogen DNA clean and concentrator kit and the clean DNA was eluted in 50 µl 10 mM Tris-HCl pH 7.8 then used in ChIP PCR.

2.2.5.4 ChIP-PCR

The PCR primers in **Table 2.3** were used to amplify across the putative binding sites from the clean sonicated DNA. The PCR reaction was optimised and each of the required components were prepared as follows: KAPA Taq Ready Mix with dye 12.5 µl, 0.6 µl for reverse as well as forward primers, 8.4 µl of clean ChIP DNA with nuclease free water added to top up the PCR reaction mix to a total of 25 µl. The PCR products generated from GeneAmp® PCR system 2700 were loaded directly (KAPA Taq has preloaded loading dye) on to 50 ml 1.5% (w/v) agarose gel stained with 1 µl of 10 mg/ml ethidium bromide stock and resolved at 100 V for 45 minutes in 1X TAE buffer. MassRuler low range DNA ladder (ThermoFisher Scientific) was used as molecular weight marker and the Bio-Rad Gel Doc XR system as well as Image Lab software version 6.0 (Bio-Rad) used to visualise PCR bands and capture images.

2.2.6 Luciferase reporter assay

Due to time constraints the project had to be submitted with the last objective for luciferase assay in progress. The Appendix F contains methods employed in preparation of luciferase assay as well as partial results obtained thus far.

The ability of PAX6 to drive PXDN expression from the *PXDN* promoter was determined using luciferase reporter assays. Only oligonucleotides for PAX6 transcription factor as well as the know target control gene *WNT5A* were designed due to time constraints resulting from delays experienced due to COVID-19 pandemic. The reasons for selection of PAX6 out of the three initially chosen transcription factors are stated in **section 2.1.2** above with PAX6 selected due to its ability to regulate FOXC1 and PITX2. The principle of luciferase reporter assay involves cloning of a reporter gene with a DNA sequence of interest into an expression vector that is then transfected into cells. Following transfection, the cells were assayed for the presence of the reporter by directly measuring the reporter protein itself or the enzymatic activity of the reporter protein (Allard and Kopish, 2008). The current study used Dual-Glo reagent (Promega) to conduct luciferase reporter assays with the enzymatic activity within transfected cells generating light, of which its intensity was directly proportional to the expression levels of the firefly luciferase enzyme translated in the transfected cells from the reporter gene.

2.2.6.1 Vector constructs preparation for luciferase

To create vectors containing the putative binding sites, we designed oligonucleotide sequences, as in **Table 2.4** below. This included the design of two negative control region (no PAX6 binding site) on *PXDN* as well as *WNT5A* gene promoter region. In addition, oligonucleotides sequences, in which conserved nucleotides from the putative binding sequences were mutated, served as controls.

Oligonucleotide sequences for each putative binding site and negative control (with no putative binding site) were modified with recognition sites sequences for restriction enzymes (RE) KpnI (5’ -end) as well as EcoRV (3’ -end), for directional cloning. The modified oligonucleotide sequences (both forward and

complementary reverse sequences) were ordered from Inqaba biotech with the lyophilised oligonucleotides resuspended in oligonucleotide annealing buffer (Appendix C). The complementary sequences for each putative binding site were mixed together in equimolar concentrations of 2 µg in 50 µl annealing buffer. The 50 µl reaction of mixed oligos (i.e., forward and reverse sequences) was prepared in a PCR tube which was incubated in a thermocycler at 95 °C for 5 minutes followed by gradual cooling over 45 minutes at 25 °C. The mixed oligos were then quantified using NanoDrop™ One (ThermoFisher Scientific) by first adding 5 µl of annealed oligos to 45 µl of nuclease-free water with the concentrations recorded. A double digest restriction was used for both the oligonucleotides and pGL4.10 as follows (**Figure 2.1**): The RE mixture comprised of 1 µl of KpnI and EcoRV (New England Biolabs), 5 µl of r2.1 10X buffer (New England Biolabs), DNA (Annealed oligos/pGL4.10) and nuclease free water up-to 50 µl volume. The mixture was incubated at 37 °C for 25 minutes followed by heat inactivation at 80 °C for 20 minutes. The restricted DNA was cleaned using the Zymo Research DNA clean-up and concentrator kit, according to manufacturers' instructions. Then the restricted oligo DNA and restricted pGL4.10 vector was used for ligation to generate vector constructs. T4 Ligase enzyme (New England Biolabs) was used to ligate 50 ng pGL4.10 vector DNA in a 3:1 ratio to the insert DNA which was then incubated at 16 °C for 18 hours followed by heat inactivation at 65 °C for 10 minutes.

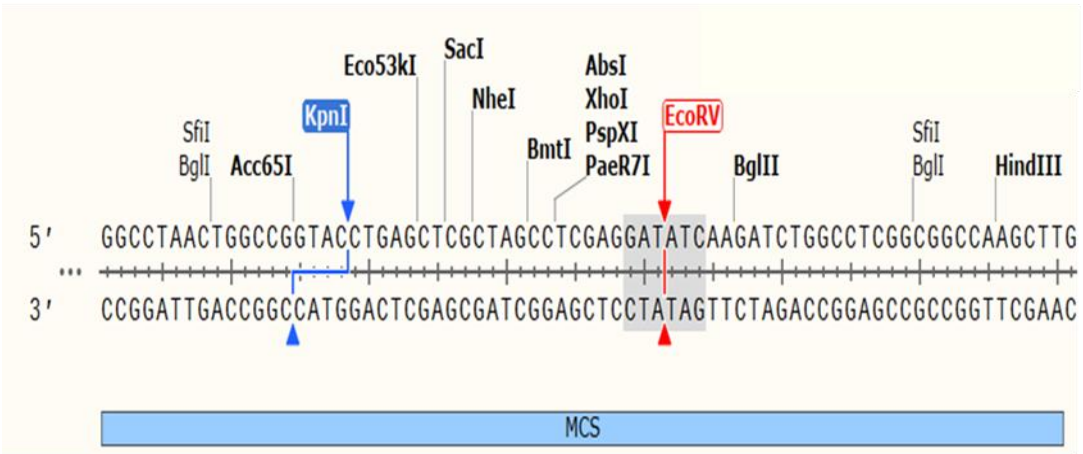

Figure 2.1: The multiple cloning site (MCS) of pGL4.10 vector prior to restriction digest. KpnI (blue) RE was used to generate sticky ends while EcoRV (red) was used to produce blunt end in a double digest reaction mix.

Table 2.4: Wild type and mutant oligonucleotide sequences for putative binding sites for PAX6 and WNT5A.

Sequence	Name	Oligonucleotides sequences of putative binding site
Wild type	PAX6 A	F = 5'-GGTACCAGAGATGGCAACTGGAGTGTGAACTGCAGATATC-3' R = 5'-GATATCTGCAGTTCACACTCCAGTTGCCATCTCTGGTACC-3'
	PAX6 B	F = 5'-GGTACCAGAGATGGCAACTGGAGTGTGAACTGGAGATATC-3' R = 5'-GATATCTCCAGTTCACACTCCAGTTGCCATCTCTGGTACC-3'
	PAX6 C	F = 5'-GGTACCAGAGAGCACATGTAGAGCGTGAACTGGAGATATC-3' R = 5'-GATATCTCCAGTTCACGCTCTACATGTGCTCTCTGGTACC-3'
Mutant	PAX6 A	F = 5'-GGTACCAGAGATGGCAAGTGCAGAACCAACTGCAGATATC-3' R = 5'-GATATCTGCAGTTGGTTCTGCACTTGCCATCTCTGGTACC-3'
	PAX6 B	F = 5'-GGTACCAGAGATGGCAAGTGCAGAACCAACTGCAGATATC-3' R = 5'-GATATCTGCAGTTGGTTCTGCACTTGCCATCTCTGGTACC-3'
	PAX6 C	F = 5'-GGTACCAGAGAGCACAGGTGCAGAATGAACTGGAGATATC-3' R = 5'-GATATCTCCAGTTCATTCTGCACCTGTGCTCTCTGGTACC-3'
Negative	$PXDN^{PAX6-}$	F = 5'-GGTACCGAGGGGTGCACAGAGGGAGCCACCCAACGATATC-3' R = 5'-GATATCGTTGGGTGGCTCCCTCTGTGCACCCCTCGGTACC-3'
Wild type	$WNT5A^{PAX6+}$	F = 5'-GGTACCAAAAAGCCATGCGCGCCTGATTGTTCTGGATATC-3' R = 5'-GATATCCAGAACAATCAGGCGCGCATGGCTTTTTGGTACC-3'
Mutant	$WNT5A^{PAX6+}$	F = 5'-GGTACCAAAAAGCCAAGCGGAAGGGCTACTTCTGGATATC-3' R = 5'-GATATCCAGAAGTAGCCCTTCCGCTTGGCTTTTTGGTACC-3'
Negative	$WNT5A^{PAX6-}$	F = 5'-GGTACCGAGCTAAGAGGCCACAGGCCTAACGACAGATATC-3' R = 5'-GATATCTGTCGTTAGGCCTGTGGCCTCTTAGCTCGGTACC-3'

F= Forward; R= Reverse; Red highlight= Putative binding site sequence; Bold= conserved mutated nucleotides.

2.2.6.2 Competent *E. coli* cells preparation

Competent cells (JM109 *E. coli*) required for transformation were prepared by inoculating *E. coli* in a falcon tube with 2% (w/v) LB broth and placed on a shaker in a 37 °C incubator overnight. Fresh 50 ml of 2% (w/v) LB broth was prepared with 0.5 ml of the previously overnight grown *E. coli* added then incubated at 37 °C with shaking for approximately 2 hours or till the absorbance at 600 nm is between 0.4 to 0.6 (arbitrary units) with the LB broth (without *E. coli*) used as a blank sample. *E. coli* was centrifuged at 5000 rpm for 10 minutes at 4 °C to collect the cells. The supernatant was discarded and the cells placed on ice then resuspended in 10 ml ice cold 0.1 M $MgCl_2$ and incubated for 30 minutes on ice. The cells were collected via centrifugation at 4 for 10 minutes at 4000 rpm with the supernatant discarded and the cells resuspended in 1 ml ice cold 0.1 M CaCl2 supplemented with 15% (v/v) glycerol. The cells were aliquoted into 50 µl pre-chilled 1.5 ml microcentrifuge tubes and stored at -80 °C. This protocol was

modified from Chang et al., (2013) with both $CaCl_2$ and $MgCl_2$ used in the current study.

2.2.6.3 Transformation and Colony PCR

Transformation of competent *E. coli* was achieved by thawing a vial of 50 µl aliquot on ice followed by addition of 5 µl of ligation mixture then incubated on ice for 30 minutes. The sample was transferred to a water bath for heat shock at 37 °C for 5 minutes which was followed by a 5 minutes incubation on ice and finally addition of 950 µl of pre-warmed 2% (w/v) LB broth then incubated for 1 hour at 37 °C with shaking to perform an outgrowth step which enables the bacteria to develop antibiotic resistance. The bacteria were then spread on LB agar plates supplemented with ampicillin (100 µg/ml) followed by incubation at 37 °C for 24 to 48 hours depending on the rate of growth of single colonies.

Colony PCR was employed in order to detect the colonies which had the insert of interest. Individual colonies were picked from the LB agar plate using a sterile P10 tip and resuspended in pre-warmed 50 µl of 2% LB broth then incubated for 1 hour with shaking at 37 °C to enable bacterial growth. The samples were then placed on ice to stop bacterial growth with 8 µl used as DNA for a PCR reaction mix comprising of 12.5 µl KappaTaq ReadyMix, 1 µl of pGL4.10 forward as well as reverse primers and topped up to a total of 25 µl with nuclease free water. The PCR products were then resolved on a 1.5% (w/v) agarose gel at 100 V for 45 minutes. Since the pGL4.10 primers amplify across the multiple cloning sites of the vector, the colonies which produced an expected size bigger (252 bp) than that of the control (243 bp) were prepared for alkaline lysis extraction. The resulting volume of 42 µl of the samples with the insert were added into a falcon tube with 5 ml of fresh 2% LB broth supplemented with (100 µg/ml) ampicillin followed by overnight incubation at 37 °C with shaking.

2.2.6.4 Alkaline Lysis

The 5 ml of successfully transformed bacteria was prepared for alkaline lysis with 1 ml added into a 1.5 ml microcentrifuge tube containing 250 µl of autoclaved

glycerol then stored at -80 °C. The remaining 4 ml of successfully transformed *E. coli* was centrifuged at 12000 rpms for 60 seconds at 4 °C to pellet the cells and the supernatant discarded. The pellet was resuspended in 150 µl of alkaline lysis solution I followed by vortexing briefly and addition of 200 µl of alkaline lysis solution II with the tube inverted 5-6 times. Alkaline lysis solution III was added to the tube (300 µl) then mixed by inverting the tube 5 to 6 times followed by centrifugation at 14000 rpm for 5 minutes with the supernatant transferred into a clean 1.5 ml microcentrifuge tube. Isopropanol was added to the supernatant in equal volume (1:1 ratio) with the tube inverted to mix the solution followed by 30 minutes incubation at -80 °C. The sample was then centrifuged for 5 minutes at 14 000 rpm with the supernatant discarded and 600 µl of 70% (v/v) ethanol added to the DNA pellet to precipitate then centrifugation repeated at 14000 rpm for 5 minutes. The supernatant was discarded with the DNA pellet air-dried for 10-30 minutes followed by resuspension with 50 µl of 10 mM Tris-HCl at pH 7.8 then stored at -20 °C after quantification with Nanodrop™ One (ThermoFisher Scientific). Sanger sequencing (carried out by Inqaba Biotech) was performed on all the successfully ligated recombinant DNA using the pGL4.10 primers to confirm presence and sequence of the insert of interest as well as the orientation prior to use of the transformed pGL4.10 vectors in luciferase reporter assay.

2.2.6.5 Luciferase reporter assay

HEK293 cells can endogenously express PAX6, FOXC1, PITX2 and PXDN proteins and have a high transfectability rate. In 200 µl SFM (DMEM), HEK293 cells with the density of $0.5 – 1.2 \times 10^4$ were seeded per well followed by incubation at 37°C with 5% CO_2 for 24 hours. The cells were further treated with 2 ng/ml FGF-2 for 24 hours. The transfection of DNA constructs (pGL4.10 plasmid) into HEK293 cells was setup by preparing 20 µl transfection reaction which comprised of 0.2 µg DNA construct diluted in 20 µl serum free medium. This was followed by addition of 2 µl of Turbofect transfection reagent (ThermoFisher Scientific) to the DNA-Serum free medium solution vortexed briefly and finally incubated for 30 minutes at room temperature. The transfection reagent-DNA mix was added into each well (20 µl) in a dropwise manner without discarding the initial 200 µl serum

free medium in each well followed by incubation of the cells at 37°C for 24 hours. Once transfection was completed, luciferase assay was performed by addition of Dual-Glo luciferase reporter assay reagent (Promega) as outlined in the assay protocol as per manufacture's instruction and luciferase reporter gene expression emitted in a form of light was measured with the aid of VICTOR Nivo® multimode plate reader (PerkinElmer®).

2.2.7 Statistical analysis

In this chapter, all results were representative of three independent experiments. Analyses of data and comparisons was done using paired Student's *t*-test where relevant; a $P < 0.05$ will be considered significant.

2.3 Results

2.3.1 Expression of PXDN, PAX6, FOXC1 and PITX2 in response to FGF-2

The three potential regulators of PXDN were observed for localisation using immunofluorescence microscopy upon treatment with 2 ng/ml of recombinant FGF-2 in HEK293 cells as depicted by the figures below. FITC (Green) and CFL (Red) conjugated secondary antibodies were used to target proteins of interest while the nucleus was counter-stained with DAPI (Blue). PXDN protein showed localisation in the ECM with the expression levels increasing from untreated (0 hours control) to 12 hours treatment with expression levels decreasing after 24- and 48-hours treatment time points. The serum medium control which had no FGF-2 treatment showed low expression levels of PXDN (**Figure 2.2**).

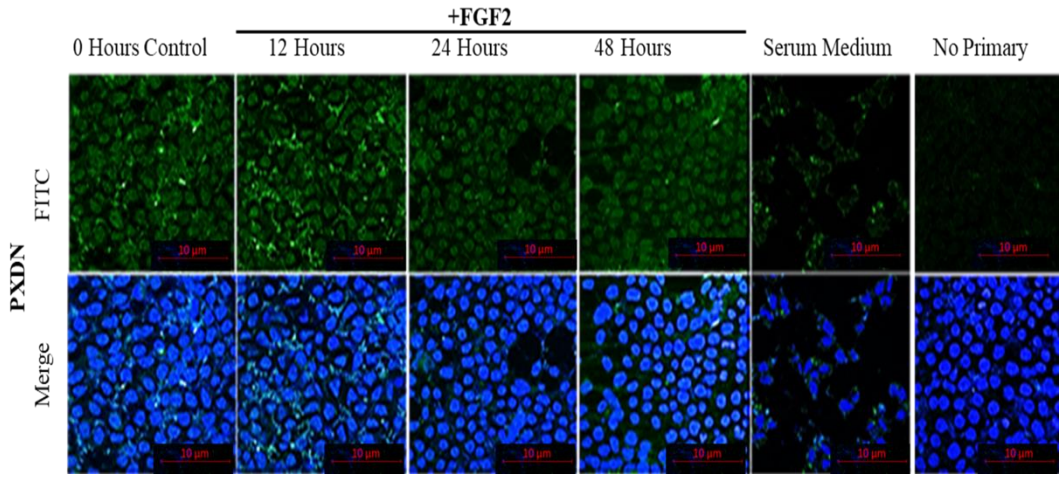

Figure 2.2: PXDN localisation in response to 2 ng/ml FGF-2 observed with the aid of Immunofluorescence confocal microscopy in HEK293 cells. PXDN is localised in the ECM and the nuclei was stained blue with DAPI. Increase in fluorescence of green shows elevated expression while a decrease in fluorescence indicates low expression levels across the different treatment time points (63X magnification; scale bar = 10µm).

The transcription factor FOXC1 (**Figure 2.3**) was found to be localised in the nucleus and varying expression patterns were observed across the selected time points with 12- and 48-hours treatment with FGF-2 showing elevated expression as the green FITC fluorescence is intensified, while the untreated 0-hour control as well as 24-hour time points showed lower levels of FOXC1 protein in contrast.

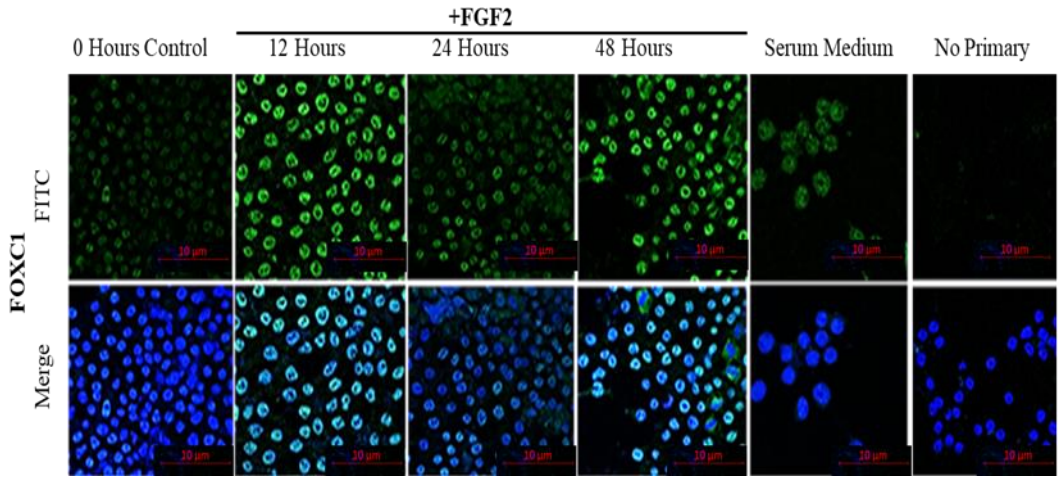

Figure 2.3: FOXC1 localisation in response to 2 ng/ml FGF-2 observed with the aid of Immunofluorescence confocal microscopy in HEK293 cells. FOXC1 localised in the nucleus and shown by FITC (green) secondary antibody while the nuclei were stained blue with DAPI (63X magnification; scale bar = 10μm).

PAX6 expression levels in HEK293 cell line (**Figure 2.4**) showed localisation in the nucleus with a constant expression level or similar expression pattern in both the presence of FGF-2 (for 12, 24 and 48 hours) as well as in its absence (0-hour control). Also, the no primary control showed specific fluorescence within the nucleus which is non-specific autofluorescence since no primary antibody was added therefore leading to no interaction with the secondary antibody.

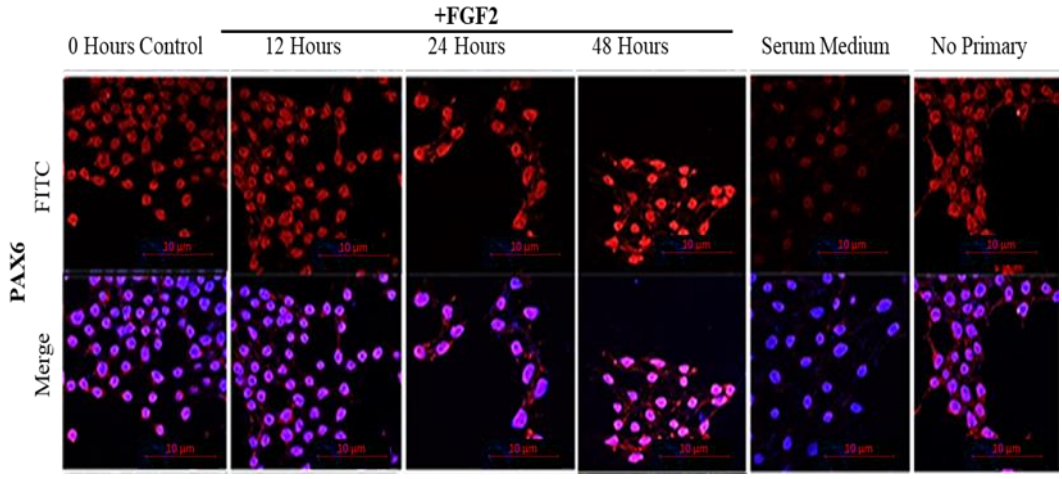

Figure 2.4: PAX6 localisation in response to 2 ng/ml FGF-2 observed with the aid of Immunofluorescence confocal microscopy in HEK293 cells. PAX6 showed nuclear localisation and shown by CFL (Red) secondary antibody while the nuclei were stained blue with DAPI (63X magnification; scale bar = 10μm).

PITX2 likewise was localised in the nucleus (**Figure 2.5**) with the no primary control showing scattered non-specific minimal fluorescence while the untreated 0-hour control showed presence of the protein with the fluorescence decreased in 12 hours' time point then was increased in 24 as well as 48 hours' time points.

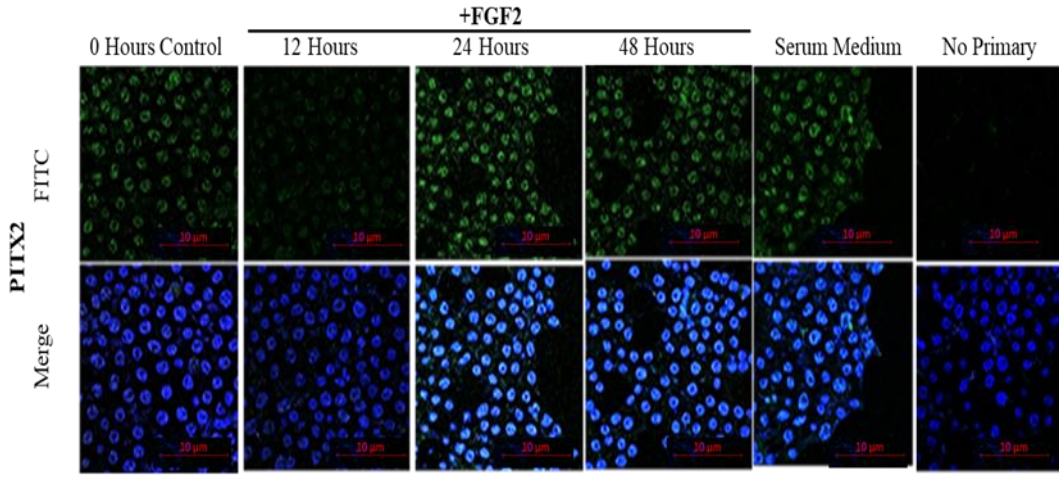

Figure 2.5: PITX2 localisation in response to 2 ng/ml FGF-2 observed with the aid of Immunofluorescence confocal microscopy in HEK293 cells. PITX2 localised in the nucleus and shown by FITC (green) secondary antibody while the nuclei were stained blue with DAPI (63X magnification; scale bar = 10μm).

2.3.2 Quantification of PXDN, PAX6, FOXC1 and PITX2 proteins in response to FGF-2

The effect of FGF-2 on PXDN (165 kDa), PAX6 (47 kDa), FOXC1 (75 kDa) and PITX2 (32 kDa) protein expression in HEK293 cells was quantified with the aid of western blot technique. Quantification of each protein was replicated three times with the signal readings of densitometry averaged and normalised with ACTB (43 kDa). The treatment time points (FGF2 + SFM) as well as the serum medium only control were analysed for significance in expression levels in comparison with the untreated 0 hours control to assess the effect of FGF2. PXDN expression levels showed an increase 414 ± 112%in PXDN at 12 hours FGF-2 treatment, relative to the 0-hour time point, with PXDN levels reducing to 185 ± 48% at 24 hours and 171 ± 86% at 48-hours. The serum medium control showed an increase of 190 ± 37%, relative to the control (**Figure 2.6**). The expression pattern of PXDN as indicated by western blot data was similar to the immunofluorescence confocal microscopy data as depicted by (**Figure 2.2**).

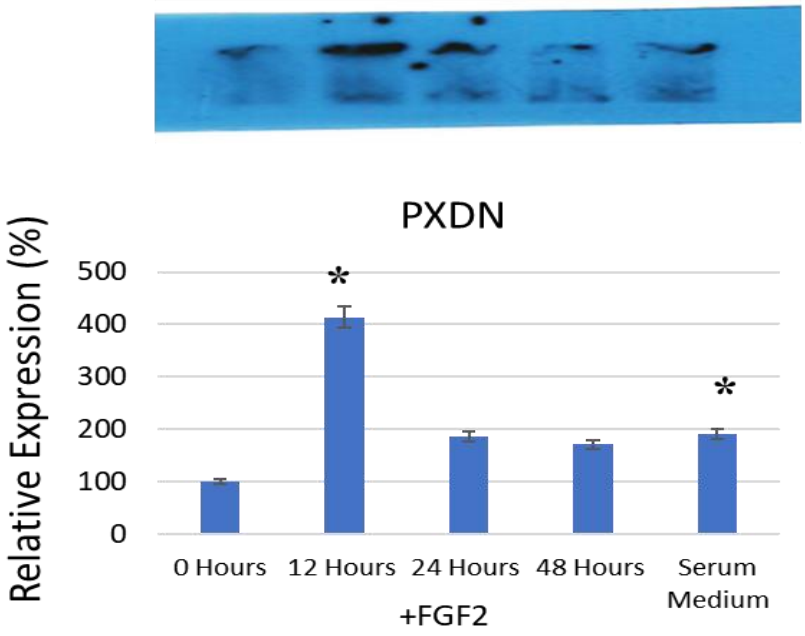

Figure 2.6: Western blot analysis of the effect of 2 ng/ml FGF-2 on protein expression of PXDN. PXDN was detected in all treatment time points with 12 hours' time point showing highest expression levels and a reduced expression through 24 and 48 hours. (n = 3, mean ± SD), P ≤ 0.05 = *..

Expression patterns of FOXC1 showed varying protein levels with a steady gradual increase of 154 ± 15%, 153 ± 17%, 166 ± 5% and 128 ± 11% for 12, 24, 48 hours and serum medium control respectively (**Figure 2.7**). The results partially match the data from confocal microscopy with 12- and 48-hours treatment time points showing highest expression levels of FOXC1.

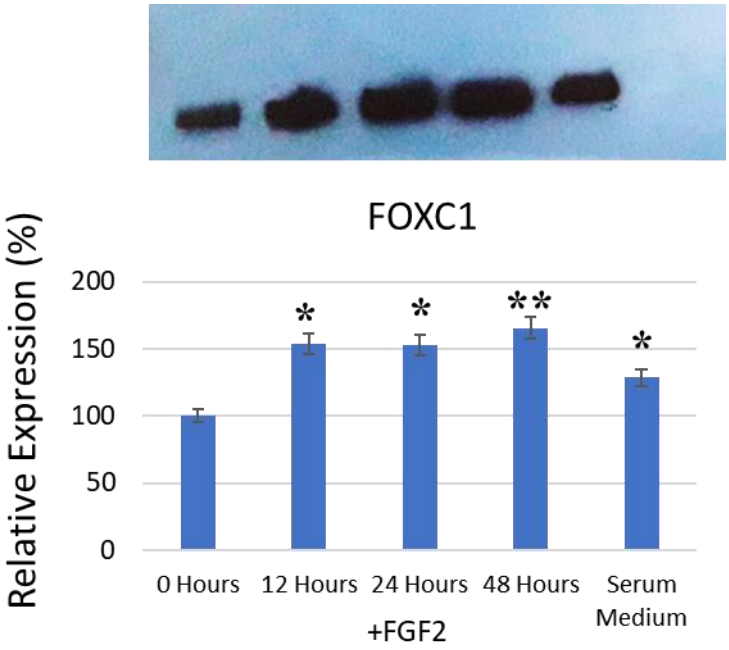

Figure 2.7: Western blot analysis of the effect of 2 ng/ml FGF-2 on protein expression of FOXC1. FOXC1 was detected in all treatment time points with a gradual increase in expression peaking at 48 hours followed by reduced expression in serum medium control. (n = 3, mean ± SD), $P \leq 0.05$ = *, $P \leq 0.01$ = **.

The FGF-2 effect on PAX6 expression levels in HEK293 cells displayed reduced levels of PAX6 as the untreated 0-hour control sample showed highest expression levels while the protein levels reduced upon treatment with FGF-2 by 71 ± 7% for 12 hours, 74 ± 7% for 24 hours, 63 ± 12% for 48 hours and 87 ± 42 for serum medium control with minimal fluctuation between the treatment time points (**Figure 2.8**). The PAX6 expression levels quantified with western blot indicated different expression patterns from those observed in confocal microscopy which showed similar expression pattern between the controls and all the treatment time points (**Figure 2.4**).

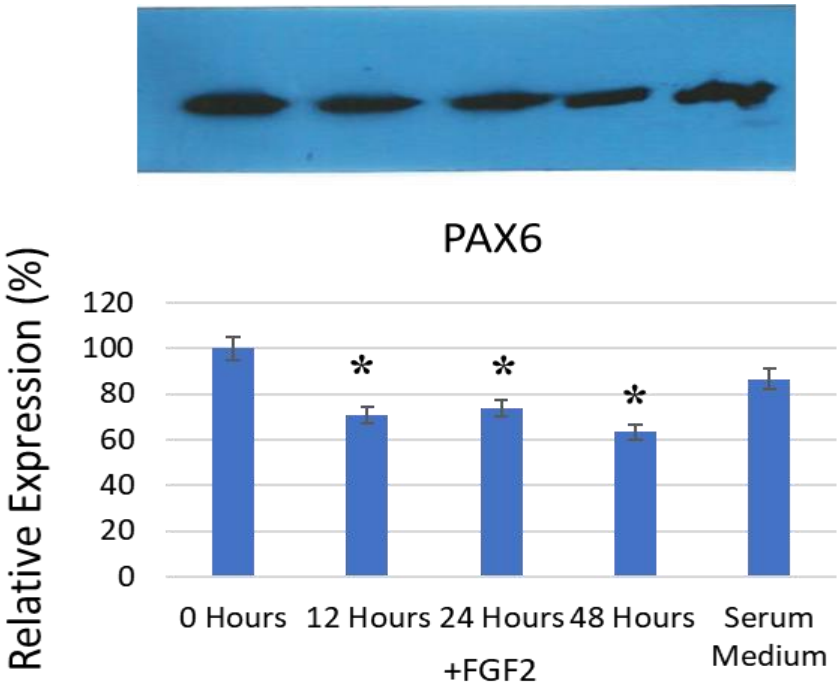

Figure 2.8: Western blot analysis of the effect of 2 ng/ml FGF-2 on protein expression of PAX6. PAX6 was detected in all treatment time points with a gradual decrease in expression across all time points followed by increased expression in serum medium control. (n = 3, mean ± SD), $P \leq 0.05$ = *.

PITX2 expression was activated by FGF-2 as little to no PITX2 protein was detected in the untreated 0-hour control sample, while all the treatment time points showed a gradual increase in PITX2 by 0 ± 17% for 12 hours, 0 ± 22% for 24 hours, 0 ± 120% for 48 hours as well as 0 ± 51% for serum medium control (**Figure 2.9**). The highest expression was observed after 48 hours' time point. This observation was not consistent with the confocal microscopy data as PITX2 was detected in the 0-hour control with reduced expression levels observed after 12 hours of treatment with FGF-2 (**Figure 2.5**). PITX2 levels further increased after 24- & 48-hours treatment time points which was similar to the quantification data generated via western blot technique.

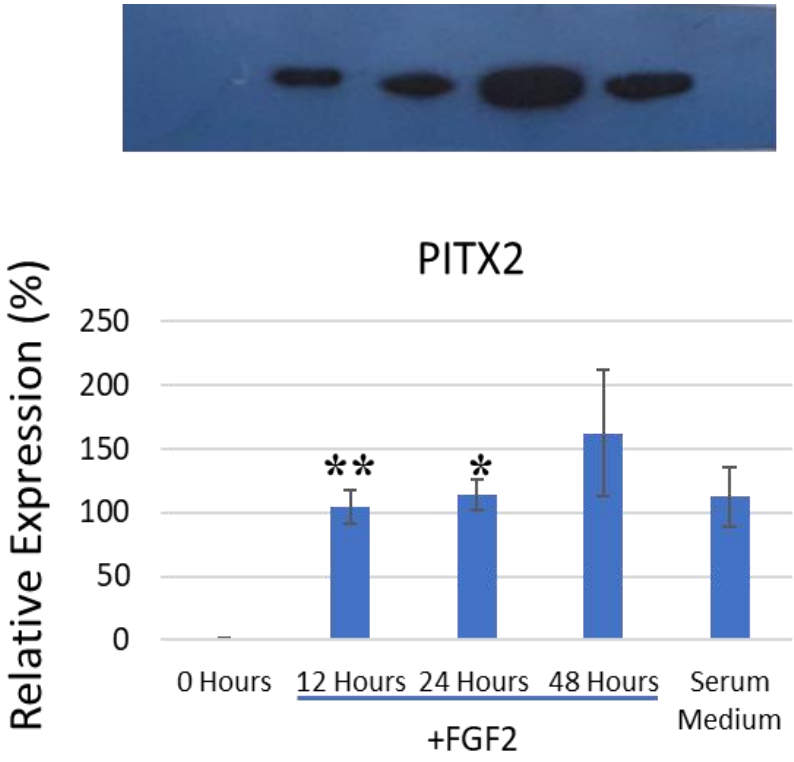

Figure 2.9: Western blot analysis of the effect of 2 ng/ml FGF-2 on protein expression of PITX2. PITX2 was only detected in 12, 24, 48 hours treatment time points which showed a gradual increase in expression and serum medium control showed reduced levels, while the untreated 0 hours control showed little to no expression of PITX2. (n = 3, mean ± SD), $P \leq 0.05$ = *, $P \leq 0.01$ = **.

ACTB (**Figure 2.10**) protein was used as loading control for normalisation during quantification of PXDN, PAX6, FOXC1 and PITX2 through densitometric calculations.

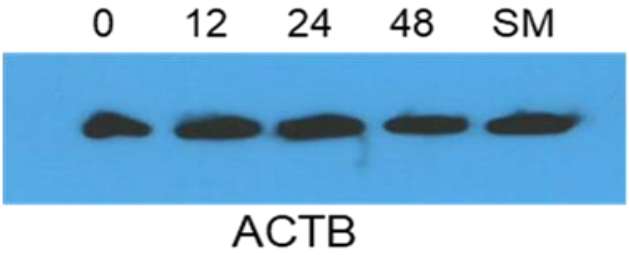

Figure 2.10: Western blot analysis of the effect of 2 ng/ml FGF-2 on protein expression of ACTB. No significant difference in expression levels of ACTB were observed across all treatment time points as expected.

2.3.3 PAX6, FOXC1 and PITX2 interaction with *PXDN* promoter

ChIP-PCR was employed in order to detect as to whether PAX6, FOXC1 and PITX2 had any interaction with *PXDN* gene promoter. A DNA sequence fragment of about 5000 bp upstream *PXDN* promoter was uploaded onto JASPAR and CONTRAV3 to detect as to whether any putative binding sites for PAX6, FOXC1 and PITX2 existed. Three putative binding sites were detected for PAX6, two for PITX2 and six for FOXC1. Confocal microscopy and western blot data was utilised in selection of treatment time points that showed elevated expression levels of PXDN, FOXC1, PAX6 and PITX2. HEK293 cells were seeded and treated with 2ng/ml FGF-2 for 12 hours for FOXC1 and 24 hours for PAX6 and PITX2, followed by harvesting of the cells for preparation for ChIP-PCR using an antibody specific for each transcription factor as well as ChIP-PCR primers as detailed in section 2.2.5.4 above. The cell lysate was sonicated and resolved on 1.5% (w/v) agarose gel with the expected fragment sizes of 200 – 1000 bps observed as shown by (**Figure 2.11)**.

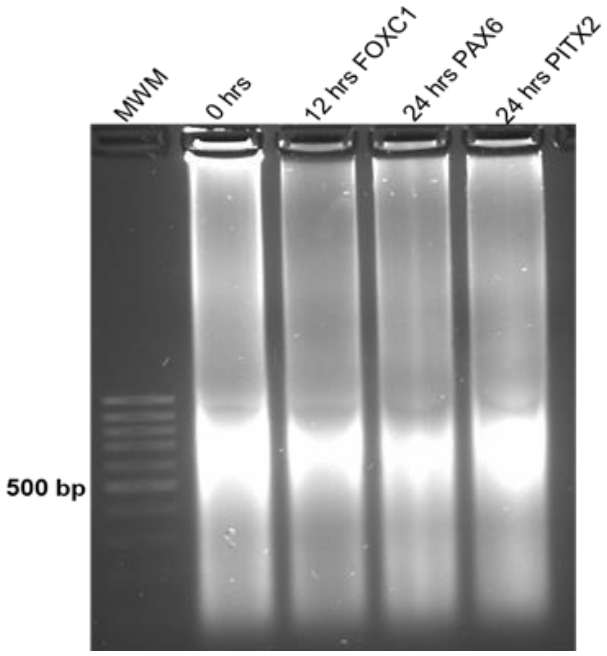

Figure 2.11: Sonicated DNA used for ChIP-PCR of PAX6, FOXC1 and PITX2 to interrogate their interaction with *PXDN* gene promoter. (A) Harvested DNA from each treatment time-point was crosslinked, quenched followed by sonication to generate fragments between 200 to 1000 bps which were resolved on 1.5% (w/v) agarose gel.

Four experimental controls were used for each ChIP-PCR run which included two positive controls namely, gDNA control for specificity of ChIP-PCR primers as well as an Input control which comprised of DNA from the sonicated chromatin prior to immunoprecipitation. Two negative controls comprised of no antibody control which comprised of sonicated DNA as well as agarose beads without the antibody and a non-template PCR control. The no antibody control provided the efficiency and specificity of the protein AG beads towards the primary antibody. ChIP-PCR showed that all putative binding sites for all three transcription factors (FOXC1, PITX2 and PAX6) do interact with the *PXDN* gene promoter region.

Transcription factor FOXC1 showed interaction with the *PXDN* gene promoter at all six (A to F) putative binding sites, as seen by clear bands after PCR while the region without FOXC1 binding site (N) showed no bands in both treated as well as untreated samples as expected (**Figure 2.12**). Putative binding site B showed no interaction of FOXC1 with *PXDN* gene in the untreated sample (Lane 2) while after treatment with FGF-2 for 12 hours FOXC1 showed a clear interaction with *PXDN* gene with a band present (Lane 3). The untreated (Lane 2) and treated (Lane 3) showed interaction of FOXC1 with *PXDN* promoter and controls such as input (Lane 4), no antibody (Lane 5), no template (Lane 6) and genomic DNA (Lane 7) confirming the specificity of the ChIP-PCR experiment as they produced expected band sizes or no bands. Heat shock protein family A (*HSPA6*) was selected as a positive control since it was a known FOXC1 downstream target (Ito et al., 2014). FOXC1 showed interaction with *HSPA6* gene promoter as both untreated and treated samples had clear expected band sizes while the control region without any known binding site for FOXC1 on *HSPA6* gene promoter showed a faint band in the untreated sample (Lane 2) and a bright band in the treated sample (Lane 3) which was unexpected (**Figure 2.12**)

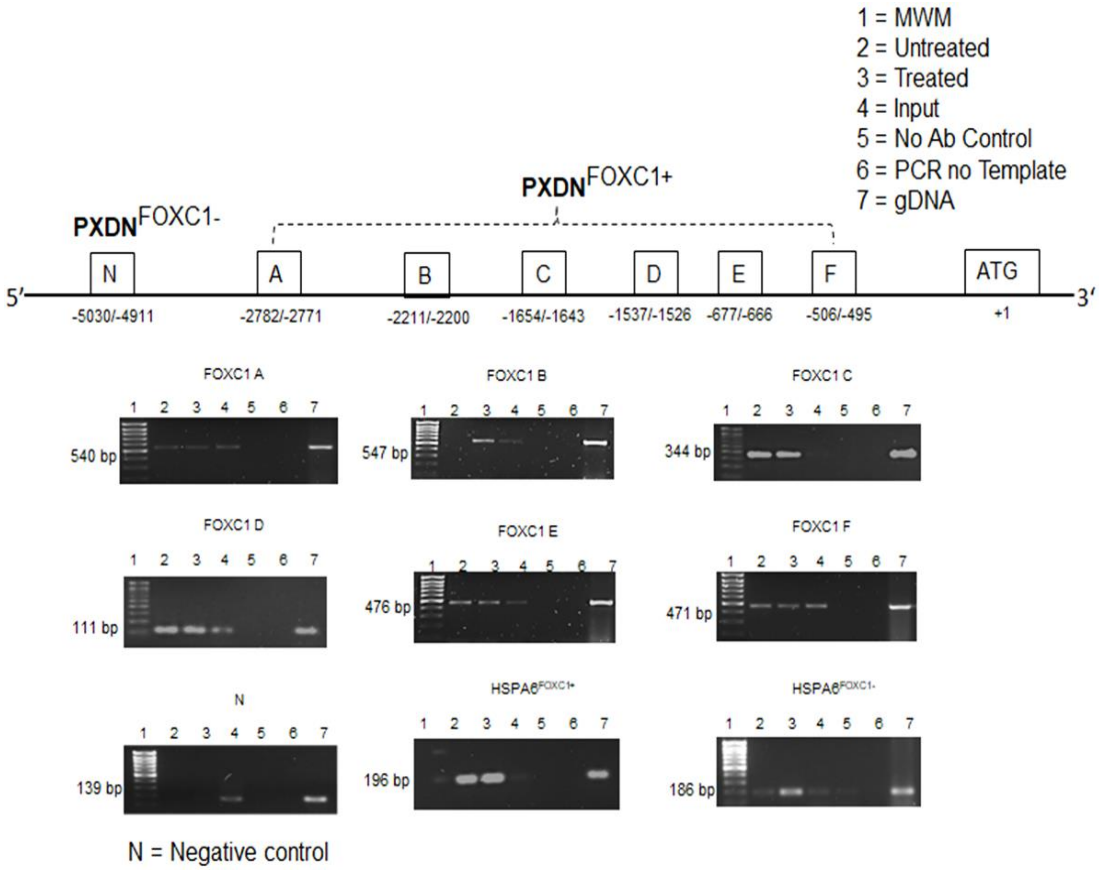

Figure 2.12: FOXC1 interaction with *PXDN* gene promoter. Bioinformatics analysis yielded six (A-F) putative binding sites for FOXC1 on *PXDN* promoter which all showed interaction with *PXDN*, while the negative control (N) showed no bands as expected. FOXC1 also showed interaction with HSPA6 which is a known FOXC1 target, while the negative control region also showed faint bands which was unexpected.

Three putative sites for PAX6 were identified in the *PXDN* gene promoter. All three putative PAX6 binding sites on *PXDN* gene promoter showed bright bands of expected sizes in the untreated as well as treated samples (**Figure 2.13**). The negative control region (N) with no known PAX6 binding site did not show any bands except for the input DNA (Lane 4) and genomic DNA (Lane 7) controls as expected. Wnt Family Member 5A (*WNT5A*) gene is a known target of PAX6 and was used as a control gene (Hu et al., 2016). ChIP-PCR revealed the interaction of PAX6 with *WNT5A* gene promoter as clear bright bands were observed in both the untreated as well as treated samples. Faint bands were observed in both treated as

well as untreated samples in the negative control region without any known PAX6 binding sites on *WNT5A* promoter.

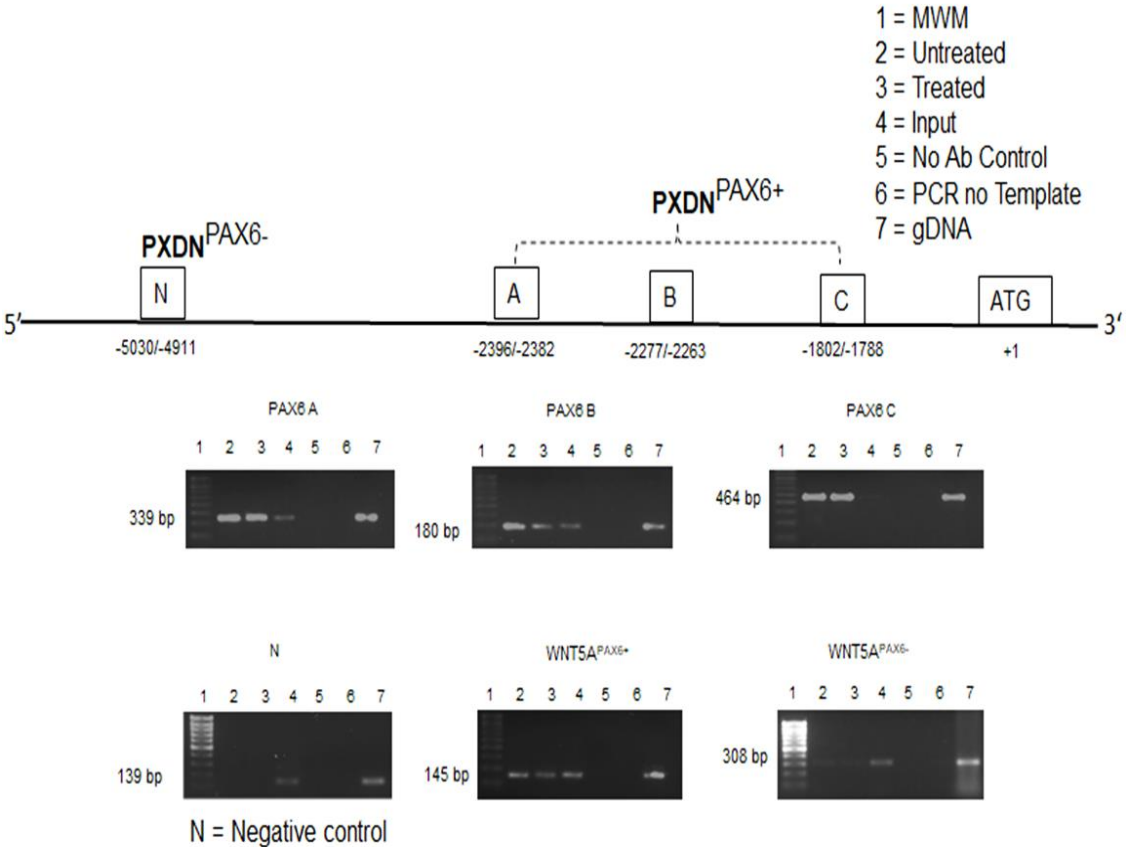

Figure 2.13: PAX6 interaction with *PXDN* gene promoter. Bioinformatics analysis yielded three (A-C) putative binding sites of PAX6 on *PXDN* promoter which all showed interaction with *PXDN*, while the negative control (N) showed no bands as expected. PAX6 also showed interaction with WNT5A which is a known PAX6 target, while the negative control region also showed faint bands which was unexpected.

JASPAR and CONTRAV3 bioinformatics tools indicated two putative PITX2 binding sites on *PXDN* gene promoter (**Figure 2.14**) of which ChIP-PCR showed that both putative binding sites interact with *PXDN* gene promoter. Putative binding site A produced two faint bands of expected sizes in both the untreated as well as treated samples, while only in the treated sample a bright band of expected size was visualised for putative binding site B. The control region within *PXDN* gene promoter without any known PITX2 binding site (N) produced no bands except for

the input (Lane 4) as well as genomic DNA (Lane 7) controls as expected. The known downstream target of PITX2, Inhibin subunit beta A (*INHBA*) gene was selected to serve as a control gene (Basu et al., 2015). ChIP-PCR revealed that PITX2 does interact with *INHBA* gene as clear bands of expected sizes were observed in both the untreated as well as treated samples, while unexpectedly the negative control region with no PITX2 binding site showed bands in both the untreated and treated samples (**Figure 2.14**).

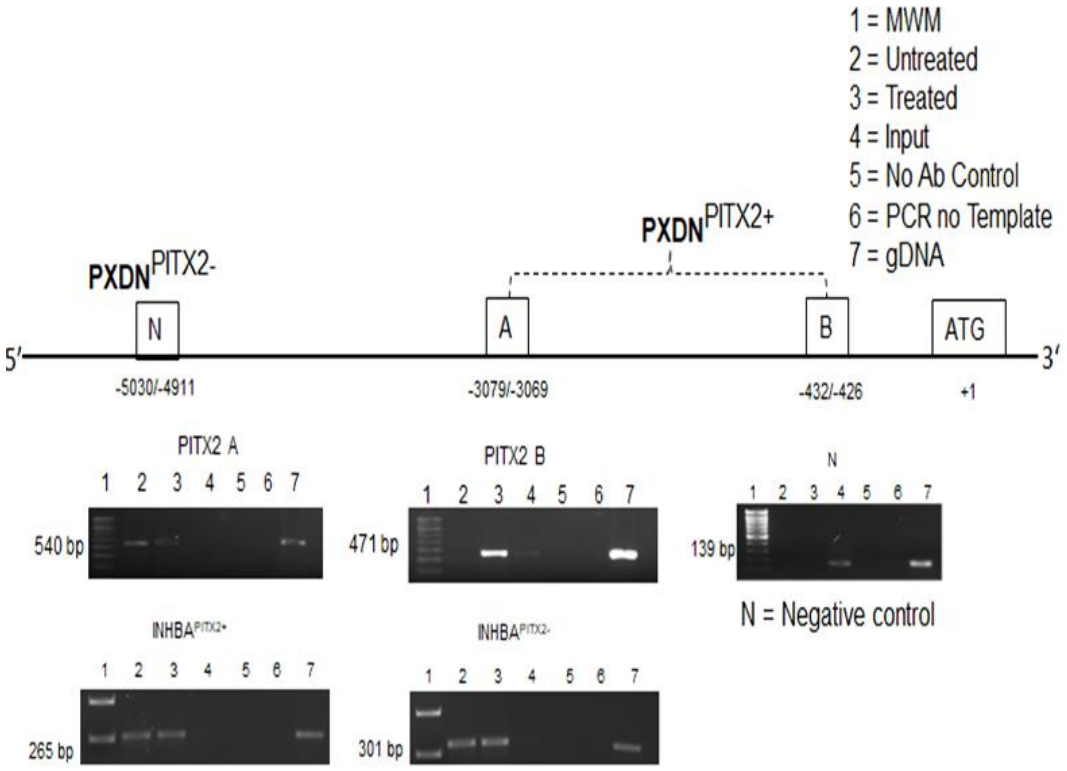

Figure 2.14: PITX2 interaction with *PXDN* gene promoter. Bioinformatics analysis yielded two (A-B) putative binding sites for PITX2 on *PXDN* promoter which all showed interaction with *PXDN*, while the negative control (N) showed no bands as expected. PITX2 also showed interaction with *INHBA* which is a known PITX2 target, while the negative control region also showed faint bands which was unexpected.

2.3.4 PAX6-PXDN luciferase reporter gene assay

Due to time constraints resulting from COVID-19, the section of luciferase assay was only conducted on PAX6 transcription factor given its supported role in the involvement of eye development as well as being known to regulate expression levels of both FOXC1 and PITX2 transcription factors which like PXDN are key players in development of the anterior segment of the eye (Graw, 2003; Berry et al., 2006; Takamiya et al., 2020).

Oligonucleotide sequences for PAX6 (**Table 2.1**) gene were successfully designed and cloned into competent *E.coli* bacteria as outline above in **Section 2.2.6**. The vector constructs were submitted for sanger sequencing (Inqaba Biotechnical Industries, Pretoria, RSA) to confirm as to whether the oligonucleotides were successfully ligated into a pGL4.10 vector (**Figure 2.1**) as well as confirmation of the insert orientation. Sanger sequencing was successful (**Figure 2.15**) as all oligonucleotide's sequences were confirmed to be ligated into pGL4.10 vector.

At the submission of this thesis, optimisation of transfection efficiency of the recombinant pGL4.10 vectors into HEK293 cells was concluded and therefore we will be moving on to the next stage of employing luciferase reporter gene assay to assess as to whether upon binding on to *PXDN* promoter does PAX6 upregulate or down regulate PXDN expression.

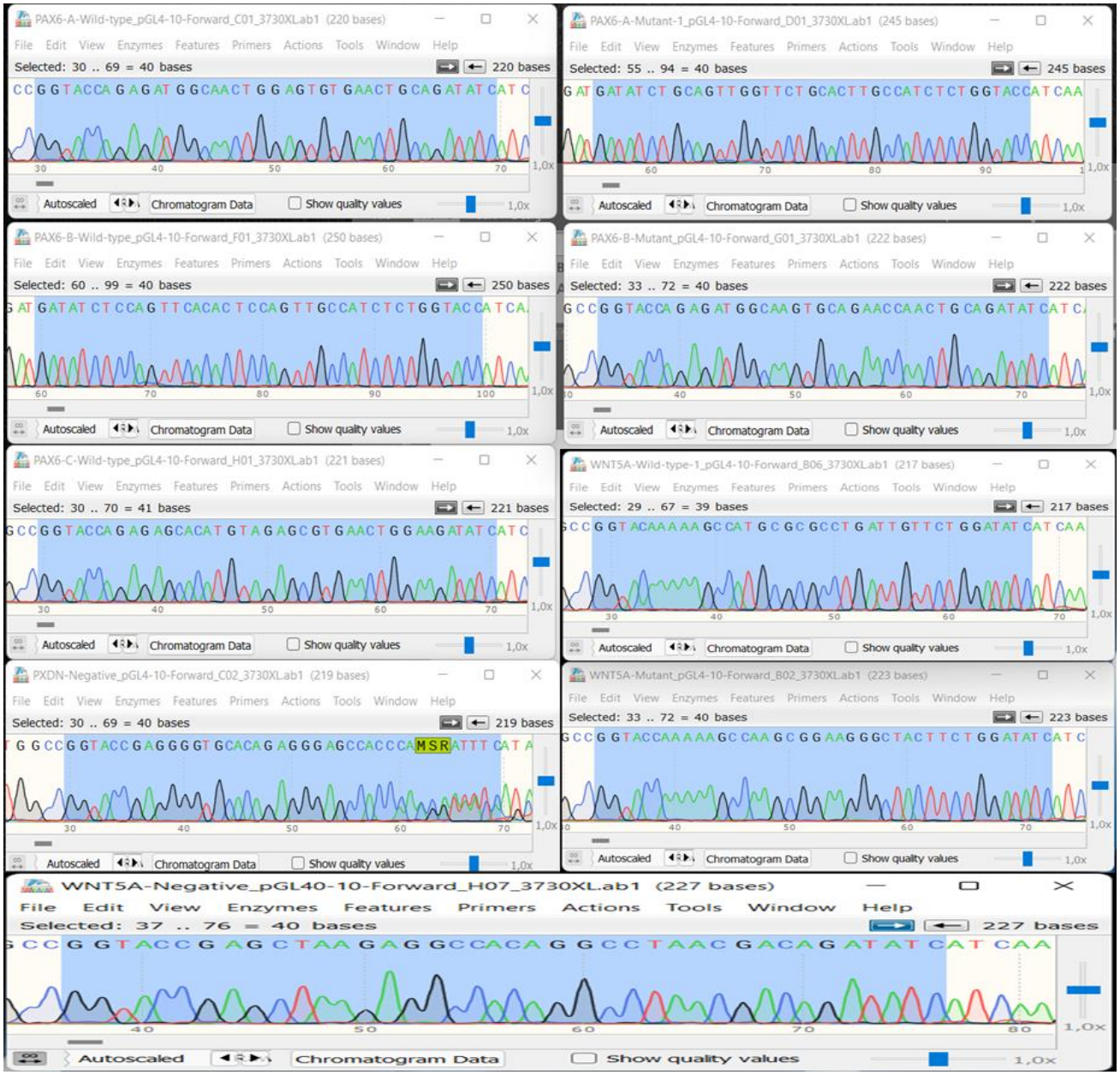

Figure 2.15: Sanger sequencing confirmation of successful ligation of oligonucleotides sequences. Putative binding sites of PAX6 and known downstream target gene WNT5A were designed as double stranded oligonucleotides modified with restriction enzyme recognition sequences. The oligos were restricted with KpnI as well as EcoRV restriction enzymes, then ligated into a restricted pGL4.10 vectors which were submitted for sequencing post colony PCR.

2.4 Discussion

PXDN belongs to the haem containing cyclooxygenase peroxidase family and in humans, PXDN is predominantly expressed in the cardiovascular system by cardiomyocytes (Cheng et al., 2008; Zhang et al., 2012; Ma et al., 2013) and in the developing eye, more specifically in the layers of lens and corneal epithelium (Homma et al., 2009; Khan et al., 2011; Lázár et al., 2015). PXDN has been implicated in the progression and pathogenesis of various diseases, most notably those affecting the cardiovascular system (; Cheng et al., 2008; Zhang et al., 2012; Ma et al., 2013), cancer (Desmond et al., 2007; Tauber et al., 2010; Liu et al., 2010; Jayachandran et al., 2016; Sitole and Mavri-Damelin, 2018), fibrosis (Peterfi et al 2009), and the eye (Khan et al., 2011, Choi et al., 2015; Micheal et al., 2016). The functions of PXDN are yet to be fully elucidated, with ECM assembly via cross-linking collagen IV to form the BM (Lázár et al., 2015) and production of hypohalous acids in the presence of H_2O_2 as well as halide ions (Klebanoff et al., 2005; Li et al., 2012) currently known.

The role PXDN plays in formation of BM, which is required for normal physiological function of tissues enabled us to investigate the regulation of PXDN expression in eye development, as this function is exclusive to PXDN (Bhave et al., 2012; Lee et al., 2020). As such, PXDN is understood to be essential for normal development of eye structures such as the lens epithelium and cornea via collagen IV crosslinking, which promotes consolidation of ocular BM (Yan et al., 2014). Three transcription factors PAX6, FOXC1 and PITX2 were chosen as potential regulators of *PXDN* in the current study due to their key involvement in the development and maintenance of eye structures (Graw, 2003; Berry et al., 2006; Sowden, 2007; Takamiya et al., 2020). This was also due to there being only two research studies thus far that examined PXDN regulation by NRF2 and SNAi1 transcription factors (Hanmer and Mavri-Damelin, 2018; Sitole and Mavri-Damelin, 2018). The interaction between the genes that regulate the development of the anterior segment of the eye is not fully understood, especially PAX6, FOXC1, PITX2 interaction with *PXDN* gene.

The data generated in the current study indicates that FGF-2 may have an impact on protein expression levels of PXDN, PAX6, FOXC1 and PITX2 in HEK293 cells. Since this study is the first to investigate FGF-2 effect on HEK293 endogenous expression of PXDN as well as the three transcription factors FOXC1, PAX6 and PITX2, no contrast (i.e., with other studies) could be made regarding expression patterns of the aforementioned proteins.

PXDN expression in the presence of FGF-2 showed elevated expression within 12 hours as compared to the control followed by reduced expression throughout the subsequent treatment time points as observed and quantified via confocal microscopy and western blot respectively. The reduction in PXDN expression could be due to the healthy state of the HEK293 cell line given that elevated PXDN expression is usually observed in pathophysiological state or oxidative stress. The cells were starved off the serum supplemented in DMEM, which could have induced the elevated expression of PXDN until the oxidative stress was alleviated by either FGF2 treatment or PXDN's ability to metabolise ROS species. The effect of FGF-2 only lasting for 12 hours in the absence of heparine could also account for the reduced expression of FGF2.

The transcription factors were also expressed throughout the treatment time points, with PAX6 showing varying expression patterns with confocal data suggesting no significant difference in protein levels across all treatment time points in contrast with the untreated 0-hour control, while quantification by western blot indicated a decrease in expression levels of PAX6 with the highest peak being in the untreated control, there after PAX6 levels were reduced throughout 12, 24, and 48 hours. The reduced expression of PAX6 could just be due to its self-regulatory ability whenever the protein is no longer required in high dosage within a specific tissue. The presence of intense fluorescence levels in the no primary antibody control for confocal data could be indicative of contamination with a tip used in the wells with both primary and secondary antibody during experiment preparation. Another reason could be that the secondary antibody CFL-594 (SC-516192) had high non-specific binding which could further be indicative of the varying expression pattern between confocal microscopy and western blotting techniques. FOXC1 expression

showed a gradual increase with peak expression observed within 48 hours. PITX2 showed an upregulated expression pattern as the control had little to no PITX2 protein, with an increment observed through the treatment time points. The FOXC1 and PITX2 transcription factors are co-expressed in discrete cell types during eye development, that they can physically interact and that they share a common subnuclear compartment. Berry et al., (2006) demonstrated a functional consequence of this interaction as PITX2A inhibits transcriptional regulatory activity by FOXC1 which might also explain the sudden increase in expression levels of PITX2 which might have been required to either form a complex with FOXC1 to upregulate their downstream targets in HEK293 cell line.

FGF2 is a potent mitogen that can activate a number of pathways some of which require PAX6, FOXC1, PITX2 and many other transcription factors (Ornitz and Itoh, 2015). FGF pathway activation drives expression of transcription factors required for normal development as well as maintenance of the eye and further induces cellular proliferation (Sinn and Wittbrodt, 2013). FGF-2 has also been shown to be required for normal proliferation as well as differentiation of corneal epithelial cells during eye development (Zhang et al., 2015) and Iris-Lens regeneration (Hayashi et al., 2004). In murine cells, it has been shown that FOXC1 is expressed in developing kidney cells and it is required for kidney organogenesis (Kume et al., 2000), while no studies have been conducted to date that examined expression levels of PAX6 as well as PITX2 expression in kidney cells, we used data obtained from protein atlas database, which has expression profiles of proteins in various commonly used cell lines (www.proteinatlas.org). In a study by Peterfi et al., (2009) it was observed that healthy kidney cells have undetectable amount of PXDN, while Hanmer and Mavri-Damelin, (2018) confirmed that PXDN is expressed in HEK293 cells.

ChIP-PCR data generated from this study, confirmed the interaction of PAX6, FOXC1 and PITX2 with *PXDN* gene promoter. The six FOXC1 potential binding sites produced bright bands signifying FOXC1-*PXDN* interaction, while three PAX6 as well as two PITX2 potential binding sites likewise produced bright bands with no bands observed for the negative control region. Overall FOXC1 binding to

PXDN showed an increased interaction on putative binding site (B) as the control did not show any band while the FGF-2 treated sample showed a bright band. PAX6-*PXDN* interaction did not shown any significant difference with or without FGF-2 in all three putative binding sites. One putative binding site (A) of PITX2 showed no difference in binding capacity in the presence or absence of FGF-2, while the second putative binding site (B), showed no interaction with *PXDN* in the absence of FGF-2, while treatment with FGF-2 increased PITX2-*PXDN* interaction. As already mentioned above, FOXC1 and PITX2 interact with each other or act independently in different tissue types. So, the data generated in this study is novel in that it is the first to examine FOXC1 and PITX2 interaction with *PXDN* gene promoter. The exact effect of both transcription factors on *PXDN* will require luciferase reporter assay in order to best assess as to whether FOXC1 and PITX2 regulate *PXDN* individually or both form a complex to initiate regulation of *PXDN*.

Our ChIP-PCR results further validated the observation from western blot and confocal data that 2 ng/ml FGF-2 has little to no impact on overall endogenous expression of PAX6 and FOXC1 in HEK293 cell line. PXDN and PITX2 expression could be driven by FGF-2 either directly or indirectly as both proteins exhibit differential expression patterns in HEK293 cells. Due to time constraints as a result of COVID-19 pandemic delays, PAX6 was selected for assessment with luciferase assay in order to determine if the interaction reported by ChIP-PCR between *PXDN*-PAX6 as to whether PAX6 initiates upregulation or downregulation of PXDN. Given the close proximity of the putative binding sites on *PXDN* promoter, it is possible that sonication of the DNA did not produce fragment sizes that contained only individual putative binding sites, which would possibly result in all putative binding sites showing positive interaction with *PXDN* gene promoter. As such we sought to employ luciferase reporter gene assay to assess the ability of each putative binding site to express reporter gene. This is why we designed double stranded short oligonucleotides sequences for each binding sequence (**Table 2.1**).

PAX6 is expressed in the very early stages of eye development to drive the organisation of the anterior segment (Takamiya et al., 2020), while FOXC1 and

PITX2 act downstream of the master control gene *PAX6* (Graw, 2003). PITX2 and FOXC1 are co-expressed during eye development in discreet cell types and they share a subnuclear compartment as well as interact with each other physically; as such they are crucial for the proper development as well as functioning of the anterior segment of the eye as they form a higher order transcription factor complex (Berry et al., 2006). During the optic cup formation stage of eye development FOXC1 and PITX2 expression is elevated showing their requirements for the process (Sowden, 2007). ECM proteins such as laminin, fibronectin, and collagen IV are also crucial for a successful optical cup formation (Kwan, 2014). Collagen IV requirement means that PXDN expression will be elevated since crosslinking of collagen IV is required in the formation of BM which is essential for normal development of the eye with the process exclusive to PXDN (Bhave et al., 2012; Lee et al., 2020).

PXDN is believed to contribute in providing support of the lens and cornea in a form of framework during their construction in the early stages of eye development (Khan et al., 2011; Choi et al., 2015). *In-situ* hybridisation found that PXDN is expressed in the eye forming region and in particular the lens of *Xenopus tropicalis* (Tindall et al., 2005). In mice, expression was observed in the lens and retina and during development of eye of the mouse, PXDN expression was detected from embryonic age (E11.5) onwards which is equivalent to 33 days in human embryology, and furthermore PXDN knock-out animals showed absence of collagen IV crosslinking (Homma et al., 2009; Lázár et al., 2015). As such, PXDN is understood to be essential for normal growth of eye structures such as the lens epithelium and cornea via collagen IV crosslinking, which promotes consolidation of ocular BM (Yan et al., 2014). The continuous expression of PAX6 throughout eye development stages in both anterior and posterior segments as well as post-development is indicative that *PXDN* could be a target of PAX6, just as FOXC1 and PITX2 are known PAX6 targets (Wang et al., 2017).

To our knowledge the transcription factors FOXC1 and PITX2 are not involved in collagen IV crosslinking or BM synthesis, while PAX6 knockdown during lens formation results in ECM proteins being significantly diminished between the optic

vesicle and ectoderm via the reduction of transcripts encoding components of the ECM (Huang et al., 2011). Once the eye is fully developed, proteins such as FOXC1, PAX6 and PXDN continue to be expressed, with FOXC1 required for cell viability as well as resistance to oxidative stress (Berry et al., 2006), while PXDN is thought to protect eye structures against oxidative stress damage (Khan et al., 2011). In a study by Shukla and Mishra, (2018), it was shown that levels of hydrogen peroxide in corneal cell lines affect expression levels and localisation of PAX6. Since PXDN and FOXC1 can regulate oxidative stress reactions, affected expression and localisation of PAX6 can contribute to the inability of PXDN to catalyse H_2O_2 therefore leading to failure in PXDN's ability to provide resistance to oxidative stress that could be harmful for eye structures. Low expression levels and affected localisation of PAX6 will definitely affect expression of downstream target genes such as FOXC1 which maintains cellular viability as well as help alleviated oxidative stress (Berry et al., 2006; Shukla and Mishra, 2018). Another reason that PAX6 may regulate *PXDN* could be during wound healing. *PXDN* has a conserved peroxidase domain as well as additional ECM-interacting domains that allow it to catalyse dityrosine cross-links, a function also noted to be performed by MPO during the inflammatory response caused by neutrophils so it is probable that PXDN may be capable of forming these cross-links during injury, since PAX6 expression was also observed to elevated in corneal injury (Heinecke et al., 1993; Cheng et al., 2011; Yu et al., 2020).

In our laboratory we have previously found out that PXDN is a novel target of the transcription factor nuclear factor erythroid-2-related factor 2 (NRF2). HeLa and HEK293 cells were treated with H_2O_2, tert-butylhydroquinone and sulforaphane which are known NRF2 inducers, elevated expression of PXDN as well as NRF2 was observed in both cell lines, with ChIP-PCR and luciferase reporter gene assay confirming NRF2 regulation of *PXDN* (Hanmer and Mavri-Damelin, 2018). NRF2 has been observed to be expressed in eye tissues where it serves a protective role against oxidative damage induced by environmental factors such as ultraviolet radiation (Nakagami, 2016; Hanmer and Mavri-Damelin, 2018; Wang et al., 2020). As a known master regulator of antioxidant response, NRF2 is able to activate ROS regulation genes such as *PXDN* to catalyse redox related processes (Hanmer and

Mavri-Damelin, 2018; Wang et al., 2020). It is possible that NRF2 is a downstream target of PAX6 given that NRF2 can regulate ECM matrix proteins (Hiebert, 2021), while PAX6 is also known to activate genes that regulate ECM proteins syntheses, while PAX6 knockdown could result in low NRF2 and PXDN expression (Huang et al., 2011).

As previously mentioned, PXDN expression is predominantly expressed in the vasculature and eye tissues. Aberrant expression of PXDN due to mis-regulation has been observed to result in various clinical phenotypes including ASD which is the focus of the current study. Various mutations in *PXDN* have been found to be present in patients diagnosed with developmental eye disorders, specifically anterior segment dysgenesis (ASD), lending support to the significance of PXDN in eye development (Khan et al., 2011; Choi et al., 2015). In various study cohorts pathogenic *PXDN* mutations have been detected (Khan et al., 2011; Choi et al., 2015; Micheal et al., 2016) and these are discussed in **Chapter 3** that follows along with other genes that may interact with *PXDN* to bring about various ocular phenotypes. No precise mechanisms are known currently as to how mutations discovered in *PXDN* cause ASD disorders, which comprise of anomalies such as glaucoma, abnormal lens and cornea development (Cheng et al., 2012). Khan et al., (2011) suggested two possible mechanisms by which pathogenic null variants in *PXDN* may be exerting their deleterious effects: (1) The lack of PXDN protein in the cornea as well as in the epithelial layers of the lens causes accumulation of ROS that generally oxidise lipids also proteins, producing aggregates that are insoluble leading to cataractogenesis and corneal clouding and (2) the accumulation of ROS in the aqueous humour can affect the differentiation also development of the structures found in the anterior segment which is involved in the development of glaucoma (Izzotti et al., 2006, Khan et al., 2011). For instance, aqueous humour of glaucoma patients contains elevated enzymes induced by oxidative stress and reduced antioxidants which promotes oxidative stress (Ferreira et al., 2004) and the trabecular meshwork is very sensitive to damage by oxidation (Khan et al., 2011).

A study by Yan et al., (2014) further provided support by using an animal model (mutant *KTA048* mouse) which displayed similar phenotypes observed in

individuals harbouring mutations in *PXDN*. The mutant mouse model was induced via N-ethyl-N-nitrosourea of which upon sequencing revealed a recessive mutation (T3816A) causing a premature stop codon in the peroxidase domain, which resulted in development of ASD as well as microphthalmia (Yan et al., 2014).

Aberrant PXDN expression has been associated with development and progression of other disorders such as kidney fibrosis (Peterfi et al., 2009), various cancers (Mitchell, 2000; Desmond et al., 2007; Tauber et al., 2010; Liu et al., 2010; Jayachandran et al., 2016; Sitole and Mavri-Damelin, 2018; Paumann-Page et al., 2021) and cardiovascular disorders (Bai et al., 2011; Shi et al., 2011; Zhang et al., 2012; Ma et al., 2013). Thus far PAX6 has not been implicated in kidney diseases while other PAX family members such as PAX2 have been implicated in chronic kidney disease (Grimley and Dressler, 2018). While elevated expression of PXDN was found in myofibroblasts that were undergoing differentiation induced by TGF-β1. The fibrillar like structure forming the ECM was formed by PXDN secreted from myofibroblasts in Kidney fibrosis (Peterfi et al., 2009). Atherosclerosis is an inflammatory condition where blood flow becomes restricted due to the narrowing and hardening of arteries (Stoneman and Bennett, 2004). PXDN has already been implicated in the mediation of ox-LDL-induced endothelial cell apoptosis– a process which is thought to increase inflammation and injury in cardiovascular tissue and accelerate atherosclerosis initiation and progression (Stoneman and Bennett, 2004; Bai et al., 2011; Ma et al., 2013).

As to how PXDN exerts its effect in the development of cancer is not known and the role of PXDN may differ per cancer type. Studies in our laboratory have found that Snail family transcriptional repressor 1 (SNAI1) which is a key player in EMT modification regulates PXDN in cervical carcinoma cell lines (Sitole and Mavri-Damelin, 2018). PAX6 expression has been observed in ependymal tumours where it acted as a tumour suppressor (Tabasaran et al., 2021), while in glioblastoma cell lines with PAX6 knockout showed elevated resistance to oxidative stress as increased production of H_2O_2 was observed while the wild type as well as healthy cell lines were not resistant to oxidative stress (Hegge et al., 2018). Also, PAX6 downstream target genes such as NRF2 showed significantly reduced protein

expression in PAX6 knockout glioblastomas as compared to wildtype and healthy cell lines (Hegge et al., 2018). Madden et al. (2004) previously showed a 17-fold increase in PXDN protein expression in glioma endothelial cells as compared to non-neoplastic endothelial brain cells. Subsequently, PXDN was found to be selectively upregulated in a set of endothelial marker genes in the microvasculature of metastatic brain tumours glioblastoma and pilocytic astrocytomas, while it was absent or detected at low quantity in the controls (non-neoplastic temporal lobe) specimens (Liu et al., 2010). This study is very important in the search for better understanding of the aetiology of congenital eye disorders such as ASD. In an African setting where the epidemiological data is lacking, data generated from this study will aid in contributing knowledge towards understanding the role of PXDN in eye development. Understanding the regulation of *PXDN* is very vital since it is implicated in development of various disorders. Transcription factors such as PAX6, FOXC1 and PITX2 like PXDN they are also implicated in a variety of disorders which makes understanding the function of their downstream targets critical.

In conclusion, this study is the first to assess the interaction of PAX6, FOXC1 and PITX2 with *PXDN* in eye development as well as maintenance. PAX6 is likely to regulate *PXDN* in eye development given the expression patterns in all stages of eye development. This can either be a direct regulation or indirect via downstream targets of PAX6 such as FOXC1, PITX2 and other ECM proteins such as NRF2. The PAX6-*PXDN* interaction as shown by ChIP-PCR data will need further validation by employing technique such as luciferase assay. Regulation of *PXDN* by master regulator of eye development would be a novel discovery as both proteins could be targeted for therapeutic approaches given the variety of disorders PXDN is implicated with including ASD. At the time of thesis submission, luciferase assay optimisation was underway.

CHAPTER 3: Variant screening in eye development genes

3.1 Introduction

3.1.1 Genetics of eye development

The human eye is a unique and complex part of the human body, and is broadly divided into two segments namely the anterior and posterior segments (Addo et al., 2016). The anterior chamber and posterior chamber are filled with aqueous humour, which provides nutrients to tissues in the anterior segment of the eye. The anterior segment of the eye comprises of trabecular meshwork, cornea, lens, iris, ciliary body and Schlemm's canal, while the retina and optic nerve form the posterior segment of the eye (Ito and Walter, 2014). The regulatory programmes that control eye development are complex and involve a myriad of both transcriptional and post transcriptional events (Dash et al., 2016; Budak et al., 2018). Master control genes of eye development refers to the genes that drive eye development at the early stages, most of which code for transcription factors and signalling molecules (Graw, 2010). PAX6, PITX2 and FOXC1 are among the key regulators in the development of the anterior segment by directing the proper differentiation of ocular mesenchyme (Baulmann et al., 2002; Graw, 2003). Joining this list is PXDN, which is understood to be essential for normal development of eye structures such as the lens epithelium as well as the cornea via collagen IV crosslinking which promotes consolidation of ocular BM (Yan et al., 2014).

3.1.2 Genetics of eye disorders

Mutations in genes that initiate and regulate the complex pathways involved in eye development can cause a spectrum of disorders such as ASD, which is heterogenic in nature and comprises of Axenfeld Rieger syndrome, Peter's anomaly, Aniridia, Sclerocornea, Primary congenital glaucoma and Microphthalmia (Choi et al., 2015). Less than a handful of studies have been conducted in South African patients with regards to the genetic aspects of eye diseases (Carstens et al., 2016; Carstens et al., 2022). Currently there are very few research studies conducted for the association of *PXDN* gene variants with ASD (Khan et al., 2011; Yan et al., 2014; Choi et al., 2015; Yang et al., 2016; Micheal et al., 2016), and none in a South African cohort.

In summary, the second aim of the current study sought to identify genetic mutations in a cohort of South African patients diagnosed with ASD, and this was achieved by performing NGS on genes known to regulate eye development pathways, including *PXDN*.

3.2 Methods

3.2.1 Phenotypic data collection and eye disorders diagnosis

The study was approved by the Human Research Ethics Committee (Medical) of the University of the Witwatersrand (**Appendix E**), South Africa (protocol number: M131125), and written informed consent was obtained from all participants (**Appendix D**). Patients were recruited through ophthalmology clinics hosted by the University of the Witwatersrand as well as Genetics clinics via the national health laboratory services and all patients were diagnosed or identified for the study by a qualified ophthalmologist and clinical geneticist. Study participants were recruited and randomly selected in the study based on their diagnoses with any congenital eye disorder falling under the umbrella of ASD.

3.2.2 Sample collection and DNA extraction

Saliva and blood samples were collected from patients diagnosed with ocular disorders categorised under ASD and DNA was extracted using prepIT®.L2P kit for saliva samples (DNA Genotek, OraSure Technologies Inc), while Monarch® genomic DNA purification kit (New England Biolabs® Inc) was used for blood samples. The DNA samples were tested for purity and quantified with the aid of the NanoDrop One spectrophotometer (ThermoFisher Scientific) at A260/280 as well as A260/230 ratios. Quantity of double stranded DNA was assessed using Qubit® 4.0 fluorometer (Invitrogen™). Also, DNA was collected from some of the parents of the patients (were possible) for use in segregation analysis in case we managed to identify putative disease-causing mutation(s) that needed validation.

3.2.3 Target gene selection and custom gene panel design

Candidate genes were chosen and prioritised according to the following criteria:

- Candidate genes were chosen for screening of any functional mutations based on their reported functional effect or involvement in the morphogenesis of the eye and/or association with ASD disorders through a thorough literature search.
- Candidate genes were also selected from databases such as iSyTE 2.0 which has catalogued various genes know to be expressed in different stages of eye development using animal models.

In total 50 candidate genes (Table 1.1 in section 1.6.5) were chosen then submitted on to Ion AmpliSeq™ Designer tool (ThermoFisher Scientific) to see if a gene panel consisting of our target genes is available or a custom on-demand panel will need to be designed. Only 43 genes were pre-validated and could be ordered on demand while 7 genes required a spike-In panel to be designed separately. The spike-In panel was not designed as this was not validated by the manufacture and it was financially expensive to construct as compared to the on-demand panel.

3.2.4 Next generation sequencing of target genes

Next-generation sequencing (NGS) has revolutionised genetic testing, as it enables many genes to be sequenced together in a single test (Hillman et al., 2014). NGS offers faster processing leading to a quicker turnaround of results therefore cutting costs. In the current study, target gene based whole exome sequencing (WES) was employed (**Figure 3.1**). The principle of WES involves extraction of DNA from samples, which will undergo shearing to produce a library of small fragments of size 200 to 400 base pairs. The resulting fragments will then be hybridised with the aid of probes which target exonic sequences and the unbound intronic sequences will be washed. The high throughput technology then facilitates sequencing of all the exonic fragments across millions of reactions in massively parallel fashion, resulting into millions of short stretches of sequences known as reads. Resulting reads are then aligned using reference genome (Gupta et al., 2017).

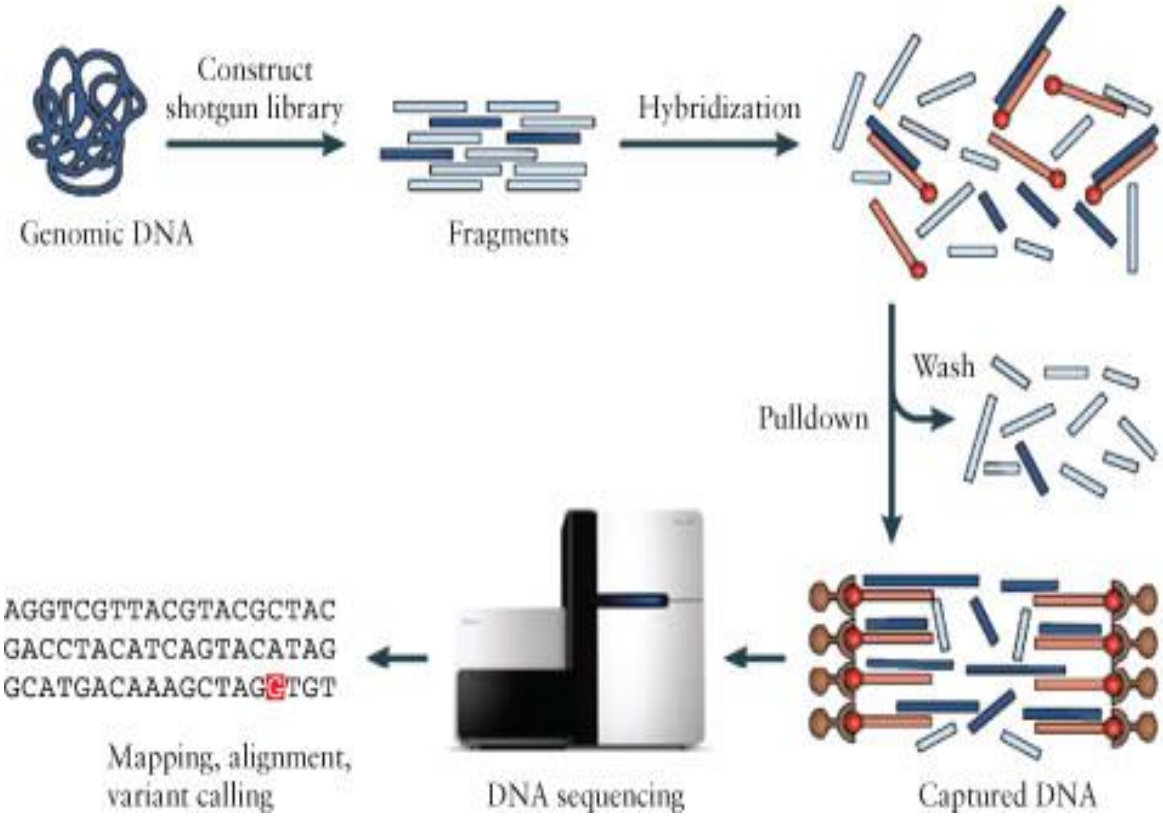

Figure 3.1: An overview of the various stages of whole exome sequencing. Genomic DNA is fragmented, hybridised with probes targeting exon sequences while intron sequences will be washed off. The exon fragments will then be sequenced then aligned to the reference genome (Hillman et al., 2014).

3.2.4.1 Library preparation of DNA samples

Extracted DNA was quantified using Nanodrop One as well as Qubit® 4.0 fluorometer with the concentration of each sample diluted to 1 ng/µl, which is in range of the required starting concentration of 0.67 ng/µl (10 ng in 15 µl total volume). As stipulated in the DNA library preparation protocol system user guide (Publication number: MAN0013432) of Ion Chef™ (ThermoFisher Scientific), the library was prepared using DL8 Ion AmpliSeq™ kit which comprised of Chef solutions, Chef reagents, Tip cartridge, PCR frame seal, Ion code 96 well PCR plate, Empty tip cartridge and Enrichment cartridge (ThermoFisher). The Ion AmpliSeq™ DL8 kit was loaded into the Ion Chef™ automated system which can prepare DNA libraries for 8 samples loaded onto the barcoded 96 well plate (A1-H1) per run via PCR using two pools of primers. The Ion Chef™ system comprises

of Ion Library Equalizer™ technology which ensures that the DNA libraries synthesised have a final concentration of 100 pM with only half (50 pM) required for downstream application (DNA templating).

3.2.4.2 DNA Templating

DNA templating was also performed on the Ion Chef™ system (ThermoFisher Scientific) with the aid of Ion 520™ Kit user guide (Publication number: MAN0016854). When templating DNA for sequencing the automated Ion Chef™ system employs the principle of emulsion PCR via clonal amplification of each amplicon on an Ion sphere particle (ISP) which results in multiple copies of the same amplicon with ISP. This is required so that optimal signal can be generated and subsequently be detected hence the synthesis of multiple copies of the same amplicon.

The wells of the Ion 520™ chip (ThermoFisher Scientific), which contain sensory coatings that can detect any change in pH during sequencing, were loaded with ISPs by the Ion Chef™ system in preparation of sequencing the Ion 520™ chip.

3.2.4.3 Ion torrent sequencing of DNA samples

Once DNA templating on the Ion Chef™ (ThermoFisher Scientific) automated system was complete, the Ion 520™ chip (ThermoFisher Scientific) was then loaded on to the Ion S5™ Sequencer. The Ion S5™ Sequencing kit reagents were stored at room temperature 45 minutes prior to them being loaded into the sequencer. All the reagents as well as solutions within the Ion S5™ Sequencing kit have been tagged with RFID technology which enables the Ion S5™ Sequencer to confirm that all reagents and solutions are loaded correctly and that they have not expired therefore affecting the pH as well as their efficacy in which case the Ion S5™ Sequencer will generate an error if reagents have expired. All this is confirmed by the Ion S5™ Sequencer during the initialisation step prior to sequencing as stipulated in the Ion 520™ kit Chef user guide (ThermoFisher Scientific).

The Ion S5™ Sequencer (ThermoFisher Scientific) employs the semiconductor sequencing technique via the Ion Torrent™ sequencing technology (ThermoFisher

Scientific) which enables the sequencing of the 200 bp DNA libraries loaded onto the Ion 520™ chip. The Ion S5™ Sequencer floods the Ion 520™ chip with PCR master mix reagents (i.e DNA polymerase, dNTPs as well as buffers) which will drive the sequencing of the DNA libraries. Using the built in pH meter, the system detects pH changes whenever there is incorporation of a nucleotide by DNA polymerase since this results in production of H^+ ion which is used in base calling. The nucleotides Adenine (A), Cytosine (C), Thymine (T) and Guanine (G) were each added to a total of four trial solutions in their native form (dATP, dCTP, dTTP and dGTP) such that whenever a trial solution of specific dNTP which is complementary to the template DNA was added to the Ion 520™ chip it resulted in base incorporation as well as the release of H^+ resulting in pH change as well as elongation of the DNA strand (Merriman et al., 2012). The built in pH meter also aids in detecting as to how many bases were incorporated into the elongated sequence. There is also a wash step/flow of the preceding trial solution subsequent to flowing of each respective trial solution for each dNTP. There will be no pH change or release of H^+ as well as nucleotide incorporation whenever there is flooding with a flow solution that is not complementary to the leading DNA strand. Also, in case of a DNA template sequence having consecutive identical bases (homopolymer) flowing of a complementary single species dNTP will allow incorporation of multiple dNTP molecules at a single cycle. This results in the release of more H^+ ions and the voltage will be doubled. The chip then records multiple bases (Merriman et al., 2012).

3.2.5 Analysis of genetic variants data

3.2.5.1 Post sequencing metrics and Read alignment

Once the sequencing run was complete, a data report comprising of metrics from before and after alignment was generated for quality assessment by the Ion Torrent Suite™ software, which is built into the Ion S5 instrument (ThermoFisher Scientific). The sequencing parameters which were indicative of a successful sequencing run had to meet the following threshold for the data to be considered useful: more than 70% for loading of the chip, less than 20% for reads of poor quality, more than 55% of excellent quality reads and less than 35% polyclonality

(de Abreu et al., 2016). All bases with sequencing coverage depth of more than 30X were considered readable given that for germline testing an average sequence depth of 30X coverage is considered ideal (Jennings et al., 2017).

The Ion Torrent Suite™ software v5.14 (ThermoFisher Scientific) was employed in the alignment of reads since the software contained plugins tools to enable such analysis using the genome reference consortium human build 37 (GRCh37/hg19) of the human reference genome to generate binary alignment map (BAM) output files for downstream analysis.

3.2.5.2 Variant calling and interpretation

The Ion Torrent Suite™ software v5.14 (Thermo Fisher Scientific) also has a plugin necessary for variant calls, the outcome of which is saved in variant call format (VCF) file type. Detected genetic variants as well as read alignment data in contrast to the human reference genome against genomic DNA from samples are contained within the VCF and BAM output files (Steward et al., 2017). Three categories/steps were employed in the interpretation of the called variants namely, annotation of variants (Ensembl Variant effect Predictor (VEP) and Ion Reporter software™ v5.14), followed by prioritisation of variants (Population, Mutation and Disease databases as well as in *silico* predictors) and finally classification of variants with the aid of ACMG guidelines for variant interpretation (**Appendix B**) (Richards et al., 2015).

3.2.5.3 Annotation of variants

To understand the meaning of each variant called, Ion Reporter™ Software v5.14 (Thermo Fisher Scientific) was used to annotate all VCF output files corresponding to each and every specific sample with the aid of VEP in contrast to the human reference genome assembly. VEP is a powerful toolset for the analysis, annotation, and prioritization of genomic variants in coding and non-coding regions. VEP is an online bioinformatics tool which requires the VCF file as an input in order to generate/categorise the variants by location, symbol of the gene harbouring the variant as well as class of the variant (McLaren et al., 2016; Sefid and Gamieldien,

2017). The online tool also further investigates the variants against population databases (frequency of variants), mutation databases (functional effect on the gene harbouring the variant) databases and disease databases (clinical phenotype associated with the variant). Further, built-in tools or plugins such as Sorting Intolerant from Tolerant (SIFT) and Polymorphism Phenotyping version 2 (PolyPhen-2), are employed by VEP to measure the severity of the consequence of changes to protein coding sequences, regulatory regions as well as splice sites by generating scores. SIFT scores range from 0.0 (deleterious) to 1.0 (tolerated) and PolyPhen-2 scores range from 0.0 (benign/tolerated) to 1.0 (deleterious). Previously reported/existing variants are tagged with identifier code which enables easy access to journals with the research articles.

3.2.5.4 Prioritisation of variants

As mentioned earlier, population, mutation and disease databases were used for prioritisation of variants coupled with bioinformatics tools to predict pathogenicity of variants. The variants were inputted into various population databases such as genome aggregation database (gnomAD), 1000 genomes project, as well as exome aggregation consortium (ExAC) to determine the minor allele frequency (MAF) which is indicative of how common (MAF > 5%) or rare (MAF < 1%) these variants are in the general population of various ethnic groups (Karczewski et al.,2017). Variants with MAF > 5% were filtered out while the rest were retained for further analysis using other criteria such as mutation and disease databases. The National Centre for Biotechnology Information (NCBI) ClinVar database was used to determine the functional effect as well as corresponding clinical phenotype associated with the variants and all variants reported as benign/likely benign were filtered out (Landrum et al., 2018). The remaining variants were then prioritised using multiple predictive bioinformatics tools such as Combined Annotation Dependent Depletion (CADD), Deleterious annotation of Genetic Variants using Neural Network (DANN), SIFT, MutationAssesor, PolyPhen2, dbscSNV and Functional Analysis Through Hidden Markov Models (FATHMM), which enabled the prediction of pathogenicity of the variants (Kumar et al., 2009; Reva et al., 2011; Adzhubei et al., 2013; Shihab et al., 2013; Jian et al., 2014; Quang et al., 2015;

Rentzsch et al., 2019). The above-mentioned tools perform such predictions by examining the type of variant, any potential deleterious effects at DNA and/or protein levels as well as evolutionary conserved regions leading to prediction of impaired or lack of functionality of proteins with variants predicted to be non-deleterious filtered out (McArthur et al., 2014; Richards et al., 2015).

3.2.5.5 Variant classification

The remaining prioritised variants underwent classification with the aid of ACMG variant interpretation guidelines which are employed by various research and diagnostic laboratories around the world (Richard et al., 2015). Under the ACMG guidelines, variants can be classified as one of the following classes, Benign (B), likely benign, pathogenic (P), likely pathogenic or variant of uncertain significance (VUS). Prior to classifying a variant, evidence from various databases such as (clinical phenotype, segregation pattern, family history, inheritance models, frequency of the variant in the general population, functional data and in silico tools) is required (Richards et al., 2015). The required evidence from the listed databases is further classified in terms of strength level as follows: Supporting (P), strong (S), moderate (M) and very strong (VS). Varsome (Kopanos et al., 2019) is a search engine which consist of data from multiple databases such as ACMG guidelines, all in *silico* tools, Genotype tissue expression (GTex), gnomAD, ExAC, ClinVar transcripts and any publications about the variant of enquiry or gene (Kopanos et al., 2019). Varsome was used in the current study to observe aggregated data of each variant from multiple database which served as a guide when classifying the variants in case there was conflicting interpretations of pathogenicity of variants from this study with any other variant submitters on ClinVar.

3.2.5.6 Integrative genomics viewer

The BAM files of all variants which were classified as VUS, pathogenic and likely pathogenic after application of ACMG guidelines, were uploaded onto Integrative genomics viewer (IGV) v2.11.2 (Thorvaldsdóttir et al., 2013), which enabled the visualisation of variant coverage to determine as to whether base calling was

consistent or it was poorly covered. This is an important post alignment quality control step given that poorly covered regions can yield sequencing artefacts during variant calling.

3.3 Results

3.3.1 Patient's clinical data

DNA from a total of 14 patients and two parents was collected for sequencing in the current study. All patients diagnosed with any congenital eye disorder categorised under ASD were invited to participate in the study. **Table 3.1** shows demographic and clinical features data for each patient with consent forms in (Appendix D).

Table 3.1: Demographic data and clinical features of patients sequenced in the study.

Sample No.	Patient ID	Sex	Age	Diagnosis	Ocular Features	Family History
1	OG131AA	*	*	Axenfeld-Rieger syndrome	No systemic features, iris atrophy and pseudopolycoria, iris processes, posterior embruotoxon, secondary glaucoma, corneal decompensation post operatively	Mother, maternal grandmother
2	OG115AA	*	*	*	*	*
3	OG136AA	M	53	Axenfeld-Rieger syndrome	Axenfeld angle with iris processes - no posterior embryotoxon noted in computer database - asymmetrical glaucoma R>L - had glaucoma surgery RE	No
4	OG137AA	*	*	*	*	*
5	OG134AA	*	*	*	*	*
6	OG113AA	F	27	Axenfeld-Rieger syndrome	Axenfeld angle with iris processes - no posterior embryotoxon noted in computer database - asymmetrical glaucoma R>L controlled on topical treatment	No
7	OG118AA	*	*	*	*	*
Sample No.	**Patient ID**	**Sex**	**Age**	**Clinical Phenotype**	**Ocular Features**	**Family History**
8	OG143AA	F	35	Axenfeld-Rieger syndrome	Asymmetrical glaucoma, RE NLP, early disease left eye - no details on angle appearance no comment on processes or embryotoxon	No
9	OG162AA	M	6	Small anterior chamber	Left eye leukocoria associated with a small anterior chamber on MRI	No
10	OG163AA	M	*	Father (OG165AA)	*	No

11	OG164AA	F	*	Mother (OG165AA)	*	No
12	OG165AA	M	4	Peter's Anomaly	Bilateral blindness due to kerato-irido-lenticular dysgenesis but with persistent hyperplastic primary vitreous with retrolental calcification on CTB.	No
13	OG167AA	F	7	Peter's Anomaly	Bilateral visual loss with corneal opacification. On the right the visual loss is due to a retinal dysplasia, while on the left it is acquired secondary to trauma.	No
14	OG141AA	F	34	Axenfeld-Rieger syndrome	Axenfeld angle with iris processes - 360 degrees with fine processes in narrow angles, advanced juvenile onset open angle glaucoma (blind left eye), no posterior embryotoxon	Family history of glaucoma - both daughters have similar angle appearance and ocu;lar hypertension but no evidence of glaucoma
15	OG151AA	M	31	Aniridia	Aniridia, Secondary glaucoma, glaucoma surgeries and laser, secondary cataracts,	Mother, Grandfather, two siblings, children.
16	DD3918	M	6	Axenfeld-Rieger Anomaly	Blue discolouration of sclera, bilateral enophthalmos.	No

3.3.2 Quality control of Ion torrent sequencing data

The quality of the NGS preparation steps was assessed by examining the parameters of each sequencing run metrics before and after alignment of sequencing reads. As described in the methods section of this chapter, a total of 16 samples comprising of 14 patients and two parents of one patient were sequenced in two separate runs each accommodating only eight samples as per NGS sequencing chip recommendations (**Figure 3.2** and **Figure 3.3**). The overall data indicated that both runs were prepared in a very high-quality manner as indicated by the following: First run showed that 59% of the reads were useable, 94% of the wells were loaded efficiently, only 7% of the reads were of low quality and 36% polyclonality (**Figure 3.2)**. The second run also showed similar quality data in that 71% of the reads were useable while 92% of the wells were loaded successfully, 6% of the reads were of low quality as well as 24% polyclonality (**Figure 3.3**). The intense red colour on both sections of **Figures 3.2** and **3.3** showed the loading density of the samples on the 96 well plate, which was indicative of ideal data quality for both sequencing runs. Genotypes with low confidence calls were identified and evaluated with the aid of the Ion Reporter™ software (ThermoFisher Scientific). The output BAM files were uploaded onto IGV to perform coverage analysis via the visualisation of sequence reads per patient in contrast to pathogenic, likely pathogenic and variants of uncertain significance.

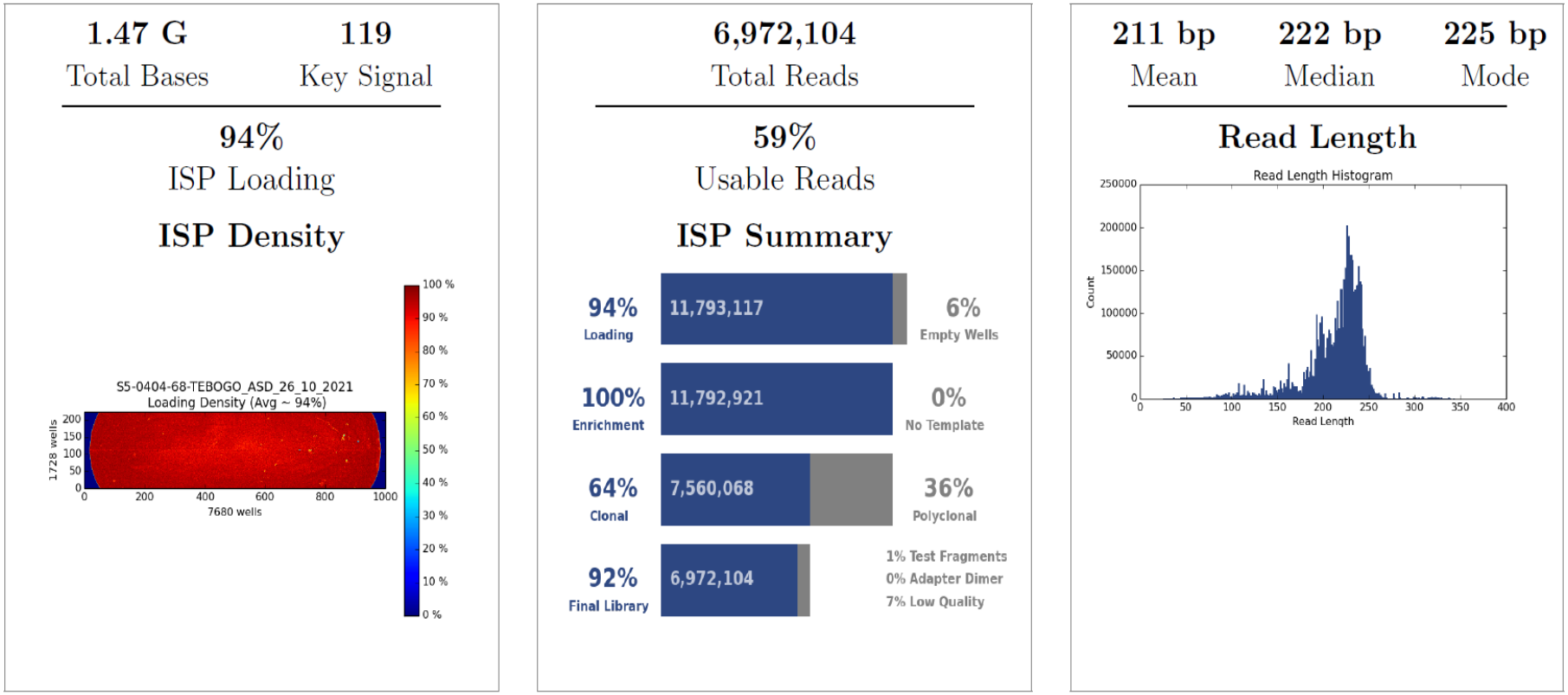

Figure 3.2: Summary of the quality of Ion Torrent NGS run for first eight samples. Data metrics for sequencing run of the first 8 samples with an ISP loading density of 94%, which generated a total of about 6.7 million reads with only 59% deemed usable and a mean read length of 211 bp.

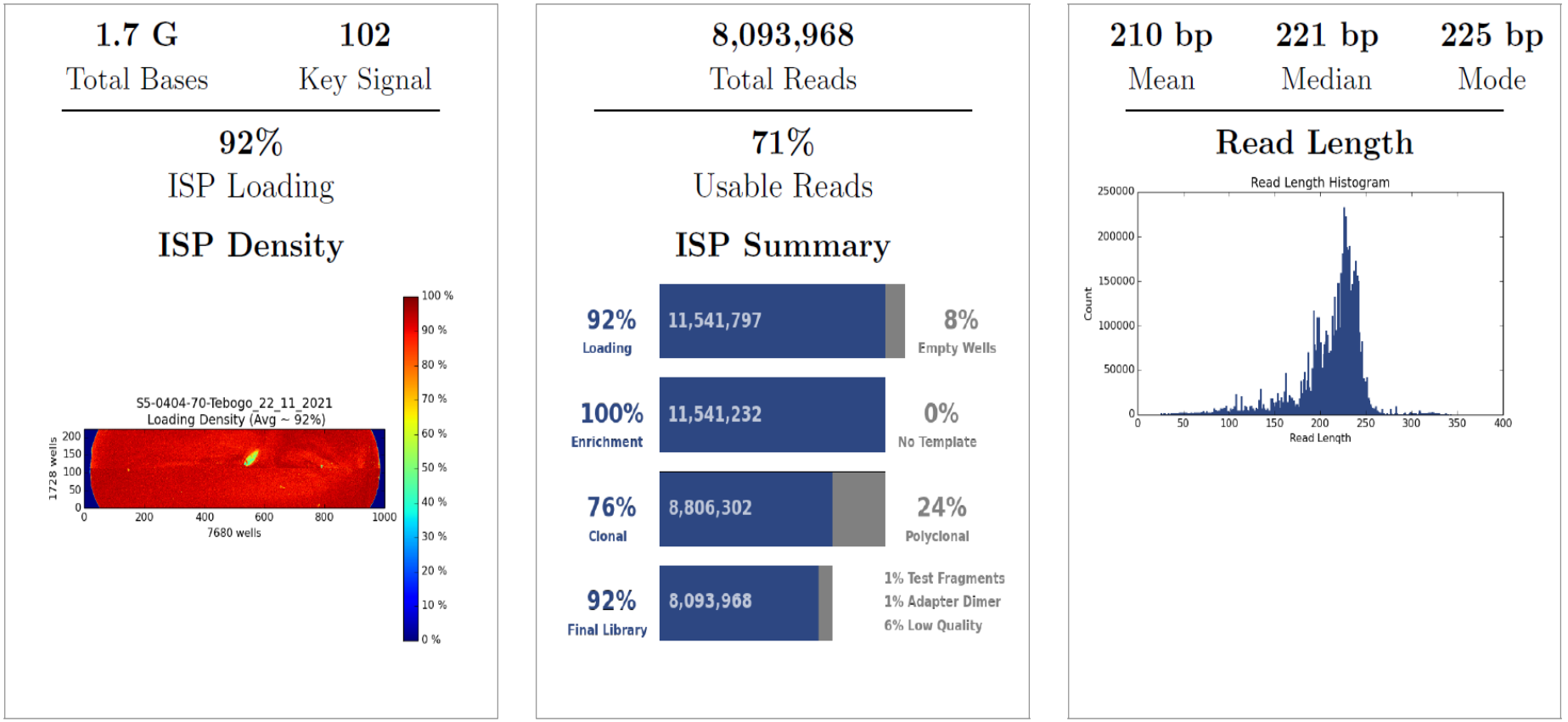

Figure 3.3: **Summary of the quality of Ion Torrent NGS run for last eight samples.** The second run had 92% ISP loading density which produced approximately 8 million reads with only 71% of the reads useable and the reads had a mean of 210 bp in length.

3.3.3 Identified variants from NGS

The first sequencing run detected a minimum of 135 variants and a maximum of 162 variants, while the second run detected a minimum of 130 and maximum of 153 variants (**Table 3.2**). These were further confirmed by Ensembl's VEP after uploading the VCF file of each patient generated by Ion Torrent Suite™ software v5.14 (ThermoFisher Scientific). The variants further underwent quality control analyses as well as filtration to eliminate poorly called variants and those not associated with the clinical phenotype of interest in our study as well as those that appeared too frequently/common within the general population.

Table 3.2: Total number of variants detected in candidate genes (Table 1.1) by Ion Torrent Suite™ software v5.14 per patient prior to filtration and interpretation.

Sample No.	Patient ID	Sequencing Run	No. of variants pre-filtration
1	OG131AA	First	162
2	OG115AA	First	156
3	OG136AA	First	137
4	OG137AA	First	135
5	OG134AA	First	152
6	OG113AA	First	154
7	OG118AA	First	143
8	OG143AA	First	158
9	OG162AA	Second	153
10	OG163AA	Second	132
11	OG164AA	Second	144
12	OG165AA	Second	144
13	OG167AA	Second	141
14	OG141AA	Second	142
15	OG151AA	Second	145
16	DD3918	Second	130

3.3.4 Putative disease-causing variants

All variants that were classified as (likely) pathogenic after filtration and prioritisation are described in the subsections below (per gene) with regards to patients harbouring the variants. Pathogenicity of the variants was detected via VEP, Varsome as well as manual application of the ACMG guidelines codes. The depth of reads for all (likely) pathogenic and VUS were visualised with the aid of IGV. ACMG guidelines were applied to variants that required reclassification as Varsome and/VEP might report some variants to have conflicting interpretation of pathogenicity which results when multiple submitters of variants claim different impact of specific variants in comparison with the corresponding clinical phenotype the variant was tested against. Submitters of variants to ClinVar usually classify variants with supporting evidence either being overwhelmingly strong in support of disease development therefore such variant will be classified as pathogenic, when evidence is moderate then such variant will be classified as VUS. When the evidence is strongly against the variant causing clinical phenotype then variants are classified as (likely) benign.

A total of 43 genes were screened for disease causing mutations in 14 patients presenting with ASD and also two parents of one patient. Quality control measures such as Annotation, filtration and prioritisation were applied to data from all 14 patients and two parents as explained in section 3.2 which yielded eight potential disease-causing variants with two in *GJA8*, *PAX6* (**Table 3.3**) which were pathogenic and six variants which were classified as VUS in *BCOR*, *EPHA2*, *PXDN* and *LTBP2* (**Table 3.4**) in this study. The (likely) pathogenic variants and VUS are described in detail per gene below in affected patients.

Table 3.3: Potential disease-causing variants detected in two patients and classified as (likely) pathogenic in this study and by Varsome database.

GENE	Impact	Variant	ClinVar Accession Number	dbSNP ID	*In Silico* tools (Benign)	*In Silico* tools (Pathogenic)	ACMG-AMP Code	ACMG classification	Presenting clinical phenotype	Patient(s) with variant
GJA8	Missense	c.22G>A (p.Gly8Arg)	-	rs202041458	Mutation Assessor	DANN, SIFT, FATHMM, MutationTaster & 7 more.	PM2, PP2, PP3	Likely Pathogenic	Axenfeld-Rieger syndrome	ID: 16
PAX6	Stop gained	c.760C>T (p.Arg254Ter)	RCV000003632.3 & RCV000536976.3	rs121907917	-	DANN, FATHMM, MutationTaster	PVS1, PP5, PM2	Pathogenic	Aniridia	ID: 15

3.3.4.1 Paired box protein 6 (PAX6)

PAX6 like many other transcription factors induces embryonic differentiation along major body axes in response to the concentration gradient of other regulatory proteins or transcription factors, which bind to DNA sequences of other genes and regulate their expression (Friedman, 1998). PAX6 belongs to the *PAX* multigene family of transcription factors that aid in the regulation of embryonic differentiation (Friedman, 1998). A nonsense stop gained *PAX6* heterozygous variant NM_001258462.3: c.760C>T (p. Arg254Ter) was detected in sample 15: A 31-year-old, black male diagnosed with aniridia and cataracts complicated by secondary glaucoma. The patient's maternal grandfather, mother, two siblings and two children are all similarly affected. The variant is located in exon 10 position 36 of 83 in PAX6 gene. This variant has three submitters on ClinVar (Accession no. RCV000003632.3, RCV000312176 & RCV000536976.3) with two associating the variant with Aniridia and classifying it as pathogenic.

Varsome further confirmed the pathogenicity of the variant by applying the ACMG-AMP codes PVS1 (very strong) given that the nonsense stop gained single nucleotide variant (SNV) results in null variants in *PAX6* gene, which usually results in loss of function in disease, PP5 (strong) due to pathogenic classification by ClinVar with strength strong support given 19 published supporting articles on this variant and finally PM2 (moderate) since the variant did not have a gnomAD genome entry and was not detected in the healthy population but has a dbSNP ID of rs121907917. Predictive In Silico tools such as DANN, FATHMM-MKL, MutationTaster as well as eight others as listed in **Table 3.3**, all predicted the variant to be pathogenic with only FATHMM-XF predicting low impact. The classification by Varsome was in agreement with our own assessment of the variant in relation to our study cohort. IGV showed that the variant call was accurate as the majority of the reads showed the presence of the alternate allele A instead of the G reference allele upon manual assessment of variant coverage (**Figure 3.4**). IGV is showing a G>A change instead of C>T which are complementary nucleotides on each DNA strand.

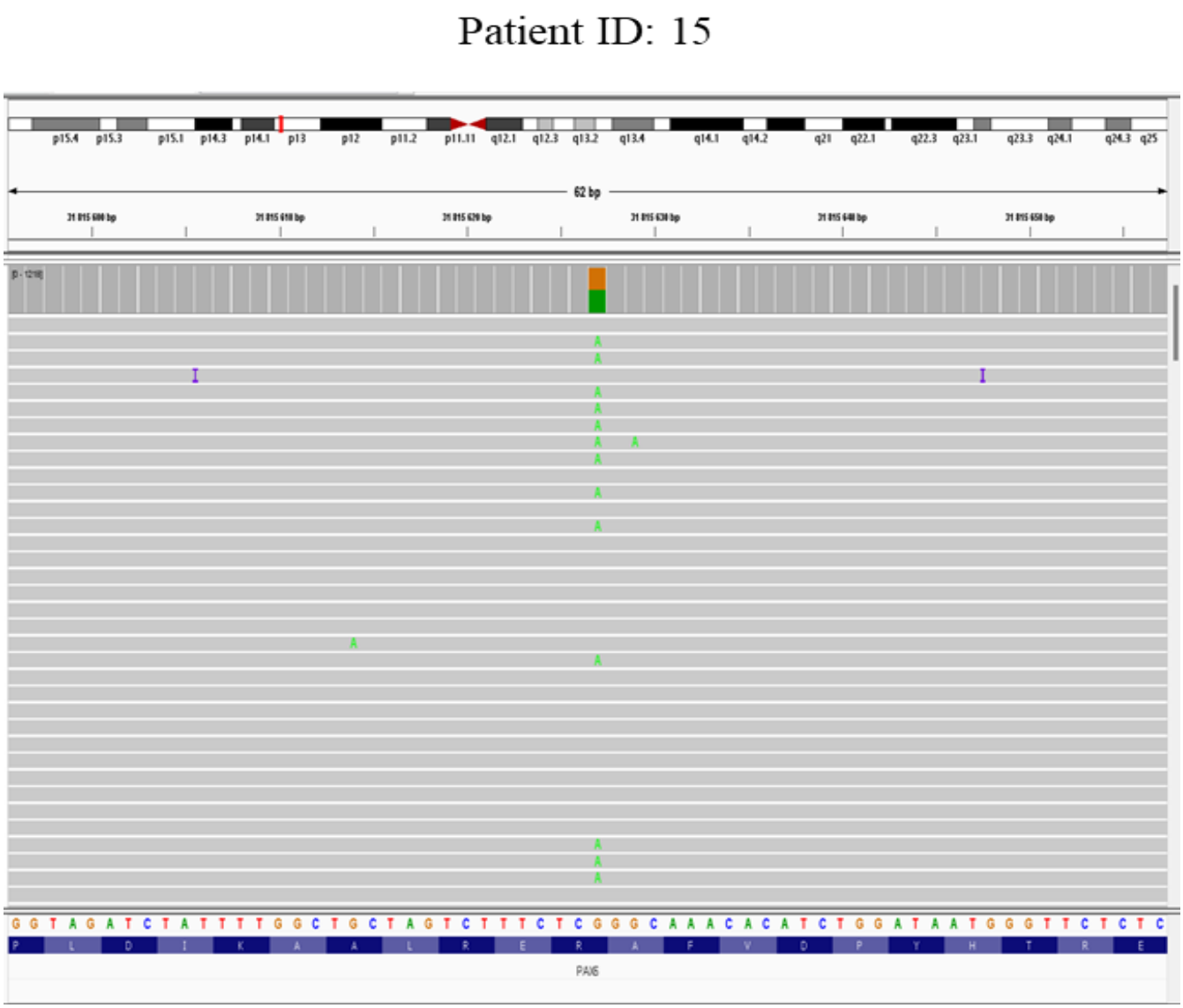

Figure 3.4: IGV image of a heterozygous *PAX6* c.760C>T (p. Arg254Ter) variant detected in a patient (sample 15) diagnosed with Aniridia. The reference genome sequence shows a reference allele as G (Mustard) which is changed to the alternate allele of A (Green).

3.3.4.2 Gap junction alpha 8 (*GJA8*)

The gap junction alpha 8 (*GJA8*) gene encode for connexin50 (Cx50) protein which belongs to a group homogenous transmembrane family of proteins crucial for intercellular communication and moderating diffusion of molecules between lens fibre cells (García et al., 2016). *GJA8* heterozygous missense variant NM_005267.5: c.22G>A (p.Gly8Arg) was detected in a 6 year old black boy who was diagnosed with Axenfeld-Rieger anomaly at birth. The child also has profound hearing loss, global neurodevelopmental delay, subtle dysmorphic features and microcephaly diagnosed with Axenfeld-Rieger anomaly (**Table 3.3**). The variant is located in exon 2 at position 33 of 1325 and was classified as likely pathogenic in the current study, which was in agreement with the classification by Varsome. This variant is not reported in ClinVar and the following ACMG-AMP classification codes were applied: PM2 (Moderate) since the variant was predicted to be located in a region that is strongly conserved, PP2 (Supporting) due to low rate of benign variants and high rate of missense mutations which are known cause of disease in GJA8 and PP3 (Supporting) as only one (MutationAssessor) computational In Silico tool predicted benign impact, while 11 more (BayesDel_addAF, DANN, DEOGEN2, EIGEN, FATHMM-MKL, LIST-S2, M-CAP, MVP, MutationTaster, PrimateAI and SIFT) predicted pathogenic impact.

The variant has dbSNP ID rs202041458 and has been reported in gnomAD with an allele frequency of 0.000185 (~ 1 in 5418) in Africans while south Asians have a frequency of 0.0000239 (~ 1 in 41902) with other ethnic groups having no entry in gnomAD. Inspection of the *GJA8* missense variant on IGV indicated that the variant was called with high confidence as the majority of the reads had the alternate allele of A, whilst the reference genome sequence has a reference allele of G (**Figure 3.5**).

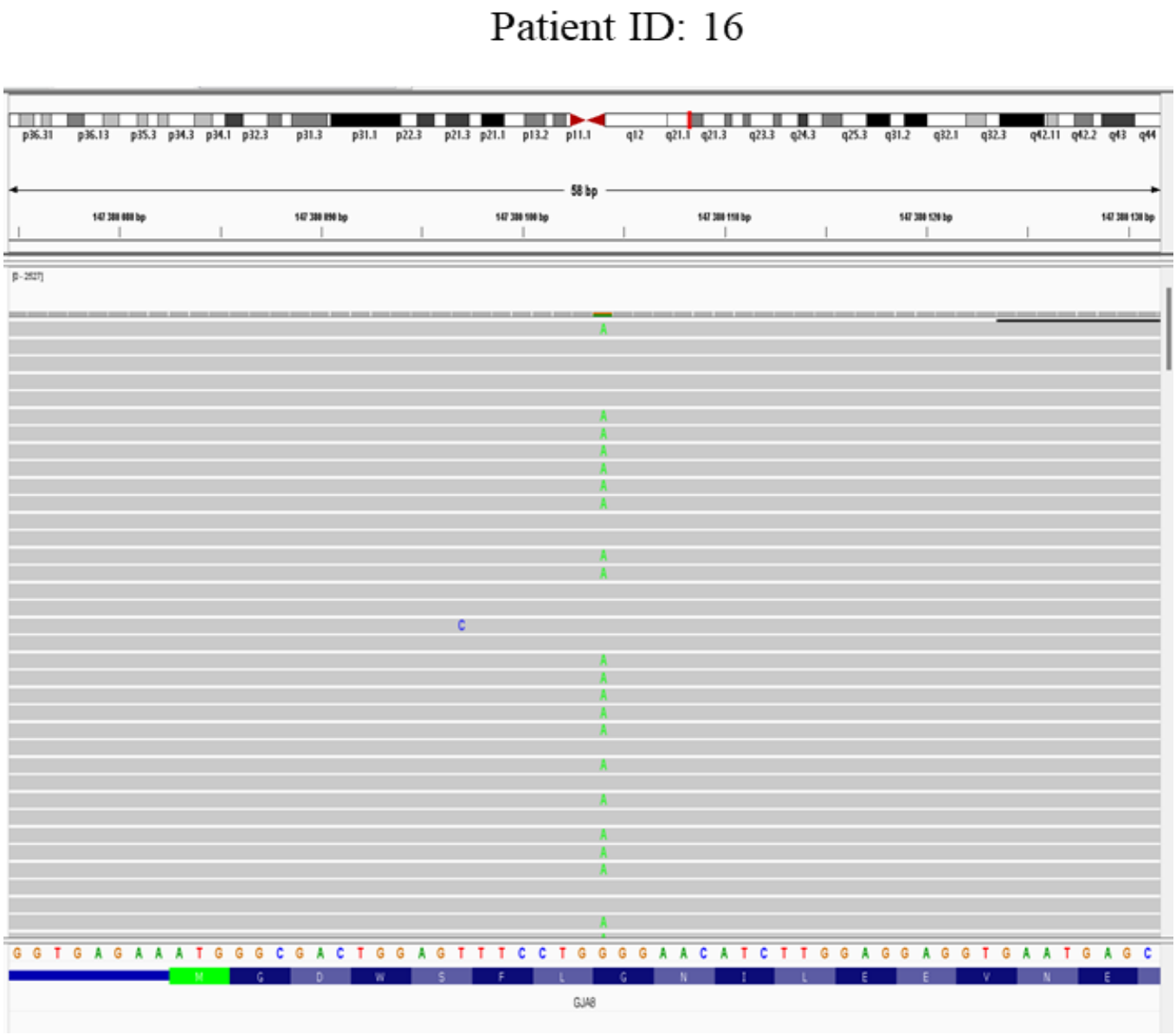

Figure 3.5: IGV plot of a heterozygous c.22G>A (p.Gly8Arg) missense variant in exon 2 of *GJA8* in a patient diagnosed with Axenfeld-Rieger syndrome. The reference sequence records a G (Mustard) allele at this position, while the reads show an alternate allele of A (Green) across the multiple reads of patient (ID: 16).

3.3.5 Variants of uncertain significance (VUS)

Mutations that were classified as VUS by Varsome and manual interpretation due to conflicting interpretation of pathogenicity were further assessed with regards to their impact in our study cohort. Once all filtration and prioritisation parameters were applied a total of six mutations were identified, with one in BCL6 corepressor (*BCOR*), one in EPH receptor A2 (*EPHA2*), two in Latent Transforming Growth Factor Beta Binding Protein 2 (*LTBP2*) and two in Peroxidasin (*PXDN*). Varsome predicted the *BCOR*, *EPHA2*, and one *LTBP2* variants to be pathogenic while we re-classified all three variants to VUS in this study as outlined in the discussion **section 3.4**.

Table 3.4: Mutations classified as VUS by Varsome and manual interpretation in relation to our study cohort.

GENE	Impact	Variant	ClinVar Accession Number	dbSNP ID	*In Silico* tools (Benign)	*In Silico* tools (Pathogenic)	ACMG-AMP Code	ACMG classification	Presenting clinical phenotype	Patient(s) with variant
BCOR	Frameshift	c.1257_1260delinsGAC (p.Asp420ThrfsTer22)	-	-	-	MutationTaster	PVS1, PM2	Likely Pathogenic (VUS in this study)	Axenfeld-Rieger syndrome, Aniridia	ID: 6, 15
EPHA2	Frameshift	c.986_987delinsT (p.Pro329LeufsTer64)	-	-	-	MutationTaster	PVS1, PM2	Pathogenic (VUS in this study)	Peters' Anomaly	ID: 13
LTBP2	Missense	c.1577G>A (p.Ser526Asn)	-	rs142979965	BayesDel_addAF, DEOGEN2, EIGEN, LIST-S2, M-CAP, MVP, PrimateAI and SIFT	DANN, FATHMM-MKL, MutationAssessor and MutationTaster	PM2 and BP4	VUS	Peter's anomaly	ID: 12
LTBP2	Splice region	c.3527-3C>A	RCV000403118	rs138194436	DANN	MutationTaster	PM4, PP3 and PM2	Pathogenic (VUS in this study)	Axenfeld-Rieger syndrome	ID: 1

GENE	Impact	Variant	ClinVar Accession Number	dbSNP ID	*In Silico* tools (Benign)	*In Silico* tools (Pathogenic)	ACMG-AMP Code	ACMG classification	Presenting clinical phenotype	Patient(s) with variant
PXDN	Missense	c.1112C>T (p.Pro371Leu)	RCV000950335	rs201592851	BayesDel_addAF, DEOGEN 2, MVP and PrimateAI	DANN, EIGEN, FATHMM-MKL, LIST-S2, M-CAP, MutationAssessor, MutationTaster and SIFT	PM2 and PP3	VUS	Axenfeld-Rieger syndrome	ID: 14
PXDN	Missense	c.2827C>T (p.Arg943Trp)	RCV001546804	rs200127189	*BayesDel_addAF, DEOGEN 2, EIGEN and MVP*	*DANN, FATHMM-MKL, LIST-S2, M-CAP, MutationAssessor, MutationTaster, PrimateAI and SIFT*	PM2 and PP3	VUS	Peter's anomaly, Axenfeld-Rieger syndrome	ID: 12, ID: 14

3.3.5.1 BCL6 corepressor (*BCOR*)

The *BCOR* gene encode for the synthesis of a BCL 6 corepressor protein that functions in specification of cellular differentiation and body structure development (Astolfi et al., 2019). A frameshift pathogenic variant in *BCOR* gene was detected in two patients: sample no. 15 (31-year-old harbouring the PAX6 mutation) and sample no. 6 (a 27-year-old black female with ARS as evidenced by an Axenfeld anterior segment angle with iris processes but no posterior embryotoxon and asymmetrical glaucoma). The variant was also observed in an unaffected parent (mother) (sample no. 11) of one of the patients (sample no. 12) not harbouring the variant. The variant is a frameshift NM_001123385.2: c.1257_1260delAGATinsGAC (p.Asp420ThrfsTer22) located in exon 4 of the *BCOR* gene in position 1092 to 1095 of 2832. The variant did not have any ClinVar submissions, gnomAD genomes entry or dbSNP ID as well as no *in silico* tools scores for pathogenicity detection. Varsome database classified the variant as likely pathogenic by assigning the ACMG-AMP codes PVS1 (very strong) given that the frameshift results in null variants in *BCOR* gene which usually results in loss of function in disease and PM2 (moderate) due to absence of gnomAD genomes entry or low representation of the variant in the controls (**Table 3.4**). This variant in the current study was reclassified as VUS due to the fact that there was no consistent co-segregation of the variant with a specific clinical phenotype since we detected the variant in two patients and a single parent (carrier) of a patient not harbouring the variant. IGV also showed that the variant was accurately called in all three samples as shown by **Figure 3.6** which indicates the read depth of the variant per patient. The reference genome sequence at the bottom of the image, indicates that there is frameshift with the reference nucleotide A (green) change to G (mustard) followed by a substitution of an insertion and deletion (**Figure 3.6**) which leads to Aspartic acid being replaced by Threonine at position 420 (D420Tfs*22).

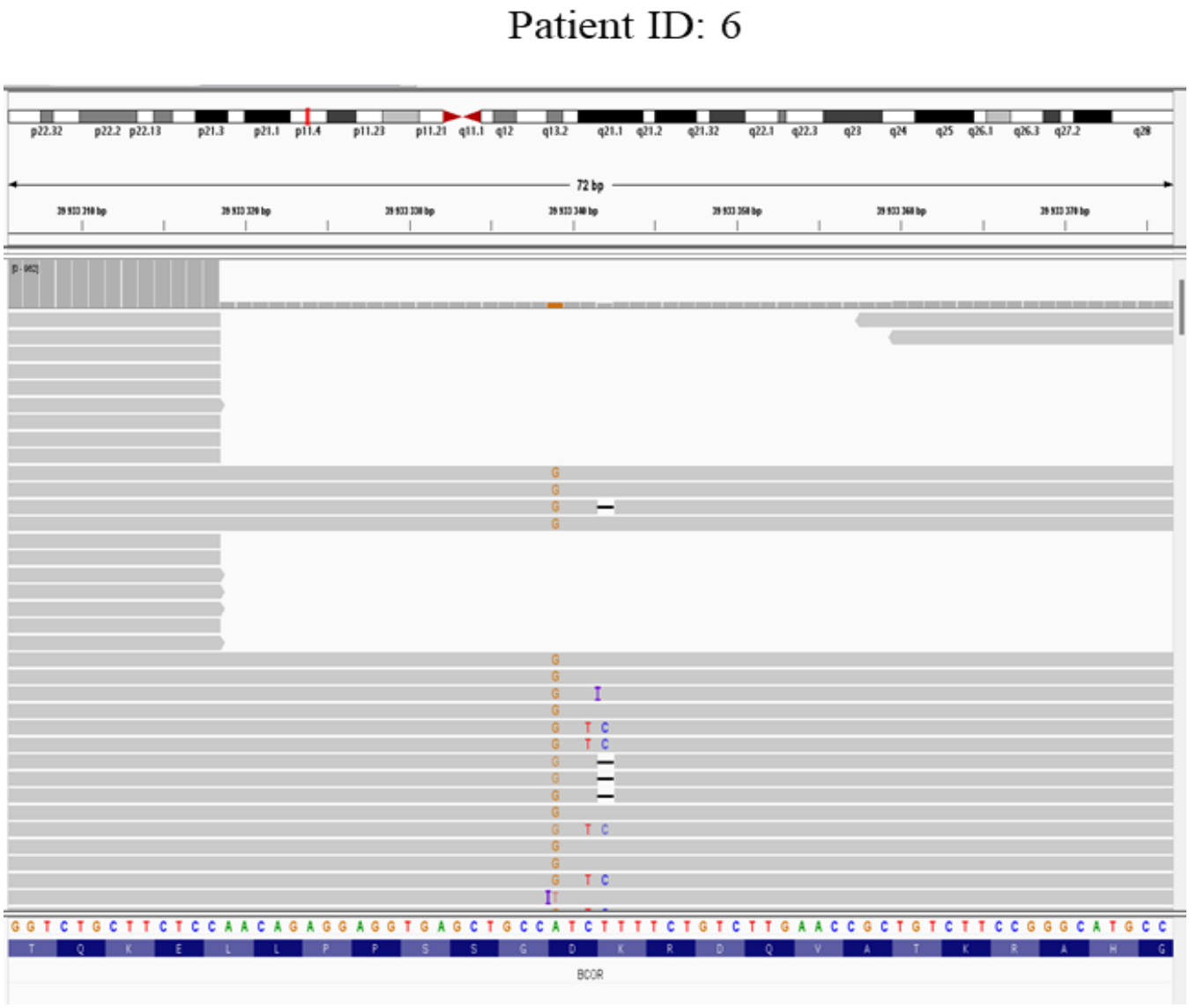

Figure 3.6: BCOR gene frameshift c.1257_1260delAGATinsGAC (p.Asp420ThrfsTer22) variant as depicted by IGV in (Patient ID: 6). The reference genome sequence is shown at the bottom of the images with the reference allele recorded as A (Green) while the reads show a frameshift at this position with the alternate allele being G (Mustard).

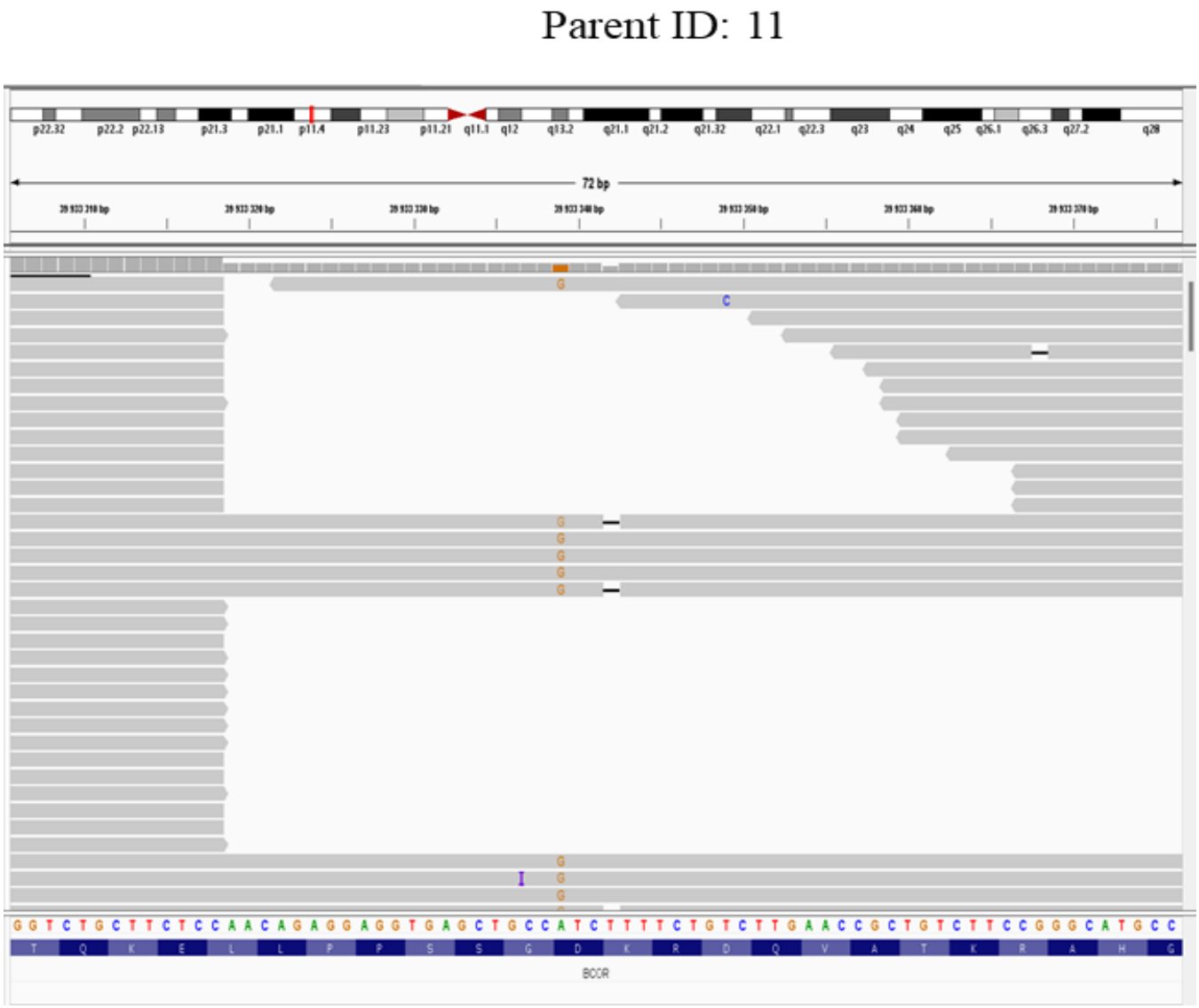

Figure 3.7: BCOR gene frameshift c.1257_1260delAGATinsGAC (p.Asp420ThrfsTer22) variant as depicted by IGV in a mother (Parent ID: 11) of one patient not harbouring the variant (Patient ID: 12). The reference genome sequence is shown at the bottom of the images with the reference allele recorded as A (Green) while the reads show a frameshift at this position with the alternate allele being G (Mustard).

Patient ID: 15

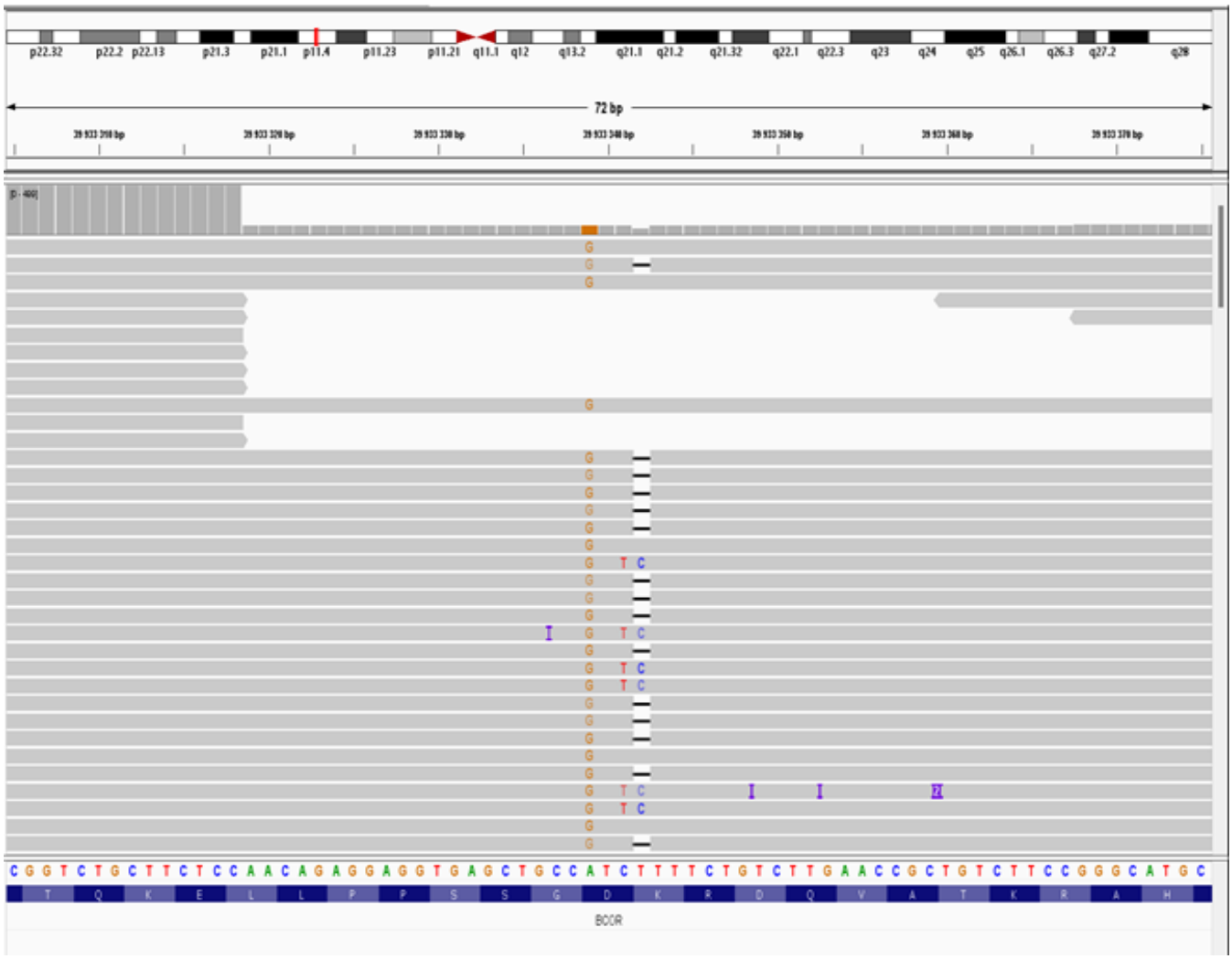

Figure 3.8: BCOR gene frameshift c.1257_1260delAGATinsGAC (p.Asp420ThrfsTer22) variant as depicted by IGV in (Patient ID: 15). The reference genome sequence is shown at the bottom of the images with the reference allele recorded as A (Green) while the reads show a frameshift at this position with the alternate allele being G (Mustard).

3.3.5.2 EPH receptor A2 (*EPHA2*)

The *EPHA2* gene encodes for ephrin receptor tyrosine kinase-type A, which is highly expressed during embryogenesis with a primary function in regulation of cell adhesion, proliferation, morphology, secretion, survival and differentiation (Miao and Wang, 2009). *EPHA2* frameshift variant NM_004431.5: c.986_987delCCinsT (p.Pro329LeufsTer64) was detected in a 7 year old black female (sample: 13) diagnosed with Peters Anomaly, age appropriate neurodevelopment, normal growth and no other congenital malformations (**Table 3.4**). The variant is located in exon 5 at position 7 to 8 of 333. Read depth coverage on IGV indicated that indeed there was a frameshift deletion with the reference genome reporting a G allele while the reads show both A allele and a deletion (**Figure 3.9**). The variant was classified as pathogenic by Varsome with the following ACMG-AMP codes applied: PSV1 (very strong) as a frameshift mutation result in null variants in *EPHA2* gene which usually loss of function results in disease and PM2 (Moderate) as the variant is located in a conserved region and the variant has a gnomAD allele frequency of 0.00006394 (~ 1 in 15639) in Africans and a global allele frequency of 0.00001636 (~ 1 in 61110). No pathogenic or benign impact prediction data by any of the *In Silico* computational tools and no ClinVar submission was present for this variant. Upon analysis of the variant in our study cohort, we classified the variant as VUS due to lack of enough supporting evidence for the gene and variant which results in difficulty in classification.

Patient ID: 13

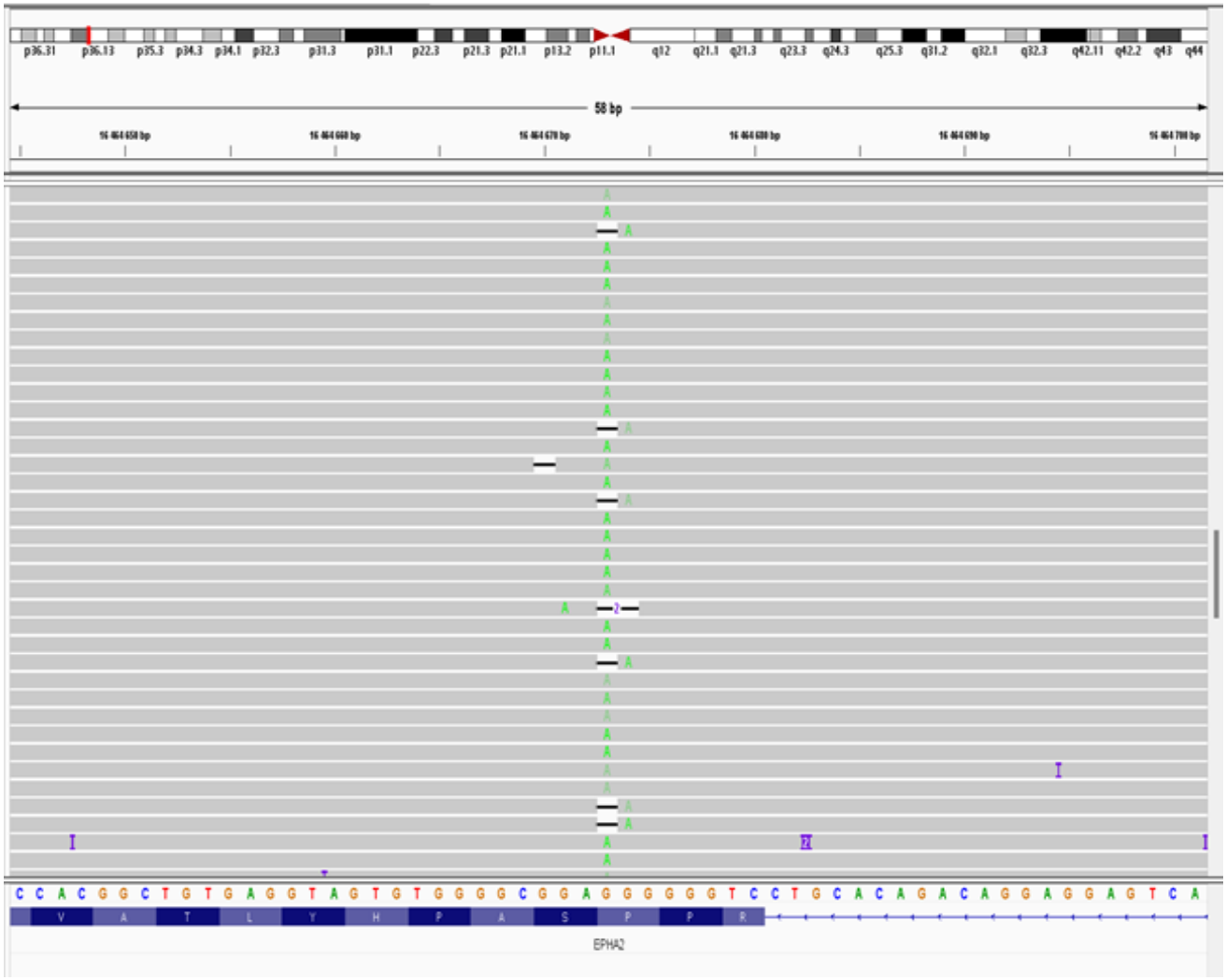

Figure 3.9: IGV plot of *EPHA2* c.986_987delCCinsT (p.Pro329LeufsTer64) frameshift variant in patient (ID: 13) diagnosed with Peter's anomaly. A reference allele of G (Mustard) is recorded by the reference genome at the variant's position, while the reads coverage shows a frameshift will allele A as well as a deletion.

3.3.5.3 Latent transforming growth factor beta binding protein 2 (*LTBP2*)

The *LTBP2* gene encode the synthesis of LTBP2 protein which is highly expressed in ciliary tissues which aid in the production of aqueous humour as well as in trabecular meshwork and functions in cell adhesion as well as tissue repair (Shipley et al., 2000). Two *LTBP2* variants were detected in two patients (ID:1 and ID:12) and the mother (parent ID: 11) of patient (ID:12).

The heterozygous missense NM_000428.3:c.1577G>A (p.Ser526Asn) in exon 7 at position 178 of 287 was detected in a 4 year old black male (sample 12) with Peters anomaly who presented with kerato-irido-lenticular dysgenesis and persistent hyperplastic primary vitreous. The patient's unaffected mother (sample 11) harboured the same variant. Varsome classified the c.1577G>A missense as VUS which was a similar classification applied in this study. The variant did not alter protein length and in silico predictive tools indicating that the variant is within a conserved region in exon 7 with ACMG-AMP code PM2 (supporting) applied, while eight pathogenicity predictive tools predicted benign impact with only four predicting a deleterious pathogenic impact therefore applying BP4 (supporting) ACMG-AMP code. The variant did not have any ClinVar submission, but had a representation of 0.00259 allele frequency in Africans in contrast to 0.000228 total minor allele frequency and dbSNP ID rs142979965. IGV confirmed presence of the variant as the depth of the reads showed the alternative allele of T while the reference genome has a C allele at the position. The C>T change recorded by IGV is a complement of the c.1577G>A variant (**Figure 3.10**) and the variant was detected in the mother (Parent ID: 11) of the diagnosed patient (ID: 12) **Figure 3.11**.

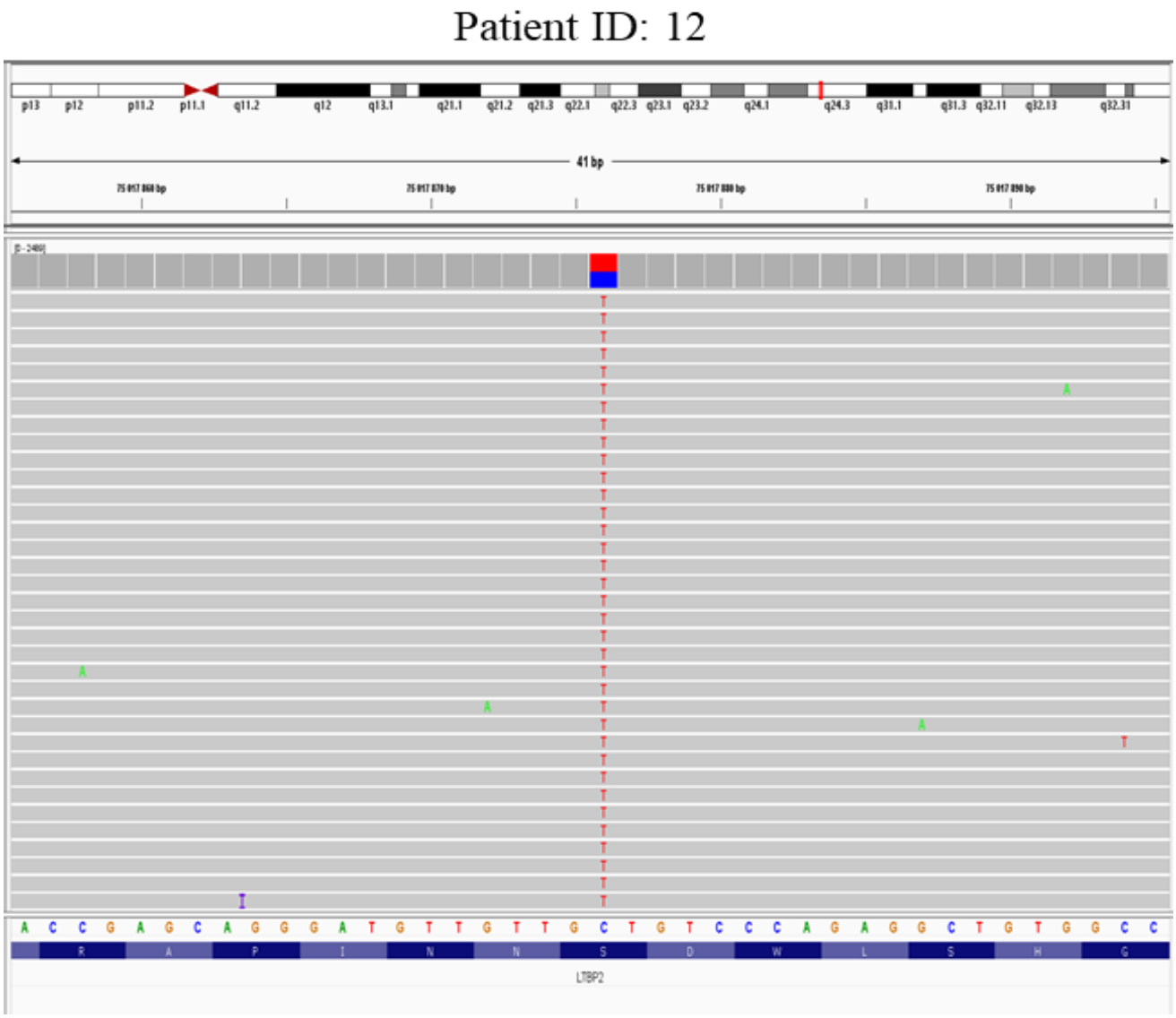

Figure 3.10: IGV plot of *LTBP2* c.1577G>A (p.Ser526Asn) missense variant in patient (ID: 12) diagnosed with Peter's anomaly. A reference allele of C (Blue) is recorded by the reference genome at the variant's position, while the reads coverage depth shows a missense variant allele T (Red).

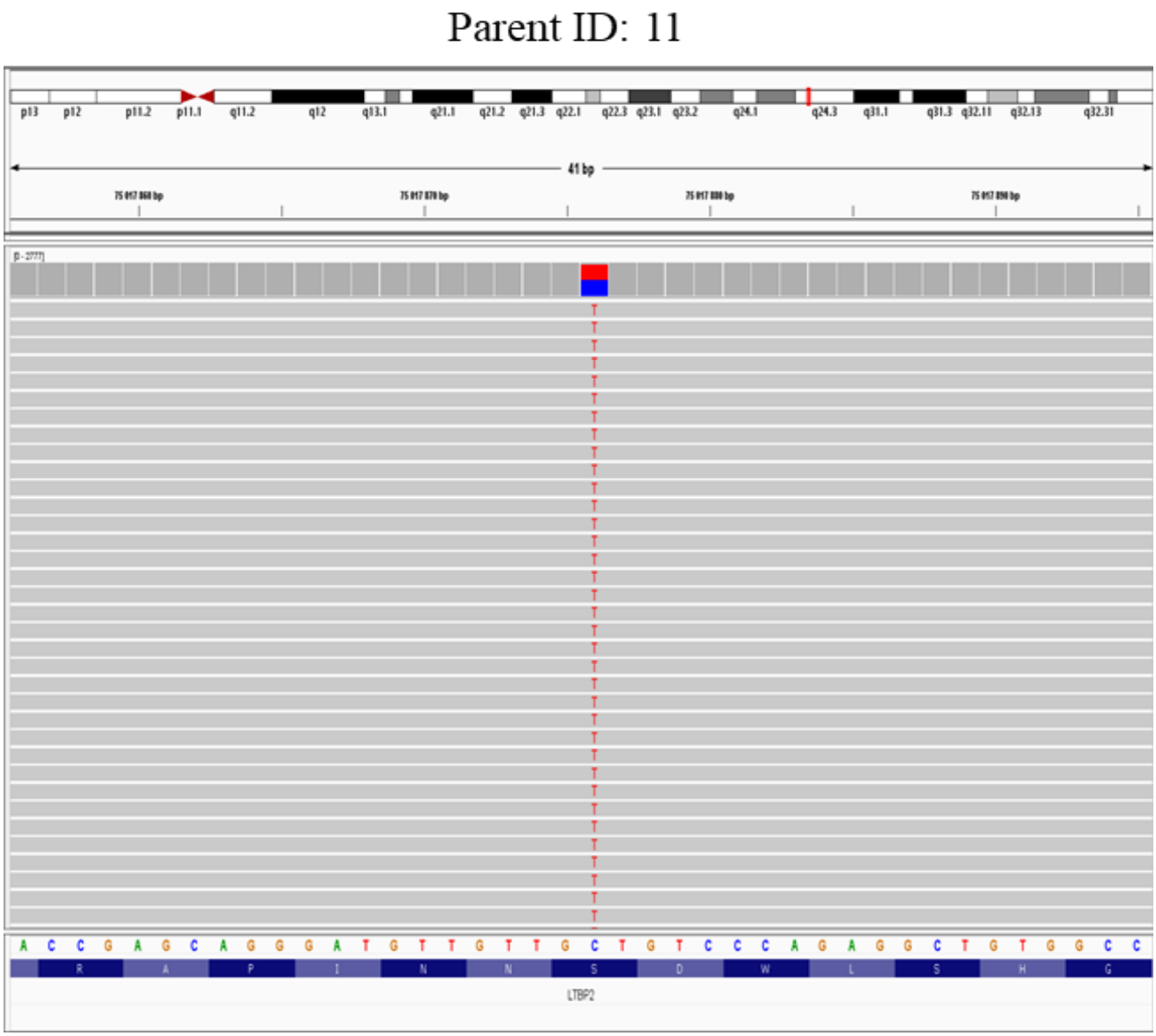

Figure 3.11: IGV plot of *LTBP2* c.1577G>A (p.Ser526Asn) missense variant in the mother (parent ID: 11) of patient (ID: 12) diagnosed with Peter's anomaly and a carrier of the same variant. A reference allele of C (Blue) is recorded by the reference genome at the variant's position, while the reads coverage depth shows a missense variant allele T (Red).

Patient (ID: 1) presenting with ARS harboured a heterozygous splice site variant NM_000428.3:c.3527-3C>A in intron 23 at position 98 of 100 (**Table 3.4**) was detected in a 56 year old black female with classic ARS. Both her mother and her maternal grandmother were similarly affected. She had no systemic features but had bilateral posterior embryotoxon, iris atrophy, pseudopolycoria and angle iris processes. Varsome classified the *LTBP2* c.3527-3C>A variant as pathogenic while we classified the variant as VUS upon further analysis in this study. The following ACMG-AMP codes were applied: PM4 (strong) since the variant is located in a noncoding region (conserved position) which is located next to a canonical splice site, PP3 (strong) given that the variant is predicted splicing and PM2 (moderate) as both exomes as well as genomes allele count is less than three for an autosomal recessive gene. The variant had a gnomAD entry with minor allele frequency of 0.0124 in Africans, while 0.0000617 was reported in Europeans (Non-Finnish), 0.00055 in Latino and 0.0000327 in south Asians. A dbSNP ID of rs138194436 is assigned to the variant with a benign impact predicted by one in silico predictive tool and another predicting a pathogenic damaging impact. ClinVar has three submitters for this variant (Accession numbers: RCV000909576, RCV000305307, RCV000403118) with all three classifying the variant as benign, likely benign and uncertain significance. This conflicting interpretation of pathogenicity led to our classification of the variant as VUS given the phenotypes the submitters were associating the variant with (Primary congenital glaucoma and Weill-Marchesani syndrome) which are attributed to *LTBP2* mutations. The depth of sequencing reads was confirmed with IGV (**Figure 3.12**) and the variant was observed throughout the reads as they reported a T (Red) allele while the reference genome shows a G (Mustard) allele at the same position of the variant.

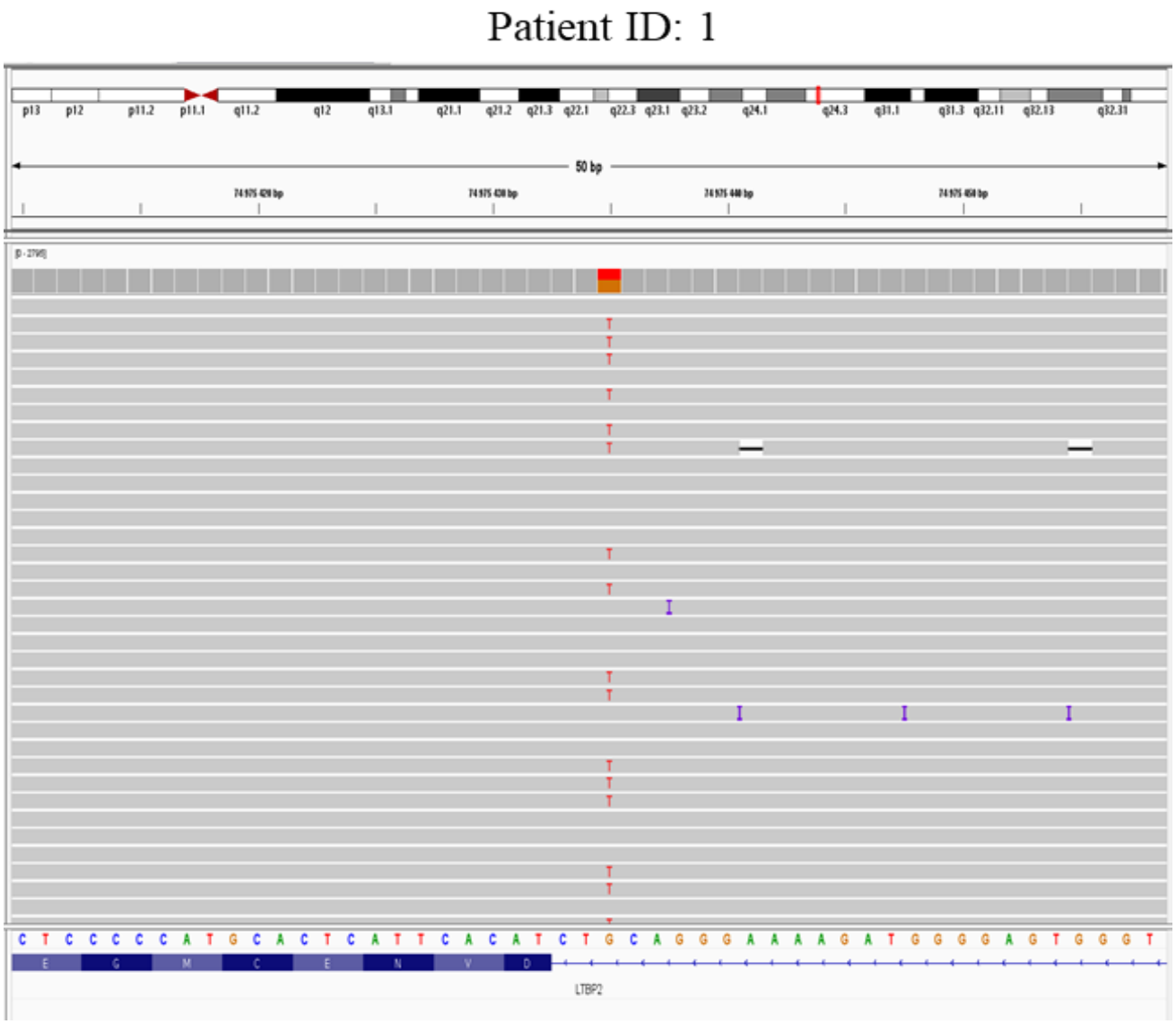

Figure 3.12: IGV plot of *LTBP2* c.3527-3C>A splice site variant in patient (ID: 1) diagnosed with ARS. The reference allele of G (Mustard) is recorded by the reference genome at the variant's position, while the reads coverage depth shows a variant allele T (Red).

3.3.5.4 Peroxidasin (*PXDN*)

A missense heterozygous NM_012293.3:c.2827C>T (p.Arg943Trp) variant located in exon 17 at position 723 of 1504 (**Table 3.4**). This variant was identified in a 4-year-old male with Peters anomaly (sample 12; described above), as well as his unaffected father (sample 10). Varsome classified the variant as VUS which was in agreement with our own classification with the following ACMG-AMP codes applied: PM2 (supporting) since the variant does not alter protein length and is not located in a conserved region and PP3 (supporting) due to eight *in silico* predictive tools predicting pathogenic computational verdict with only four predicting benign impact. ClinVar also reports conflicting interpretation of pathogenicity as two submitters have classified the variant as VUS and likely benign (Accession numbers: RCV001546804 and RCV000533505) after testing the variants against ASD and Sclerocornea with other ocular anomalies. The variant has also been catalogued in dbSNP database with ID rs200127189 and a gnomAD minor allele frequency of 0.00491 in Africans as well as a total minor allele frequency of 0.000349. Observation of the variant in IGV showed a G>A change from reference genome and the sequence reads (**Figure 3.13**). The c.2827C>T variant was also detected in the father (parent ID: 10) of this patient (ID: 12) as confirmed with IGV (**Figure 3.14**).

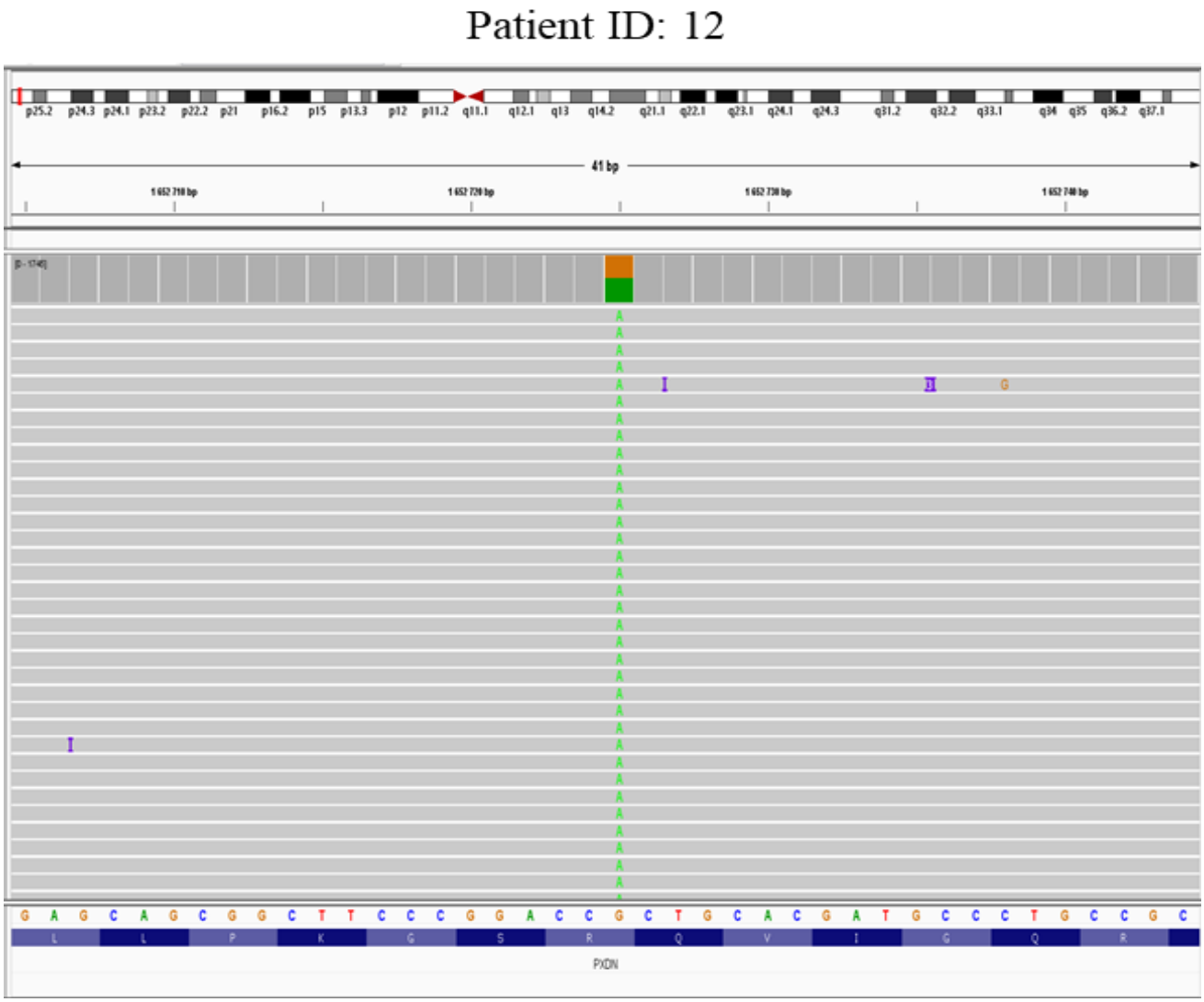

Figure 3.13: IGV plot of *PXDN* c.2827C>T missense variant in patient (ID: 12) diagnosed with Peter's Anomaly. The reference allele of G (Mustard) is recorded by the reference genome at the variant's position, while the reads coverage depth shows a variant allele A (Green).

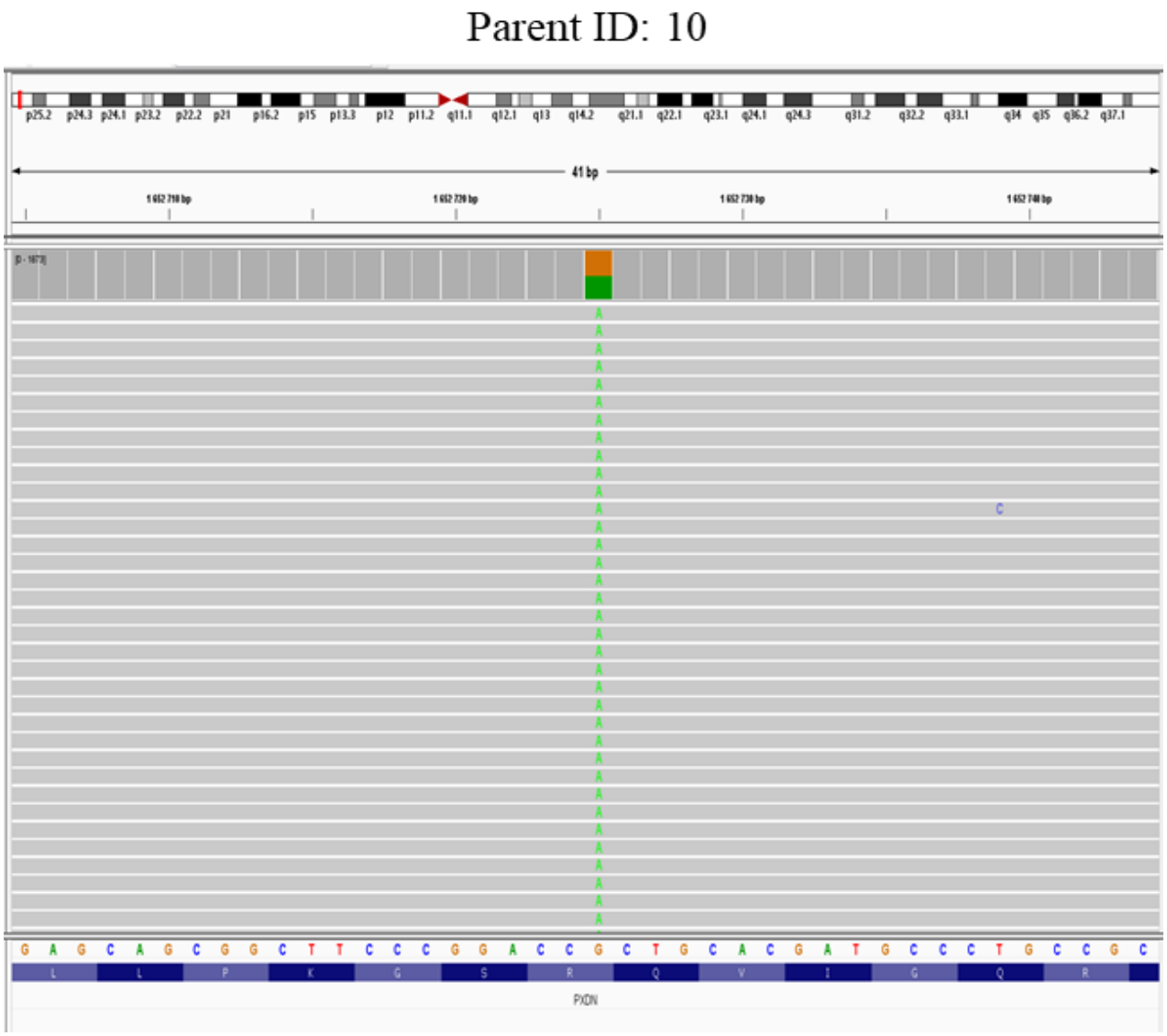

Figure 3.14: IGV plot of *PXDN* c.2827C>T missense variant in the father (parent ID: 10) of patient (ID: 12) diagnosed with Peter's Anomaly. The reference allele of G (Mustard) is recorded by the reference genome at the variant's position, while the reads coverage depth shows a variant allele A (Green).

A 34-year-old black female diagnosed with ARS (sample 14) presented with advanced juvenile onset open angle glaucoma with an Axenfeld angle with numerous iris processes but no posterior embryotoxon or systemic features was found to be harbouring both the missense heterozygous NM_012293.3:c.2827C>T (p.Arg943Trp) (**Figure 3.15**) detailed above and missense heterozygous NM_012293.3:c.1112C>T (p.Pro371Leu) located in exon 10 at position 94 of 273 (**Table 3.4**). The variant was classified as VUS by Varsome as it was the same in

the current study, with two ACMG-AMP codes applied: PM2 (strong) due to the position of the variant being strongly conserved and PP3 (supporting) as a total of eight *in silico* predictive tools deemed the variant to have a pathogenic impact while only four predicted benign impact. In ClinVar two submissions have been recorded (Accession numbers: RCV001556898 and RCV000950335) with both submitters classifying the variant as likely benign and VUS. The c.1112C>T variant has a dbSNP ID of rs201592851 and a gnomAD entry for minor allele frequency of 0.00352 in Africans with a total minor allele frequency of 0.000282. IGV confirmed the presence of the c.1112C>T variant in the reads as the reference genome showed a G allele at the position of the variant (**Figure 3.16**). IGV records a G>A change which is complimentary to C>T change presented with the variant.

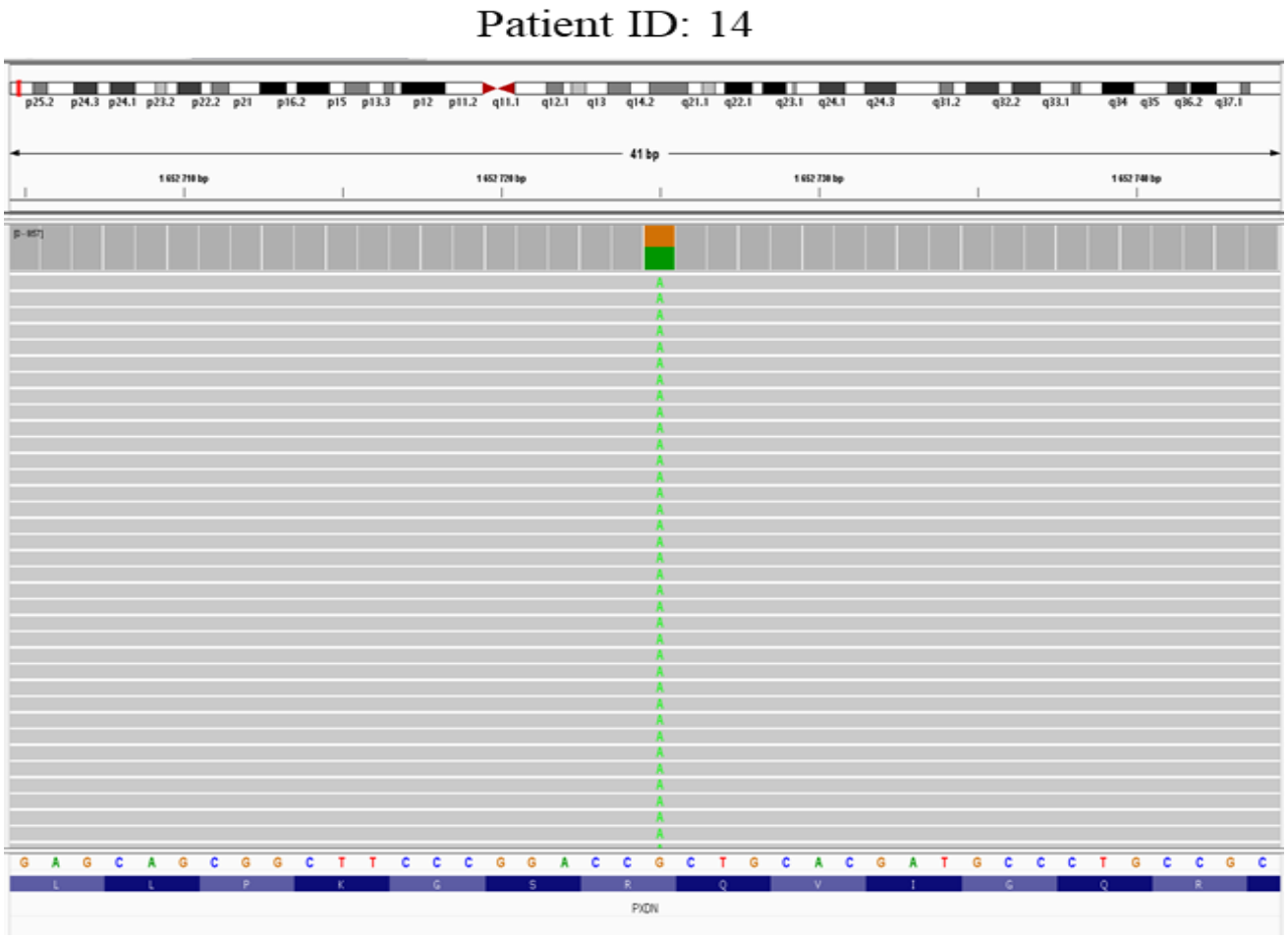

Figure 3.15: IGV plot of *PXDN* c.2827C>T missense variant in patient (ID: 14) diagnosed with ARS. The reference allele of G (Mustard) is recorded by the reference genome at the variant's position, while the reads coverage depth shows a variant allele A (Green).

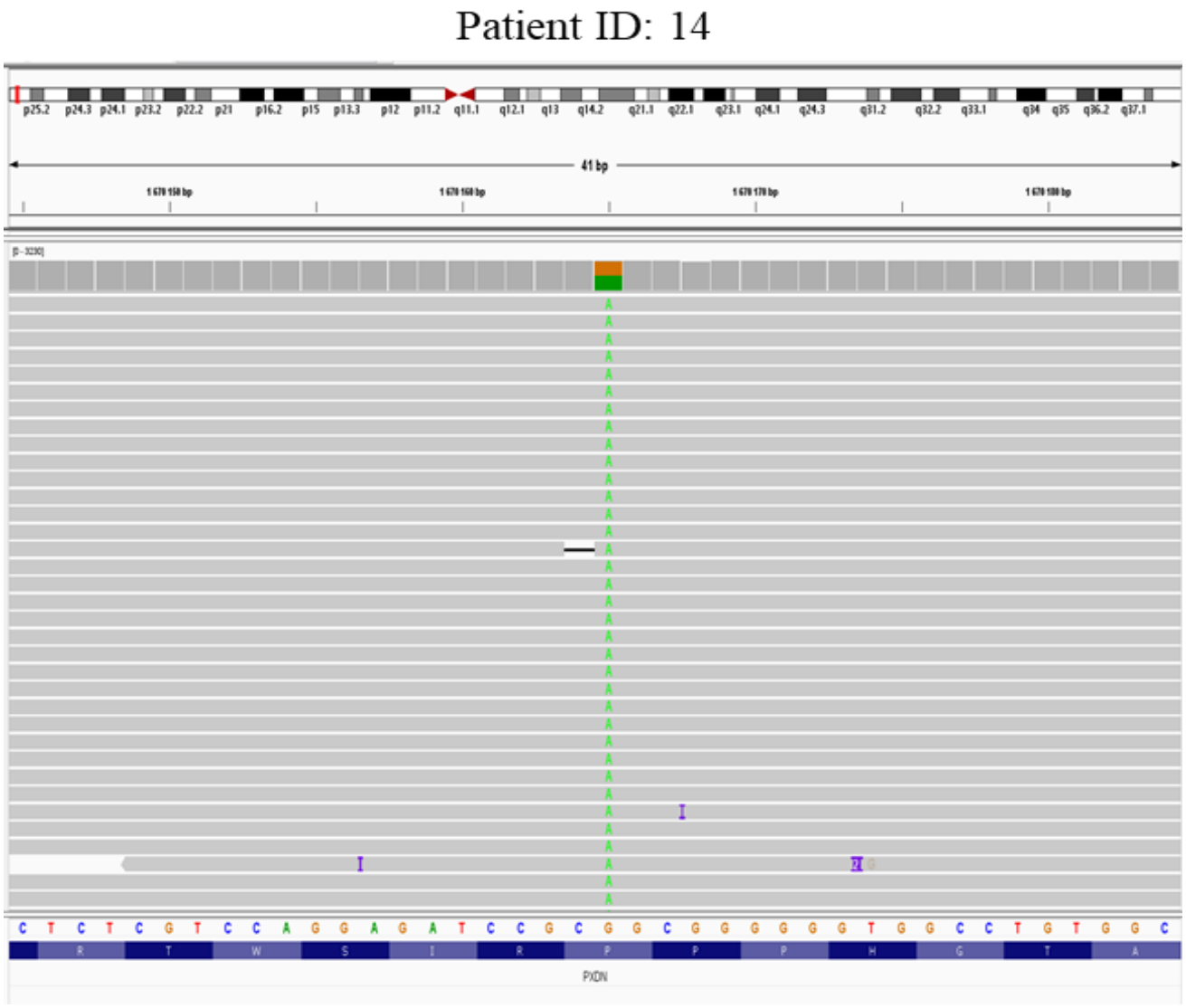

Figure 3.16: IGV plot of *PXDN* c.1112C>T missense variant in patient (ID: 14) diagnosed with ARS. The reference allele of G (Mustard) is recorded by the reference genome at the variant's position, while the reads coverage depth shows a variant allele A (Green).

3.4 Discussion

ASD is a collection of rare complex heterogenous congenital eye disorders that affect structures within the anterior segment of the eye such as the cornea, iris, trabecular meshwork, Schlemm's canal and ciliary body (Sowden, 2007; Reis and Semina, 2011). ASD is comprised of disorders such as microphthalmia, and Peter's anomaly, ARS, and sclerocornea, which can lead to cataract formation, corneal opacity and glaucoma (Reis and Semina, 2011). ASD consist of congenital disorders, which affect the lens, cornea and iris and are usually accompanied by a 50% increased predisposition to glaucoma (Alward, 2000; Sowden, 2007; Ito and Walter, 2014). Mutations in genes that regulate eye development (*PXDN*, *PAX6*, *FOXC1* and *PITX2*) have been associated with ASD in various population groups (Khan et al., 2011; Slavotinek et al., 2015; Ullah et al., 2016; Choi et al., 2015; Prokudin et al., 2014; Micheal et al., 2016), with very few studies conducted in African/South African cohorts with regards to the genetic aspects of eye diseases (Carstens et al., 2016; Goolam et al., 2018; Carstens et al., 2022). Furthermore, there is only one research study conducted for the association of *PXDN* gene variants with ASD in Africans (Thanikachalam et al., 2020) and none in a South African cohort. As such, the second aim of this study was to identify genetic mutations in South African patients diagnosed with ASD with the addition of *PXDN* and this was achieved by performing NGS (Exome sequencing) on genes known to regulate eye development pathways. This was to also help in potentially developing an ASD gene panel that would be gene specific for testing of ASD in African patients diagnosed with such disorders.

To summarise, a total of 50 genes of interest were selected for exome sequencing in a total of 14 patients and two parents with the aid of Ion Torrent NGS with 43 genes available on demand and with 7 only available in a spike-in panel which was not designed and therefore not sequenced. The 7 genes included *FOXC1, FOXC2, FOXE3, GDF6, SMOC1, RARB* and *MAF*. NGS data analysis identified disease causing variants in *PAX6* (Pathogenic) and *GJA8* (Likely pathogenic) genes in our study cohort, while variants in *BCOR, EPHA2, LTBP2* and *PXDN* were classified as VUS in this study.

3.4.1 Pathogenic *PAX6* variant

A heterozygous stop gained *PAX6* mutation NM_001258462.3:c.760C>T (p. Arg254Ter) with dbSNP ID rs121907917, was detected in a single patient (ID:15) diagnosed with Aniridia. Aniridia (lack of iris), is a rare autosomal dominant disease which is described by varying eye abnormalities such as corneal opacity, lens dislocation, ciliary body hypoplasia, and iris hypoplasia (Lee et al., 2008). Aniridia affects approximately 1 in 50 000 and can occur as an isolated or a syndromic form (Fischbach et al., 2005) with about 67% of all reported cases being familial and co-segregating in an autosomal dominant manner with high penetrance while the rest are sporadic (Valenzuela and Cline, 2004). *FOXC1*, *PITX2*, *WNT5A*, *TGFβ2* and *BMP4* are some of the know downstream targets which play an important role in the normal development of the eye (Wang et al., 2012; Hu et al., 2016; Wang et al., 2017) with failure to express proteins from these genes due to aberrant PAX6 or direct mutation within their genes resulting in ASD (Berry et al., 2006; Sowden, 2007; Berry et al., 2008; Weisschuh et al., 2008; Tümer and Bach-Holm, 2009; Thanikachalam et al., 2020).

PAX6 like many other transcription factors induces embryonic differentiation along major body axes in response to the concentration gradient of other regulatory proteins or transcription factors, which bind to DNA sequences of other genes and regulate their expression (Friedman, 1998). PAX6 belongs to the *PAX* multigene family of transcription factors that aid in the regulation of embryonic differentiation (Friedman, 1998). PAX6 is termed a master control gene since mutations in the highly conserved transcription factor interrupts development of the eye in both insects and mammals (; Hill et al., 1991; Quiring et al., 1994).

The *PAX6* variant c760C>T (p. Arg254Ter) is located in exon 10 at position 36 of 83 and has been observed (recurrent variant) in multiple patients of different ethnicities (Japanese, Egyptians, Chinese, Arabians, Thai, Indians and Italians) whom were all diagnosed with Aniridia (Neethirajan et al., 2003; Atchaneeyasakul et al., 2006; Khan and Aldahmesh, 2008; Abouzeid et al., 2009; Khondo-Saitoh et

al., 2009; Khang et al., 2016; Lin et al., 2018). A novel heterozygous *PAX6* missense variant c.152G>T (p.Gly51Val) in the conserved paired box domain was detected in a patient diagnosed with Peter's Anomaly with the variant being absent from the controls as well as unaffected parents (Prokudin et al., 2014). Our data with regards to the reported *PAX6* variant further confirms the important role PAX6 plays in development of the eye. *In Silico* predictive computational tools deemed the variant pathogenic or damaging as it results in a premature stop codon which could subsequently result in nonsense mediated decay of mRNA transcript containing the premature stop codon in which case no protein synthesis will occur.

The c.760C>T variant reported in this study is located within the transactivation domain enriched with proline-serine-threonine (PST) residues at the C terminus which is strongly conserved (Dansault et al., 2007). The PAX proteins contain a PST domain which is tightly regulated by phosphorylation in the C-terminal region with the key function of this region being downstream target genes transactivation (Singh et al., 2001). Mutations such as missense variants that occur within the DNA binding domain of PAX6 can result in poor recognition or complete failure in recognising binding sites sequences in target genes of which can result in partial or complete loss of function (Singh et al., 2001).

The role of PAX6 in organogenesis including eye development is not fully understood (Takamiya et al., 2020). The identified c760C>T (p. Arg254Ter) variant may result in impaired function of PAX6 leading to development of the diagnosed Aniridia in our patient via haploinsufficiency. Expression of *PAX6* is very precise within the different tissues, therefore normal eye development requires the correct dosage of PAX6. Reduced expression of *PAX6*, due to mutations, results in clinical phenotypes such as small eye in mice and rats (Kroeber et al., 2010), whereas in humans it results in Aniridia (Yokoi et al., 2016; Lim et al., 2017). Overexpression in mice was found to also cause severe eye phenotypes (Schedl et al., 1996; Chanas et al., 2009).

To the best of our knowledge this study is the first to report the identification of a *PAX6* pathogenic variant in a South African patient diagnosed with Aniridia. Previously, a *PAX6* variant NM_000280.3:c.622G>A (p.Gly208Arg) was

identified in a total of 27 admixed South African family members diagnosed with nystagmus, coloboma as well as familial congenital cataracts and co-segregation of the variant with the clinical phenotypes was observed in all 27 family members (Goolam et al., 2018). Our study has further validated the importance of screening for variants in the PAX6 gene in African patients diagnosed with ASD.

3.4.2 Likely pathogenic *GJA8* variant

A single patient (ID: 16) diagnosed with ARS harboured a missense *GJA8* heterozygous NM_005267.5: c.22G>A (p.Gly8Arg) variant. The variant has an existing dbSNP ID of rs202041458 but has not been reported in the literature for association with any clinical phenotype, including ASD. The gap junction alpha 8 (*GJA8*) gene encode for the connexin50 (Cx50) protein, which belongs to a group homogenous transmembrane family of proteins crucial for intercellular communication and moderating diffusion of molecules between lens fibre cells (García et al., 2016). Gap junction channels are formed by connexons when they dock with the juxtaposed cells' counterparts or they can form hemichannels (HCs), which allows them to function independently. Mutations in the genes that encode transmembrane family of proteins have been implicated in various clinical phenotypes such as hearing loss disorders, skin disorders, heart malformations, cataract, microphthalmia, microcornea (Pfenniger et al., 2011) and various biological processes owing to their primary function of cell-to-cell communication as well as tissue homeostasis (García et al., 2016).

GJA8 and GJA3 are the most abundant gap junction proteins with expression levels high in lens and fiber cells respectively (García et al., 2016). Animal model studies have demonstrated that knockout of *GJA8* results in cataract development at an early age with impaired lens development, as well as microphthalmia (Rong et al., 2002). The importance of GJA8 requirement for normal eye development was also seen in mouse models with missense mutations, which lead to the development of cataracts and microphthalmia (Xi et al., 2012; Berthoud et al., 2013). This observation has also been seen in humans whereby missense mutations in *GJA8* have been associated with cataracts (Yu et al., 2016) and in rare occasions the variants have been observed in patients diagnosed with other ocular disorders such

as iris hypoplasia, microphthalmia, sclerocornea, microcornea and also defects in normal development of lens (Hansen et al., 2007; Prokudin et al. 2014; Ma et al., 2016; Ma et al., 2018). Missense mutations in *GJA8* are mostly heterozygous with only a few cases of homozygous variants reported, all of which were in consanguineous families (Ponnam et al., 2013; Ma et al., 2016).

The c.22G>A (p.Gly8Arg) missense variant detected in our study cohort is located in exon 2 at position 33 of 1325 in a conserved region of GJA8 (Willoughby et al., 2003; Mackay et al., 2014; Ma et al., 2016), which causes a glycine to arginine change at position 22 in the intramembrane N-terminal domain (NT) and was classified as likely pathogenic variant. A total of 11 computational *In Silico* predictive tools predicted the variant to be damaging as well as pathogenic with only one tool predicting a benign impact. In a study by a (Devi and Vijayalakwshmi, 2006), a heterozygous novel variant c.593G>A (p.Arg198Gln) was detected in Indian patients diagnosed with congenital cataract/microcornea and another variant, c.593G>A, was also detected in a patient diagnosed with cataracts/microcornea in a second study with a different cohort (Prokudin et al., 2014). Missense variants in *GJA8* have been observed to affect the protein via alteration of distributed amino acids specifically those localised between transmembrane domain 1 (TM1) and transmembrane domain 2 (TM2) (Yu et al., 2016). The predicted effect of these variants is thought to be achieved via mis-localisation and/or misfolding, which leads to alteration of channel properties (Beyer et al., 2013). The most common variant detected in *GJA8* gene is the heterozygous (p.Glu46Val) mutation known to cause microcornea and congenital cataracts (Beyer et al., 2013) as shown by functional studies that the variant in TM1 domain causes elevated hemichannels formation, which leads to severe damage of the cells (Minogue et al., 2009).

The c.139G>T (p.Asp47T) in Extracellular loop one (ECL1), and c.586G>A (p.Val196Met) in Extracellular loop two (ECL2) as well as c.773C>T (p.Ser258Phe) in C-terminal (CT) domain have also been observed to associate with nuclear cataract as well as microcornea in Chinese (Lin et al., 2008), Indian (Ponnam et al., 2013) and Chinese (Gao et al., 2010) study cohorts respectively. A c.166A>C (p.Thr56Pro) in ECL1 was observed in a Mauritanian family diagnosed

with nuclear cataracts with the variant absent from controls and segregating with the disease (Hadrami et al., 2019). Only three pathogenic variants c.20T>C (p.Leu7Pro), c.68 G>C (p.Arg23Thr) and c.89dupT p.lle31Hisfs*18 located in the NT domain have been observed thus far in Caucasian-Americans (Mackay et al., 2014), Iranians (Willoughby et al., 2003) and Caucasian-Australians (Ma et al., 2016) presenting with nuclear cataracts respectively, with the reported c.22G>A variant in the current study being the fourth although in a patient presenting with ARS.

Null pathogenic variants in *FOXC1* and *PITX2* genes are known to causes ARS (Tümer and Bach-Holm, 2009; Chang et al., 2012). The most frequently detected mutations in patients presenting with ARS are point mutations such as c.236C>T (p.Pro79Leu), c.358C>T (p.Gln120Ter) in *FOXC1* (Nishimura et al., 2001; Weisschuh et al., 2008) and c.385G>C (p.Val129Leu) in *PITX2* (Preston et al., 2001). The alteration of functional FOXC1 and PITX2 proteins due to pathogenic variants or deletions, duplications and/or insertions can result in either dosage increase or decrease of either protein which is a causative mechanism for ARS (Tümer and Bach-Holm, 2009; Chang et al., 2012). In a study by Berry et al., (2006) it was shown that both FOXC1 and PITX2 interact with each other and are co-expressed in the developing anterior segment of the eye, with PITX2 downregulating FOXC1 expression which in turn inhibits expression of FOXC1 downstream targets. The relationship between the two proteins might also explain why aberrant expression of either protein due to null mutations can lead to phenotypes such as ARS. In the absence of functional PITX2, expression levels of FOXC1 are elevated which can also lead to ARS development.

Both *FOXC1* and *PITX2* were selected for variant screening in the current study with only *PITX2* successfully sequenced in all 14 patients, while *FOXC1* was not sequenced due to the gene being only available in a Spike In gene panel (not sequenced) instead of on demand gene panel. No pathogenic *PITX2* were detected in all 14 patients with only the reported c.22G>A *GJA8* variant detected in a single patient presenting with ARS.

Our detection of this *GJA8* missense variant in a patient diagnosed with ARS further broadens the phenotype spectrum associated with aberrant expression of this protein. The minor allele frequency of the c.22G>A (p.Gly8Arg) variant from the current study was reported in gnomAD as 0.000185 in Africans, in comparison to 0.0000239 (~ 1 in 41902) in south Asians, with other ethnic groups having no entry in gnomAD. Thus far, *GJA8* heterozygous missense variants have not been detected in patients diagnosed with ARS since GJA8 is known as a cataract only gene, which leads to the exclusion of this gene when testing patients for possible causes of ARS. ARS is a rare autosomal dominant heterogenous group of disorders which are congenital and affect the normal development of the anterior segment of the eye (Chang et al., 2012). These conditions include developmental abnormalities, which affect both the extraocular as well as ocular structures and they show genetic heterogeneity with null variants in FOXC1 and PITX2 implicated in ARS development thus far (Tümer and Bach-Holm, 2009). Our data suggest that the *GJA8* gene should be included in the gene panel for testing of patients diagnosed with ARS or ASD in general since this may have clinical implications especially in adult patients diagnosed with ASD or ARS as they would have a 50% risk of passing the mutation onto their offspring, and as such impacts reproductive planning. The lack of broader genomic sequencing in African study cohorts also creates a problem when screening patients diagnosed with ASD disorders given their genetic diversity, which can contribute to the heterogeneity of ASD disorders between various ethnic groups (Campbell and Tishkoff, 2010; Choudhury et al., 2017).

3.4.3 Varsome pathogenic *BCOR* and *EPHA2* but VUS in this study

Two possibly novel frameshift variants were identified in this study, one in *BCOR* NM_001123385.2: c.1257_1260delAGATinsGAC (p.Asp420ThrfsTer22) and one in *EPHA2* NM_004431.5:c.986_987delinsT (p.Pro329LeufsTer64). The *BCOR* c.1257_1260delAGATinsGAC variant was detected in two patients, diagnosed with Aniridia (ID: 15) as well as ARS (ID: 6). The *EPHA2* c.986_987delinsT variant was observed in a patient (ID: 13) presenting with Peter's anomaly. The two variants were classified as pathogenic by VARSOME database while upon further examination of the variants relative to our study cohort were then classified as VUS.

The *BCOR* gene encodes for the synthesis of a BCL 6 corepressor protein that functions in specification of cellular differentiation and body structure development (Astolfi et al., 2019). Two domains primarily regulate the function of BCOR namely the PCGF Ub-like fold discriminator (PUFD) domain, which is implicated in histone regulation, and BCL-6 binding domain that interacts with BCL-6 transcriptional repressor (Astolfi et al., 2019). The *BCOR* frameshift variant c.1257_1260delAGATinsGAC (p.Asp420ThrfsTer22) is located in exon 4 at position 1092 to 1095 of 2832. The BCL6 binding domain is located within exon 4 of the *BCOR* gene, which evidently our detected frameshift variant is also located in the same domain. Aberrant expression of *BCOR* is associated with various disorders such as cancer (Astolfi et al., 2019) and X-linked microphthalmia disorders, which include oculofaciocardiodental disorder (OFCD) (Hilton et al., 2009; Ragge et al., 2019). BCOR variants affect males and females differently owing to the location of the gene on the X chromosome, such that OFCD are observed in females and is lethal in males, while lenz microphthalmia which an X-linked condition comprising of microphthalmia or anophthalmia presenting with mental retardation, malformed ears, skeletal, renal, and urogenital anomalies is observed in males harbouring *BCOR* null mutations (Ng et al., 2004; Ragge et al., 2019). In a study by Ng et al., (2004) it was observed that a *BCOR* missense variant c.254C>T (p.Pro85Leu) was the cause of X-linked recessive lenz microphthalmia in an affected male patient as the variant segregated with the clinical phenotype, and other similar observations have been described (Hilton et al., 2009; Suzumori

et al., 2013) with the variants absent in unaffected control cohort. Zhu et al., (2015) screened genes such as *PITX2, BCOR* and *FOXC1* in a male patient presenting with complex cardiac anomalies, dextrocardia and congenital glaucoma with a denovo novel *BCOR* missense variant c.1619G>A (pArg540Gln) detected in the patient. Here our data shows that two patients, ID: 6 with ARS and ID: 15 with aniridia, harboured a frameshift pathogenic *BCOR* variant. The patient diagnosed with Aniridia also harboured a pathogenic *PAX6* stop-gained variant NM_001258462.3: c760C>T (p. Arg254Ter), which is a known recurrent mutation directly associated with Aniridia (Neethirajan et al., 2003; Atchaneeyasakul et al., 2006; Khan and Aldahmesh, 2008; Abouzeid et al., 2009; Khondo-Saitoh et al., 2009; Khang et al., 2016; Lin et al., 2018). This made it difficult when manually examining the *BCOR* variant as to whether it could be contributory to the development of the two patient's clinical phenotype since *BCOR* pathogenic mutations have not been associated with Aniridia as well as ARS in any ethnic groups. The *BCOR* variant was also observed in the mother of one of the patients (ID: 12) who did not inherit the variant. This could be due to the parent being partially mosaic in which case she would have a healthy clinical phenotype. It is also possible that the variant could be a partial sequencing artefact which will require validation with the aid of sanger sequencing. Our study is also the first to present a possible pathogenic *BCOR* variant in Africans diagnosed with ASD. The variant did not have a gnomAD entry for allele frequency and *in silico* computational tool MutationTaster predicting the variant to have a pathogenic impact. The literature currently available on *BCOR* pathogenic mutations shows that further studies are warranted to understand the role of BCOR in eye development (Hilton et al., 2009; Suzumori et al., 2013; Zhu et al., 2015; Ragge et al., 2019).

The *EPHA2* NM_004431.5: c.986_987delinsT (p.Pro329LeufsTer64) frameshift variant was detected in a single patient (ID: 13) diagnosed with Peters anomaly. Peters anomaly is a developmental abnormality in the anterior section of the eye. In 1906, Peters described the syndrome as it was characterised by cornea-iris adhesion, corneal leukoma and shallow anterior chamber (Harissi-Dagher and Colby, 2008). The severity of the disorder can vary from mild opacification of the cornea to severe glaucoma, cataract and microphthalmia (Stahl, 2014). The variant did not have a

gnomAD entry or ClinVar submission, and the *in silico* computational tool MutationTaster predicted a pathogenic impact, which was supported by Varsome. The *EPHA2* gene encodes for ephrin receptor tyrosine kinase-type A2 (EPHA2), which is highly expressed during embryogenesis with a primary function in regulation of cell adhesion, proliferation, morphology, secretion, survival and differentiation (Miao and Wang, 2009). EPHA2 is required for the normal development of various organs with elevated expression observed in developing eye, kidney and ear tissues (Xu et al., 2005; Saeger et al., 2011; Son et al., 2013; Park et al., 2013). In the eye, lens transparency is achieved by organisation and tight packing of lens fibre cells, which is maintained via gap and tight junctions as well as extensive cell to cell adhesion that aids in sustaining lens transparency by transporting between cells water, ions, minerals, nutrients, solutes and waste products (Cooper et al., 2008; Dave et al., 2012; Son et al., 2013). Studies conducted using mice animal model indicate that knockout or loss of function of EPHA2 results in disruption of the N-cadherin dependent intercellular adherens junctions that regulate lens fiber cell to cell interaction resulting in cell morphological change, weak cellular connections resulting in cataracts development (Jung et al., 2009; Dave et al., 2013). Various studies have shown that *EPHA2* null variants cause eye development disorders such as cataracts and microphthalmia (Zhang et al., 2009; Dave et al., 2013; Park et al., 2013).

In this study we report of a frameshift variant c.986_987delinsT (p.Pro329LeufsTer64) detected in *EPHA2* gene in a patient diagnosed with Peter's anomaly and the variant is located in exon 5 position 7 to 8 of 333. The EPHA2 protein is required for normal development of lens and patients harbouring mutations in the *EPHA2* gene resulting in aberrant expression, have been diagnosed with congenital eye disorders. In a family diagnosed with bilateral nuclear lens opacities, which were congenital, a c.1751C>T (p.Pro584Leu) variant was found to be the cause of the opacities as the variant resulted in an alteration in amino acids in exon 10 that are highly conserved. This resulted in the juxta membrane region of EPHA2 being dysfunctional as this region is responsible for tyrosine residue auto-phosphorylation, which subsequently regulates signalling activity of the receptor (Dave et al., 2013; Park et al., 2013). Zhang et al., (2009) also detected two disease

causing variants in a British family (frameshift mutation c.2915_2916delTG) as well as an Australian family (splicing mutation c.2826-9G>A) diagnosed with congenital cataracts. The c.2826-9G>A splice site variant introduces a splice acceptor site which results in an additional 7 base pairs in an intron, which is included in the final processed transcript (Zhang et al., 2009). Most recently it was observed that *EPHA2* variants, heterozygous missense c.1751C>T (p.Pro584Leu) and splice site c.2826-9G>A, segregated with microphthalmia as well as congenital cataracts in two unrelated families (Harding et al., 2021). The data presented from literature coupled with data obtained in the current study add support to the importance of EPHA2 in eye development since the protein is required for lens homeostasis through regulating adherens junctions, both during embryological development and throughout life. Our data also demonstrate a potential novel association of *EPHA2* gene variants with Peter's anomaly in a study cohort comprising of South Africans, which could potentially aid in diagnostic rates if *EPHA2* gene is added to the list of genes screened for mutations in association with Peter's anomaly.

3.4.4 Variants of uncertain significance: *LTBP2* and *PXDN*

VUS mutations that had conflicting interpretation of pathogenicity (i.e., reported as pathogenic in one testing centre, while reported as likely benign by another) during data analysis were also filtered out for quality control. Variants located within the untranslated regions were analysed for any effect on splicing, with those not having any deleterious impact filtered out. Variants with allele count greater than five in ExAC and gnomAD were filtered out. Three variants in (*PXDN* (two) and *LTBP2* (one)) were prioritised from the filtered data set.

PXDN heterozygous missense mutations NM_012293.3:c.1112C>T (p.Pro371Leu) in exon 10 at position 94 of 273 and NM_012293.3:c.2827C>T (p.Arg943Trp) in exon 17 at position 723 of 1504 were detected in two patients, ID: 12 and ID: 14, respectively. Patient (ID: 14) harboured both *PXDN* missense mutations and was diagnosed with ARS, while Patient (ID: 12) was diagnosed with Peter's anomaly and only harboured the c.2827C>T variant, which was also observed in the patient's father (Sample ID: 10). PXDN is a novel player in the development of the eye since

less than a handful of studies have been conducted with regards to its function in the eye as well as the regulation of gene expression, and as the impact of pathogenic mutations in the gene (Khan et al., 2011; Choi et al., 2015; Micheal et al., 2016).

In a study by Khan et al. (2011), it was found that two consanguineous Pakistani families and one consanguineous Cambodian family, harboured homozygous mutations in *PXDN* (Khan et al., 2011). The two Pakistani families presented with congenital cataract and corneal opacity which was mild to moderate, while the Cambodian family presented with severe corneal opacification and congenital glaucoma. An exon 17 *PXDN* missense mutation at position 534 of 1504 NM_012293.3:c.2638C>T (p.Arg880Cys) was detected via direct sequencing in one Pakistani family (Khan et al., 2011). *In silico* computational tools predicted the c.2638C>T to be deleterious as the amino acid change was within the conserved haem peroxidase domain, which could affect both protein structure and enzymatic ability of the domain (Khan et al., 2011). A homozygous 1-bp deletion NM_012293.3:c.2568delC (p.Cys857fs) in exon 17 of the PXDN gene, causing a frameshift predicted to result in premature termination of the protein (Cys857AlafsTer5) within the haem peroxidase domain was observed to be segregating in an affected Pakistani consanguineous family (Khan et al., 2011). Another pathogenic *PXDN* variant in exon 10 at position 3 of 273 NM_012293.3:c.1021C>T (p.Arg341Ter) located within the Ig-like domain was detected in the Cambodian family and was found to likely cause protein truncation, which can also be deleterious (Khan et al., 2011). These mutations were only observed in the affected patients and absent in the controls (Khan et al., 2011).

Choi et al. (2015) detected additional mutations in *PXDN* including the c.1021C>T reported by Khan et al. (2011) in a study cohort of a different ethnic group (Caucasian-Americans). The c.1021C>T variant was inherited maternally and a paternally inherited 23-base-pair deletion causing a frameshift and premature protein truncation c.2375_2397del23 (p.Leu792Hisfs*67) was observed in two siblings presenting with microphthalmia, developmental delays, ASD, hypotonia and sclerocornea from a Caucasian family with no history of consanguinity (Choi et al., 2015). Data from another 20 patients was investigated for any *PXDN* gene

mutations and two were identified in one patient (male) presenting with ASD, microphthalmia and cataracts: the mutations were a c.1192delT (p.Tyr398Thrfs*40), frameshift mutation, which was inherited maternally, and a c.947A>C (p.Gln316Pro) missense mutation considered to be deleterious, which was paternally inherited (Choi et al., 2015).

In 2016, Micheal et al. screened three consanguineous families from Pakistan diagnosed with primary congenital glaucoma (PCG) and developmental glaucoma for pathogenic variants in *PXDN* and *LTBP2* genes. In two families, two causative variants (novel missense mutation c.4934G>A (p.Arg1645Glu) and a novel frameshift mutation c.4031_4032insA (p.Asp1345Glyfs*6)) in the *LTBP2* gene were detected and co-segregated with the disease phenotype. A novel *PXDN* mutation c.3496G>A (p.Gly1166Arg) was identified in the third family diagnosed with developmental glaucoma and the variant was observed to be segregating with the disease. The variants detected in *PXDN* and *LTBP2* were absent in healthy controls of 150 Pakistani (Micheal et al., 2016).

The two *PXDN* variants identified in our study were located in exons 10 (p.Pro371Leu) and 17 (p.Arg943Trp), regions in which pathogenic variants have been previously reported (Khan et al., 2011, Choi et al., 2015; Micheal et al., 2016). The two exons fall within the Ig-like domain (231 to 333 of 1470) and haem peroxidase domain (741 to 1289 of 1470) respectively, with amino acid changes within the two conserved domains could affect both protein structure and enzymatic ability of the domain. The variants reported in this study were also predicted to be damaging by eight *in silico* predictive tools vs four predicting benign impact. The c.1112C>T variant was found to have a minor allele frequency of 0.003 in Africans versus 0.0000558 in East Asians, 0.0000183 in Europeans (Non-Finnish) and 0.000262nin Latinos., while the c.2827C>T variant has a minor allele frequency of 0.004 also in Africans as reported by gnomAD, versus 0.000333 in South Asians, 0.00000958 in Europeans (Non-Finnish) and 0.000353 in Latinos.

PXDN requirement for normal eye development has also been shown by Yan et al. (2014) whereby a mutant mouse model was induced via N-ethyl-N-nitrosourea of which upon sequencing revealed a recessive mutation (T3816A) causing a

premature stop codon in the peroxidase domain, which resulted in development of ASD as well as microphthalmia. In mouse animal models, the developing eye expresses PXDN from embryonic age (E11.5) onwards, which is equivalent to 33 days in human embryology, and when PXDN is knocked out, the outcome is absence of collagen IV crosslinking (Lázár et al., 2015). As such, PXDN is understood to be essential for normal development of eye structures such as the lens epithelium and cornea via collagen IV crosslinking, which promotes consolidation of ocular BM (Yan et al., 2014).

The LTBP2 protein is involved in cell adhesion as well as tissue repair and is highly expressed in ciliary processes which regulate the synthesis of aqueous humour and in trabecular meshwork (Shipley et al., 2000). Here we report two *LTBP2* heterozygous missense variants, NM_000428.3:c.1577G>A (p.Ser526Asn) in exon 7 at position 178 of 287, and heterozygous splice site variant NM_000428.3:c.3527-3C>A in intron 23 at position 98 of 100, which were detected in Patient (ID: 12) with Peter's anomaly and Patient (ID: 1) with ARS, respectively. Varsome classified the *LTBP2* c.3527-3C>A variant as pathogenic with three ClinVar submitters (Accession number: RCV000909576, RCV000305307, RCV000403118) classifying the variant as benign, likely benign and uncertain significance while the c.1577G>A missense was classified as VUS and had no ClinVar submission.

The mother (Sample ID: 11) of the diagnosed patient (ID: 12) was also a carrier of the variant. The two variants reported in the current study were not novel and have a gnomAD entry for minor allele frequency of 0.002 for c.1577G>A in Africans versus 0.00000884 in Europeans (Non-Finnish), 0.000347 in Latino. The c.3527-3C>A had a minor allele frequency of 0.001 in contrast with 0.0000612 in Europeans (Non-Finnish), 0.00055 in Latino and 0.0000327 in South Asians. The variants are all located in a conserved region within the *LTBP2* gene with i*n silico* predictions indicating a pathogenic impact (one) for c.3527-3C>A while the c.1577G>A was predicted to be pathogenic by (four) vs benign (eight).

Homozygous null mutations in the *LTBP2* gene have been previously reported in four consanguineous Pakistani and Gypsy families (Ali, et al., 2009). Micheal et al.

(2016) reported two causative variants (novel missense mutation c.4934G>A (p.Arg1645Glu) and a novel frameshift mutation c.4031_4032insA (p.Asp1345Glyfs*6) in the *LTBP2* gene detected via sequencing of two unrelated consanguineous Pakistani families with the variants co-segregating with the disease phenotype Primary congenital glaucoma (PCG). In eight Indian families a nonsense missense mutation c.2421G>A (p.Trp807Ter) was detected and observed to be co-segregating with PCG (Yan et al., 2017), and the same variant was also detected in three consanguineous Pakistani family diagnosed with PCG with the variant absent in 200 healthy controls (Rauf et al., 2020). There are only two studies to date (excluding the current study) that have been conducted in African cohorts (Mauritanians and South Africans) to screen for potential pathogenic variants in *LTBP2* gene in patients diagnosed with PCG and in both studies no pathogenic variants were detected in the patients (Hadrami et al., 2019; Carstens et al., 2022).

The processes by which pathogenic variants in *LTBP2* results in clinical phenotypes such as PCG is not well understood. Given the function of LTBP2 in ciliary process which involve ciliary muscles that control the lens, the protein is involved in regulation of elastic fibers in developing elastic tissues (Vehviläinen et al., 2009). Fibrillin 1 (FBN1) interacts with LTBP2 which integrates it into the ECM (Hirani et al., 2007), with dysregulation of *FBN1* associated with Marfan syndrome while *LTBP2* null variants have also been associated lens dislocation, secondary glaucoma, megalocornea, microspherophakia and Weill Marchesani syndrome (Désir et al., 2010; Kumar et al., 2010; Haji-Seyed-Javadi et al., 2012). The studies that have reported on pathogenic variants in *LTBP2,* including the current study, have all shown the underlying involvement of aberrant LTBP2 protein expression in various eye disorders given as shown by expression patterns in the ciliary body, trabecular meshwork and ciliary processes (Ali et al., 2009).

The link between PXDN and LTBP2 with regards to their involvement in the development of glaucoma is also not well understood. PXDN plays a pivotal role in the assembly of the ECM by cross-linking Collagen IV to form the BM (Lázár et al., 2015). LTBP2, like PXDN, is also an ECM protein (i.e., glycoprotein) that interacts with fibronectin as well as FBN1, which are also required for normal ECM

formation (Vehviläinen et al., 2009). It is possible that either collagen IV or other ECM proteins directly or indirectly facilitate their interaction. Null variants in any of the genes that encodes *PXDN*, *LTBP2*, collagen IV (*COL4A*) or *FBN1* could results in poor or no development of the anterior segment of the eye due to affected ECM assembly in eye tissues such as the trabecular meshwork, which regulates IOP of the eye leading to development of vision impairment disorders such as ASD (Vranka et al., 2015; Lázár et al., 2015).

In conclusion, our data confirms that ASD is indeed heterogenous in nature, as out of the total of 14 patients presenting with ASD no pathogenic variant was observed to be segregating with the disease in more than one patient. Sanger sequencing of family members of the patients harbouring both pathogenic variants as well as variants of uncertain significance will need to be performed for validation. This will aid in better understanding as to whether these variants are de novo or if they are partial sequencing artefacts especially the *BCOR*, *LTBP2* and *EPHA2* variants. At the time of submission of this work, no research studies have been conducted with regards to *PXDN* gene variant screening in African patients presenting with congenital eye disorders under the umbrella of ASD. Although the cohort size was not big enough to draw broad conclusions from, the data generated will contribute in adding some much-needed knowledge in understanding *PXDN* role in eye development as well as providing clarity as to whether gene panels for eye disease testing in cohorts of different ethnic background can be used for testing in African cohorts. Thus far a handful of studies have been conducted in a South African cohort with regards to the genetic aspect of eye disease. In Africa, more specifically South Africa there is limited epidemiological data regarding the burden of eye diseases. The data generated in this study was novel in that it is the first to be conducted in a South African cohort presenting with ASD.

CHAPTER 4: Overall conclusions and future experiments

4.1 Summary conclusions

In this study we have demonstrated that PAX6, FOXC1 and PITX2 are potential regulators of PXDN. We have also demonstrated the heterogeneity of ASD in a South African cohort.

Our data confirmed the novel interaction of PAX6, FOXC1 and PITX2 with *PXDN* gene promoter as confirmed by ChIP-PCR and that our model HEK293 cell line endogenously expressed all three transcription factors as well as PXDN in the presence of FGF-2. We have also demonstrated through literature as to why PAX6 is more likely to regulate PXDN as compared to FOXC1 and PITX2 which are already known to be regulated by PAX6. PXDN is an ECM protein that is able to catalyse oxidative stress reaction in response to elevated production of H_2O_2 in various tissue. Knockout of PAX6 in glioblastomas has been showed to result in the cells being more resilient to H_2O_2 induced oxidative stress than wild type cells. With a similar observation noted in corneal cell lines exposed to H_2O_2 which resulted in reduced expression as well as localisation of PAX6. PAX6 as master regulator of eye development and other organs, it has been shown to regulate expression of key genes that regulate oxidative stress such as NRF2 which has already been proven to be regulating expression of PXDN in HEK293 cell lines. Given the known roles as well as putative functions of PXDN, PAX6 is likely to be a direct or indirect regulator of PXDN by either upregulating its expression to synthesise BM through collagen IV cross-linking in the establishment of ECM or catalysis of ROS generated in eye, vascular or kidney tissues. The limitation of our first aim is the requirement for luciferase reporter gene data, which will aid in completely understanding as to which specific binding site results in regulation of PXDN. FOXC1 and PITX2 are known downstream targets of PAX6 and as such could also be regulators of PXDN, although our ChIP-PCR data will need to be validated with luciferase reporter gene assays. The interaction of these proteins will be key in better understanding the respective clinical phenotypes they are currently implicated in more especially ASD which is congenital in nature. The ChIP-PCR data was also supposed to be replicated in human corneal cell line in order to see as to whether the data generated using HEK293 cell line will be similar or not but due to COVID-19 this aim was not achieved.

In the second aim of this study, we proceeded to sequence 43 genes, known to be involved in eye development pathways, in a South African cohort presenting with ASD. Out of all 14 patients sequenced in this study, one patient presenting with Aniridia harboured a pathogenic *PAX6* gene variant. Four patients presenting with ARS harboured variants of uncertain significance in *PXDN, LTBP2* and *BCOR*, while one harboured a pathogenic *GJA8* variant. Two patients presenting with Peter's anomaly also harboured a *PXDN* as well as *LTBP2* variants, which were observed in two patients presenting with ARS. The data generated in this study further confirms the heterogeneity of ASD disorders and further broadens the ASD spectrum as genes such as *GJA8* are known as cataracts gene which is never tested in patients presenting with other ocular anomalies other than cataracts, microphthalmia, sclerocornea and iris hypoplasia. This observed heterogeneity could also be due to the lack of broader genomic sequencing in African study cohorts as this also creates a problem when screening patients diagnosed with ASD disorders given their genetic diversity, which can contribute to the heterogeneity of ASD disorders between various ethnic groups (Campbell and Tishkoff, 2010; Choudhury et al., 2017).

One key limitation of in this study was the sample size which was also lower than expected as a direct consequence of COVID-19 delays in collection of samples as clinics/hospitals were closed for research purposes during lockdowns. Another limitation was with regards to the validation of some of the variants such as the two *BCOR* and *EPHA2* frameshifts with sanger sequencing and the unavailability of other family members of the study participants for sequencing to screen for any possible segregation of the prioritised variants in this study. The patient presenting with pathogenic *GJA8* variant will require screening for *FOXC1* mutations given that *GJA8* variants thus far have not been associated with ARS development.

4.2 Future experiments

Luciferase assay for PAX6, FOXC1 and PITX2 will confirm the ChIP-PCR work in this study, which has already shown that these transcription factors do interact with PXDN in HEK293 cell line. Replication of *PXDN* interaction with FOXC1, PITX2 and PAX6 in human corneal cell line will further validate this study in the context of the eye.

While for the NGS work, seven genes were filtered out from the total of 50, as they were not available on the on-demand gene panel but only on spike-in panel which was not ordered due to financial reasons. The filtered-out genes included *FOXC1*, which is known as key transcription factor required for development of the anterior segment of the eye. The patients for which no pathogenic variants were detected could be harbouring disease causing variants in these genes and as such would be an important addition.

References

Abouzeid, H., Youssef, M.A., ElShakankiri, N., Hauser, P., Munier, F.L., Schorderet, D.F., 2009. PAX6 aniridia and interhemispheric brain anomalies. Mol Vis 15, 2074–2083.

Abrahamson, D.R., Hudson, B.G., Stroganova, L., Borza, D.-B., St John, P.L., 2009. Cellular origins of type IV collagen networks in developing glomeruli. J. Am. Soc. Nephrol. 20, 1471–1479. https://doi.org/10.1681/ASN.2008101086

Adzhubei, I., Jordan, D.M., Sunyaev, S.R., 2013. Predicting functional effect of human missense mutations using PolyPhen-2. Curr Protoc Hum Genet Chapter 7, Unit7.20. https://doi.org/10.1002/0471142905.hg0720s76

Aldahmesh, M.A., Khan, A.O., Hijazi, H., Alkuraya, F.S., 2013. Mutations in ALDH1A3 cause microphthalmia. Clin. Genet. 84, 128–131. https://doi.org/10.1111/cge.12184

Ali, M., McKibbin, M., Booth, A., Parry, D.A., Jain, P., Riazuddin, S.A., Hejtmancik, J.F., Khan, S.N., Firasat, S., Shires, M., Gilmour, D.F., Towns, K., Murphy, A.-L., Azmanov, D., Tournev, I., Cherninkova, S., Jafri, H., Raashid, Y., Toomes, C., Craig, J., Mackey, D.A., Kalaydjieva, L., Riazuddin, S., Inglehearn, C.F., 2009. Null Mutations in LTBP2 Cause Primary Congenital Glaucoma. Am J Hum Genet 84, 664–671. https://doi.org/10.1016/j.ajhg.2009.03.017

Alizadeh, A., Clark, J., Seeberger, T., Hess, J., Blankenship, T., FitzGerald, P.G., 2003. Targeted Deletion of the Lens Fiber Cell–Specific Intermediate Filament Protein Filensin. Investigative Ophthalmology & Visual Science 44, 5252–5258. https://doi.org/10.1167/iovs.03-0224

Alward, W.L., 2000. Axenfeld-Rieger syndrome in the age of molecular genetics. Am. J. Ophthalmol. 130, 107–115.

Alzuhairy, S., Abu-Amero, K.K., Al-Shahwan, S., Edward, D.P., 2015. A novel CYP1B1 mutation with congenital glaucoma and total aniridia. Ophthalmic Genet. 36, 89–91. https://doi.org/10.3109/13816810.2013.833635

Amendt, B.A., Semina, E.V., Alward, W.L.M., 2000. Rieger syndrome: a clinical, molecular, and biochemical analysis. CMLS, Cell. Mol. Life Sci. 57, 1652–1666. https://doi.org/10.1007/PL00000647

Anatomy of the Eye and Common Diseases Affecting the Eye | SpringerLink [WWW Document], n.d. URL https://link.springer.com/chapter/10.1007/978-3-319-47691-9_2 (accessed 11.11.20).

Añazco, C., López-Jiménez, A.J., Rafi, M., Vega-Montoto, L., Zhang, M.-Z., Hudson, B.G., Vanacore, R.M., 2016. Lysyl Oxidase-like-2 Cross-links Collagen IV of Glomerular Basement Membrane. J. Biol. Chem. 291, 25999–26012. https://doi.org/10.1074/jbc.M116.738856

Arneson, M.L., Louis, C.F., 1998. Structural Arrangement of Lens Fiber Cell Plasma Membrane Protein MP20. Experimental Eye Research 66, 495–509. https://doi.org/10.1006/exer.1998.0477

Asai-Coakwell, M., French, C.R., Berry, K.M., Ye, M., Koss, R., Somerville, M., Mueller, R., van Heyningen, V., Waskiewicz, A.J., Lehmann, O.J., 2007. GDF6, a Novel Locus for a Spectrum of Ocular Developmental Anomalies. The American Journal of Human Genetics 80, 306–315. https://doi.org/10.1086/511280

Astolfi, A., Fiore, M., Melchionda, F., Indio, V., Bertuccio, S.N., Pession, A., n.d. BCOR involvement in cancer. Epigenomics 11, 835–855. https://doi.org/10.2217/epi-2018-0195

Atchaneeyasakul, L., Trinavarat, A., Dulayajinda, D., Kumpornsin, K., Thongnoppakhun, W., Yenchitsomanus, P., Limwongse, C., 2006. Novel and De-novo Truncating PAX6 Mutations and Ocular Phenotypes in Thai Aniridia Patients. Ophthalmic Genetics 27, 21–27. https://doi.org/10.1080/13816810500481667

Bai, Y.-P., Hu, C.-P., Yuan, Q., Peng, J., Shi, R.-Z., Yang, T.-L., Cao, Z.-H., Li, Y.-J., Cheng, G., Zhang, G.-G., 2011. Role of VPO1, a newly identified heme-containing peroxidase, in ox-LDL induced endothelial cell apoptosis. Free Radic. Biol. Med. 51, 1492–1500. https://doi.org/10.1016/j.freeradbiomed.2011.07.004

Bardakjian, T.M., Schneider, A., 2011. The genetics of anophthalmia and microphthalmia. Curr Opin Ophthalmol 22, 309–313. https://doi.org/10.1097/ICU.0b013e328349b004

Basu, M., Bhattacharya, R., Ray, U., Mukhopadhyay, S., Chatterjee, U., Roy, S.S., 2015. Invasion of ovarian cancer cells is induced byPITX2-mediated activation of TGF-β and Activin-A. Mol Cancer 14, 162. https://doi.org/10.1186/s12943-015-0433-y

Bathish, B., Paumann-Page, M., Paton, L.N., Kettle, A.J., Winterbourn, C.C., 2020. Peroxidasin mediates bromination of tyrosine residues in the extracellular matrix. J Biol Chem 295, 12697–12705. https://doi.org/10.1074/jbc.RA120.014504

Battaglia, R.A., Delic, S., Herrmann, H., Snider, N.T., 2018. Vimentin on the move: new developments in cell migration. F1000Res 7, F1000 Faculty Rev-1796. https://doi.org/10.12688/f1000research.15967.1

Battistuzzi, G., Bellei, M., Bortolotti, C. A., & Sola, M. (2010). Redox properties of heme peroxidases. *Archives of biochemistry and biophysics*, *500*(1), 21–36. https://doi.org/10.1016/j.abb.2010.03.002

Beby, F., Lamonerie, T., 2013. The homeobox gene Otx2 in development and disease. Experimental Eye Research 111, 9–16. https://doi.org/10.1016/j.exer.2013.03.007

Bejjani, B.A., Lewis, R.A., Tomey, K.F., Anderson, K.L., Dueker, D.K., Jabak, M., Astle, W.F., Otterud, B., Leppert, M., Lupski, J.R., 1998. Mutations in CYP1B1, the gene for cytochrome P4501B1, are the predominant cause of primary congenital glaucoma in Saudi Arabia. Am. J. Hum. Genet. 62, 325–333. https://doi.org/10.1086/301725

Bella, J., Hindle, K.L., McEwan, P.A., Lovell, S.C., 2008. The leucine-rich repeat structure. Cell Mol Life Sci 65, 2307–2333. https://doi.org/10.1007/s00018-008-8019-0

Berry, F.B., Lines, M.A., Oas, J.M., Footz, T., Underhill, D.A., Gage, P.J., Walter, M.A., 2006. Functional interactions between FOXC1 and PITX2 underlie the

sensitivity to FOXC1 gene dose in Axenfeld–Rieger syndrome and anterior segment dysgenesis. Human Molecular Genetics 15, 905–919. https://doi.org/10.1093/hmg/ddl008

Berry, F.B., Skarie, J.M., Mirzayans, F., Fortin, Y., Hudson, T.J., Raymond, V., Link, B.A., Walter, M.A., 2008. FOXC1 is required for cell viability and resistance to oxidative stress in the eye through the transcriptional regulation of FOXO1A. Human Molecular Genetics 17, 490–505. https://doi.org/10.1093/hmg/ddm326

Berthoud, V.M., Minogue, P.J., Yu, H., Schroeder, R., Snabb, J.I., Beyer, E.C., 2013. Connexin50D47A Decreases Levels of Fiber Cell Connexins and Impairs Lens Fiber Cell Differentiation. Invest Ophthalmol Vis Sci 54, 7614–7622. https://doi.org/10.1167/iovs.13-13188

Beyer, E.C., Ebihara, L., Berthoud, V.M., 2013. Connexin Mutants and Cataracts. Front Pharmacol 4, 43. https://doi.org/10.3389/fphar.2013.00043

Bhave, G., Cummings, C.F., Vanacore, R.M., Kumagai-Cresse, C., Ero-Tolliver, I.A., Rafi, M., Kang, J.-S., Pedchenko, V., Fessler, L.I., Fessler, J.H., Hudson, B.G., 2012. Peroxidasin forms sulfilimine chemical bonds using hypohalous acids in tissue genesis. Nat. Chem. Biol. 8, 784–790. https://doi.org/10.1038/nchembio.1038

Bodunde, O.T., Ajibode, H.A., 2006. Congenital eye diseases at Olabisi Onabanjo University Teaching Hospital, Sagamu, Nigeria. Niger J Med 15, 291–294.

Bonnans, C., Chou, J., Werb, Z., 2014. Remodelling the extracellular matrix in development and disease. Nat. Rev. Mol. Cell Biol. 15, 786–801. https://doi.org/10.1038/nrm3904

Borza, D.B., Bondar, O., Ninomiya, Y., Sado, Y., Naito, I., Todd, P., Hudson, B.G., 2001. The NC1 domain of collagen IV encodes a novel network composed of the alpha 1, alpha 2, alpha 5, and alpha 6 chains in smooth muscle basement membranes. J. Biol. Chem. 276, 28532–28540. https://doi.org/10.1074/jbc.M103690200

Bucher, P.J., Ijsselmuiden, C.B., 1988. Prevalence and causes of blindness in the northern Transvaal. British Journal of Ophthalmology 72, 721–726. https://doi.org/10.1136/bjo.72.10.721

Budak, G., Dash, S., Srivastava, R., Lachke, S.A., Janga, S.C., 2018. Express: A database of transcriptome profiles encompassing known and novel transcripts across multiple development stages in eye tissues. Exp. Eye Res. 168, 57–68. https://doi.org/10.1016/j.exer.2018.01.009

Budde, W.M., Velten, I.M., Jonas, J.B., 1998. Optic Disc Size and Iris Color. Arch Ophthalmol 116, 545–545.

Burdon, K.P., McKay, J.D., Sale, M.M., Russell-Eggitt, I.M., Mackey, D.A., Wirth, M.G., Elder, J.E., Nicoll, A., Clarke, M.P., FitzGerald, L.M., Stankovich, J.M., Shaw, M.A., Sharma, S., Gajovic, S., Gruss, P., Ross, S., Thomas, P., Voss, A.K., Thomas, T., Gécz, J., Craig, J.E., 2003. Mutations in a Novel Gene, NHS, Cause the Pleiotropic Effects of Nance-Horan Syndrome, Including Severe Congenital Cataract, Dental Anomalies, and Mental Retardation. Am J Hum Genet 73, 1120–1130.

Busby, S.A., Burris, T.P., 2012. Retinoic Acid Receptors (RARA, RARB, and RARC), in: Choi, S. (Ed.), Encyclopedia of Signaling Molecules. Springer, New York, NY, pp. 1648–1655. https://doi.org/10.1007/978-1-4419-0461-4_385

Callaerts, P., Halder, G., Gehring, W.J., 1997. PAX-6 in development and evolution. Annu. Rev. Neurosci. 20, 483–532. https://doi.org/10.1146/annurev.neuro.20.1.483

Campbell, M.C., Tishkoff, S.A., 2008. AFRICAN GENETIC DIVERSITY: Implications for Human Demographic History, Modern Human Origins, and Complex Disease Mapping. Annu Rev Genomics Hum Genet 9, 403–433. https://doi.org/10.1146/annurev.genom.9.081307.164258

Carstens, N., Goolam, S., Hulley, M., Brandenburg, J.-T., Ramsay, M., Williams, S.E.I., 2022. Exome-based mutation screening in South African children with primary congenital glaucoma. Eye 1–7. https://doi.org/10.1038/s41433-022-01941-7

Carstens, N., Williams, S., Goolam, S., Carmichael, T., Cheung, M.S., Büchmann-Møller, S., Sultan, M., Staedtler, F., Zou, C., Swart, P., Rice, D.S., Lacoste, A., Paes, K., Ramsay, M., 2016. Novel mutation in the CHST6 gene causes macular corneal dystrophy in a black South African family. BMC Med Genet 17, 47. https://doi.org/10.1186/s12881-016-0308-0

Casey, J., Kawaguchi, R., Morrissey, M., Sun, H., McGettigan, P., Nielsen, J.E., Conroy, J., Regan, R., Kenny, E., Cormican, P., Morris, D.W., Tormey, P., Chróinín, M.N., Kennedy, B.N., Lynch, S., Green, A., Ennis, S., 2011. First implication of STRA6 mutations in isolated anophthalmia, microphthalmia and coloboma: a new dimension to the STRA6 phenotype. Hum Mutat 32, 1417–1426. https://doi.org/10.1002/humu.21590

Castronovo, V., Waltregny, D., Kischel, P., Roesli, C., Elia, G., Rybak, J.-N., Neri, D., 2006. A chemical proteomics approach for the identification of accessible antigens expressed in human kidney cancer. Mol. Cell Proteomics 5, 2083–2091. https://doi.org/10.1074/mcp.M600164-MCP200

Cataracts and Microphthalmia Caused by a Gja8 Mutation in Extracellular Loop 2 [WWW Document], n.d. URL https://journals.plos.org/plosone/article?id=10.1371/journal.pone.0052894 (accessed 3.8.22).

Cavodeassi, F., Creuzet, S., Etchevers, H.C., 2019. The hedgehog pathway and ocular developmental anomalies. Hum Genet 138, 917–936. https://doi.org/10.1007/s00439-018-1918-8

Ceroni, F., Aguilera-Garcia, D., Chassaing, N., Bax, D.A., Blanco-Kelly, F., Ramos, P., Tarilonte, M., Villaverde, C., da Silva, L.R.J., Ballesta-Martínez, M.J., Sanchez-Soler, M.J., Holt, R.J., Cooper-Charles, L., Bruty, J., Wallis, Y., McMullan, D., Hoffman, J., Bunyan, D., Stewart, A., Stewart, H., Lachlan, K., Fryer, A., McKay, V., Roume, J., Dureau, P., Saggar, A., Griffiths, M., Calvas, P., Ayuso, C., Corton, M., Ragge, N.K., DDD Study, 2019. New GJA8 variants and phenotypes highlight its critical role in a broad spectrum of eye anomalies. Hum Genet 138, 1027–1042. https://doi.org/10.1007/s00439-018-1875-2

Chan, Y.M., Keramaris-Vrantsis, E., Lidov, H.G., Norton, J.H., Zinchenko, N., Gruber, H.E., Thresher, R., Blake, D.J., Ashar, J., Rosenfeld, J., Lu, Q.L., 2010. Fukutin-related protein is essential for mouse muscle, brain and eye development and mutation recapitulates the wide clinical spectrums of dystroglycanopathies. Human Molecular Genetics 19, 3995–4006. https://doi.org/10.1093/hmg/ddq314

Chanas, S.A., Collinson, J.M., Ramaesh, T., Dorà, N., Kleinjan, D.A., Hill, R.E., West, J.D., 2009. Effects of Elevated Pax6 Expression and Genetic Background on Mouse Eye Development. Invest Ophthalmol Vis Sci 50, 4045–4059. https://doi.org/10.1167/iovs.07-1630

Chang, T.C., Summers, C.G., Schimmenti, L.A., Grajewski, A.L., 2012. Axenfeld-Rieger syndrome: new perspectives. British Journal of Ophthalmology 96, 318–322. https://doi.org/10.1136/bjophthalmol-2011-300801

Cheng, C., Wang, K., Hoshino, M., Uesugi, K., Yagi, N., Pierscionek, B., 2022. EphA2 Affects Development of the Eye Lens Nucleus and the Gradient of Refractive Index. Investigative Ophthalmology & Visual Science 63, 2. https://doi.org/10.1167/iovs.63.1.2

Cheng, G., Salerno, J.C., Cao, Z., Pagano, P.J., Lambeth, J.D., 2008. Identification and characterization of VPO1, a new animal heme-containing peroxidase. Free Radical Biology and Medicine 45, 1682–1694. https://doi.org/10.1016/j.freeradbiomed.2008.09.009

Choi, A., Lao, R., Ling-Fung Tang, P., Wan, E., Mayer, W., Bardakjian, T., Shaw, G.M., Kwok, P.-Y., Schneider, A., Slavotinek, A., 2015. Novel mutations in PXDN cause microphthalmia and anterior segment dysgenesis. Eur. J. Hum. Genet. 23, 337–341. https://doi.org/10.1038/ejhg.2014.119

Choudhury, A., Ramsay, M., Hazelhurst, S., Aron, S., Bardien, S., Botha, G., Chimusa, E.R., Christoffels, A., Gamieldien, J., Sefid-Dashti, M.J., Joubert, F., Meintjes, A., Mulder, N., Ramesar, R., Rees, J., Scholtz, K., Sengupta, D., Soodyall, H., Venter, P., Warnich, L., Pepper, M.S., 2017. Whole-genome sequencing for an enhanced understanding of genetic variation among South Africans. Nat Commun 8, 2062. https://doi.org/10.1038/s41467-017-00663-9

Clause, K.C., Barker, T.H., 2013. Extracellular matrix signaling in morphogenesis and repair. Curr. Opin. Biotechnol. 24, 830–833. https://doi.org/10.1016/j.copbio.2013.04.011

Cooper, M.A., Son, A.I., Komlos, D., Sun, Y., Kleiman, N.J., Zhou, R., 2008. Loss of ephrin-A5 function disrupts lens fiber cell packing and leads to cataract. Proc Natl Acad Sci U S A 105, 16620–16625. https://doi.org/10.1073/pnas.0808987105

Coordinating Proliferation and Tissue Specification to Promote Regional Identity in the Drosophila Head - ScienceDirect [WWW Document], n.d. URL https://www.sciencedirect.com/science/article/pii/S1534580703002430 (accessed 4.13.18).

Cvekl, A., Callaerts, P., 2017. PAX6: 25th anniversary and more to learn. Experimental Eye Research, In honour of David Beebe 156, 10–21. https://doi.org/10.1016/j.exer.2016.04.017

Cvekl, A., Tamm, E.R., 2004. Anterior eye development and ocular mesenchyme. Bioessays 26, 374–386. https://doi.org/10.1002/bies.20009

Dash, S., Siddam, A.D., Barnum, C.E., Janga, S.C., Lachke, S.A., 2016. RNA-binding proteins in eye development and disease: implication of conserved RNA granule components. Wiley Interdiscip Rev RNA 7, 527–557. https://doi.org/10.1002/wrna.1355

Dave, A., Craig, J.E., Sharma, S., 2012. The status of intercellular junctions in established lens epithelial cell lines. Mol Vis 18, 2937–2946.

Dave, A., Laurie, K., Staffieri, S.E., Taranath, D., Mackey, D.A., Mitchell, P., Wang, J.J., Craig, J.E., Burdon, K.P., Sharma, S., 2013. Mutations in the EPHA2 Gene Are a Major Contributor to Inherited Cataracts in South-Eastern Australia. PLoS One 8, e72518. https://doi.org/10.1371/journal.pone.0072518

Davies, M.J., 2011. Myeloperoxidase-derived oxidation: mechanisms of biological damage and its prevention. J Clin Biochem Nutr 48, 8–19. https://doi.org/10.3164/jcbn.11-006FR

Davies, M.J., Hawkins, C.L., Pattison, D.I., Rees, M.D., 2008. Mammalian heme peroxidases: from molecular mechanisms to health implications. Antioxid. Redox Signal. 10, 1199–1234. https://doi.org/10.1089/ars.2007.1927

de la Houssaye, G., Bieche, I., Roche, O., Vieira, V., Laurendeau, I., Arbogast, L., Zeghidi, H., Rapp, P., Halimi, P., Vidaud, M., Dufier, J.-L., Menasche, M., Abitbol, M., 2006. Identification of the first intragenic deletion of the PITX2 gene causing an Axenfeld-Rieger Syndrome: case report. BMC Med Genet 7, 82. https://doi.org/10.1186/1471-2350-7-82

DeNichilo, M.O., Panagopoulos, V., Rayner, T.E., Borowicz, R.A., Greenwood, J.E., Evdokiou, A., 2015. Peroxidase enzymes regulate collagen extracellular matrix biosynthesis. Am. J. Pathol. 185, 1372–1384. https://doi.org/10.1016/j.ajpath.2015.01.013

Désir, J., Sznajer, Y., Depasse, F., Roulez, F., Schrooyen, M., Meire, F., Abramowicz, M., 2010. LTBP2 null mutations in an autosomal recessive ocular syndrome with megalocornea, spherophakia, and secondary glaucoma. Eur J Hum Genet 18, 761–767. https://doi.org/10.1038/ejhg.2010.11

Desmond, J.C., Raynaud, S., Tung, E., Hofmann, W.-K., Haferlach, T., Koeffler, H.P., 2007. Discovery of epigenetically silenced genes in acute myeloid leukemias. Leukemia 21, 1026–1034. https://doi.org/10.1038/sj.leu.2404611

Devi, R.R., Vijayalakshmi, P., 2006. Novel mutations in GJA8 associated with autosomal dominant congenital cataract and microcornea. Mol Vis 12, 190–195.

Doward, W., Perveen, R., Lloyd, I., Ridgway, A., Wilson, L., Black, G., 1999. A mutation in the RIEG1 gene associated with Peters' anomaly. J Med Genet 36, 152–155.

Duester, G., 2009. Keeping an eye on retinoic acid signaling during eye development. Chem Biol Interact 178, 178–181. https://doi.org/10.1016/j.cbi.2008.09.004

Eiraku, M., Adachi, T., Sasai, Y., 2012. Relaxation-expansion model for self-driven retinal morphogenesis: a hypothesis from the perspective of biosystems dynamics

at the multi-cellular level. Bioessays 34, 17–25. https://doi.org/10.1002/bies.201100070

Erickson, R.P., 2001. Forkhead genes and human disease. J Appl Genet 42, 211–221.

Ero-Tolliver, I.A., Hudson, B.G., Bhave, G., 2015. The Ancient Immunoglobulin Domains of Peroxidasin Are Required to Form Sulfilimine Cross-links in Collagen IV. J Biol Chem 290, 21741–21748. https://doi.org/10.1074/jbc.M115.673996

Reis, L.M., Semina, E.V., 2011. GENETICS OF ANTERIOR SEGMENT DYSGENESIS DISORDERS. Curr Opin Ophthalmol 22, 314–324. https://doi.org/10.1097/ICU.0b013e328349412b

Fischbach, B.V., Trout, K.L., Lewis, J., Luis, C.A., Sika, M., 2005. WAGR Syndrome: A Clinical Review of 54 Cases. Pediatrics 116, 984–988. https://doi.org/10.1542/peds.2004-0467

Fitzpatrick, D.R., van Heyningen, V., 2005. Developmental eye disorders. Curr. Opin. Genet. Dev. 15, 348–353. https://doi.org/10.1016/j.gde.2005.04.013

Ford, D.A., 2010. Lipid oxidation by hypochlorous acid: chlorinated lipids in atherosclerosis and myocardial ischemia. Clin Lipidol 5, 835–852. https://doi.org/10.2217/clp.10.68

Frantz, C., Stewart, K.M., Weaver, V.M., 2010. The extracellular matrix at a glance. J. Cell. Sci. 123, 4195–4200. https://doi.org/10.1242/jcs.023820

Fuhrmann, S., 2010. Eye morphogenesis and patterning of the optic vesicle. Curr. Top. Dev. Biol. 93, 61–84. https://doi.org/10.1016/B978-0-12-385044-7.00003-5

Fukai, T., Ushio-Fukai, M., 2011. Superoxide dismutases: role in redox signaling, vascular function, and diseases. Antioxid. Redox Signal. 15, 1583–1606. https://doi.org/10.1089/ars.2011.3999

Furtmüller, P.G., Zederbauer, M., Jantschko, W., Helm, J., Bogner, M., Jakopitsch, C., Obinger, C., 2006. Active site structure and catalytic mechanisms of human

peroxidases. Archives of Biochemistry and Biophysics, Chemistry and Biology of Human Peroxidases 445, 199–213. https://doi.org/10.1016/j.abb.2005.09.017

Furukawa, T., Kozak, C.A., Cepko, C.L., 1997. Rax, a novel paired-type homeobox gene, shows expression in the anterior neural fold and developing retina. Proc Natl Acad Sci U S A 94, 3088–3093.

Gage, P.J., Camper, S.A., 1997. Pituitary homeobox 2, a novel member of the bicoid-related family of homeobox genes, is a potential regulator of anterior structure formation. Hum Mol Genet 6, 457–464. https://doi.org/10.1093/hmg/6.3.457

Gage, P.J., Rhoades, W., Prucka, S.K., Hjalt, T., 2005. Fate maps of neural crest and mesoderm in the mammalian eye. Invest. Ophthalmol. Vis. Sci. 46, 4200–4208. https://doi.org/10.1167/iovs.05-0691

Gage, P.J., Suh, H., Camper, S.A., 1999. Dosage requirement of Pitx2 for development of multiple organs. Development 126, 4643–4651.

Gao, X., Cheng, J., Lu, C., Li, X., Li, F., Liu, C., Zhang, M., Zhu, S., Ma, X., 2010. A Novel Mutation in the Connexin 50 Gene (GJA8) Associated with Autosomal Dominant Congenital Nuclear Cataract in a Chinese Family. Current Eye Research 35, 597–604. https://doi.org/10.3109/02713681003725831

García, I.E., Prado, P., Pupo, A., Jara, O., Rojas-Gómez, D., Mujica, P., Flores-Muñoz, C., González-Casanova, J., Soto-Riveros, C., Pinto, B.I., Retamal, M.A., González, C., Martínez, A.D., 2016. Connexinopathies: a structural and functional glimpse. BMC Cell Biology 17, S17. https://doi.org/10.1186/s12860-016-0092-x

Gavrilov, A., Eivazova, E., Pirozhkova, I., Lipinski, M., Razin, S., Vassetzky, Y., 2009. Chromosome Conformation Capture (from 3C to 5C) and Its ChIP-Based Modification, in: Chromatin Immunoprecipitation Assays, Methods in Molecular Biology. Humana Press, Totowa, NJ, pp. 171–188. https://doi.org/10.1007/978-1-60327-414-2_12

Geiszt, M., Witta, J., Baffi, J., Lekstrom, K., Leto, T.L., 2003. Dual oxidases represent novel hydrogen peroxide sources supporting mucosal surface host defense. FASEB J. 17, 1502–1504. https://doi.org/10.1096/fj.02-1104fje

Gerido, D.A., White, T.W., 2004. Connexin disorders of the ear, skin, and lens. Biochimica et Biophysica Acta (BBA) - Biomembranes, The Connexins 1662, 159–170. https://doi.org/10.1016/j.bbamem.2003.10.017

Girelli, D., Corrocher, R., Bisceglia, L., Olivieri, O., Franceschi, L.D., Zelante, L., Gasparini, P., 1995. Molecular Basis for the Recently Described Hereditary Hyperferritinemia-Cataract Syndrome: A Mutation in the Iron-Responsive Element of Ferritin L-Subunit Gene (the "Verona Mutation"). Blood 86, 4050–4053. https://doi.org/10.1182/blood.V86.11.4050.bloodjournal86114050

Goolam, S., Carstens, N., Ross, M., Bentley, D., Lopes, M., Peden, J., Kingsbury, Z., Tsogka, E., Barlow, R., Carmichael, T.R., Ramsay, M., Williams, S.E., 2018. Familial congenital cataract, coloboma, and nystagmus phenotype with variable expression caused by mutation in PAX6 in a South African family. Mol Vis 24, 407–413.

Gotenstein, J.R., Swale, R.E., Fukuda, T., Wu, Z., Giurumescu, C.A., Goncharov, A., Jin, Y., Chisholm, A.D., 2010. The C. elegans peroxidasin PXN-2 is essential for embryonic morphogenesis and inhibits adult axon regeneration. Development 137, 3603–3613.

Gould, D.B., John, S.W.M., 2002. Anterior segment dysgenesis and the developmental glaucomas are complex traits. Hum. Mol. Genet. 11, 1185–1193.

Graw, J., 2003. The genetic and molecular basis of congenital eye defects. Nature Reviews Genetics 4, 876–888. https://doi.org/10.1038/nrg1202

Graw, J., 2009. Genetics of crystallins: Cataract and beyond. Experimental Eye Research, Studies on the Ocular Lens 88, 173–189. https://doi.org/10.1016/j.exer.2008.10.011

Graw, J., 2010. Eye development. Curr Top Dev Biol 90, 343–386. https://doi.org/10.1016/S0070-2153(10)90010-0

Graw, J., Löster, J., 2003. Developmental genetics in ophthalmology. Ophthalmic Genet 24, 1–33. https://doi.org/10.1076/opge.24.1.1.13888

Green, M.R., Sambrook, J., 2017. Isolation of High-Molecular-Weight DNA Using Organic Solvents. Cold Spring Harb Protoc 2017, pdb.prot093450. https://doi.org/10.1101/pdb.prot093450

Grimley, E., Dressler, G.R., 2018. Are Pax Proteins Potential Therapeutic Targets in Kidney Disease and Cancer? Kidney Int 94, 259–267. https://doi.org/10.1016/j.kint.2018.01.025

Gunwar, S., Bejarano, P.A., Kalluri, R., Langeveld, J.P., Wisdom, B.J., Noelken, M.E., Hudson, B.G., 1991. Alveolar basement membrane: molecular properties of the noncollagenous domain (hexamer) of collagen IV and its reactivity with Goodpasture autoantibodies. Am. J. Respir. Cell Mol. Biol. 5, 107–112.

Gupta, S., Chatterjee, S., Mukherjee, A., Mutsuddi, M., 2017. Whole exome sequencing: Uncovering causal genetic variants for ocular diseases. Exp. Eye Res. 164, 139–150. https://doi.org/10.1016/j.exer.2017.08.013

Hadrami, M., Bonnet, C., Veten, F., Zeitz, C., Condroyer, C., Wang, P., Biya, M., Sidi Ahmed, M.A., Zhang, Q., Cheikh, S., Audo, I., Petit, C., Houmeida, A., 2019a. A novel missense mutation of GJA8 causes congenital cataract in a large Mauritanian family. European Journal of Ophthalmology 29, 621–628. https://doi.org/10.1177/1120672118804757

Hadrami, M., Bonnet, C., Zeitz, C., Veten, F., Biya, M., Hamed, C.T., Condroyer, C., Wang, P., Sidi, M.M., Cheikh, S., Zhang, Q., Audo, I., Petit, C., Houmeida, A., 2019b. Mutation profile of glaucoma candidate genes in Mauritanian families with primary congenital glaucoma. Mol Vis 25, 373–381.

Haji-Seyed-Javadi, R., Jelodari-Mamaghani, S., Paylakhi, S.H., Yazdani, S., Nilforushan, N., Fan, J.-B., Klotzle, B., Mahmoudi, M.J., Ebrahimian, M.J., Chelich, N., Taghiabadi, E., Kamyab, K., Boileau, C., Paisan-Ruiz, C., Ronaghi, M., Elahi, E., 2012. LTBP2 mutations cause Weill–Marchesani and Weill–Marchesani-like syndrome and affect disruptions in the extracellular matrix. Human Mutation 33, 1182–1187. https://doi.org/10.1002/humu.22105

Halestrap, A.P., Meredith, D., 2004. The SLC16 gene family—from monocarboxylate transporters (MCTs) to aromatic amino acid transporters and beyond. Pflugers Arch - Eur J Physiol 447, 619–628. https://doi.org/10.1007/s00424-003-1067-2

Hanmer, K.L., Mavri-Damelin, D., 2018. Peroxidasin is a novel target of the redox-sensitive transcription factor Nrf2. Gene 674, 104–114. https://doi.org/10.1016/j.gene.2018.06.076

Hansen, L., Yao, W., Eiberg, H., Kjaer, K.W., Baggesen, K., Hejtmancik, J.F., Rosenberg, T., 2007. Genetic Heterogeneity in Microcornea-Cataract: Five Novel Mutations in CRYAA, CRYGD, and GJA8. Investigative Ophthalmology & Visual Science 48, 3937–3944. https://doi.org/10.1167/iovs.07-0013

Harding, P., Toms, M., Schiff, E., Owen, N., Bell, S., Lloyd, I.C., Moosajee, M., 2021. EPHA2 Segregates with Microphthalmia and Congenital Cataracts in Two Unrelated Families. Int J Mol Sci 22, 2190. https://doi.org/10.3390/ijms22042190

Harissi-Dagher, M., Colby, K., 2008. Anterior segment dysgenesis: Peters anomaly and sclerocornea. Int Ophthalmol Clin 48, 35–42. https://doi.org/10.1097/IIO.0b013e318169526c

Haro, C., Uribe, M.L., Quereda, C., Cruces, J., Martín-Nieto, J., 2018. Expression in retinal neurons of fukutin and FKRP, the protein products of two dystroglycanopathy-causative genes. Mol Vis 24, 43–58.

Hayashi, T., Mizuno, N., Ueda, Y., Okamoto, M., Kondoh, H., 2004. FGF2 triggers iris-derived lens regeneration in newt eye. Mechanisms of Development 121, 519–526. https://doi.org/10.1016/j.mod.2004.04.010

Hiebert, P., 2021. The Nrf2 transcription factor: A multifaceted regulator of the extracellular matrix. Matrix Biol Plus 10, 100057. https://doi.org/10.1016/j.mbplus.2021.100057

Hillman, S.C., Willams, D., Carss, K.J., McMullan, D.J., Hurles, M.E., Kilby, M.D., 2015. Prenatal exome sequencing for fetuses with structural abnormalities:

the next step. Ultrasound Obstet Gynecol 45, 4–9. https://doi.org/10.1002/uog.14653

Hirani, R., Hanssen, E., Gibson, M.A., 2007. LTBP-2 specifically interacts with the amino-terminal region of fibrillin-1 and competes with LTBP-1 for binding to this microfibrillar protein. Matrix Biology 26, 213–223. https://doi.org/10.1016/j.matbio.2006.12.006

Hjalt, T.A., Semina, E.V., Amendt, B.A., Murray, J.C., 2000. The Pitx2 protein in mouse development. Developmental Dynamics 218, 195–200. https://doi.org/10.1002/(SICI)1097-0177(200005)218:1<195::AID-DVDY17>3.0.CO;2-C

Homma, S., Shimada, T., Hikake, T., Yaginuma, H., 2009. Expression pattern of LRR and Ig domain-containing protein (LRRIG protein) in the early mouse embryo. Gene Expression Patterns 9, 1–26. https://doi.org/10.1016/j.gep.2008.09.004

Horikoshi, N., Cong, J., Kley, N., Shenk, T., 1999. Isolation of Differentially Expressed cDNAs from p53-Dependent Apoptotic Cells: Activation of the Human Homologue of the Drosophila Peroxidasin Gene. Biochemical and Biophysical Research Communications 261, 864–869. https://doi.org/10.1006/bbrc.1999.1123

Hornby, S.J., Gilbert, C.E., Rahi, J.K., Sil, A.K., Xiao, Y., Dandona, L., Foster, A., 2000. Regional variation in blindness in children due to microphthalmos, anophthalmos and coloboma. Ophthalmic Epidemiol 7, 127–138.

Hu, B., Wang, Q., Wang, Y.A., Hua, S., Sauvé, C.-E.G., Ong, D., Lan, Z.D., Chang, Q., Ho, Y.W., Monasterio, M.M., Lu, X., Zhong, Y., Zhang, Jianhua, Deng, P., Tan, Z., Wang, G., Liao, W.-T., Corley, L.J., Yan, H., Zhang, Junxia, You, Y., Liu, N., Cai, L., Finocchiaro, G., Phillips, J.J., Berger, M.S., Spring, D.J., Hu, J., Sulman, E.P., Fuller, G.N., Chin, L., Verhaak, R.G.W., DePinho, R.A., 2016. Epigenetic Activation of WNT5A Drives Glioblastoma Stem Cell Differentiation and Invasive Growth. Cell 167, 1281-1295.e18. https://doi.org/10.1016/j.cell.2016.10.039

Huynh, K.D., Fischle, W., Verdin, E., Bardwell, V.J., 2000. BCoR, a novel corepressor involved in BCL-6 repression. Genes Dev 14, 1810–1823.

Hynes, R.O., 2009. Extracellular matrix: not just pretty fibrils. Science 326, 1216–1219. https://doi.org/10.1126/science.1176009

Hynes, R.O., 2012. The evolution of metazoan extracellular matrix. J Cell Biol 196, 671–679. https://doi.org/10.1083/jcb.201109041

Idrees, F., Vaideanu, D., Fraser, S.G., Sowden, J.C., Khaw, P.T., 2006. A review of anterior segment dysgeneses. Surv Ophthalmol 51, 213–231. https://doi.org/10.1016/j.survophthal.2006.02.006

Ito, Y.A., Footz, T.K., Berry, F.B., Mirzayans, F., Yu, M., Khan, A.O., Walter, M.A., 2009. Severe Molecular Defects of a Novel FOXC1 W152G Mutation Result in Aniridia. Invest. Ophthalmol. Vis. Sci. 50, 3573–3579. https://doi.org/10.1167/iovs.08-3032

Ito, Y.A., Walter, M.A., 2014. Genomics and anterior segment dysgenesis: a review. Clin. Experiment. Ophthalmol. 42, 13–24. https://doi.org/10.1111/ceo.12152

Jalali Sefid Dashti, M., Gamieldien, J., 2017. A practical guide to filtering and prioritizing genetic variants. BioTechniques 62, 18–30. https://doi.org/10.2144/000114492

Jayachandran, A., Prithviraj, P., Lo, P.-H., Walkiewicz, M., Anaka, M., Woods, B.L., Tan, B., Behren, A., Cebon, J., McKeown, S.J., 2016. Identifying and targeting determinants of melanoma cellular invasion. Oncotarget 7, 41186–41202. https://doi.org/10.18632/oncotarget.9227

Jian, X., Boerwinkle, E., Liu, X., 2014. In silico prediction of splice-altering single nucleotide variants in the human genome. Nucleic Acids Res 42, 13534–13544. https://doi.org/10.1093/nar/gku1206

Jun, G., Guo, H., Klein, B.E.K., Klein, R., Wang, J.J., Mitchell, P., Miao, H., Lee, K.E., Joshi, T., Buck, M., Chugha, P., Bardenstein, D., Klein, A.P., Bailey-Wilson, J.E., Gong, X., Spector, T.D., Andrew, T., Hammond, C.J., Elston, R.C., Iyengar, S.K., Wang, B., 2009. EPHA2 Is Associated with Age-Related Cortical Cataract in

Mice and Humans. PLoS Genet 5, e1000584. https://doi.org/10.1371/journal.pgen.1000584

Kahsai, T.Z., Enders, G.C., Gunwar, S., Brunmark, C., Wieslander, J., Kalluri, R., Zhou, J., Noelken, M.E., Hudson, B.G., 1997. Seminiferous tubule basement membrane. Composition and organization of type IV collagen chains, and the linkage of alpha3(IV) and alpha5(IV) chains. J. Biol. Chem. 272, 17023–17032.

Kalluri, R., Gattone, V.H., Hudson, B.G., 1998. Identification and localization of type IV collagen chains in the inner ear cochlea. Connect. Tissue Res. 37, 143–150.

Kalluri, R., Weinberg, R.A., 2009. The basics of epithelial-mesenchymal transition. J. Clin. Invest. 119, 1420–1428. https://doi.org/10.1172/JCI39104

Kang, J., Neidigh, J.W., 2008. Hypochlorous acid damages histone proteins forming 3-chlorotyrosine and 3,5-dichlorotyrosine. Chemical Research in Toxicology 21, 1028–1038. https://doi.org/10.1021/tx7003486

Kang, Y., Li, X., Wu, Q., Zhou, W., Li, Q., Hu, Q., 2016. [Analysis of PAX6 gene mutation in a family affected with congenital aniridia]. Zhonghua Yi Xue Yi Chuan Xue Za Zhi 33, 519–522. https://doi.org/10.3760/cma.j.issn.1003-9406.2016.04.021

Kaplan, H.J., 2007. Anatomy and Function of the Eye. Immune Response and the Eye 92, 4–10. https://doi.org/10.1159/000099236

Kenyon, K.R., 1975. Mesenchymal dysgenesis in Peter's anomaly, sclerocornea and congenital endothelial dystrophy. Exp. Eye Res. 21, 125–142.

Khan, A.O., Aldahmesh, M.A., 2008. PAX6 analysis of two unrelated families from the Arabian Peninsula with classic hereditary aniridia. Ophthalmic Genet 29, 145–148. https://doi.org/10.1080/13816810802078195

Khan, K., Rudkin, A., Parry, D.A., Burdon, K.P., McKibbin, M., Logan, C.V., Abdelhamed, Z.I., Muecke, J.S., Fernandez-Fuentes, N., Laurie, K.J., 2011. Homozygous mutations in PXDN cause congenital cataract, corneal opacity, and developmental glaucoma. The American Journal of Human Genetics 89, 464–473.

Khoshnoodi, J., Pedchenko, V., Hudson, B.G., 2008. Mammalian collagen IV. Microsc. Res. Tech. 71, 357–370. https://doi.org/10.1002/jemt.20564

Kidson, S.H., Kume, T., Deng, K., Winfrey, V., Hogan, B.L.M., 1999. The Forkhead/Winged-Helix Gene, Mf1, Is Necessary for the Normal Development of the Cornea and Formation of the Anterior Chamber in the Mouse Eye. Developmental Biology 211, 306–322. https://doi.org/10.1006/dbio.1999.9314

Kim, H.-J., Suh, W., Park, S.C., Kim, C.Y., Park, K.H., Kook, M.S., Kim, Y.Y., Kim, C.-S., Park, C.K., Ki, C.-S., Kee, C., 2011. Mutation spectrum of CYP1B1 and MYOC genes in Korean patients with primary congenital glaucoma. Mol. Vis. 17, 2093–2101.

Kita, T., Kume, N., Minami, M., Hayashida, K., Murayama, T., Sano, H., Moriwaki, H., Kataoka, H., Nishi, E., Horiuchi, H., Arai, H., Yokode, M., 2001. Role of Oxidized LDL in Atherosclerosis. Annals of the New York Academy of Sciences 947, 199–206. https://doi.org/10.1111/j.1749-6632.2001.tb03941.x

Koksal, Z., Gulcin, I., Ozdemir, H., 2016. An Important Milk Enzyme: Lactoperoxidase. Milk Proteins - From Structure to Biological Properties and Health Aspects. https://doi.org/10.5772/64416

Komori, T., Ono, M., Hara, E.S., Ueda, J., Nguyen, H.T.T., Nguyen, H.T., Yonezawa, T., Maeba, T., Kimura-Ono, A., Takarada, T., Momota, R., Maekawa, K., Kuboki, T., Oohashi, T., 2018a. Type IV collagen α6 chain is a regulator of keratin 10 in keratinization of oral mucosal epithelium. Scientific Reports 8, 2612. https://doi.org/10.1038/s41598-018-21000-0

Kondo-Saitoh, A., Matsumoto, N., Sasaki, T., Egashira, M., Saitoh, A., Yamada, K., Niikawa, N., Amemiya, T., 2000. Two Nonsense Mutations of PAX6 in Two Japanese Aniridia Families: Case Report and Review of the Literature. European Journal of Ophthalmology 10, 167–172. https://doi.org/10.1177/112067210001000213

Kopanos, C., Tsiolkas, V., Kouris, A., Chapple, C.E., Albarca Aguilera, M., Meyer, R., Massouras, A., 2019. VarSome: the human genomic variant search engine. Bioinformatics 35, 1978–1980. https://doi.org/10.1093/bioinformatics/bty897

Kreft, Ł., Soete, A., Hulpiau, P., Botzki, A., Saeys, Y., De Bleser, P., 2017. ConTra v3: a tool to identify transcription factor binding sites across species, update 2017. Nucleic Acids Res 45, W490–W494. https://doi.org/10.1093/nar/gkx376

Kroeber, M., Davis, N., Holzmann, S., Kritzenberger, M., Shelah-Goraly, M., Ofri, R., Ashery-Padan, R., Tamm, E.R., 2010. Reduced expression of Pax6 in lens and cornea of mutant mice leads to failure of chamber angle development and juvenile glaucoma. Hum Mol Genet 19, 3332–3342. https://doi.org/10.1093/hmg/ddq237

Kumar, A., Duvvari, M.R., Prabhakaran, V.C., Shetty, J.S., Murthy, G.J., Blanton, S.H., 2010. A homozygous mutation in LTBP2 causes isolated microspherophakia. Hum Genet 128, 365–371. https://doi.org/10.1007/s00439-010-0858-8

Kumar, P., Henikoff, S., Ng, P.C., 2009. Predicting the effects of coding non-synonymous variants on protein function using the SIFT algorithm. Nat Protoc 4, 1073–1081. https://doi.org/10.1038/nprot.2009.86

Kume, T., Deng, K., Hogan, B.L., 2000. Murine forkhead/winged helix genes Foxc1 (Mf1) and Foxc2 (Mfh1) are required for the early organogenesis of the kidney and urinary tract. Development 127, 1387–1395. https://doi.org/10.1242/dev.127.7.1387

Kussendrager, K.D., Hooijdonk, A.C.M. van, 2000. Lactoperoxidase: physico-chemical properties, occurrence, mechanism of action and applications. British Journal of Nutrition 84, 19–25. https://doi.org/10.1017/S0007114500002208

Kwan, K.M., 2014. Coming into focus: The role of extracellular matrix in vertebrate optic cup morphogenesis. Developmental Dynamics 243, 1242–1248. https://doi.org/10.1002/dvdy.24162

Lachke, S.A., Ho, J.W.K., Kryukov, G.V., O'Connell, D.J., Aboukhalil, A., Bulyk, M.L., Park, P.J., Maas, R.L., 2012. iSyTE: Integrated Systems Tool for Eye Gene Discovery. Invest. Ophthalmol. Vis. Sci. 53, 1617–1627. https://doi.org/10.1167/iovs.11-8839

Lambeth, J.D., Neish, A.S., 2014. Nox enzymes and new thinking on reactive oxygen: a double-edged sword revisited. Annu Rev Pathol 9, 119–145. https://doi.org/10.1146/annurev-pathol-012513-104651

Lamouille, S., Xu, J., Derynck, R., 2014. Molecular mechanisms of epithelial-mesenchymal transition. Nat. Rev. Mol. Cell Biol. 15, 178–196. https://doi.org/10.1038/nrm3758

Laurila, P., Leivo, I., 1993. Basement membrane and interstitial matrix components form separate matrices in heterokaryons of PYS-2 cells and fibroblasts. J. Cell. Sci. 104 (Pt 1), 59–68.

Lázár, E., Péterfi, Z., Sirokmány, G., Kovács, H.A., Klement, E., Medzihradszky, K.F., Geiszt, M., 2015. Structure-function analysis of peroxidasin provides insight into the mechanism of collagen IV crosslinking. Free Radic. Biol. Med. 83, 273–282. https://doi.org/10.1016/j.freeradbiomed.2015.02.015

Le, S.N., Porebski, B.T., McCoey, J., Fodor, J., Riley, B., Godlewska, M., Góra, M., Czarnocka, B., Banga, J.P., Hoke, D.E., Kass, I., Buckle, A.M., 2015. Modelling of Thyroid Peroxidase Reveals Insights into Its Enzyme Function and Autoantigenicity. PLOS ONE 10, e0142615. https://doi.org/10.1371/journal.pone.0142615

Lee, H., Khan, R., O'Keefe, M., 2008. Aniridia: current pathology and management. Acta Ophthalmologica 86, 708–715. https://doi.org/10.1111/j.1755-3768.2008.01427.x

Lee, S.-W., Kim, H.-K., Naidansuren, P., Ham, K.A., Choi, H.S., Ahn, H.-Y., Kim, M., Kang, D.H., Kang, S.W., Joe, Y.A., 2020. Peroxidasin is essential for endothelial cell survival and growth signaling by sulfilimine crosslink-dependent matrix assembly. The FASEB Journal 34, 10228–10241. https://doi.org/10.1096/fj.201902899R

Lehmann, O.J., Sowden, J.C., Carlsson, P., Jordan, T., Bhattacharya, S.S., 2003. Fox's in development and disease. Trends in Genetics 19, 339–344. https://doi.org/10.1016/S0168-9525(03)00111-2

Lengler, J., Bittner, T., Münster, D., Gawad, A.E.-D.A., Graw, J., 2005. Agonistic and Antagonistic Action of AP2, Msx2, Pax6, Prox1 and Six3 in the Regulation of Sox2 Expression. ORE 37, 301–309. https://doi.org/10.1159/000087774

Lévigne, D., Modarressi, A., Krause, K.-H., Pittet-Cuénod, B., 2016. NADPH oxidase 4 deficiency leads to impaired wound repair and reduced dityrosine-crosslinking, but does not affect myofibroblast formation. Free Radical Biology and Medicine 96, 374–384. https://doi.org/10.1016/j.freeradbiomed.2016.04.194

Li, H., Cao, Z., Moore, D.R., Jackson, P.L., Barnes, S., Lambeth, J.D., Thannickal, V.J., Cheng, G., 2012. Microbicidal Activity of Vascular Peroxidase 1 in Human Plasma via Generation of Hypochlorous Acid. Infect Immun 80, 2528–2537. https://doi.org/10.1128/IAI.06337-11

Lim, H.T., Kim, D.H., Kim, H., 2017. PAX6 aniridia syndrome: clinics, genetics, and therapeutics. Curr Opin Ophthalmol 28, 436–447. https://doi.org/10.1097/ICU.0000000000000405

Lin Y., Liu N., Lei C., Fan Y., Liu X., Yang Y., Wang J., Liu B., Yang Z., 2008. A novel GJA8 mutation in a Chinese family with autosomal dominant congenital cataract. Chinese Journal of Medical Genetics 59–62.

Lin, J.-S., Lai, E.-M., 2017. Protein–Protein Interactions: Co-Immunoprecipitation, in: Bacterial Protein Secretion Systems, Methods in Molecular Biology. Humana Press, New York, NY, pp. 211–219. https://doi.org/10.1007/978-1-4939-7033-9_17

Lin, Y., Gao, H., Zhu, Y., Chen, C., Li, T., Liu, B., Lyu, C., Huang, Y., Li, H., Wu, Q., Jin, C., Liang, X., Huang, X., Lu, L., 2018. Two Paired Box 6 mutations identified in Chinese patients with classic congenital aniridia and cataract. Mol Med Rep 18, 4439–4445. https://doi.org/10.3892/mmr.2018.9469

Lines, M.A., Kozlowski, K., Walter, M.A., 2002. Molecular genetics of Axenfeld-Rieger malformations. Hum Mol Genet 11, 1177–1184. https://doi.org/10.1093/hmg/11.10.1177

Little, A.G., Seebacher, F., 2014. The evolution of endothermy is explained by thyroid hormone-mediated responses to cold in early vertebrates. Journal of Experimental Biology 217, 1642–1648. https://doi.org/10.1242/jeb.088880

Long, X., Huang, Y., Tan, H., Li, Z., Zhang, R., Linpeng, S., Lv, W., Cao, Y., Li, H., Liang, D., Wu, L., 2018. Identification of a novel MIP frameshift mutation associated with congenital cataract in a Chinese family by whole-exome sequencing and functional analysis. Eye 32, 1359–1364. https://doi.org/10.1038/s41433-018-0084-5

Lu, J., Mitra, S., Wang, X., Khaidakov, M., Mehta, J.L., 2011. Oxidative stress and lectin-like ox-ldl-receptor lox-1 in atherogenesis and tumorigenesis. Antioxidants and Redox Signaling 15, 2301–2333. https://doi.org/10.1089/ars.2010.3792

Ma, A. s., Grigg, J. r., Prokudin, I., Flaherty, M., Bennetts, B., Jamieson, R. v., 2018. New mutations in GJA8 expand the phenotype to include total sclerocornea. Clinical Genetics 93, 155–159. https://doi.org/10.1111/cge.13045

Ma, A.S., Grigg, J.R., Ho, G., Prokudin, I., Farnsworth, E., Holman, K., Cheng, A., Billson, F.A., Martin, F., Fraser, C., Mowat, D., Smith, J., Christodoulou, J., Flaherty, M., Bennetts, B., Jamieson, R.V., 2016. Sporadic and Familial Congenital Cataracts: Mutational Spectrum and New Diagnoses Using Next- Generation Sequencing. Hum Mutat 37, 371–384. https://doi.org/10.1002/humu.22948

Ma, Q.-L., Zhang, G.-G., Peng, J., 2013. Vascular peroxidase 1: A novel enzyme in promoting oxidative stress in cardiovascular system. Trends in Cardiovascular Medicine 23, 179–183. https://doi.org/10.1016/j.tcm.2012.11.002

Mackay, D.S., Bennett, T.M., Culican, S.M., Shiels, A., 2014. Exome sequencing identifies novel and recurrent mutations in GJA8 and CRYGD associated with inherited cataract. Hum Genomics 8, 19. https://doi.org/10.1186/s40246-014-0019-6

Madden, S.L., Cook, B.P., Nacht, M., Weber, W.D., Callahan, M.R., Jiang, Y., Dufault, M.R., Zhang, X., Zhang, W., Walter-Yohrling, J., Rouleau, C., Akmaev, V.R., Wang, C.J., Cao, X., St Martin, T.B., Roberts, B.L., Teicher, B.A., Klinger, K.W., Stan, R.-V., Lucey, B., Carson-Walter, E.B., Laterra, J., Walter, K.A., 2004.

Vascular gene expression in nonneoplastic and malignant brain. Am. J. Pathol. 165, 601–608.

Mahmood, T., Yang, P.-C., 2012. Western Blot: Technique, Theory, and Trouble Shooting. N Am J Med Sci 4, 429–434. https://doi.org/10.4103/1947-2714.100998

Manral, P., Colon, S., Bhave, G., Zhao, M.-H., Jain, S., Borza, D.-B., 2019. Peroxidasin Is a Novel Target of Autoantibodies in Lupus Nephritis. Kidney Int Rep 4, 1004–1006. https://doi.org/10.1016/j.ekir.2019.04.009

Mao, M., Smith, R.S., Alavi, M.V., Marchant, J.K., Cosma, M., Libby, R.T., John, S.W.M., Gould, D.B., 2015. Strain-Dependent Anterior Segment Dysgenesis and Progression to Glaucoma in Col4a1 Mutant Mice. Invest. Ophthalmol. Vis. Sci. 56, 6823–6831. https://doi.org/10.1167/iovs.15-17527

Markitantova, Yu.V., Firsova, N.V., Smirnova, Yu.A., Panova, I.G., Sukhikh, G.T., Zinovieva, R.D., Mitashov, V.I., 2008. Localization of the PITX2 gene expression in human eye cells in the course of prenatal development. Biol Bull Russ Acad Sci 35, 113–120. https://doi.org/10.1134/S1062359008020039

Martin, D.M., Skidmore, J.M., Philips, S.T., Vieira, C., Gage, P.J., Condie, B.G., Raphael, Y., Martinez, S., Camper, S.A., 2004. PITX2 is required for normal development of neurons in the mouse subthalamic nucleus and midbrain. Developmental Biology 267, 93–108. https://doi.org/10.1016/j.ydbio.2003.10.035

McCall, A.S., Bhave, G., Pedchenko, V., Hess, J., Free, M., Little, D.J., Baker, T.P., Pendergraft, W.F., Falk, R.J., Olson, S.W., Hudson, B.G., 2018. Inhibitory Anti-Peroxidasin Antibodies in Pulmonary-Renal Syndromes. J Am Soc Nephrol 29, 2619–2625. https://doi.org/10.1681/ASN.2018050519

McLaren, W., Gil, L., Hunt, S.E., Riat, H.S., Ritchie, G.R.S., Thormann, A., Flicek, P., Cunningham, F., 2016. The Ensembl Variant Effect Predictor. Genome Biol 17, 122. https://doi.org/10.1186/s13059-016-0974-4

McMillen, T.S., Heinecke, J.W., LeBoeuf, R.C., 2005. Expression of human myeloperoxidase by macrophages promotes atherosclerosis in mice. Circulation 111, 2798–2804. https://doi.org/10.1161/CIRCULATIONAHA.104.516278

Merriman, B., R&D Team, I.T., Rothberg, J.M., 2012. Progress in Ion Torrent semiconductor chip based sequencing. ELECTROPHORESIS 33, 3397–3417. https://doi.org/10.1002/elps.201200424

Miao, H., Wang, B., 2009. Eph/ephrin signaling in epithelial development and homeostasis. The International Journal of Biochemistry & Cell Biology 41, 762–770. https://doi.org/10.1016/j.biocel.2008.07.019

Micheal, S., Siddiqui, S.N., Zafar, S.N., Iqbal, A., Khan, M.I., den Hollander, A.I., 2016. Identification of Novel Variants in LTBP2 and PXDN Using Whole-Exome Sequencing in Developmental and Congenital Glaucoma. PLoS One 11, e0159259. https://doi.org/10.1371/journal.pone.0159259

Li, H., Cao, Z., Moore, D.R., Jackson, P.L., Barnes, S., Lambeth, J.D., Thannickal, V.J., Cheng, G., 2012. Microbicidal Activity of Vascular Peroxidase 1 in Human Plasma via Generation of Hypochlorous Acid. Infect Immun 80, 2528–2537. https://doi.org/10.1128/IAI.06337-11

Miner, J.H., 2012. The Glomerular Basement Membrane. Exp Cell Res 318, 973–978. https://doi.org/10.1016/j.yexcr.2012.02.031

Minogue, P.J., Tong, J.-J., Arora, A., Russell-Eggitt, I., Hunt, D.M., Moore, A.T., Ebihara, L., Beyer, E.C., Berthoud, V.M., 2009. A Mutant Connexin50 with Enhanced Hemichannel Function Leads to Cell Death. Invest Ophthalmol Vis Sci 50, 5837–5845. https://doi.org/10.1167/iovs.09-3759

Mucchielli, M.-L., Mitsiadis, T.A., Raffo, S., Brunet, J.-F., Proust, J.-P., Goridis, C., 1997. MouseOtlx2/RIEGExpression in the Odontogenic Epithelium Precedes Tooth Initiation and Requires Mesenchyme-Derived Signals for Its Maintenance. Developmental Biology 189, 275–284. https://doi.org/10.1006/dbio.1997.8672

Nakagami, Y., 2016. Nrf2 Is an Attractive Therapeutic Target for Retinal Diseases. Oxidative Medicine and Cellular Longevity 2016, e7469326. https://doi.org/10.1155/2016/7469326

Nauseef, W.M., 1988. Myeloperoxidase deficiency. Hematol. Oncol. Clin. North Am. 2, 135–158.

Nauseef, W.M., Borregaard, N., 2014. Neutrophils at work. Nat Immunol 15, 602–611. https://doi.org/10.1038/ni.2921

Neethirajan, G., Hanson, I.M., Krishnadas, S.R., Vijayalakshmi, P., Anupkumar, K., Sundaresan, P., 2003. A novel PAX6 gene mutation in an Indian aniridia patient. Mol Vis 9, 205–209.

Ng, D., Thakker, N., Corcoran, C.M., Donnai, D., Perveen, R., Schneider, A., Hadley, D.W., Tifft, C., Zhang, L., Wilkie, A.O.M., van der Smagt, J.J., Gorlin, R.J., Burgess, S.M., Bardwell, V.J., Black, G.C.M., Biesecker, L.G., 2004. Oculofaciocardiodental and Lenz microphthalmia syndromes result from distinct classes of mutations in BCOR. Nat Genet 36, 411–416. https://doi.org/10.1038/ng1321

Nieto, M.A., 2013. Epithelial plasticity: a common theme in embryonic and cancer cells. Science 342, 1234850. https://doi.org/10.1126/science.1234850

Nishimura, D.Y., Searby, C.C., Alward, W.L., Walton, D., Craig, J.E., Mackey, D.A., Kawase, K., Kanis, A.B., Patil, S.R., Stone, E.M., Sheffield, V.C., 2001. A Spectrum of FOXC1 Mutations Suggests Gene Dosage as a Mechanism for Developmental Defects of the Anterior Chamber of the Eye. Am J Hum Genet 68, 364–372.

Nishina, S., Kohsaka, S., Yamaguchi, Y., Handa, H., Kawakami, A., Fujisawa, H., Azuma, N., 1999. PAX6 expression in the developing human eye. Br J Ophthalmol 83, 723–727.

Okada, I., Hamanoue, H., Terada, K., Tohma, T., Megarbane, A., Chouery, E., Abou-Ghoch, J., Jalkh, N., Cogulu, O., Ozkinay, F., Horie, K., Takeda, J., Furuichi, T., Ikegawa, S., Nishiyama, K., Miyatake, S., Nishimura, A., Mizuguchi, T., Niikawa, N., Hirahara, F., Kaname, T., Yoshiura, K., Tsurusaki, Y., Doi, H., Miyake, N., Furukawa, T., Matsumoto, N., Saitsu, H., 2011. SMOC1 Is Essential for Ocular and Limb Development in Humans and Mice. Am J Hum Genet 88, 30–41. https://doi.org/10.1016/j.ajhg.2010.11.012

Oliver, G., Mailhos, A., Wehr, R., Copeland, N.G., Jenkins, N.A., Gruss, P., 1995. Six3, a murine homologue of the sine oculis gene, demarcates the most anterior

border of the developing neural plate and is expressed during eye development. Development 121, 4045–4055.

Ornitz, D.M., Itoh, N., 2015. The Fibroblast Growth Factor signaling pathway. Wiley Interdiscip Rev Dev Biol 4, 215–266. https://doi.org/10.1002/wdev.176

Panagopoulos, V., Zinonos, I., Leach, D.A., Hay, S.J., Liapis, V., Zysk, A., Ingman, W.V., DeNichilo, M.O., Evdokiou, A., 2015. Uncovering a new role for peroxidase enzymes as drivers of angiogenesis. The International Journal of Biochemistry & Cell Biology 68, 128–138. https://doi.org/10.1016/j.biocel.2015.09.006

Park, J.E., Son, A.I., Zhou, R., 2013. Roles of EphA2 in Development and Disease. Genes (Basel) 4, 334–357. https://doi.org/10.3390/genes4030334

Paumann-Page, M., Kienzl, N.F., Motwani, J., Bathish, B., Paton, L.N., Magon, N.J., Sevcnikar, B., Furtmüller, P.G., Traxlmayr, M.W., Obinger, C., Eccles, M.R., Winterbourn, C.C., 2021. Peroxidasin protein expression and enzymatic activity in metastatic melanoma cell lines are associated with invasive potential. Redox Biology 46, 102090. https://doi.org/10.1016/j.redox.2021.102090

Pedchenko, V., Bondar, O., Fogo, A.B., Vanacore, R., Voziyan, P., Kitching, A.R., Wieslander, J., Kashtan, C., Borza, D.-B., Neilson, E.G., Wilson, C.B., Hudson, B.G., 2010. Molecular Architecture of the Goodpasture Autoantigen in Anti-GBM Nephritis. N Engl J Med 363, 343–354. https://doi.org/10.1056/NEJMoa0910500

Péterfi, Z., Donkó, A., Orient, A., Sum, A., Prókai, A., Molnár, B., Veréb, Z., Rajnavölgyi, E., Kovács, K.J., Müller, V., 2009. Peroxidasin is secreted and incorporated into the extracellular matrix of myofibroblasts and fibrotic kidney. The American journal of pathology 175, 725–735.

Péterfi, Z., Geiszt, M., 2014. Peroxidasins: novel players in tissue genesis. Trends in biochemical sciences 39, 305–307.

Pfenniger, A., Wohlwend, A., Kwak, B.R., 2011. Mutations in connexin genes and disease. European Journal of Clinical Investigation 41, 103–116. https://doi.org/10.1111/j.1365-2362.2010.02378.x

Plásilová, M., Stoilov, I., Sarfarazi, M., Kádasi, L., Feráková, E., Ferák, V., 1999. Identification of a single ancestral CYP1B1 mutation in Slovak Gypsies (Roms) affected with primary congenital glaucoma. J. Med. Genet. 36, 290–294.

Ponnam, S.P.G., Ramesha, K., Matalia, J., Tejwani, S., Ramamurthy, B., Kannabiran, C., 2013. Mutational screening of Indian families with hereditary congenital cataract. Mol Vis 19, 1141–1148.

Prokudin, I., Simons, C., Grigg, J.R., Storen, R., Kumar, V., Phua, Z.Y., Smith, J., Flaherty, M., Davila, S., Jamieson, R.V., 2014. Exome sequencing in developmental eye disease leads to identification of causal variants in GJA8, CRYGC, PAX6 and CYP1B1. Eur. J. Hum. Genet. 22, 907–915. https://doi.org/10.1038/ejhg.2013.268

Quang, D., Chen, Y., Xie, X., 2015. DANN: a deep learning approach for annotating the pathogenicity of genetic variants. Bioinformatics 31, 761–763. https://doi.org/10.1093/bioinformatics/btu703

Ragge, N., Isidor, B., Bitoun, P., Odent, S., Giurgea, I., Cogné, B., Deb, W., Vincent, M., Le Gall, J., Morton, J., Lim, D., Le Meur, G., Zazo Seco, C., Zafeiropoulou, D., Bax, D., Zwijnenburg, P., Arteche, A., Swafiri, S.T., Cleaver, R., McEntagart, M., Kini, U., Newman, W., Ayuso, C., Corton, M., Herenger, Y., Jeanne, M., Calvas, P., Chassaing, N., DDD Study, 2019. Expanding the phenotype of the X-linked BCOR microphthalmia syndromes. Hum Genet 138, 1051–1069. https://doi.org/10.1007/s00439-018-1896-x

Ragge, N.K., Subak-Sharpe, I.D., Collin, J.R.O., 2007. A practical guide to the management of anophthalmia and microphthalmia. Eye (Lond) 21, 1290–1300. https://doi.org/10.1038/sj.eye.6702858

Rauf, B., Irum, B., Khan, S.Y., Kabir, F., Naeem, M.A., Riazuddin, S., Ayyagari, R., Riazuddin, S.A., 2020. Novel mutations in LTBP2 identified in familial cases of primary congenital glaucoma. Mol Vis 26, 14–25.

Reis, L.M., Semina, E.V., 2011. Genetics of anterior segment dysgenesis disorders. Curr Opin Ophthalmol 22, 314–324. https://doi.org/10.1097/ICU.0b013e328349412b

Rentzsch, P., Witten, D., Cooper, G.M., Shendure, J., Kircher, M., 2019. CADD: predicting the deleteriousness of variants throughout the human genome. Nucleic Acids Res 47, D886–D894. https://doi.org/10.1093/nar/gky1016

Reva, B., Antipin, Y., Sander, C., 2011. Predicting the functional impact of protein mutations: application to cancer genomics. Nucleic Acids Res 39, e118. https://doi.org/10.1093/nar/gkr407

Reza, H.M., Yasuda, K., 2004. Roles of maf family proteins in lens development. Developmental Dynamics 229, 440–448. https://doi.org/10.1002/dvdy.10467

Ricard-Blum, S., 2011. The Collagen Family. Cold Spring Harb Perspect Biol 3. https://doi.org/10.1101/cshperspect.a004978

Richards, S., Aziz, N., Bale, S., Bick, D., Das, S., Gastier-Foster, J., Grody, W.W., Hegde, M., Lyon, E., Spector, E., Voelkerding, K., Rehm, H.L., ACMG Laboratory Quality Assurance Committee, 2015. Standards and guidelines for the interpretation of sequence variants: a joint consensus recommendation of the American College of Medical Genetics and Genomics and the Association for Molecular Pathology. Genet. Med. 17, 405–424. https://doi.org/10.1038/gim.2015.30

Risteli, J., Bächinger, H.P., Engel, J., Furthmayr, H., Timpl, R., 1980. 7-S collagen: characterization of an unusual basement membrane structure. Eur. J. Biochem. 108, 239–250.

Roberts, L., Goliath, R., Rebello, G., Bardien, S., September, A.V., Bartmann, L., Loubser, F., Greenberg, L.J., Ramesar, R.S., 2016. Inherited retinal disorders in South Africa and the clinical impact of evolving technologies. South African Medical Journal 106, S33. https://doi.org/10.7196/SAMJ.2016.v106i6.10988

Rong, P., Wang, X., Niesman, I., Wu, Y., Benedetti, L.E., Dunia, I., Levy, E., Gong, X., 2002. Disruption of Gja8 (α8 connexin) in mice leads to microphthalmia associated with retardation of lens growth and lens fiber maturation. Development 129, 167–174. https://doi.org/10.1242/dev.129.1.167

Ronsein, G.E., Winterbourn, C.C., Di Mascio, P., Kettle, A.J., 2014. Cross-linking methionine and amine residues with reactive halogen species. Free Radical Biology and Medicine 70, 278–287. https://doi.org/10.1016/j.freeradbiomed.2014.01.023

Rozario, T., DeSimone, D.W., 2010. The extracellular matrix in development and morphogenesis: a dynamic view. Dev. Biol. 341, 126–140. https://doi.org/10.1016/j.ydbio.2009.10.026

Rubio-Gozalbo, M.E., Derks, B., Das, A.M., Meyer, U., Möslinger, D., Couce, M.L., Empain, A., Ficicioglu, C., Juliá Palacios, N., De Los Santos De Pelegrin, M.M., Rivera, I.A., Scholl-Bürgi, S., Bosch, A.M., Cassiman, D., Demirbas, D., Gautschi, M., Knerr, I., Labrune, P., Skouma, A., Verloo, P., Wortmann, S.B., Treacy, E.P., Timson, D.J., Berry, G.T., 2021. Galactokinase deficiency: lessons from the GalNet registry. Genet Med 23, 202–210. https://doi.org/10.1038/s41436-020-00942-9

Ruf, J., Carayon, P., 2006. Structural and functional aspects of thyroid peroxidase. Arch Biochem Biophys 445, 269–277. https://doi.org/10.1016/j.abb.2005.06.023

Sadler, J.E., 2009. von Willebrand factor assembly and secretion. J Thromb Haemost 7 Suppl 1, 24–27. https://doi.org/10.1111/j.1538-7836.2009.03375.x

Saeger, B.M., Suhm, M., Neubüser, A., 2011. Ephrin/ephrin receptor expression during early stages of mouse inner ear development. Developmental Dynamics 240, 1578–1585. https://doi.org/10.1002/dvdy.22632

Saito, K., Yonezawa, T., Minaguchi, J., Kurosaki, M., Suetsugu, S., Nakajima, A., Nomoto, H., Morizane, Y., Sado, Y., Sugimoto, M., Kusachi, S., Ninomiya, Y., 2011. Distribution of α(IV) collagen chains in the ocular anterior segments of adult mice. Connective Tissue Research 52, 147–156. https://doi.org/10.3109/03008207.2010.492062

Sarfarazi, M., Stoilov, I., Schenkman, J.B., 2003. Genetics and biochemistry of primary congenital glaucoma. Ophthalmol Clin North Am 16, 543–554, vi.

Schedl, A., Ross, A., Lee, M., Engelkamp, D., Rashbass, P., van Heyningen, V., Hastie, N.D., 1996. Influence of PAX6 gene dosage on development: overexpression causes severe eye abnormalities. Cell 86, 71–82.

Schneider, A., Bardakjian, T., Reis, L.M., Tyler, R.C., Semina, E.V., 2009. Novel SOX2 mutations and genotype-phenotype correlation in anophthalmia and microphthalmia. Am. J. Med. Genet. A 149A, 2706–2715. https://doi.org/10.1002/ajmg.a.33098

Semina, E.V., Brownell, I., Mintz-Hittner, H.A., Murray, J.C., Jamrich, M., 2001. Mutations in the human forkhead transcription factor FOXE3 associated with anterior segment ocular dysgenesis and cataracts. Hum. Mol. Genet. 10, 231–236.

Seo, S., Kume, T., 2006. Forkhead transcription factors, Foxc1 and Foxc2, are required for the morphogenesis of the cardiac outflow tract. Dev Biol 296, 421–436. https://doi.org/10.1016/j.ydbio.2006.06.012

Sevcnikar, B., Schaffner, I., Chuang, C.Y., Gamon, L., Paumann-Page, M., Hofbauer, S., Davies, M.J., Furtmüller, P.G., Obinger, C., 2020. The leucine-rich repeat domain of human peroxidasin 1 promotes binding to laminin in basement membranes. Archives of Biochemistry and Biophysics 689, 108443. https://doi.org/10.1016/j.abb.2020.108443

Shaham, O., Menuchin, Y., Farhy, C., Ashery-Padan, R., 2012. Pax6: A multi-level regulator of ocular development. Progress in Retinal and Eye Research 31, 351–376. https://doi.org/10.1016/j.preteyeres.2012.04.002

Shakes, D.C., Miller, D.M., Nonet, M.L., 2012. Chapter 2 - Immunofluorescence Microscopy, in: Rothman, J.H., Singson, A. (Eds.), Methods in Cell Biology, Caenorhabditis Elegans: Cell Biology and Physiology. Academic Press, pp. 35–66. https://doi.org/10.1016/B978-0-12-394620-1.00002-3

Shi, R., Hu, C., Yuan, Q., Yang, T., Peng, J., Li, Y., Bai, Y., Cao, Z., Cheng, G., Zhang, G., 2011. Involvement of vascular peroxidase 1 in angiotensin II-induced vascular smooth muscle cell proliferation. Cardiovasc. Res. 91, 27–36. https://doi.org/10.1093/cvr/cvr042

Shi, Y., Jones, W., Beatty, W., Tan, Q., Mecham, R.P., Kumra, H., Reinhardt, D.P., Gibson, M.A., Reilly, M.A., Rodriguez, J., Bassnett, S., 2021. Latent-transforming growth factor beta-binding protein-2 (LTBP-2) is required for longevity but not for development of zonular fibers. Matrix Biology 95, 15–31. https://doi.org/10.1016/j.matbio.2020.10.002

Shiels, A., Hejtmancik, J.F., 2015. Chapter Twelve - Molecular Genetics of Cataract, in: Hejtmancik, J.F., Nickerson, J.M. (Eds.), Progress in Molecular Biology and Translational Science, Molecular Biology of Eye Disease. Academic Press, pp. 203–218. https://doi.org/10.1016/bs.pmbts.2015.05.004

Shihab, H.A., Gough, J., Cooper, D.N., Stenson, P.D., Barker, G.L.A., Edwards, K.J., Day, I.N.M., Gaunt, T.R., 2013. Predicting the functional, molecular, and phenotypic consequences of amino acid substitutions using hidden Markov models. Hum Mutat 34, 57–65. https://doi.org/10.1002/humu.22225

Shipley, J.M., Mecham, R.P., Maus, E., Bonadio, J., Rosenbloom, J., McCarthy, R.T., Baumann, M.L., Frankfater, C., Segade, F., Shapiro, S.D., 2000. Developmental Expression of Latent Transforming Growth Factor β Binding Protein 2 and Its Requirement Early in Mouse Development. Mol Cell Biol 20, 4879–4887.

Shoulders, M.D., Raines, R.T., 2009. Collagen structure and stability. Annu. Rev. Biochem. 78, 929–958. https://doi.org/10.1146/annurev.biochem.77.032207.120833

Shukla, S., Mishra, R., 2018. Level of hydrogen peroxide affects expression and sub-cellular localization of Pax6. Mol Biol Rep 45, 533–540. https://doi.org/10.1007/s11033-018-4190-z

Singh, S., Chao, L.Y., Mishra, R., Davies, J., Saunders, G.F., 2001. Missense mutation at the C-terminus of PAX6 negatively modulates homeodomain function. Human Molecular Genetics 10, 911–918. https://doi.org/10.1093/hmg/10.9.911

Sinn, R., Wittbrodt, J., 2013. An eye on eye development. Mech. Dev. 130, 347–358. https://doi.org/10.1016/j.mod.2013.05.001

Sitole, B.N., Mavri-Damelin, D., 2018. Peroxidasin is regulated by the epithelial-mesenchymal transition master transcription factor Snai1. Gene 646, 195–202. https://doi.org/10.1016/j.gene.2018.01.011

Skalicky, S.E., White, A.J.R., Grigg, J.R., Martin, F., Smith, J., Jones, M., Donaldson, C., Smith, J.E.H., Flaherty, M., Jamieson, R.V., 2013. Microphthalmia, Anophthalmia, and Coloboma and Associated Ocular and Systemic Features: Understanding the Spectrum. JAMA Ophthalmol 131, 1517–1524. https://doi.org/10.1001/jamaophthalmol.2013.5305

Slavotinek, A.M., Chao, R., Vacik, T., Yahyavi, M., Abouzeid, H., Bardakjian, T., Schneider, A., Shaw, G., Sherr, E.H., Lemke, G., Youssef, M., Schorderet, D.F., 2012. VAX1 mutation associated with microphthalmia, corpus callosum agenesis, and orofacial clefting: the first description of a VAX1 phenotype in humans. Hum. Mutat. 33, 364–368. https://doi.org/10.1002/humu.21658

Slavotinek, A.M., Garcia, S.T., Chandratillake, G., Bardakjian, T., Ullah, E., Wu, D., Umeda, K., Lao, R., Tang, P.L.-F., Wan, E., Madireddy, L., Lyalina, S., Mendelsohn, B.A., Dugan, S., Tirch, J., Tischler, R., Harris, J., Clark, M.J., Chervitz, S., Patwardhan, A., West, J.M., Ursell, P., de Alba Campomanes, A., Schneider, A., Kwok, P.-Y., Baranzini, S., Chen, R.O., 2015. Exome sequencing in 32 patients with anophthalmia/microphthalmia and developmental eye defects. Clin. Genet. 88, 468–473. https://doi.org/10.1111/cge.12543

Söder, S., Pöschl, E., 2004. The NC1 domain of human collagen IV is necessary to initiate triple helix formation. Biochemical and Biophysical Research Communications 325, 276–280. https://doi.org/10.1016/j.bbrc.2004.10.034

Son, A.I., Cooper, M.A., Sheleg, M., Sun, Y., Kleiman, N.J., Zhou, R., 2013. Further analysis of the lens of ephrin-A5−/− mice: development of postnatal defects. Mol Vis 19, 254–266.

Soudi, M., Paumann-Page, M., Delporte, C., Pirker, K.F., Bellei, M., Edenhofer, E., Stadlmayr, G., Battistuzzi, G., Boudjeltia, K.Z., Furtmüller, P.G., Van Antwerpen, P., Obinger, C., 2015. Multidomain Human Peroxidasin 1 Is a Highly Glycosylated

and Stable Homotrimeric High Spin Ferric Peroxidase. J Biol Chem 290, 10876–10890. https://doi.org/10.1074/jbc.M114.632273

Soudi, M., Zamocky, M., Jakopitsch, C., Furtmüller, P.G., Obinger, C., 2012. Molecular Evolution, Structure, and Function of Peroxidasins. Chem Biodivers 9, 1776–1793. https://doi.org/10.1002/cbdv.201100438

Sowden, J.C., 2007. Molecular and developmental mechanisms of anterior segment dysgenesis. Eye (Lond) 21, 1310–1318. https://doi.org/10.1038/sj.eye.6702852

Stahl, E.D., 2014. Anterior segment dysgenesis. Int Ophthalmol Clin 54, 95–104. https://doi.org/10.1097/IIO.0000000000000031

Strobel, N.A., Fassett, R.G., Marsh, S.A., Coombes, J.S., 2011. Oxidative stress biomarkers as predictors of cardiovascular disease. International Journal of Cardiology 147, 191–201. https://doi.org/10.1016/j.ijcard.2010.08.008

Suzumori, N., Kaname, T., Muramatsu, Y., Yanagi, K., Kumagai, K., Mizuno, S., Naritomi, K., Saitoh, S., Sugiura-Ogasawara, M., 2013. Prenatal diagnosis of X-linked recessive Lenz microphthalmia syndrome. Journal of Obstetrics and Gynaecology Research 39, 1545–1547. https://doi.org/10.1111/jog.12081

Tabasaran, J., Schuhmann, M., Ebinger, M., Honegger, J., Renovanz, M., Schittenhelm, J., 2021. PAX6 is frequently expressed in ependymal tumours and associated with prognostic relevant subgroups. J Clin Pathol jclinpath-2021-207526. https://doi.org/10.1136/jclinpath-2021-207526

Takamiya, M., Stegmaier, J., Kobitski, A.Y., Schott, B., Weger, B.D., Margariti, D., Cereceda Delgado, A.R., Gourain, V., Scherr, T., Yang, L., Sorge, S., Otte, J.C., Hartmann, V., van Wezel, J., Stotzka, R., Reinhard, T., Schlunck, G., Dickmeis, T., Rastegar, S., Mikut, R., Nienhaus, G.U., Strähle, U., 2020. Pax6 organizes the anterior eye segment by guiding two distinct neural crest waves. PLoS Genet 16, e1008774. https://doi.org/10.1371/journal.pgen.1008774

Tanwar, M., Dada, T., Sihota, R., Dada, R., 2009. Identification of four novel cytochrome P4501B1 mutations (p.I94X, p.H279D, p.Q340H, and p.K433K) in primary congenital glaucoma patients. Mol. Vis. 15, 2926–2937.

Taranova, O.V., Magness, S.T., Fagan, B.M., Wu, Y., Surzenko, N., Hutton, S.R., Pevny, L.H., 2006. SOX2 is a dose-dependent regulator of retinal neural progenitor competence. Genes Dev 20, 1187–1202. https://doi.org/10.1101/gad.1407906

Tassi, E., Al-Attar, A., Aigner, A., Swift, M.R., McDonnell, K., Karavanov, A., Wellstein, A., 2001. Enhancement of Fibroblast Growth Factor (FGF) Activity by an FGF-binding Protein*. Journal of Biological Chemistry 276, 40247–40253. https://doi.org/10.1074/jbc.M104933200

Tauber, S., Jais, A., Jeitler, M., Haider, S., Husa, J., Lindroos, J., Knöfler, M., Mayerhofer, M., Pehamberger, H., Wagner, O., Bilban, M., 2010. Transcriptome analysis of human cancer reveals a functional role of Heme Oxygenase-1 in tumor cell adhesion. Mol Cancer 9, 200. https://doi.org/10.1186/1476-4598-9-200

Taurog, A., Dorris, M.L., Doerge, D.R., 1996. Mechanism of Simultaneous Iodination and Coupling Catalyzed by Thyroid Peroxidase. Archives of Biochemistry and Biophysics 330, 24–32. https://doi.org/10.1006/abbi.1996.0222

Thanikachalam, S., Hodapp, E., Chang, T.C., Morel Swols, D., Cengiz, F.B., Guo, S., Zafeer, M.F., Seyhan, S., Bademci, G., Scott, W.K., Grajewski, A., Tekin, M., 2020. Spectrum of Genetic Variants Associated with Anterior Segment Dysgenesis in South Florida. Genes (Basel) 11, 350. https://doi.org/10.3390/genes11040350

Thorvaldsdóttir, H., Robinson, J.T., Mesirov, J.P., 2013. Integrative Genomics Viewer (IGV): high-performance genomics data visualization and exploration. Briefings in Bioinformatics 14, 178–192. https://doi.org/10.1093/bib/bbs017

Tindall, A.J., Pownall, M.E., Morris, I.D., Isaacs, H.V., 2005. Xenopus tropicalis peroxidasin gene is expressed within the developing neural tube and pronephric kidney. Dev. Dyn. 232, 377–384. https://doi.org/10.1002/dvdy.20226

Tümer, Z., Bach-Holm, D., 2009. Axenfeld–Rieger syndrome and spectrum of PITX2 and FOXC1 mutations. Eur J Hum Genet 17, 1527–1539. https://doi.org/10.1038/ejhg.2009.93

Ullah, E., Nadeem Saqib, M.A., Sajid, S., Shah, N., Zubair, M., Khan, M.A., Ahmed, I., Ali, G., Dutta, A.K., Danda, S., Lao, R., Ling-Fung Tang, P., Kwok, P.-

Y., Ansar, M., Slavotinek, A., 2016. Genetic analysis of consanguineous families presenting with congenital ocular defects. Exp. Eye Res. 146, 163–171. https://doi.org/10.1016/j.exer.2016.03.014

van der Veen, B.S., de Winther, M.P.J., Heeringa, P., 2009. Myeloperoxidase: molecular mechanisms of action and their relevance to human health and disease. Antioxid. Redox Signal. 11, 2899–2937. https://doi.org/10.1089/ars.2009.2538

Vanacore, R., Ham, A.-J.L., Voehler, M., Sanders, C.R., Conrads, T.P., Veenstra, T.D., Sharpless, K.B., Dawson, P.E., Hudson, B.G., 2009. A sulfilimine bond identified in collagen IV. Science 325, 1230–1234. https://doi.org/10.1126/science.1176811

Vasiliou, V., Gonzalez, F.J., 2008. Role of CYP1B1 in glaucoma. Annu Rev Pharmacol Toxicol 48, 333–358. https://doi.org/10.1146/annurev.pharmtox.48.061807.154729

Vehviläinen, P., Hyytiäinen, M., Keski-Oja, J., 2009a. Matrix association of latent TGF-beta binding protein-2 (LTBP-2) is dependent on fibrillin-1. Journal of Cellular Physiology 221, 586–593. https://doi.org/10.1002/jcp.21888

Verma, A.S., Fitzpatrick, D.R., 2007. Anophthalmia and microphthalmia. Orphanet J Rare Dis 2, 47. https://doi.org/10.1186/1750-1172-2-47

Verwey, V.F., Mahomed, S., 2020. Burden of eye conditions at a specialised eye hospital in KwaZulu-Natal, South Africa. African Vision and Eye Health 79, 5. https://doi.org/10.4102/aveh.v79i1.518

Vincent, A., Billingsley, G., Priston, M., Williams-Lyn, D., Sutherland, J., Glaser, T., Oliver, E., Walter, M., Heathcote, G., Levin, A., Heon, E., 2001. Phenotypic heterogeneity of CYP1B1: mutations in a patient with Peters' anomaly. J Med Genet 38, 324–326. https://doi.org/10.1136/jmg.38.5.324

von Castelmur, E., Marino, M., Svergun, D.I., Kreplak, L., Ucurum-Fotiadis, Z., Konarev, P.V., Urzhumtsev, A., Labeit, D., Labeit, S., Mayans, O., 2008. A regular pattern of Ig super-motifs defines segmental flexibility as the elastic mechanism of

the titin chain. Proc Natl Acad Sci U S A 105, 1186–1191. https://doi.org/10.1073/pnas.0707163105

Vranka, J.A., Kelley, M.J., Acott, T.S., Keller, K.E., 2015. Extracellular matrix in the trabecular meshwork: Intraocular pressure regulation and dysregulation in glaucoma. Exp Eye Res 133, 112–125. https://doi.org/10.1016/j.exer.2014.07.014

Walter, M.A., 2003. PITs and FOXes in ocular genetics: the Cogan lecture. Invest Ophthalmol Vis Sci 44, 1402–1405. https://doi.org/10.1167/iovs.02-0618

Wang, H., Zhang, T., Wu, D., Zhang, J., 2013. A novel beaded filament structural protein 1 (BFSP1) gene mutation associated with autosomal dominant congenital cataract in a Chinese family. Mol Vis 19, 2590–2595.

Wang, M., Zhao, J., Zhang, H., Li, K., Niu, L., Wang, Y., Zheng, Y., 2020. Potential Protective and Therapeutic Roles of the Nrf2 Pathway in Ocular Diseases: An Update. Oxid Med Cell Longev 2020, 9410952. https://doi.org/10.1155/2020/9410952

Wang, W.H., McNatt, L.G., Shepard, A.R., Jacobson, N., Nishimura, D.Y., Stone, E.M., Sheffield, V.C., Clark, A.F., 2001. Optimal procedure for extracting RNA from human ocular tissues and expression profiling of the congenital glaucoma gene FOXC1 using quantitative RT-PCR. Mol Vis 7, 89–94.

Wang, X., Gregory-Evans, C.Y., 2012. Identification Of The Downstream Targets Of Pax6 In The Developing Iris Relevant To Aniridia. Invest. Ophthalmol. Vis. Sci. 53, 4932–4932.

Wang, X., Shan, X., Gregory-Evans, C.Y., 2017. A mouse model of aniridia reveals the in vivo downstream targets of Pax6 driving iris and ciliary body development in the eye. Biochimica et Biophysica Acta (BBA) - Molecular Basis of Disease 1863, 60–67. https://doi.org/10.1016/j.bbadis.2016.10.018

Weisschuh, N., Wolf, C., Wissinger, B., Gramer, E., 2008. A novel mutation in the FOXC1 gene in a family with Axenfeld–Rieger syndrome and Peters' anomaly. Clinical Genetics 74, 476–480. https://doi.org/10.1111/j.1399-0004.2008.01025.x

Wen, J., Hu, Q., Li, M., Wang, S., Zhang, L., Chen, Y., Li, L., 2008. Pax6 directly modulate Sox2 expression in the neural progenitor cells. Neuroreport 19, 413–417. https://doi.org/10.1097/WNR.0b013e3282f64377

Whittaker, C.A., Bergeron, K.-F., Whittle, J., Brandhorst, B.P., Burke, R.D., Hynes, R.O., 2006. The echinoderm adhesome. Dev. Biol. 300, 252–266. https://doi.org/10.1016/j.ydbio.2006.07.044

Willoughby, C.E., Arab, Sara, Gandhi, R., Zeinali, S., Arab, Seddigheh, Luk, D., Billingsley, G., Munier, F.L., Héon, E., 2003. A novel GJA8 mutation in an Iranian family with progressive autosomal dominant congenital nuclear cataract. Journal of Medical Genetics 40, e124–e124. https://doi.org/10.1136/jmg.40.11.e124

Winterbourn, C.C., 2008. Reconciling the chemistry and biology of reactive oxygen species. Nat. Chem. Biol. 4, 278–286. https://doi.org/10.1038/nchembio.85

Wu, Z., Meng, D., Fang, C., Li, J., Zheng, X., Lin, J., Zeng, H., Lv, S., Zhang, Z., Luan, B., Zhong, Z., Chen, J., 2019. PITX3 mutations associated with autosomal dominant congenital cataract in the Chinese population. Molecular Medicine Reports 19, 3123–3131. https://doi.org/10.3892/mmr.2019.9989

Wurm, F.M., 2004. Production of recombinant protein therapeutics in cultivated mammalian cells. Nat Biotechnol 22, 1393–1398. https://doi.org/10.1038/nbt1026

Wynn, T.A., 2007. Common and unique mechanisms regulate fibrosis in various fibroproliferative diseases. J Clin Invest 117, 524–529. https://doi.org/10.1172/JCI31487

Xia, C., Chang, B., DeRosa, A.M., Cheng, C., White, T.W., Gong, X., 2012. Cataracts and Microphthalmia Caused by a Gja8 Mutation in Extracellular Loop 2. PLoS One 7, e52894. https://doi.org/10.1371/journal.pone.0052894

Xu, H., Tian, W., Lindsley, J.N., Oyama, T.T., Capasso, J.M., Rivard, C.J., Cohen, H.T., Bagnasco, S.M., Anderson, S., Cohen, D.M., 2005. EphA2: expression in the renal medulla and regulation by hypertonicity and urea stress in vitro and in vivo. American Journal of Physiology-Renal Physiology 288, F855–F866. https://doi.org/10.1152/ajprenal.00347.2004

Yan, X., Sabrautzki, S., Horsch, M., Fuchs, H., Gailus-Durner, V., Beckers, J., Hrabě de Angelis, M., Graw, J., 2014. Peroxidasin is essential for eye development in the mouse. Hum. Mol. Genet. 23, 5597–5614. https://doi.org/10.1093/hmg/ddu274

Yang, L.L., Lambert, S.R., 2001. Peters' anomaly. A synopsis of surgical management and visual outcome. Ophthalmol Clin North Am 14, 467–477.

Yang, Y., Zhang, L., Li, S., Zhu, X., Sundaresan, P., 2017. Candidate Gene Analysis Identifies Mutations in CYP1B1 and LTBP2 in Indian Families with Primary Congenital Glaucoma. Genetic Testing and Molecular Biomarkers 21, 252–258. https://doi.org/10.1089/gtmb.2016.0203

Yokoi, T., Nishina, S., Fukami, M., Ogata, T., Hosono, K., Hotta, Y., Azuma, N., 2016. Genotype–phenotype correlation of *PAX6* gene mutations in aniridia. Human Genome Variation 3, 15052. https://doi.org/10.1038/hgv.2015.52

Yu, Y., Wu, M., Chen, X., Zhu, Y., Gong, X., Yao, K., 2016. Identification and functional analysis of two novel connexin 50 mutations associated with autosome dominant congenital cataracts. Sci Rep 6, 26551. https://doi.org/10.1038/srep26551

Yun, S., Saijoh, Y., Hirokawa, K.E., Kopinke, D., Murtaugh, L.C., Monuki, E.S., Levine, E.M., 2009. Lhx2 links the intrinsic and extrinsic factors that control optic cup formation. Development 136, 3895–3906. https://doi.org/10.1242/dev.041202

Yurchenco, P.D., 2011. Basement membranes: cell scaffoldings and signaling platforms. Cold Spring Harb Perspect Biol 3. https://doi.org/10.1101/cshperspect.a004911

Zámocký, M., Hofbauer, S., Schaffner, I., Gasselhuber, B., Nicolussi, A., Soudi, M., Pirker, K.F., Furtmüller, P.G., Obinger, C., 2015. Independent evolution of four heme peroxidase superfamilies. Archives of Biochemistry and Biophysics, A protein fold with multiple functions: chlorite dismutase, HemQ and DyP-type peroxidase 574, 108–119. https://doi.org/10.1016/j.abb.2014.12.025

Zhang, J., Upadhya, D., Lu, L., Reneker, L.W., 2015. Fibroblast Growth Factor Receptor 2 (FGFR2) Is Required for Corneal Epithelial Cell Proliferation and

Differentiation during Embryonic Development. PLOS ONE 10, e0117089. https://doi.org/10.1371/journal.pone.0117089

Zhang, T., Hua, R., Xiao, W., Burdon, K.P., Bhattacharya, S.S., Craig, J.E., Shang, D., Zhao, X., Mackey, D.A., Moore, A.T., Luo, Y., Zhang, J., Zhang, X., 2009. Mutations of the EPHA2 receptor tyrosine kinase gene cause autosomal dominant congenital cataract. Human Mutation 30, E603–E611. https://doi.org/10.1002/humu.20995

Zhang, X., Friedman, A., Heaney, S., Purcell, P., Maas, R.L., 2002. Meis homeoproteins directly regulate Pax6 during vertebrate lens morphogenesis. Genes Dev. 16, 2097–2107. https://doi.org/10.1101/gad.1007602

Zhang, Y.-S., He, L., Liu, B., Li, N.-S., Luo, X.-J., Hu, C.-P., Ma, Q.-L., Zhang, G.-G., Li, Y.-J., Peng, J., 2012. A novel pathway of NADPH oxidase/vascular peroxidase 1 in mediating oxidative injury following ischemia-reperfusion. Basic Res. Cardiol. 107, 266. https://doi.org/10.1007/s00395-012-0266-4

Zhu, X., Dai, F.-R., Wang, J., Zhang, Yu, Tan, Z.-P., Zhang, Yi, 2015. Novel BCOR mutation in a boy with Lenz microphthalmia/oculo-facio-cardio-dental (OFCD) syndrome. Gene 571, 142–144. https://doi.org/10.1016/j.gene.2015.07.061

Zhuan, B., Yu, Y., Yang, Z., Zhao, X., Li, P., 2017. Mechanisms of oxidative stress effects of the NADPH oxidase-ROS-NF-κB transduction pathway and VPO1 on patients with chronic obstructive pulmonary disease combined with pulmonary hypertension. Eur Rev Med Pharmacol Sci 21, 3459–3464.

Zou, C., Levine, E.M., 2012. Vsx2 Controls Eye Organogenesis and Retinal Progenitor Identity Via Homeodomain and Non-Homeodomain Residues Required for High Affinity DNA Binding. PLOS Genetics 8, e1002924. https://doi.org/10.1371/journal.pgen.1002924

Appendices

Appendix A

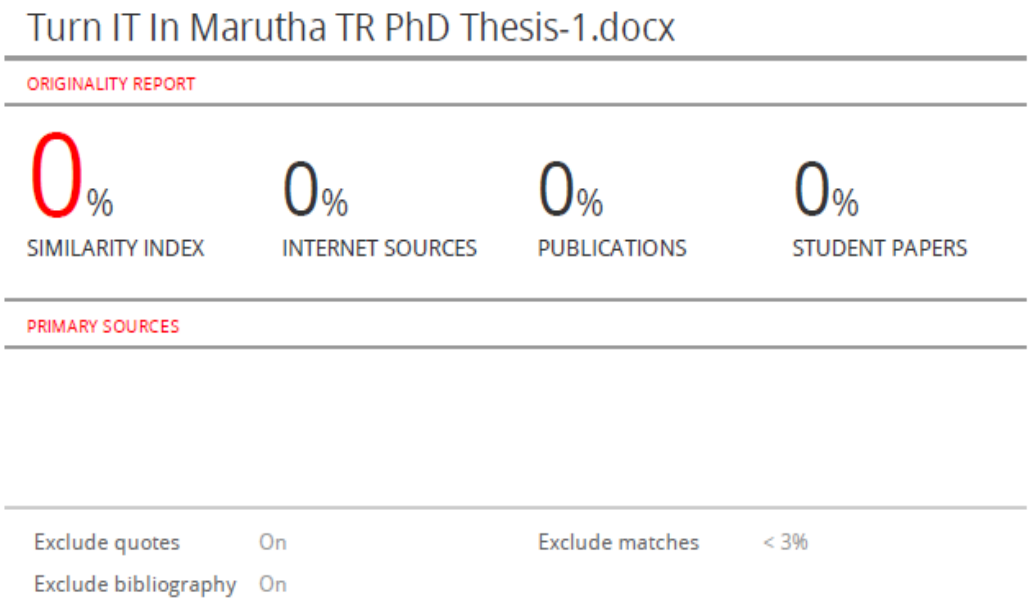

Turn IT In Marutha TR PhD Thesis-1.docx

ORIGINALITY REPORT

0%	0%	0%	0%
SIMILARITY INDEX	INTERNET SOURCES	PUBLICATIONS	STUDENT PAPERS

PRIMARY SOURCES

Exclude quotes	On	Exclude matches	< 3%
Exclude bibliography	On		

Appendix B

Criteria for Classifying Pathogenic Variants

Very strong evidence of pathogenicity

PVS1 = Null variant (nonsense, frameshift, canonical +/−1 or 2 splice sites, initiation codon, single or multi-exon deletion) in a gene where loss of function (LOF) is a known mechanism of disease

Caveats:

- Beware of genes where LOF is not a known disease mechanism (e.g GFAP, MYH7)
- Use caution interpreting LOF variants at the extreme 3' end of a gene
- Use caution with splice variants that are predicted to lead to exon skipping but leave the remainder of the protein intact
- Use caution in the presence of multiple transcripts

Strong evidence of pathogenicity

PS1 = Same amino acid change as a previously established pathogenic variant regardless of nucleotide change

Example: Val->Leu caused by either G>C or G>T in the same codon

Caveat: Beware of changes that impact splicing rather than at the amino acid/protein level

PS2 = De novo (both maternity and paternity confirmed) in a patient with the disease and no family history

Note: Confirmation of paternity only is insufficient. Egg donation, surrogate motherhood, errors in embryo transfer, etc. can contribute to non-maternity.

PS3 = Well-established in vitro or in vivo functional studies supportive of a damaging effect on the gene or gene product

Note: Functional studies that have been validated and shown to be reproducible and robust in a clinical diagnostic laboratory setting are considered the most well-established

PS4 = The prevalence of the variant in affected individuals is significantly increased compared to the prevalence in controls

Note 1: Relative risk (RR) or odds ratio (OR), as obtained from case-control studies, is >5.0 and the confidence interval around the estimate of RR or OR does not include 1.0. See manuscript for detailed guidance.

Note 2: In instances of very rare variants where case-control studies may not reach statistical significance, the prior observation of the variant in multiple unrelated patients with the same phenotype, and its absence in controls, may be used as moderate level of evidence.

Moderate evidence of pathogenicity

PM1 = Located in a mutational hot spot and/or critical and well-established functional domain (e.g active site of an enzyme) without benign variation

PM2 = Absent from controls (or at extremely low frequency if recessive) (see Table 6) in Exome Sequencing Project, 1000 Genomes or ExAC

Caveat: Population data for indels may be poorly called by next generation sequencing

PM3 = For recessive disorders, detected in trans with a pathogenic variant

Note: This requires testing of parents (or offspring) to determine phase

PM4 = Protein length changes due to in-frame deletions/insertions in a non-repeat region or stop-loss variants

PM5 = Novel missense change at an amino acid residue where a different missense change determined to be pathogenic has been seen before

Example: Arg156His is pathogenic; now you observe Arg156Cys

Caveat: Beware of changes that impact splicing rather than at the amino acid/protein level

PM6 = Assumed de novo, but without confirmation of paternity and maternity

Supporting evidence of pathogenicity

PP1 = Co-segregation with disease in multiple affected family members in a gene definitively known to cause the disease.

Note: May be used as stronger evidence with increasing segregation data PP2 Missense variant in a gene that has a low rate of benign missense variation and where missense variants are a common mechanism of disease.

PP3 = Multiple lines of computational evidence support a deleterious effect on the gene or gene product (conservation, evolutionary, splicing impact, etc)

Caveat: As many in silico algorithms use the same or very similar input for their predictions, each algorithm should not be counted as an independent criterion. PP3 can be used only once in any evaluation of a variant.

PP4 = Patient's phenotype or family history is highly specific for a disease with a single genetic etiology

PP5 = Reputable source recently reports variant as pathogenic but the evidence is not available to the laboratory to perform an independent evaluation

Criteria for Classifying Benign Variants

Stand-Alone evidence of benign impact

BA1 = Allele frequency is above 5% in Exome Sequencing Project, 1000 Genomes, or ExAC

Strong evidence of benign impact

BS1 = Allele frequency is greater than expected for disorder (see table 6)

BS2 = Observed in a healthy adult individual for a recessive (homozygous), dominant (heterozygous), or X-linked (hemizygous) disorder with full penetrance expected at an early age

BS3 = Well-established in vitro or in vivo functional studies shows no damaging effect on protein function or splicing

BS4 = Lack of segregation in affected members of a family

Caveat: The presence of phenocopies for common phenotypes (i.e. cancer, epilepsy) can mimic lack of segregation among affected individuals. Also, families may have more than one pathogenic variant contributing to an autosomal dominant disorder, further confounding an apparent lack of segregation.

Supporting evidence of benign impact

BP1 = Missense variant in a gene for which primarily truncating variants are known to cause disease

BP2 = Observed in trans with a pathogenic variant for a fully penetrant dominant gene/disorder; or observed in cis with a pathogenic variant in any inheritance pattern

BP3 = In-frame deletions/insertions in a repetitive region without a known function

BP4 = Multiple lines of computational evidence suggest no impact on gene or gene product (conservation, evolutionary, splicing impact, etc)

Caveat: As many in silico algorithms use the same or very similar input for their predictions, each algorithm cannot be counted as an independent criterion. BP4 can be used only once in any evaluation of a variant.

BP5 = Variant found in a case with an alternate molecular basis for disease

BP6 = Reputable source recently reports variant as benign but the evidence is not available to the laboratory to perform an independent evaluation

BP7 = A synonymous (silent) variant for which splicing prediction algorithms predict no impact to the splice consensus sequence nor the creation of a new splice site AND the nucleotide is not highly conserved

Appendix C

Recipes of buffers and solutions used in gene regulation experiments.

Buffer/ solution	**Recipe**
1X PBS	137 mM NaCl, 2.7 mM KCl, 8.1 mM $Na_2HPO_4 \cdot 12H_2O$, 1.8 mM KH_2PO_4, pH 7.2, autoclaved
Trypan Blue	0.2% (w/v) Trypan blue in 1X PBS, filter sterilised
1X RIPA buffer	50 mM Tris-HCl pH 8.0, 150 mM NaCl, 0.1% (w/v) SDS, 1% (v/v) Triton X-100, 0.5% (w/v) sodium deoxycholate, 1 mM PMSF, 10 μM leupeptin
Native lysis buffer	25 mM Tris-HCl pH 8.0, 75 mM NaCl, 0.5% (v/v) Triton X-100, 1 mM PMSF, 10 μM leupeptin
Coomassie blue dye	3 mM Coomassie Brilliant Blue G-250, 50% (v/v) methanol, 10% (v/v) glacial acetic acid
Destain solution	12% (v/v) Glacial acetic acid, 10% (v/v) methanol
Elution buffer	66% (v/v) Methanol, 1% (v/v) 25% (v/v) ammonia
4X protein loading buffer	240 mM Tris-HCl pH 6.8, 8% (w/v) SDS, 0.04% (w/v) bromophenol blue, 5% (v/v) β-mercaptoethanol, 40% (v/v) glycerol
SDS-PAGE Running Buffer	3.5 mM SDS, 192 mM glycine, 25 mM Tris, pH 8.8
Transfer buffer	192 mM Glycine, 25 mM Tris, 20% (v/v) methanol, pH 8.3
1X TBS/T	20 mM Tris-HCl pH 7.6, 137 mM NaCl, 0.1% (v/v) Tween-20
Blocking buffer	5% (w/v) Fat-free milk, 1X TBS/T
Developer	6.4 M Metol, 0.6 M sodium sulphite, 80 mM hydroquinone, 45 mM sodium carbonate, 34 mM potassium bromide
Fixer	0.8 M Sodium thiosulphate, 0.2 M sodium metasulphite
1X TAE	40 mM Tris-HCl pH 8, 0.11% (v/v) glacial acetic acid, 1 mM EDTA pH 8.0
6X DNA loading dye	30% (v/v) Glycerol, 3.7 mM bromophenol blue
IP buffer	20 mM Tris-HCl pH 8.0, 150 mM NaCl, 0.5% (v/v) Triton X-100, 1 mM PMSF, 10 μM leupeptin
ChIP IP buffer	20 mM Tris-HCl pH 8.0, 2 mM EDTA pH 8.0, 150 mM NaCl, 1% (v/v) Triton X-100, 1 mM PMSF, 10 μM leupeptin
ChIP wash buffer	20 mM Tris-HCl pH 8.0, 2 mM EDTA pH 8.0, 150 mM NaCl, 1% (v/v) Triton X-100, 0.1% (v/v) SDS
ChIP final wash buffer	20 mM Tris-HCl pH 8.0, 2 mM EDTA pH 8.0, 500 mM NaCl, 1% (v/v) Triton X-100, 0.1% (v/v) SDS
ChIP elution buffer	1% (v/v) SDS, 100 mM $NaHCO_3$
SOC broth	2% (w/v) LB broth, 10 mM $MgCl_2$
Solution A	25 mM Tris-HCl, 10 mM EDTA, pH 8.0
Solution B	0.4 M NaOH, 2% (v/v) SDS
Crystal violet	0.2% (w/v) Crystal violet powder, 20% (v/v) ethanol
2X cell culture medium	1.5% (w/v) DMEM and 0.5% (w/v) F12 (3:1), 0.4% (w/v) $NaHCO_3$, 10% (v/v) FBS, 0.1% (v/v) penicillin/streptomycin, filter sterilised

Appendix D

PARTICIPANT INFORMATION SHEET

Eye development disorders

Hello,

We (Dr Carstens, Dr Williams, Dr Goolam and Prof Ramsay) are undertaking research into the underlying genetic cause for eye development disorders that affect the front of the eye (anterior segment). Dr Carstens and Prof Ramsay are specialists in the field of human genetics and we are working with consultant eye specialists at Charlotte Maxeke Johannesburg Academic Hospital. We will be conducting the study we are speaking about. The research will be conducted at the Charlotte Maxeke Johannesburg Academic Hospital and the University of the Witwatersrand.

We are studying the eye development conditions that you/your child has. It seems that this is a disease that is passed on in our genes. It can be inherited or it can be a completely new mutation that occurs for the first time in the family. The genes are contained in the DNA, which is found in every cell of our bodies.

We would like to invite you and your children, those with the condition and those who do not have it, to participate in this study. At some stage we may also, with your permission, contact other family members who may assist us with the study. If you would like to participate (and if you and your children are willing to be a part of the study), we will first arrange for your family to see a genetic counsellor or doctor who can explain inheritance and what it means in this disease and in your family. Then we will examine your child's eyes and take a blood sample from his/her arm. We will also examine your eyes and take a blood sample from you. We may also ask for a saliva sample. We will then take the DNA out of the blood or saliva without doing any other tests on the sample. Some of the DNA may be sent out of the country to look at all the genetic material in the DNA. We hope that this will help us to find the genes that are associated with developmental eye disorders. All the information that is discovered with this process will return to South Africa where it may be used in other genetic studies. We would also like to use the records from all your eye related tests to help us find patterns between specific results from these tests or examinations and the DNA changes.

You and your children do not have to join this study. You can also decide to leave the study at any time. If you do not want to be part of this study or decide to leave the study it will not affect your child's regular treatments or medical care in any way. We invite your child to approach the researchers to be re-consented when he/she turns 18 if he/she wishes. He/she can also decide to leave the study at any time.

INFORMATION ABOUT DEVELOPMENTAL EYE DISORDERS

The purpose of this research is to look for genes that are associated with developmental eye disorders in South Africans. We hope that the results will help us to better understand the causes of developmental eye disorders.

The human eye forms through a complex program during embryonic development. Problems in this developmental process can lead to congenital eye malformations, such as **anophthalmia** (no eye), **microphthalmia** (small eye), **coloboma** (failure of the optic fissure to close), **aniridia** (absent or partial iris), **anterior segment dysgenesis** (a range of disorders that affect the development of the front of the eye) and **optic nerve hypoplasia** (underdeveloped optic nerve). These eye development disorders are usually apparent in an eye examination. Children with these problems need the kind of specialized experience found among ophthalmologists. Eye development disorders can affect one or many parts of the eye, such as the iris, cornea and lens. There are a number of genes that have been linked to eye development disorders and it is not always possible to identify or predict the likely causal gene based on a clinical examination. This is why we would like to examine many genes in the same study to try and identify the gene that's causing a particular developmental eye disorder.

INFORMATION ABOUT DNA SAMPLING

If your family would like to be a part of this study, then we will arrange for a genetic counsellor or doctor to meet with you to explain genes, genetics and how they are involved in developmental eye disorders and how this is likely to affect your family. Then in order to study your genes we will take a sample of blood from your arms. We may also ask for a saliva (spit) sample from you or your affected child. Our blood and saliva contains cells. All the cells in our bodies contain a chemical called DNA that we inherit from our parents. It carries the instructions for making us living organisms. It contains all our genes. We can take the DNA out of the cells that are in your sample. Once we have removed the DNA from the sample we can study the genes. In this study we will examine every gene in the DNA to try and find the gene that causes a developmental eye disorder. Sometimes we have to send a little bit of the DNA overseas to experienced service providers or collaborators to examine these genes, because we don't always have the equipment and machines that are necessary to do this work in the country. All the information that is discovered with this process will, however, return to South Africa where it can be analysed and perhaps used in other genetic studies.

If your family is interested in helping us with further research then the remainder of your DNA will be stored in the Sydney Brenner Institute for Molecular Biosciences (SBIMB) Biobank here in South Africa for an indefinite period of time. It can sometimes take a long time and lots of experiments to fully understand the cause of a particular disease, which is why we ask to keep the samples. You may sign a separate consent form for this and your children may sign a separate assent form for this. In the future if further tests become available for genes involved in developmental eye disorders we may then use this DNA to look for these genes. We will only use the DNA for tests related to genetic- and

ophthalmology-related research and it will not be used for any other purpose. Any further tests will be monitored by the Wits Ethics Committee. If samples are to be sent overseas they will be protected by a legal agreement with Wits University. This will also be monitored by this Ethics Committee. You may choose to have the DNA destroyed at any time.

EXPECTED BENEFITS

This study is unlikely to help you in any way but it will help us to understand developmental eye disorders better and may help us to develop new ways to treat the disease in the future. If information relative to the eye condition is identified, the information will be conveyed to you by a genetic counsellor or doctor.

Through this research, we may find that you and your child has an abnormal gene or gene product (RNA or protein). These results may also indirectly provide information about your entire family. Some people involved in genetic studies have felt anxious about the possibility of carrying an abnormal gene that places them at risk or that can be passed on to their children. If you have these feelings at any time during the study, you may contact the investigator(s) who will arrange for you to speak to a genetic counsellor.

WHAT TO EXPECT FROM THE STUDY

Once you have signed the consent form and your children have signed the assent form we will ask you some questions about your and your children's background, health and eyes. A complete eye examination will be performed on your affected child that is no different from his/her usual follow-up eye examination. Unaffected family members will also have an eye examination to confirm that they do not have the condition. This information will be used in the research study, but your family's personal details will be withheld. Then a nursing sister or doctor will take up to two teaspoons (10ml or 2 tubes) of blood from a vein in each participating family member. Venipunctures (drawing blood) are normally done as part of routine medical care and present a slight risk of discomfort. Drawing blood may result in faintness, inflammation of the vein, pain, bruising or bleeding at the puncture site. There is also a slight possibility of infection. Your protection is that experienced personnel perform the procedures under sterile conditions.

We may also ask for a saliva (spit) sample from you or your affected child. A nursing sister or doctor will use a small, soft sponge to collect the saliva sample. The sponge is placed inside the mouth against the cheek and gently moved along the gums and cheek to soak up as much saliva as possible. He/she will then place the saliva in a special container and might repeat the process if we do not get enough saliva the first time. This procedure is painless and harmless.

CONFIDENTIALITY

Only the investigators of the study will know your and your children's names and personal details. You will each be given a code and number for the study so that no one knows who you are. The blood samples, DNA and/or saliva samples will not be attached to your names – they will only have their code and number on them.

CONTACT DETAILS

If you have any problems you can contact me at any time on this telephone number: -
Dr Nadia Carstens – 011 489 9230.

If you have any concern over the way the study is being conducted, please contact the Chairperson of this Committee who is Professor Clement Penny, who may be contacted on telephone number 011 717 2301, or by e-mail on Clement.Penny@wits.ac.za. The telephone numbers for the Committee secretariat are 011 717 2700/1234 and the e-mail addresses are Zanele.Ndlovu@wits.ac.za and Rhulani.Mukansi@wits.ac.za.

CONSENT FORM for adults

"The purpose of this study, procedures to be followed, risks and benefits, have been explained to me. I have been allowed to ask the questions I have, and my questions have been answered to my satisfaction. I have been told whom to contact if I have questions, to discuss problems, concerns, or suggestions related to the research, or to obtain information or offer input about the research. I have read this consent form and agree to participate in this research study with the understanding that I may withdraw at any time. I have been told that I will be given a signed and dated copy of this consent form if I would like one."

_____ _____

Signature of Participant Date

_____ _____

Signature of Person Obtaining Consent Date

CONSENT FORM for children

"The purpose of this study, procedures to be followed, risks and benefits, have been explained to me and my child. I have been allowed to ask the questions I have, and my questions have been answered to my satisfaction. I have been told whom to contact if I have questions, to discuss problems, concerns, or suggestions related to the research, or to obtain information or offer input about the research. I have read this consent form and agree to allow my child to participate in this research study with the understanding that I may withdraw my child at any time. We have discussed the study with my child to the best of our ability, who agrees to be in the study. We have explained to my child that he/she may approach the researchers to be re-consented when he/she turns 18 if he/she wishes and that he/she may withdraw from the study at any time. I have been told that I will be given a signed and dated copy of this consent form if I would like one."

_____ _____

Name of Child Date

_____ _____

Signature of Parent or Legal Guardian Date

_____ _____

Signature of Person Obtaining Consent Date

ASSENT FORM

"The purpose of this study, procedures to be followed, risks and benefits, have been explained to me. I have been allowed to ask the questions I have, and my questions have been answered to my satisfaction. I have been told whom to contact if I have questions, to discuss problems, concerns, or suggestions related to the research, or to obtain information or offer input about the research. I have read this assent form (or had it read to me) and agree to participate in this research study with the understanding that I may withdraw at any time. I understand that that I may approach the researchers to be re-consented when I turn 18 if I want to and that I may withdraw from the study at any time. I have been told that I will be given a signed and dated copy of this consent form if I would like one."

_____	_____
Signature of Child/ thumb print	Date
_____	_____
Signature of Parent or Legal Guardian	Date
_____	_____
Signature of Person Obtaining Consent	Date

CONSENT FORM for ADULTS for DNA storage for possible future use

I, the undersigned, have been fully informed as to the procedure to be followed and have been given a description of the risks and benefits of having my DNA extracted and stored for possible further research.

In signing this form, I agree to have my DNA stored at the Division of Human Genetics in the Molecular Genetics Laboratory.

I understand that most of the DNA that is extracted from my blood will be stored in Johannesburg for an indefinite period of time and may be used for further genetic testing for genetic- or developmental disorder-related research only. This may include sending a portion of the sample overseas for further tests. Any further testing on these samples will be monitored by the Wits Ethics Committee.

I understand that if I have any questions at any time, they will be answered.

I understand that I can choose to have my DNA destroyed at any time.

I understand that confidentiality will be maintained at all times through the use of a code and numbering system.

A signed copy of this consent form will be made available to me if I want one.

The information around the blood and DNA samples taken from me is clear.

YES ☐ NO ☐

The purpose of this consent is for me to inform the study what they can or cannot do with these samples.

YES ☐ NO ☐

I acknowledge that all procedure/tests on the stored blood and DNA samples have been or will be approved by the Human Research Ethics Committee of the University of the Witwatersrand.

YES ☐ NO ☐

I am in agreement that my DNA may be stored and used for the purposes described above.

YES ☐ NO ☐

I am in agreement that the data generated from my DNA may be made available in a public domain without any identifiers.

YES ☐ NO ☐

I agree that a small bit of my DNA may be sent out of the country if the research cannot easily be done in South Africa.

YES ☐ NO ☐

I understand that every time a new study is done on my DNA, permission will be obtained from the ethics committee for the study to make sure that it is used only for the purposes stated above.

YES ☐ NO ☐

I understand that I may not benefit directly from the research done on my DNA and my family's DNA. I understand that the tests will reveal information about my biological ancestors, about my ability to respond to certain drugs and that genetic variants that may affect my risk for some diseases may be identified.

YES ☐ NO ☐

If this research does identify information that would be important or of benefit to me or my family, I would like to be contacted to receive the information.

YES ☐ NO ☐

I understand that my family and I may withdraw from the study at any time.

YES ☐ NO ☐

RESEARCHER:

Printed Name Signature Date

PARTICIPANT:

_____

Printed name Signature Date

WITNESS:

Printed Name Signature Date

CONSENT FORM for CHILDREN for DNA storage for possible future use

I, the undersigned, have been fully informed as to the procedure to be followed and have been given a description of the risks and benefits of having my child's blood sampled for the purpose of DNA extraction and storage for possible further research.

In signing this form, I agree to have my child's DNA stored at the Division of Human Genetics in the Molecular Genetics Laboratory.

I understand that most of the DNA that is extracted from my child's blood will be stored in Johannesburg for an indefinite period of time and may be used for further genetic testing for genetic- or developmental disorder-related research only. This may include sending a portion of the sample overseas for further tests. Any further testing on these samples will be monitored by the Wits Ethics Committee. I understand that that my child may approach the researchers to be re-consented when he/she turns 18 if he/she wants to and that he/she may withdraw from the study at any time.

I understand that if I have any questions at any time, they will be answered.

I understand that I can choose to have my child's DNA destroyed at any time.

I understand that confidentiality will be maintained at all times through the use of a code and numbering system.

I have discussed the study with my child, who agrees to the DNA storage.

A signed copy of this consent form will be made available to me if I want one.

The information around the blood and DNA samples taken from my child is clear.

YES ☐ NO ☐

The purpose of this consent form is for me to inform the study what they can or cannot do with these samples.

YES ☐ NO ☐

I acknowledge that all procedure/tests on the stored blood and DNA samples have been or will be approved by the Human Research Ethics Committee of the University of the Witwatersrand.

YES ☐ NO ☐

I am in agreement that my child's DNA may be stored and used for the purposes described above.

YES ☐ NO ☐

I am in agreement that the data generated from my child's DNA may be made available in a public domain without any identifiers.

YES ☐ NO ☐

I agree that a small bit of my child's DNA may be sent out of the country if the research cannot easily be done in South Africa.

YES ☐ NO ☐

I understand that every time a new study is done on my child's DNA, permission will be obtained from the ethics committee for the study to make sure that it is used only for the purposes stated above.

YES ☐ NO ☐

I understand that my child is unlikely to benefit directly from the research done on the DNA. I understand that the tests will reveal information about my child's biological ancestors, about my child's ability to respond to certain drugs and that genetic variants that may affect my child's risk for some diseases may be identified.

YES ☐ NO ☐

I understand that my child withdraw from the study at any time.

YES ☐ NO ☐

CHILD:

Printed Name

RESEARCHER:

Printed Name Signature Date

PARENT OR LEGAL GUARDIAN:

_____

Printed name Signature Date

WITNESS:

Printed Name Signature Date

ASSENT FORM for DNA storage for possible future use

"The purpose of storing my DNA has been explained to me – it may be used for health studies related to developmental disorders. I have been allowed to ask the questions I have, and my questions have been answered to my satisfaction. I have been told whom to contact if I have questions, to discuss problems, concerns, or suggestions related to the research, or to obtain information or offer input about the research. I have read this assent form (or had it read to me) and agree to participate in this research study with the understanding that I may withdraw at any time. I understand that if I want to withdraw from the research my DNA sample will be destroyed. I understand that that I may approach the researchers to be re-consented when I turn 18 if I want to and that I may withdraw from the study at any time. I have been told that I will be given a signed and dated copy of this consent form if I would like one."

_____ _____

Signature of Child/ thumb print Date

_____ _____

Signature of Parent or Legal Guardian Date

_____ _____

Signature of Person Obtaining Consent Date

Appendix E

NATIONAL HEALTH LABORATORY SERVICE
School of Pathology, University of the Witwatersrand
DIVISION OF HUMAN GENETICS
Hospital Street, Johannesburg, 2001 | PO Box 1038, Johannesburg, 2000
[T]: +27 11 489 9211 | [F]: +27 11 489 9226 | [E]: human.genetics@nhls.ac.za

13 February 2019

To the Chair, Wits Human Research Ethics Committee (Medical)

RE: Application for sub-study clearance certificate for Mr Tebogo Marutha's PhD project under protocol M1811126

Mr Tebogo Marutha's PhD project falls under the bigger project entitled "Using next-generation sequencing approaches to identify ocular disease genes in South African populations". An ethics clearance certificate was originally awarded to this project under my name (protocol number M131125) and this was renewed on 03/12/2018 (protocol number M1811126). Mr Marutha will use the information sheet and informed consent documents that were submitted to and approved by the HREC(Medical) under protocol M1811126.

I am supervising this PhD project together with Prof Demetra Mavri-Damelin from the School of Molecular and Cell Biology.

Please do not hesitate to contact me if you have any questions.

Sincerely,

Dr Nadia Carstens
Medical Scientist | Researcher
Division of Human Genetics
National Health Laboratory Service & The University of the Witwatersrand
Tel (011) 489 9230 | nadia.carstens@nhls.ac.za or nadia.carstens@wits.ac.za

UNIVERSITY OF THE WITWATERSRAND, JOHANNESBURG

R14/49 Dr N Carstens, et al

HUMAN RESEARCH ETHICS COMMITTEE (MEDICAL)
CLEARANCE CERTIFICATE NO. M1811126

NAME: (Principal Investigator)	Dr N Carstens, et al
DEPARTMENT:	School of Pathology Department of Human Genetics South African Institute for Medical Research
PROJECT TITLE:	Using next-generation sequencing approaches to identify ocular disease genes in South African populations
DATE CONSIDERED:	Ad hoc
DECISION:	Approved unconditionally
CONDITIONS:	Renewal of M 131125
SUPERVISOR:	Not applicable
APPROVED BY:	Dr CB Penny, Chairperson, HREC (Medical)
DATE OF APPROVAL:	03/12/2018

This clearance certificate is valid for 5 years from date of approval. Extension may be applied for.

DECLARATION OF INVESTIGATORS

To be completed in duplicate and **ONE COPY** returned to the Research Office Secretary on 3rd floor, Phillip V Tobias Building, Parktown, University of the Witwatersrand, Johannesburg.

I/We fully understand the conditions under which I am/we are authorised to carry out the above-mentioned research and I/we undertake to ensure compliance with these conditions. Should any departure be contemplated from the research protocol as approved, I/we undertake to resubmit to the Committee. **I agree to submit a yearly progress report**. When a funder requires annual re-certification, the application date will be one year after the date of the meeting when the study was initially reviewed. In this case, the study was initially reviewed in **November** and will therefore reports and re-certification will be due early in the month of **November** each year. Unreported changes to the application may invalidate the clearance given by the HREC (Medical).

Principal Investigator Signature

Date

PLEASE QUOTE THE PROTOCOL NUMBER IN ALL ENQUIRIES